CHAPTER 6

THE RETARDED-MOTION EXPANSION

In this chapter the object of study is the "retarded-motion expansion," which is an expansion about the Newtonian fluid. Successive terms in the expansion account systematically for the deviations from Newtonian behavior because of "elastic effects." When the expansion is truncated after the second-order terms, the *second-order fluid* results; truncation after the third-order terms yields the *third-order fluid*, and so forth. Whereas the generalized Newtonian fluid models have been used mainly by engineers and the linear viscoelastic models have been used mainly by chemists, the second- and third-order fluid models have been studied primarily by mathematicians and continuum physicists. Because it is generally agreed that the retarded-motion expansion is the correct constitutive equation for flows in which the rate-of-strain tensor and its time derivatives are small, considerable effort has been expended to solve flow problems and to develop general theorems for this constitutive equation. These results obtained for the second-, third-,... order fluids (the "ordered fluids") have an aura of permanence, since no empiricism is involved in the development of the retarded-motion expansion.

A great deal of physical insight about "elastic effects" has been obtained by solving flow problems with the ordered-fluid models. One learns about the sign attached to the elastic effects and how elasticity results in secondary flows. One develops some qualitative feelings about how elasticity affects bubble shapes and particle orientations. In addition, one begins to develop an understanding of the mathematical procedures needed for coping with nonlinear viscoelastic problems and the role of boundary and initial conditions.

However, it must be kept in mind that the retarded-motion expansion is of little use to the engineer, since in industrial problems the non-Newtonian viscosity often plays the dominant role, and, as we shall see, the ordered fluids cannot describe the η vs. $\dot{\gamma}$ relation faithfully. Also, the retarded-motion expansion is of little use to the chemist doing linear viscoelasticity experiments, since the ordered fluids cannot describe the full range of time-dependent behavior. The retarded-motion expansion has a niche of its own and it provides valuable insight into some problems that cannot be studied by the generalized Newtonian fluids or by linear viscoelastic models. Keep in mind that all three of these models, covered in Chapters 4, 5, and 6, can be obtained as special cases of a much more general constitutive equation, as discussed in Chapter 9.

The chapter begins in §6.1 with the definition of the "nth rate-of-strain tensors". A full discussion of their derivation and geometrical significance is postponed until Chapter 9. In §6.2 we give the retarded-motion expansion and define a Deborah number to describe the importance of the elastic effects. Then in §6.3 some general theorems are given for the second-order fluid, which facilitate problem solving for certain important classes of flows. Examples in §§6.4 and 6.5 illustrate the fluid dynamical behavior of viscoelastic liquids in the limit of slow flows. Finally in §6.6 the use and limitations of the retarded-motion expansion are discussed.

§6.1 CONVECTED DERIVATIVES OF THE RATE-OF-STRAIN TENSOR

In this section we define the kinematic tensors to be used in the chapter. Imagine a velocity field specified by the function $\boldsymbol{v}(x_1, x_2, x_3, t)$ where (x_1, x_2, x_3) is a set of Cartesian coordinates. With respect to this coordinate system we define the following three kinematic tensors:[1]

		*ij*th *Cartesian Component*	
Velocity gradient tensor:	$\nabla \boldsymbol{v}$	$\frac{\partial}{\partial x_i} v_j$	(6.1-1)
Rate-of-strain tensor:	$\dot{\gamma} = \nabla \boldsymbol{v} + (\nabla \boldsymbol{v})^\dagger$	$\frac{\partial}{\partial x_i} v_j + \frac{\partial}{\partial x_j} v_i$	(6.1-2)
Vorticity tensor:	$\boldsymbol{\omega} = \nabla \boldsymbol{v} - (\nabla \boldsymbol{v})^\dagger$	$\frac{\partial}{\partial x_i} v_j - \frac{\partial}{\partial x_j} v_i$	(6.1-3)

We have already encountered the rate-of-strain tensor $\dot{\gamma}$ in earlier chapters. We see from the definitions that $\dot{\gamma}$ is a symmetric tensor, whereas the vorticity tensor $\boldsymbol{\omega}$ is an antisymmetric tensor. The velocity gradient tensor is equal to one half the sum of the rate-of-strain tensor and the vorticity tensor:

$$\nabla \boldsymbol{v} = \tfrac{1}{2}(\dot{\gamma} + \boldsymbol{\omega}) \tag{6.1-4}$$

That is, the velocity gradient tensor can be decomposed into its symmetric and antisymmetric parts. The symmetric tensor $\dot{\gamma}$ has six independent Cartesian components, whereas the antisymmetric tensor $\boldsymbol{\omega}$ has three independent components to give a total of nine independent components, corresponding to the number of components of $\nabla \boldsymbol{v}$. For convenience the components of $\nabla \boldsymbol{v}$ in four coordinate systems are given in Tables A.7-1 to 4, and the components of $\dot{\gamma}$ and $\boldsymbol{\omega}$ are presented in Tables B.3 and B.4.

The rate-of-strain tensor $\dot{\gamma}$ describes the rate at which neighboring particles move with respect to each other independently of superposed rigid rotations. The vorticity tensor is a measure of the local rate of rotation of the fluid. For this reason the vorticity tensor does not appear in the constitutive equation for the Newtonian liquid. Thus the use of the rate-of-strain tensor rather than the velocity gradient tensor in the Newtonian fluid relation ensures that the stresses depend only on the rate at which neighboring particles move relative to each other, and not on superposed rigid rotations.

We now introduce the fundamental kinematic tensors[2] of this chapter, $\gamma_{(1)}$, $\gamma_{(2)} \cdots \gamma_{(n)}$, called the *first, second, $\cdots$, nth rate-of-strain tensors.* The first of these is defined to be identical to the rate-of-strain tensor and the remaining are defined through a recurrence relation:

$$\gamma_{(1)} \equiv \dot{\gamma} \tag{6.1-5}$$

$$\gamma_{(n+1)} = \frac{D}{Dt} \gamma_{(n)} - \{(\nabla \boldsymbol{v})^\dagger \cdot \gamma_{(n)} + \gamma_{(n)} \cdot (\nabla \boldsymbol{v})\} \tag{6.1-6}$$

[1] *Caution*: There is considerable diversity in the literature regarding the definitions of these quantities. Some authors define the *ij*th component of $\nabla \boldsymbol{v}$ to be $\partial v_i / \partial x_j$. Factors of $\frac{1}{2}$ are commonly included on the right side of Eqs. 6.1-2 and 3, and some authors use a vorticity tensor that is the negative of, or $\frac{1}{2}$ the negative of, the one defined here.

[2] J. G. Oldroyd, *Proc. Roy. Soc.*, **A200**, 523–541 (1950).

The tensor $\boldsymbol{\gamma}_{(n+1)}$ is the nth *convected derivative*[3] of the rate-of-strain tensor $\boldsymbol{\gamma}_{(1)}$. These derivatives are defined in a manner such that they have a significance independent of superposed rigid rotations. The detailed explanation of the origin of these tensors is postponed until Chapter 9, and in this chapter we shall be concerned with the consequences of using the tensors in constitutive equations. Explicit expressions for $\boldsymbol{\gamma}_{(1)}$ and $\boldsymbol{\gamma}_{(2)}$ for homogeneous shear flows and shearfree flows are given as matrix displays in Appendix C. The following example illustrates how $\boldsymbol{\gamma}_{(1)}$, $\boldsymbol{\gamma}_{(2)}$, and $\boldsymbol{\gamma}_{(3)}$ can be written explicitly for homogeneous shear flow.

EXAMPLE 6.1-1 The Rate-of-Strain Tensors in Simple Shear Flow

Consider the simple shear flow $v_x = \dot{\gamma}_{yx}(t)y$, and display the first three rate-of-strain tensors in matrix form.

SOLUTION The standard procedure is to represent all tensors by their Cartesian components arranged in matrices. Tensor multiplications may then be performed as matrix multiplications. First we obtain for the velocity gradient tensor, its transpose, and the (first) rate-of-strain tensor:

$$\nabla \boldsymbol{v} = \begin{pmatrix} 0 & 0 & 0 \\ 1 & 0 & 0 \\ 0 & 0 & 0 \end{pmatrix} \dot{\gamma}_{yx}(t); \qquad (\nabla \boldsymbol{v})^{\dagger} = \begin{pmatrix} 0 & 1 & 0 \\ 0 & 0 & 0 \\ 0 & 0 & 0 \end{pmatrix} \dot{\gamma}_{yx}(t) \tag{6.1-7}$$

$$\boldsymbol{\gamma}_{(1)} \equiv \dot{\boldsymbol{\gamma}} = \begin{pmatrix} 0 & 1 & 0 \\ 1 & 0 & 0 \\ 0 & 0 & 0 \end{pmatrix} \dot{\gamma}_{yx}(t) \tag{6.1-8}$$

Then we use the definition in Eq. 6.1-6 written for $n = 1$. Since the flow is homogeneous the term $\{\boldsymbol{v} \cdot \nabla \boldsymbol{\gamma}_{(1)}\}$ is identically zero and we obtain

$$\begin{aligned} \boldsymbol{\gamma}_{(2)} &= \frac{\partial}{\partial t} \begin{pmatrix} 0 & 1 & 0 \\ 1 & 0 & 0 \\ 0 & 0 & 0 \end{pmatrix} \dot{\gamma}_{yx} - \begin{pmatrix} 0 & 1 & 0 \\ 0 & 0 & 0 \\ 0 & 0 & 0 \end{pmatrix} \begin{pmatrix} 0 & 1 & 0 \\ 1 & 0 & 0 \\ 0 & 0 & 0 \end{pmatrix} \dot{\gamma}_{yx}^2 - \begin{pmatrix} 0 & 1 & 0 \\ 1 & 0 & 0 \\ 0 & 0 & 0 \end{pmatrix} \begin{pmatrix} 0 & 0 & 0 \\ 1 & 0 & 0 \\ 0 & 0 & 0 \end{pmatrix} \dot{\gamma}_{yx}^2 \\ &= \begin{pmatrix} 0 & 1 & 0 \\ 1 & 0 & 0 \\ 0 & 0 & 0 \end{pmatrix} \frac{\partial \dot{\gamma}_{yx}}{\partial t} - 2 \begin{pmatrix} 1 & 0 & 0 \\ 0 & 0 & 0 \\ 0 & 0 & 0 \end{pmatrix} \dot{\gamma}_{yx}^2 \end{aligned} \tag{6.1-9}$$

For $\boldsymbol{\gamma}_{(3)}$ we obtain similarly

$$\boldsymbol{\gamma}_{(3)} = \begin{pmatrix} 0 & 1 & 0 \\ 1 & 0 & 0 \\ 0 & 0 & 0 \end{pmatrix} \frac{\partial^2 \dot{\gamma}_{yx}}{\partial t^2} - 6 \begin{pmatrix} 1 & 0 & 0 \\ 0 & 0 & 0 \\ 0 & 0 & 0 \end{pmatrix} \dot{\gamma}_{yx} \frac{\partial \dot{\gamma}_{yx}}{\partial t} \tag{6.1-10}$$

Notice that $\boldsymbol{\gamma}_{(n)} = 0$ for $n \geq 3$ if the flow is steady.

Before leaving this section we define the "order" of an expression in the rate-of-strain tensors. Notice from Example 6.1-1 that the tensor $\boldsymbol{\gamma}_{(n)}$ may contain terms up through

[3] In Chapter 9 this is called a "contravariant convected derivative."

nth degree in the components of the velocity gradient and their time derivatives taken together. The tensor $\gamma_{(n)}$ is then defined[4] to be "of order n." We also define the order of any product involving rate-of-strain tensors as the sum of the orders of the factors. Such products could be scalar products, tensor products, or multiplication of a tensor by a scalar invariant. For example,

$$\gamma_{(3)}, \quad \{\gamma_{(2)} \cdot \gamma_{(1)}\}, \quad \{\gamma_{(1)} \cdot \gamma_{(1)} \cdot \gamma_{(1)}\}, \quad \text{and } (\gamma_{(1)} : \gamma_{(1)})\gamma_{(1)}$$

are all terms of order three. Note that terms of order one have dimensions of reciprocal time; terms of order two, reciprocal time squared; terms of order three, reciprocal time cubed; and so on.

§6.2 THE RETARDED-MOTION EXPANSION

We wish to construct a constitutive equation that describes small departures from Newtonian behavior. To account systematically for such departures one could try developing a series expression involving increasing powers of the rate-of-strain tensor as well as powers of the first-, second-, and higher-order partial time derivatives. This idea is explored in Problem 6B.12, and it is shown that such an expression for τ fails to give reasonable results in the turntable experiment discussed at the end of Chapter 5. The continuum-mechanics development in Chapter 9 shows that partial time derivatives of the rate-of-strain tensor should not appear in constitutive equations, but rather convected time derivatives.

We are then led to construct a constitutive equation as follows. First we assume[1] that the fluid is incompressible and that the stress tensor is symmetric and can be expressed as a polynomial in the rate-of-strain tensors $\gamma_{(n)}$. Second we arrange the terms in the polynomial to be of increasing order, and terms of equal order are collected together. Then we arrive at the *retarded-motion expansion*, given here through terms of third order:[2]

$$\tau = -[b_1\gamma_{(1)} + b_2\gamma_{(2)} + b_{11}\{\gamma_{(1)} \cdot \gamma_{(1)}\} + b_3\gamma_{(3)} + b_{12}\{\gamma_{(1)} \cdot \gamma_{(2)} + \gamma_{(2)} \cdot \gamma_{(1)}\} + b_{1:11}(\gamma_{(1)} : \gamma_{(1)})\gamma_{(1)} + \cdots] \tag{6.2-1}$$

The scalars b_1, b_2, b_{11}, etc. are material parameters, and we shall call them *retarded-motion constants*. If we retain only the first-order term, this expansion reduces to the constitutive equation for the *incompressible Newtonian fluid*, and b_1 is then the viscosity. If all terms

[4] H. Giesekus, *Z. Angew. Math. Mech.*, **42**, 32–61 (1962).

[1] This assumption is inherent in R. S. Rivlin and J. L. Ericksen, *J. Rat. Mech. Anal.*, **4**, 323–425 (1955), for unsteady flow and in H. Giesekus, *Kolloid Z.*, **147**, 29–45 (1956), for steady flow.

[2] Among the third-order terms there is one containing $(\dot\gamma : \dot\gamma)\dot\gamma$ and another containing $\{\dot\gamma \cdot \dot\gamma \cdot \dot\gamma\}$. The latter may be eliminated in favor of an additional term of the form $(\dot\gamma : \dot\gamma)\dot\gamma$ by using the Cayley-Hamilton theorem (Eq. A.3-2[8])

$$\dot\gamma^3 - \dot\gamma^2 \operatorname{tr} \dot\gamma + \tfrac{1}{2}\dot\gamma[(\operatorname{tr} \dot\gamma)^2 - \operatorname{tr} \dot\gamma^2] - \delta[\tfrac{1}{6}(\operatorname{tr} \dot\gamma)^3 - \tfrac{1}{2} \operatorname{tr} \dot\gamma \operatorname{tr} \dot\gamma^2 + \tfrac{1}{3} \operatorname{tr} \dot\gamma^3] = \mathbf{0} \tag{6.2-1a}$$

and the fact that $\operatorname{tr} \dot\gamma = 0$ for an incompressible fluid. In addition the term containing the unit tensor δ can be discarded, inasmuch as the normal components of τ can be determined only to within an additive isotropic function. H. Giesekus, *Z. Angew. Math. Mech.*, **42**, 32–61 (1962), developed the expansion complete through sixth order. When the fluid is compressible, additional terms have to be included in the retarded-motion expansion [see R. K. Prud'homme and R. B. Bird, *J. Non-Newtonian Fluid Mech.*, **3**, 261–279 (1978)].

through second order (i.e., the dashed underlined terms) are included, we obtain the *incompressible second-order fluid.*[3] Finally if all terms shown explicitly are included, we have the *incompressible third-order fluid.* That is, the "ordered fluids" are represented by constitutive equations obtained by truncating the retarded-motion expansion. Most of this chapter is concerned with second- and third-order fluids. In the following illustrative example we work out the expressions for the viscosity and normal stress coefficients for the third-order fluid.

EXAMPLE 6.2-1 Viscometric Functions for the Third-Order Fluid

Consider the steady shear flow $v_x = \dot{\gamma} y$ to find the viscometric functions η, Ψ_1, and Ψ_2 for the third-order fluid. Discuss conditions under which the shear stress is a monotone increasing function of shear rate.

SOLUTION The rate-of-strain tensors $\boldsymbol{\gamma}_{(1)}$, $\boldsymbol{\gamma}_{(2)}$ and $\boldsymbol{\gamma}_{(3)}$ may be obtained by simplifying the expressions found in Example 6.1-1 to steady state. The other combinations are found by matrix multiplication

$$\{\boldsymbol{\gamma}_{(1)} \cdot \boldsymbol{\gamma}_{(1)}\} = \begin{pmatrix} 1 & 0 & 0 \\ 0 & 1 & 0 \\ 0 & 0 & 0 \end{pmatrix} \dot{\gamma}^2, \qquad (\boldsymbol{\gamma}_{(1)} : \boldsymbol{\gamma}_{(1)}) = \mathrm{tr}\{\boldsymbol{\gamma}_{(1)} \cdot \boldsymbol{\gamma}_{(1)}\} = 2\dot{\gamma}^2 \tag{6.2-2}$$

$$\{\boldsymbol{\gamma}_{(1)} \cdot \boldsymbol{\gamma}_{(2)} + \boldsymbol{\gamma}_{(2)} \cdot \boldsymbol{\gamma}_{(1)}\} = \begin{pmatrix} 0 & 1 & 0 \\ 1 & 0 & 0 \\ 0 & 0 & 0 \end{pmatrix} (-2\dot{\gamma}^3) \tag{6.2-3}$$

Up through terms of third order, Eq. 6.2-1 may now be written explicitly for steady simple shear flow as

$$\begin{pmatrix} \tau_{xx} & \tau_{yx} & 0 \\ \tau_{yx} & \tau_{yy} & 0 \\ 0 & 0 & \tau_{zz} \end{pmatrix} = - \left[\begin{pmatrix} 0 & 1 & 0 \\ 1 & 0 & 0 \\ 0 & 0 & 0 \end{pmatrix} (b_1 \dot{\gamma} - 2(b_{12} - b_{1:11})\dot{\gamma}^3) + \begin{pmatrix} 1 & 0 & 0 \\ 0 & 0 & 0 \\ 0 & 0 & 0 \end{pmatrix} (-2b_2 \dot{\gamma}^2) + \begin{pmatrix} 1 & 0 & 0 \\ 0 & 1 & 0 \\ 0 & 0 & 0 \end{pmatrix} b_{11} \dot{\gamma}^2 \right] \tag{6.2-4}$$

so that the viscometric functions for the third-order fluid are

$$\eta = b_1 - (b_{12} - b_{1:11}) 2\dot{\gamma}^2 \tag{6.2-5}$$

$$\Psi_1 = -2b_2 \tag{6.2-6}$$

$$\Psi_2 = b_{11} \tag{6.2-7}$$

[3] The second-order fluid is usually given in the literature in terms of the kinematic tensors $\boldsymbol{\gamma}^{(n)}$ (commonly denoted $\boldsymbol{A}_n$ and called the "Rivlin–Ericksen tensors"; see Chapter 9) thus,

$$\boldsymbol{\tau} = -[a_1 \boldsymbol{\gamma}^{(1)} + a_2 \boldsymbol{\gamma}^{(2)} + a_{11}\{\boldsymbol{\gamma}^{(1)} \cdot \boldsymbol{\gamma}^{(1)}\}] \tag{6.2-1b}$$

The a's and the b's are interrelated by

$$b_1 = a_1; \quad b_2 = a_2; \quad b_{11} = a_{11} + 2a_2 \tag{6.2-1c}$$

From these results it is clear that the second-order fluid has a constant viscosity and constant first and second normal stress coefficients. In particular we see that $\Psi_{1,0}/2\eta_0 = -b_2/b_1$; furthermore from Table 5.3-1 it can be seen that $-b_2/b_1$ is equal to $\int_0^\infty sG(s)\,ds/\int_0^\infty G(s)\,ds$. In addition we note that the third-order fluid exhibits departure from a constant viscosity if $(b_{12} - b_{1:11}) \neq 0$. If $(b_{12} - b_{1:11}) < 0$ the fluid is shear thickening, and the negative of the shear stress is continually increasing with shear rate. If $(b_{12} - b_{1:11}) > 0$ the derivative of the negative of the shear stress with respect to shear rate is

$$d(-\tau_{yx})/d\dot{\gamma} = b_1[1 - 6\alpha^2\dot{\gamma}^2] \tag{6.2-8}$$

where $\alpha^2 = (b_{12} - b_{1:11})/b_1$. In order that this derivative be positive, we must require that $\dot{\gamma}^2 < 1/6\alpha^2$. Notice also that when $\dot{\gamma}^2 = 1/6\alpha^2$, we have $\eta = (2/3)b_1$, so that the third-order fluid can describe a shear-thinning viscosity that drops only by one third of its zero-shear-rate value (see Fig. 6.2-1).

In Example 6.2-1 we demonstrated that there must be a restriction on the shear rate in steady simple shear flow of a third-order fluid with coefficients chosen such that the fluid shows shear thinning. For the second-order fluid no such limitation appeared. In other kinds of flow, however, there will also be a restriction on the strain rates for the second-order fluid, as we may see, for example, from the elongational viscosity of a second-order fluid (Problem 6B.4):

$$\bar{\eta}(\dot{\varepsilon}) = 3b_1 - 3(b_2 - b_{11})\dot{\varepsilon} \tag{6.2-9}$$

We see that unless $b_2 = b_{11}$ we must require $\dot{\varepsilon} < b_1/(b_2 - b_{11})$ to ensure that $\bar{\eta}(\dot{\varepsilon})$ is positive. Since $\dot{\varepsilon}$ may be both positive (uniaxial elongation) or negative (biaxial extension) the above inequality is a real restriction irrespective of the sign of $(b_2 - b_{11})$. Such restrictions serve to illustrate that the retarded-motion expansion is indeed a constitutive equation designed for systematic investigations of small-velocity-gradient departure from Newtonian behavior.

We now show that the restriction of the retarded-motion expansion to "small velocity gradients" is really a restriction to small Deborah number. To do this we let κ denote a characteristic rate of strain for the flow. For example in tube flow we could take κ to be the average velocity divided by the tube radius, and for flow around a submerged object we could choose the velocity of the fluid far from the object (measured relative to the object) divided by a dimension of the object transverse to the flow (cf. Fig. 2.8-1). It is then reasonable to define a dimensionless stress $\boldsymbol{\tau}^*$ to be $\boldsymbol{\tau}/b_1\kappa = \boldsymbol{\tau}/\eta_0\kappa$ and a dimensionless nth rate-of-strain tensor $\boldsymbol{\gamma}^*_{(n)}$ to be $\boldsymbol{\gamma}_{(n)}/\kappa^n$. From Example 6.2-1 a good choice for a characteristic

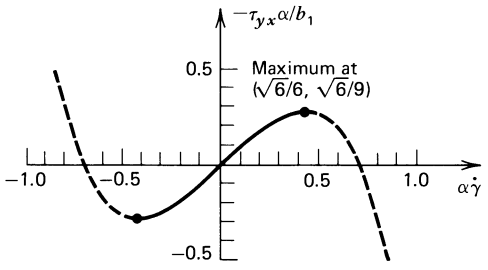

FIGURE 6.2-1. Illustration of the maximum in the shear stress for the third-order fluid. The maximum is located at $(\alpha\dot{\gamma}, -\tau_{yx}\alpha/b_1) = (\sqrt{6}/6, \sqrt{6}/9)$. If $\alpha\dot{\gamma}$ is increased above $\sqrt{6}/6$ the flow is unattainable. The model predicts an unacceptable negative viscosity at shear stresses $|\tau_{yx}\alpha/b_1| > \sqrt{6}/9$. The quantity α is defined below Eq. 6.2-8.

time for the fluid is $-b_2/b_1$, since this ratio is equal to the characteristic time found in linear viscoelasticity in Chapter 5. Thus we take the *Deborah number*[4] to be

$$\mathrm{De} = \lambda\kappa = (-b_2/b_1)\kappa = (\Psi_{1,0}/2\eta_0)\kappa \tag{6.2-10}$$

Finally we denote dimensionless ratios of the retarded-motion expansion coefficients as follows:

$$B_{11} = \frac{b_{11}}{b_2}; \quad B_3 = \frac{b_3 b_1}{b_2^2}; \quad B_{12} = \frac{b_{12} b_1}{b_2^2}; \quad B_{1:11} = \frac{b_{1:11} b_1}{b_2^2} \tag{6.2-11}$$

With these definitions the dimensionless form of the retarded-motion expansion can be written:

$$\begin{aligned} \boldsymbol{\tau}^* = & -\boldsymbol{\gamma}^*_{(1)} + \mathrm{De}[\boldsymbol{\gamma}^*_{(2)} + B_{11}\boldsymbol{\gamma}^{*2}_{(1)}] \\ & -\mathrm{De}^2[B_3\boldsymbol{\gamma}^*_{(3)} + B_{12}\{\boldsymbol{\gamma}^*_{(1)}\cdot\boldsymbol{\gamma}^*_{(2)} + \boldsymbol{\gamma}^*_{(2)}\cdot\boldsymbol{\gamma}^*_{(1)}\} \\ & + B_{1:11}(\boldsymbol{\gamma}^*_{(1)}:\boldsymbol{\gamma}^*_{(1)})\boldsymbol{\gamma}^*_{(1)}] + O(\mathrm{De}^3) \end{aligned} \tag{6.2-12}$$

The Deborah number is seen to be a measure of the importance of nonlinear terms on the flow. It is important to note, in addition, that the absolute values of the B's are expected to be less than unity, according to the kinetic-theory results described below.

The retarded-motion constants should ideally be determined from experiments. We note for instance from Example 6.2-1 that a knowledge of the viscometric functions at low shear rates determines the three constants in the second-order fluid. Rheogoniometer measurements may, however, not be sufficiently sensitive to determine these parameters for all fluids, and in §6.5 we illustrate how other flow situations may be used to obtain information about the retarded-motion constants. There is currently no available systematic tabulation of retarded-motion constants for real polymeric fluids.

Because of the limited experimental information available about the retarded-motion constants, it is important to utilize the results of molecular theories. Constitutive equations obtained from molecular theories can be cast in the form of a retarded-motion expansion. In so doing one obtains expressions for the retarded-motion constants in terms of the parameters appearing in specific molecular models. Table 6.2-1 gives the constants for two molecular theories for dilute polymer solutions and for one molecular theory for polymer melts. From the table we note that these theories, involving various structural models, lead to

1. The b_n alternate in sign with $b_1 > 0$.
2. At second order, $|b_2| > |b_{11}|$.
3. At third order, $b_3 > b_{12} > b_{1:11}$.

The positive value of b_1 corresponds, of course, to the fact that η_0 is positive, and it is shown in Chapter 9 that the alternation in the sign of the b_n can be deduced from continuum-mechanical arguments. However, the inequalities above, suggested by several molecular theories, cannot be obtained from continuum mechanics.

[4] For a discussion of the Deborah number see §2.8.

TABLE 6.2-1

Constants in the Retarded-Motion Expansion (Eq. 6.2-1) from Kinetic-Theory Models (Made Dimensionless with a_i)[a]

Order k	Constants	FENE Dumbbells (Dilute Solution)[b]	Multibead Rods (Dilute Solution)[c]	Freely Jointed Bead-Rod Chain (Melt)[d]
		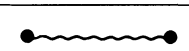	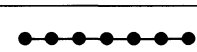	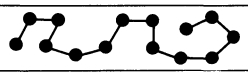
1	b_1/a_1	$\frac{\eta_s}{a_1} + \frac{b}{b+5}$	$\frac{\eta_s}{a_1} + \left[1 - \frac{2}{5}\left(1 - \frac{\lambda_N^{(2)}}{\lambda_N^{(1)}}\right)\right]$	$\frac{1}{60} + \frac{\varepsilon}{90}$
2	b_2/a_2	$-\frac{b^2}{(b+5)(b+7)}$	$-\frac{3}{5}$	$-\frac{1}{600}$
	b_{11}/a_2	0	$-\frac{12}{35}\left(1 - \frac{\lambda_N^{(2)}}{\lambda_N^{(1)}}\right)$	$-\frac{1}{1050} + \frac{\varepsilon}{1050}$
3	b_3/a_3	$\frac{b^3(2b+11)/(2b+7)}{(b+5)(b+7)(b+9)}$	$\frac{3}{5}$	$\frac{17}{100{,}800}$
	b_{12}/a_3	$\frac{4b^3/(2b+7)}{(b+5)(b+7)(b+9)}$	$\frac{12}{35}\left[1 - \frac{1}{2}\left(1 - \frac{\lambda_N^{(2)}}{\lambda_N^{(1)}}\right)\right]$	$\frac{17}{117{,}600} - \frac{17\varepsilon}{352{,}800}$
	$b_{1:11}/a_3$	$\frac{3b^3/(2b+7)}{(b+5)^2(b+7)(b+9)}$	$\frac{3}{35}\left[1 + \frac{6}{5}\left(1 - \frac{\lambda_N^{(2)}}{\lambda_N^{(1)}}\right)\right]$	$\frac{17}{705{,}600}$
	a_k	$nkT\lambda_H^k$	$nkT\lambda_N^{(1)k}$	$NnkT\lambda^k$

[a] The second-order fluid constants are related to the zero-shear-rate values of the viscometric functions as follows: $b_1 = \eta_0$; $b_2 = -\frac{1}{2}\Psi_{1,0}$; $b_{11} = \Psi_{2,0}$. In the molecular-theory formulas n is the number density of polymer molecules, k is the Boltzmann constant, T is the absolute temperature, and η_s is the solvent viscosity. The lambdas are all time constants; b and ε are dimensionless parameters.

[b] The constants for the FENE (Finitely Extensible Nonlinear Elastic) dumbbells with no hydrodynamic interaction were derived by R. C. Armstrong, *J. Chem. Phys.*, **60**, 724–728 (1974); the parameter b is found to be in the range of about 10 to 300, and $b = \infty$ corresponds to dumbbells with linear (Hookean) springs. See §13.5.

[c] The constants for the multibead rod with hydrodynamic interaction were obtained by X. J. Fan, using R. B. Bird and C. F. Curtiss, *J. Non-Newtonian Fluid Mech.*, **14**, 85–101 (1984). For osculating beads the quantity $[1 - (\lambda_N^{(2)}/\lambda_N^{(1)})]$ varies with the number of beads, N, from -0.5000 for $N = 2$ to -0.0284 for $N = 6$ and from $+0.0102$ for $N = 7$ to $+0.3082$ for $N = 70$. See also §§14.6 and 16.1–16.4.

[d] The constants for an undiluted system of interacting, freely jointed bead-rod chains are taken from C. F. Curtiss and R. B. Bird, *J. Chem. Phys.*, **74**, 2016–2025, 2026–2033 (1981). N is the number of beads in the chain, and ε is a parameter which is found to be in the range of 0.3 to 0.5 for some polymer melts. See also Chapter 19.

TABLE 6.2-2

Retarded-Motion Constants for Selected Empirical Constitutive Equations[a]

Order	Retarded-Motion Constants	Oldroyd Six-Constant[b] Model (Eq. 7.3-2)	Giesekus Model (Eq. 7.3-3)	Factorized K-BKZ Equation (Eq. 8.3-11)[c]	Factorized Rivlin-Sawyers Equation (Eq. 8.3-12)[c]
1	b_1	η_0	η_0	M_1	M_1
2	b_2	$-\eta_0(\lambda_1 - \lambda_2)$	$-\eta_0(\lambda_1 - \lambda_2)$	$-\frac{1}{2}M_2$	$-\frac{1}{2}M_2$
	b_{11}	$-\eta_0(\lambda_3 - \lambda_4)$	$-\alpha\eta_0(\lambda_1 - \lambda_2)$	$-W^{(01)}M_2$	$-\phi_2^{(00)}M_2$
3	b_3	$\eta_0\lambda_1(\lambda_1(\lambda_1 - \lambda_2)$	$\eta_0\lambda_1(\lambda_1 - \lambda_2)$	$\frac{1}{6}M_3$	$\frac{1}{6}M_3$
	b_{12}	$\eta_0[\lambda_1(\lambda_3 - \lambda_4) + \frac{1}{2}\lambda_3(\lambda_1 - \lambda_2)]$	$2\alpha\eta_0\lambda_1(\lambda_1 - \lambda_2)$	$\frac{1}{2}W^{(01)}M_3$	$\frac{1}{2}\phi_2^{(00)}M_3$
	$b_{1:11}$	$\frac{1}{2}\eta_0[(\lambda_1 + \lambda_3)(\lambda_3 - \lambda_4) - \lambda_5(\lambda_1 - \lambda_2 - \lambda_3 + \lambda_4)]$	$\alpha(\alpha + \frac{1}{2})\eta_0\lambda_1(\lambda_1 - \lambda_2)$	$\frac{1}{2}(W^{(01)} + W^{(20)} + 2W^{(11)} + W^{(02)}M_3)$	$\frac{1}{2}[\phi_2^{(00)} + \phi_1^{(10)} + (\phi_1^{(01)} + \phi_2^{(10)}) + \phi_2^{(10)}]$

[a] See Problems 7B.6 and 9B.8 for the method involved in obtaining these entries.

[b] λ_6 and λ_7 have been set equal to zero in Eq. 7.3-2.

[c] The $W^{(mn)}$ and $\phi_j^{(mn)}$ are defined in Eq. 8.3-17; the M_j are given in Eq. 8.2-12.

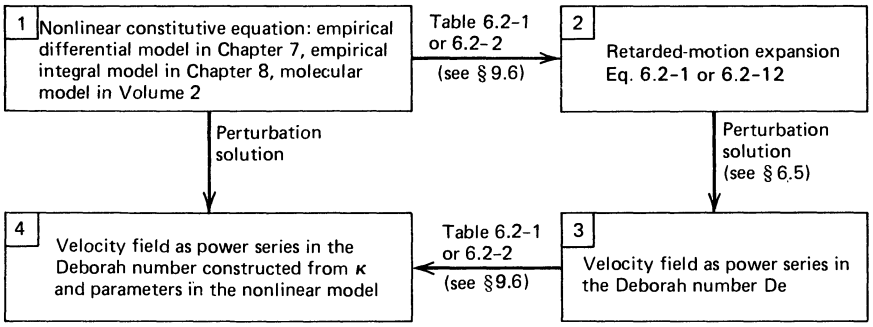

FIGURE 6.2-2. Use of the retarded-motion expansion to obtain perturbation solutions to flow problems for nonlinear constitutive equations.

In Chapters 7 and 8 a number of empirical nonlinear constitutive equations will be introduced. These empirical models will not have the restrictions inherent in the retarded-motion expansion, and are proposed with the hope of describing experimental data over a wider range of strain rates than is possible with the retarded-motion expansion. In the limit of small Deborah number, however, all these empirical models are equivalent[5] to a retarded-motion expansion with retarded-motion constants given in terms of the parameters of the empirical model. Values of such retarded-motion constants corresponding to a number of empirical constitutive equations are given in Table 6.2-2. Therefore any material function for a homogeneous flow field that has been calculated for the retarded-motion expansion may be immediately taken over for the empirical models in the limit of small Deborah number. For example, to obtain the lowest order terms in a power-series expansion of the viscometric functions of any of the nonlinear models in Table 6.2-2, all that is needed is to replace the retarded-motion constants in Eqs. 6.2-5 through 7 with the appropriate entries in Table 6.2-2. A more important application of Table 6.2-2, however, arises in connection with nonhomogeneous flow situations. In §6.5 it will be shown that the retarded-motion expansion is particularly well suited for developing perturbation solutions in which the velocity field is given as a power series in the Deborah number. Then Table 6.2-2 may be used to find the velocity field that would be obtained if the perturbation solution were performed with any of the empirical models in the table. This procedure, shown in the block diagram in Fig. 6.2-2, is important since the route from box 1 to box 4 via boxes 2 and 3 in the figure is usually both simpler and more systematic than the direct route from box 1 to box 4.

§6.3 USEFUL THEOREMS FOR THE SECOND-ORDER FLUID

In this section we consider three special theorems for the flow of second-order fluids: (a) the three-dimensional flow theorem of Giesekus, (b) the plane flow theorem of Tanner and Pipkin, and (c) the rectilinear flow theorem of Langlois, Rivlin, and Pipkin. These theorems are useful in reducing the total amount of work needed to obtain solutions of flow problems with the second-order fluid. The first two apply to creeping flow only.

We begin by giving the equations that one has to solve for an incompressible second-order fluid when the inertial terms can be neglected, (i.e., in the creeping-flow limit) or are

[5] K. Walters, *Z. Angew. Math. Phys.*, **21**, 592-600 (1970); see §9.6.

identically equal to zero. The incompressibility condition is Eq. 1.1-5, and the equation of motion is Eq. 1.1-8 with $\rho D\boldsymbol{v}/Dt = \boldsymbol{0}$. One then arrives at the following partial differential equations:

$$(\nabla \cdot \boldsymbol{v}) = 0 \tag{6.3-1}$$

$$[\nabla \cdot \{b_1\gamma_{(1)} + b_2\gamma_{(2)} + b_{11}\gamma_{(1)} \cdot \gamma_{(1)}\}] = \nabla\mathscr{P} \tag{6.3-2}$$

Here $\boldsymbol{\pi}$ in Eq. 1.1-8 has been decomposed into $\boldsymbol{\tau} + p\boldsymbol{\delta}$, and the dashed-underlined terms of Eq. 6.2-1 have been substituted for $\boldsymbol{\tau}$. In addition we have included the gravitational acceleration term in the modified pressure $\mathscr{P}$ so that $\nabla\mathscr{P} = \nabla p - \rho\boldsymbol{g}$.

In all three theorems it is assumed that we already know a solution for the creeping flow of an incompressible Newtonian fluid. That is, we know a velocity field $\boldsymbol{v}$ and a modified pressure field $\mathscr{P}_N$ that satisfy the boundary conditions, the incompressibility condition (Eq. 6.3-1), and the creeping-flow equation of motion:

$$[\nabla \cdot b_1\gamma_{(1)}] = b_1\nabla^2\boldsymbol{v} = \nabla\mathscr{P}_N \tag{6.3-3}$$

where b_1 is the viscosity. The modified pressure has the subscript "N" to indicate that it is associated with the first-order (i.e., Newtonian) fluid; the reason for doing this will be clear later.

For the Newtonian fluid it is possible to get a very useful expression involving the following combination of kinematic tensors:

$$\gamma_{(2)} + \{\gamma_{(1)} \cdot \gamma_{(1)}\} = \frac{D}{Dt}\gamma_{(1)} + \{(\nabla\boldsymbol{v}) \cdot (\nabla\boldsymbol{v})^\dagger - (\nabla\boldsymbol{v})^\dagger \cdot (\nabla\boldsymbol{v})\} \tag{6.3-4}$$

where the definition of $\gamma_{(n)}$ in Eq. 6.1-6 has been used, and the rate-of-strain tensor has been split into the sum of the velocity gradient and its transpose. Next we form the divergence of Eq. 6.3-4, and in so doing we make use of the fact that the velocity field satisfies the incompressibility relation, Eq. 6.3-1, to obtain

$$\begin{aligned}[\nabla \cdot \{\gamma_{(2)} + \gamma_{(1)} \cdot \gamma_{(1)}\}] &= \frac{D}{Dt}\nabla^2\boldsymbol{v} + [(\nabla\boldsymbol{v}) \cdot \nabla^2\boldsymbol{v}] + \frac{1}{2}\nabla((\nabla\boldsymbol{v}) : (\nabla\boldsymbol{v}) + (\nabla\boldsymbol{v}) : (\nabla\boldsymbol{v})^\dagger) \\ &= \frac{D}{Dt}\nabla^2\boldsymbol{v} + [(\nabla\boldsymbol{v}) \cdot \nabla^2\boldsymbol{v}] + \frac{1}{4}\nabla(\gamma_{(1)} : \gamma_{(1)})\end{aligned} \tag{6.3-5}$$

Up to this point we have used only definitions and the incompressibility condition for the velocity field. If we now make use of the assumption that $\boldsymbol{v}$ satisfies Eq. 6.3-3 we find the *Giesekus equation*:

$$[\nabla \cdot \{\gamma_{(2)} + \gamma_{(1)} \cdot \gamma_{(1)}\}] = \nabla\left[\frac{1}{b_1}\frac{D}{Dt}\mathscr{P}_N + \frac{1}{4}(\gamma_{(1)} : \gamma_{(1)})\right] \tag{6.3-6}$$

This equation will be used several times in the remainder of this section for obtaining the pressure field in simple flows of the second-order fluid, and again in §6.5 for simplifying the procedure for obtaining perturbation solutions for the retarded-motion expansion.

a. The Three-Dimensional Flow Theorem[1] of Giesekus

Consider a three-dimensional creeping flow for a second-order fluid which has the restriction that:

$$b_{11} = b_2 \tag{6.3-7}$$

Note that this corresponds to $-\Psi_{2,0}/\Psi_{1,0} = \frac{1}{2}$, and that experimental values of this ratio are generally $\frac{1}{4}$ or smaller.

If Eq. 6.3-6 is multiplied by b_2 and added to Eq. 6.3-3, the result takes precisely the form of Eq. 6.3-2, with $\mathscr{P}$ now given by

$$\mathscr{P} = \mathscr{P}_N + \frac{b_2}{b_1}\frac{D}{Dt}\mathscr{P}_N + \frac{b_2}{4}(\boldsymbol{\gamma}_{(1)}:\boldsymbol{\gamma}_{(1)}) \tag{6.3-8}$$

Keep in mind that by the definition of the modified pressure $\mathscr{P} - \mathscr{P}_N = p - p_N$, so that a formula explicit in p is

$$p = p_N + \frac{b_2}{b_1}\frac{D}{Dt}\mathscr{P}_N + \frac{b_2}{4}(\boldsymbol{\gamma}_{(1)}:\boldsymbol{\gamma}_{(1)}) \tag{6.3-9}$$

The $\mathscr{P}_N$ operated on by the substantial derivative may be replaced by p_N only if gravity is negligible. This gives rise to the following theorem which we shall refer to as the *three-dimensional flow theorem of Giesekus*:

> Given a velocity field $\boldsymbol{v}$ and a pressure field $\mathscr{P}_N$ that satisfy the equations for creeping flow of an incompressible Newtonian fluid, then the same velocity field $\boldsymbol{v}$ and the pressure field $\mathscr{P}$ given by Eq. 6.3-8 satisfy the equations for creeping flow of an incompressible second-order fluid with $b_{11} = b_2$.

Note that the next two theorems do *not* have the restriction $b_{11} = b_2$.

b. The Plane Flow Theorem[2] of Tanner and Pipkin

This theorem is limited to *plane flow* defined by

$$v_1 = v_1(x_1, x_2); \quad v_2 = v_2(x_1, x_2); \quad v_3 = 0 \tag{6.3-10}$$

in which the x_i are Cartesian coordinates. For this flow the rate-of-strain tensor may be

[1] The treatment here closely follows H. Giesekus, *Rheol. Acta*, **3**, 59–71 (1963); see "Anhang II," p. 70. The theorem has been rederived by Fosdick and Rajagopal, who in addition gave a condition for uniqueness of the velocity field in the second-order fluid [R. L. Fosdick and K. R. Rajagopal, *Int. J. Non-Linear Mech.*, **13**, 131–137 (1978)].

[2] This theorem was developed by R. I. Tanner and A. C. Pipkin, *Trans. Soc. Rheol.*, **13**, 471–484 (1969), and R. I. Tanner, *Phys. Fluids*, **9**, 1246–1247 (1968), who were apparently unaware of Giesekus' earlier work. A condition for uniqueness of the flow is given by R. R. Huilgol, *SIAM J. Appl. Math.*, **24**, 226–233 (1973).

represented in matrix form by

$$\boldsymbol{\gamma}_{(1)} = \begin{pmatrix} 2(\partial v_1/\partial x_1) & (\partial v_1/\partial x_2) + (\partial v_2/\partial x_1) & 0 \\ (\partial v_1/\partial x_2) + (\partial v_2/\partial x_1) & 2(\partial v_2/\partial x_2) & 0 \\ 0 & 0 & 0 \end{pmatrix} \tag{6.3-11}$$

If we take the dot product of this tensor with itself and use the incompressibility condition it follows that

$$[\nabla \cdot \{\boldsymbol{\gamma}_{(1)} \cdot \boldsymbol{\gamma}_{(1)}\}] = \tfrac{1}{2}\nabla(\boldsymbol{\gamma}_{(1)} : \boldsymbol{\gamma}_{(1)}) \tag{6.3-12}$$

This simple equation, along with the Giesekus equation (Eq. 6.3-6), is all that is needed to derive the plane flow theorem. Indeed if we multiply Eq. 6.3-12 by $(b_{11} - b_2)$, multiply Eq. 6.3-6 by b_2, and add both results to Eq. 6.3-3, the final equation takes the form of Eq. 6.3-2 with $\mathscr{P}$ now given by

$$\mathscr{P} = \mathscr{P}_N + \frac{b_2}{b_1}\frac{D}{Dt}\mathscr{P}_N + \left(\frac{b_{11}}{2} - \frac{b_2}{4}\right)(\boldsymbol{\gamma}_{(1)} : \boldsymbol{\gamma}_{(1)}) \tag{6.3-13}$$

Here again note that a formula explicit in p is obtained just by replacing the two $\mathscr{P}$'s on either side of the equality sign by p's. This then gives the *plane flow theorem of Tanner and Pipkin*:

> Given a plane velocity field $\boldsymbol{v}$ and a pressure field $\mathscr{P}_N$ that satisfy the equations for creeping plane flow of an incompressible Newtonian fluid, then the same velocity field and the pressure field $\mathscr{P}$ given by Eq. 6.3-13 satisfy the equations for creeping plane flow of an incompressible second-order fluid.

EXAMPLE 6.3-1 Force Exerted on a Solid Surface by a Second-Order Fluid in Steady Plane Flow

Use Eq. 6.3-13 to obtain an expression for the force per unit area exerted locally on an arbitrary, curved solid surface by an incompressible second-order fluid in steady plane flow.

SOLUTION With origin at the wall we introduce a local Cartesian coordinate system x_1, x_2, x_3 with $\boldsymbol{\delta}_1$ tangent to the wall and parallel to the direction of the fluid flow, $\boldsymbol{\delta}_2$ normal to the wall and pointing into the fluid, and $\boldsymbol{\delta}_3$ in the direction of no flow (see Fig. 6.3-1). In this coordinate system the velocity field is that of Eq. 6.3-10. In addition, we assume that the wall may slide relative to the axes in its own plane which means that at $x_2 = 0$ we have $v_2 = 0$ and $v_1 = \text{constant}$. It follows that $\partial v_2/\partial x_1 = 0$ and $\partial v_1/\partial x_1 = 0$ at the origin, and therefore on account of incompressibility we also have $\partial v_2/\partial x_2 = 0$ at the origin. The velocity gradient and the rate-of-strain tensors therefore take the following simple forms at $x_1 = 0$ and $x_2 = 0$:

$$\nabla \boldsymbol{v} = \begin{pmatrix} 0 & 0 & 0 \\ 1 & 0 & 0 \\ 0 & 0 & 0 \end{pmatrix} [\dot{\gamma}_{12}]_w; \quad \dot{\boldsymbol{\gamma}} = \begin{pmatrix} 0 & 1 & 0 \\ 1 & 0 & 0 \\ 0 & 0 & 0 \end{pmatrix} [\dot{\gamma}_{12}]_w \tag{6.3-14}$$

where $\dot{\gamma}_{12} = (\partial v_1/\partial x_2)$, and the subscript "$w$" on a bracket indicates that the quantity inside the bracket is to be evaluated "at the origin," that is, at $x_1 = 0$ and $x_2 = 0$. The quantity $[\dot{\gamma}_{12}]_w$ may be

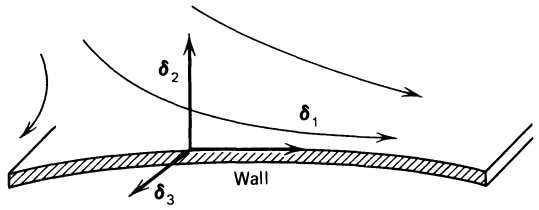

FIGURE 6.3-1. Steady plane flow of a second-order fluid near a curved wall. Unit vectors $\boldsymbol{\delta}_1, \boldsymbol{\delta}_2, \boldsymbol{\delta}_3$ define a local coordinate system with origin at the wall. At $x_2 = 0$, the velocity component $v_2 = 0$, but v_1 may be nonzero if the wall is moving.

either positive or negative, and its magnitude is equal to the shear rate at the wall. The second-order fluid pressure p given by Eq. 6.3-13 then becomes at the wall

$$p_w = \left[p_N + \frac{b_2}{b_1} v_1 \left(\frac{\partial \mathscr{P}_N}{\partial x_1} \right) + \left(b_{11} - \frac{b_2}{2} \right) \dot{\gamma}_{12}^2 \right]_w \tag{6.3-15}$$

Here we have also used the fact that $v_2 = 0$ at $x_2 = 0$. We now need to obtain the stress tensor components from the dashed-underlined terms in Eq. 6.2-1. When the expression is written out in matrix notation, and account is again taken of the simplifications at the origin of the coordinate system one obtains for the 22-component

$$[\tau_{22}]_w = -[b_{11}\dot{\gamma}_{12}^2]_w \tag{6.3-16}$$

Consequently we obtain the following expression for the total normal stress exerted by the second-order fluid on the wall

$$\begin{aligned} [-\pi_{22}]_w &= [-(p + \tau_{22})]_w \\ &= \left[-p_N - \frac{b_2}{b_1} v_1 \left(\frac{\partial \mathscr{P}_N}{\partial x_1} \right) + \frac{b_2}{2} \dot{\gamma}_{12}^2 \right]_w \end{aligned} \tag{6.3-17}$$

A similar development for the shear stress gives

$$[-\tau_{21}]_w = \left[b_1 \dot{\gamma}_{12} + b_2 v_1 \frac{\partial}{\partial x_1} \dot{\gamma}_{12} \right]_w \tag{6.3-18}$$

These results may be combined to give the following expression for the force per unit area exerted by the fluid on the wall (cf. Example 1.2-1)

$$\begin{aligned} [-\boldsymbol{\delta}_2 \cdot \boldsymbol{\pi}]_w = &\left[p_N + \tfrac{1}{2}\Psi_{1,0} \left(-\frac{1}{\eta_0} (\mathbf{v} \cdot \nabla \mathscr{P}_N) + \tfrac{1}{2}\dot{\gamma}_{12}^2 \right) \right]_w (-\boldsymbol{\delta}_2) \\ &+ [\eta_0 \dot{\gamma}_{12} - \tfrac{1}{2}\Psi_{1,0}(\mathbf{v} \cdot \nabla \dot{\gamma}_{12})]_w \boldsymbol{\delta}_1 \end{aligned} \tag{6.3-19}$$

where the magnitude of $[\dot{\gamma}_{12}]_w = [\partial v_1 / \partial x_2]_w$ is equal to the shear rate at the wall.

In connection with Eqs. 6.3-16 to 18 keep in mind that $\boldsymbol{\delta}_1$ must be in the direction of flow and $\boldsymbol{\delta}_2$ must be normal to the surface and pointing into the fluid. Each of these expressions may be used at several different locations; however, it is important that each set of local axes $\boldsymbol{\delta}_1, \boldsymbol{\delta}_2, \boldsymbol{\delta}_3$ have the same orientation with respect to the same global Cartesian coordinate system in which the flow is steady.

c. The Rectilinear Flow Theorem[3] of Langlois, Rivlin, and Pipkin

This theorem is limited to *rectilinear* flow defined by

$$v_1 = 0, \quad v_2 = 0, \quad v_3 = v_3(x_1, x_2) \tag{6.3-20}$$

in which the x_i are Cartesian coordinates. For rectilinear flow[4] it may be shown (Problem 6B.10) that if $\boldsymbol{v}$ satisfies Eq. 6.3-3 and if the pressure gradient $\nabla \mathscr{P}_N$ does not change in the direction of flow, then,

$$[\nabla \cdot \{\boldsymbol{\gamma}_{(1)} \cdot \boldsymbol{\gamma}_{(1)}\}] = \nabla\left(\frac{1}{b_1}(\boldsymbol{v} \cdot \nabla \mathscr{P}_N) + \tfrac{1}{2}((\nabla \boldsymbol{v}) : (\nabla \boldsymbol{v})^\dagger)\right) \tag{6.3-21}$$

This equation along with the Giesekus equation may now be used to derive the rectilinear flow theorem in a manner analogous to the derivation of the plane flow theorem. This time we multiply Eq. 6.3-21 by $(b_{11} - b_2)$, multiply Eq. 6.3-6 by b_2, and add the results to Eq. 6.3-3. Then the result may be written in the form of Eq. 6.3-2, with $\mathscr{P}$ now given by

$$\mathscr{P} = \mathscr{P}_N + \frac{b_2}{b_1}\frac{\partial}{\partial t}\mathscr{P}_N + \frac{b_{11}}{b_1}(\boldsymbol{v} \cdot \nabla \mathscr{P}_N) + \frac{b_2}{4}(\dot{\boldsymbol{\gamma}} : \dot{\boldsymbol{\gamma}}) + \frac{(b_{11} - b_2)}{2}((\nabla \boldsymbol{v}) : (\nabla \boldsymbol{v})^\dagger) \tag{6.3-22}$$

This gives rise to the *rectilinear flow theorem of Langlois, Rivlin, and Pipkin*:

> Given a rectilinear velocity field $\boldsymbol{v}$ and a pressure field $\mathscr{P}_N$ that satisfy the equation of motion for a Newtonian fluid and such that $\nabla \mathscr{P}_N$ does not change with distance in the flow direction, then the same velocity field and the pressure field $\mathscr{P}$ given by Eq. 6.3-22 satisfy the equations of continuity and motion for an incompressible second-order fluid.

Notice that the definition of rectilinear flow implies that the continuity equation is automatically satisfied and also that inertial terms do not enter into the equation of motion. This theorem, unlike the two preceding theorems, is not limited to creeping flow.

EXAMPLE 6.3-2 Force Exerted on a Solid Surface by a Second-Order Fluid in Steady Rectilinear Flow

Use Eq. 6.3-22 to obtain an expression for the total force per unit area exerted locally on a solid surface by an incompressible second-order fluid in steady rectilinear flow.

SOLUTION Arrange the coordinate system x_1, x_2, x_3 with origin at the wall and with $\boldsymbol{\delta}_1$ tangent to the wall, $\boldsymbol{\delta}_2$ locally normal to the wall and pointing into the fluid, and $\boldsymbol{\delta}_3$ tangent to the wall

[3] W. E. Langlois and R. S. Rivlin, *Rend. Mat.*, **22**, 169–185 (1963); A. C. Pipkin and R. S. Rivlin, *Z. Angew. Math. Phys.*, **14**, 738–742 (1963). See also E. A. Kearsley, *Trans. Soc. Rheol.*, **14**, 419–424 (1970); A. C. Pipkin, *Lectures on Viscoelasticity Theory*, Springer Verlag, Berlin (1972), Chapt. VIII, Sec. 11.

[4] Note that rectilinear flow is possible for Newtonian, second-order, and third-order fluids, but not in general for higher-order fluids (see Fig. 6.6-1).

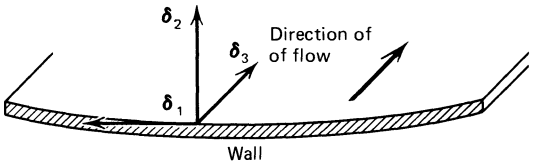

FIGURE 6.3-2. Steady rectilinear flow of a second-order fluid along a solid surface. Unit vectors $\boldsymbol{\delta}_1$ $\boldsymbol{\delta}_2$, $\boldsymbol{\delta}_3$ define a local coordinate system with origin at the wall. At $x_2 = 0$ the velocity component v_3 may be nonzero if the wall is moving, but $\partial v_3/\partial x_1$ and $\partial v_3/\partial x_3$ are zero.

and in the direction of flow (see Fig. 6.3-2). The velocity gradient and the rate-of-strain tensors become:

$$\nabla \boldsymbol{v} = \begin{pmatrix} 0 & 0 & \partial v_3/\partial x_1 \\ 0 & 0 & \partial v_3/\partial x_2 \\ 0 & 0 & 0 \end{pmatrix}; \quad \dot{\boldsymbol{\gamma}} = \begin{pmatrix} 0 & 0 & \partial v_3/\partial x_1 \\ 0 & 0 & \partial v_3/\partial x_2 \\ \partial v_3/\partial x_1 & \partial v_3/\partial x_2 & 0 \end{pmatrix} \tag{6.3-23}$$

By writing out all terms in Eq. 6.3-22 for steady flow one obtains

$$p = p_N + \frac{b_{11}}{b_1} v_3 \frac{\partial}{\partial x_3} \mathscr{P}_N + \frac{b_{11}}{2} \left[\left(\frac{\partial v_3}{\partial x_1} \right)^2 + \left(\frac{\partial v_3}{\partial x_2} \right)^2 \right] \tag{6.3-24}$$

This expression can then be simplified further at $x_2 = 0$ by noting that $\partial v_3/\partial x_1 = 0$ at the wall.

Similarly the expression for the stress tensor, the dotted-underlined terms in Eq. 6.2-1, may be written out in matrix form based on the velocity gradient in Eq. 6.3-23. When account is again taken of the fact that $\partial v_3/\partial x_1 = 0$ at the wall one obtains for τ_{22} at the wall,

$$[\tau_{22}]_w = -b_{11}[\dot{\gamma}_{23}^2]_w \tag{6.3-25}$$

Here $\dot{\gamma}_{23} = (\partial v_3/\partial x_2)$, and the subscript "$w$" on a bracket indicates that the quantity inside the bracket is to be evaluated "at the wall," that is, at $x_2 = 0$. Consequently we obtain the following simple expression for the total normal stress exerted by the fluid on the wall:

$$[\pi_{22}]_w = \left[p_N + \frac{b_{11}}{b_1} v_3 \frac{\partial}{\partial x_3} \mathscr{P}_N - \frac{b_{11}}{2} \dot{\gamma}_{23}^2 \right]_w \tag{6.3-26}$$

Similarly we find also the only non-zero shear stress component, which is identical to that for a Newtonian fluid:

$$[\tau_{23}]_w = -b_1[\dot{\gamma}_{23}]_w \tag{6.3-27}$$

Finally a compact expression for the force per unit area exerted by the fluid on the solid wall is

$$[-\boldsymbol{\delta}_2 \cdot \boldsymbol{\pi}]_w = \left[p_N - \Psi_{2,0} \left(\left(-\frac{v_3}{\eta_0} \frac{\partial \mathscr{P}_N}{\partial x_3} \right) + \tfrac{1}{2} \dot{\gamma}_{23}^2 \right) \right]_w (-\boldsymbol{\delta}_2) + [\eta_0 \dot{\gamma}_{23}]_w \boldsymbol{\delta}_3 \tag{6.3-28}$$

where the magnitude of $[\dot{\gamma}_{23}]_w = [\partial v_3/\partial x_2]_w$ is equal to the shear rate at the wall.

Notice that the first normal stress coefficient does not enter in the resultant normal force. In addition keep in mind that all available data show that $\Psi_{2,0}$ is negative or zero (Chapter 3).

§6.4 TWO-DIMENSIONAL AND RECTILINEAR FLOW PROBLEMS FOR THE SECOND-ORDER FLUID

In this section we turn to the application of the two-dimensional flow theorem and the rectilinear flow theorem, derived in the previous section. These theorems state that for two-dimensional creeping flows and rectilinear flows the velocity field for creeping motion of an incompressible Newtonian fluid will also be possible for a second-order fluid. This means that there is *no secondary motion due to fluid elasticity* in the examples considered here. The stresses and pressures are not, however, the same as in a Newtonian fluid, and therefore *the forces exerted on the boundaries are influenced by fluid elasticity*. Both examples considered in this section are concerned with investigations of such extra forces due to fluid elasticity. The reader may find that even though the derivations of the theorems were a bit tedious, their application to problem solving is straightforward.

EXAMPLE 6.4-1 Axial Eccentric Annular Flow[1]

Here we consider the axial motion of a second-order fluid in an eccentric annular region; a rod moves with speed V inside a circular cylindrical cavity as shown in Fig. 6.4-1. The rod has radius R_1,

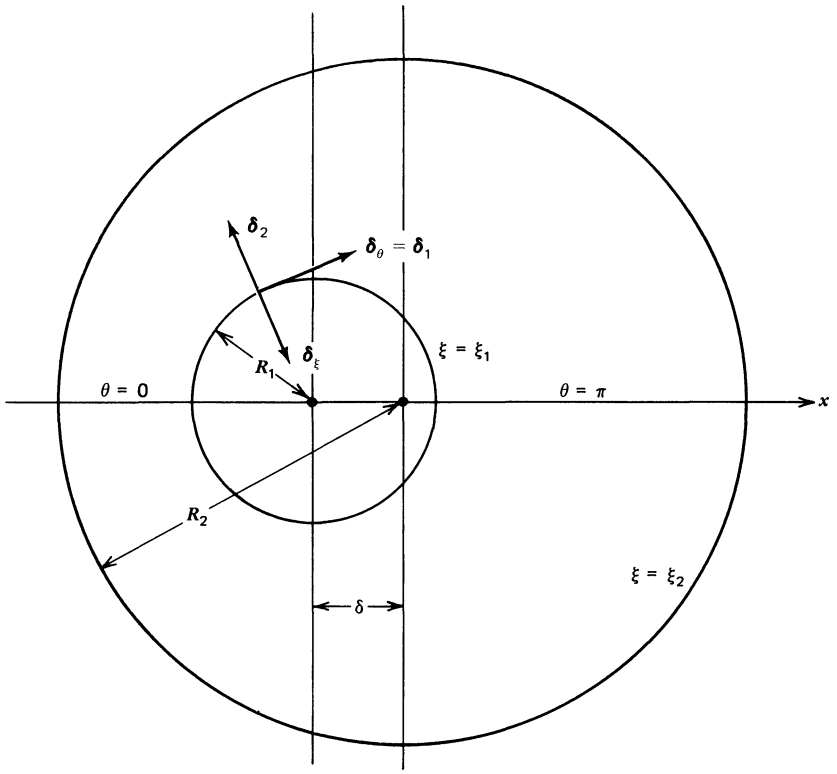

FIGURE 6.4-1. An off-centered circular rod of radius R_1 moving axially with speed V in a cylindrical cavity of radius R_2 filled with a viscoelastic coating material. The coordinates ξ and θ are coordinates in the bipolar coordinate system (see Fig. A.7-1).

[1] This problem was solved for an Oldroyd model by J. R. Jones, *J. Méch.*, **3**, 79–99 (1964); **4**, 121–132 (1965). For an alternative treatment based on the CEF equation of §9.6 see Z. Tadmor and R. B. Bird, *Polym. Eng. Sci.*, **14**, 124–136 (1974); see also Example 4.3-2.

and the radius of the cavity is R_2. The rod axis and cavity axis are not coincident, but separated by a distance δ. Because of the eccentric arrangement, the flow is most easily described in terms of bipolar coordinates (see Fig. A.7-1). It is desired to find the lateral force acting by the second-order fluid on the off-centered cylindrical rod.

This arrangement is of interest in connection with the stabilizing forces acting on an off-center wire in a wire-coating operation, where speeds of up to 25 m/s are encountered. Since wire-coating materials in their molten form are usually viscoelastic liquids, it is important to know whether the normal stresses in these liquids will help or hinder in the stabilizing of the wire-coating operation. Therefore it is of interest to find out if there is a force on an off-center cylinder that tends to push the cylinder toward the center of the cavity or in the opposite direction.

SOLUTION We anticipate that the flow will be a rectilinear flow, which in bipolar coordinates means that we look for a solution of the form

$$v_\xi = 0, \quad v_\theta = 0, \quad v_z = v_z(\xi, \theta) \tag{6.4-1}$$

We further imagine that $p = p(\xi, \theta)$ so that $\partial p/\partial z = 0$. The situation with a constant pressure gradient in the z-direction still results in a rectilinear flow. The equations of motion of a Newtonian fluid are

$$0 = \frac{X}{a}\frac{\partial p_N}{\partial \xi} \tag{6.4-2}$$

$$0 = \frac{X}{a}\frac{\partial p_N}{\partial \theta} \tag{6.4-3}$$

$$\left(\frac{X}{a}\right)^2 \frac{\partial^2 v_z}{\partial \xi^2} + \left(\frac{X}{a}\right)^2 \frac{\partial^2 v_z}{\partial \theta^2} = 0 \tag{6.4-4}$$

in which $X = \cosh \xi + \cos \theta$, and a is defined in Fig. A.7-1. Equations 6.4-2 through 4 are to be solved with the boundary conditions

$$v_z(\xi, \theta) = V, \qquad at \quad \xi = \xi_1, \qquad \text{for all } \theta \tag{6.4-5}$$

$$v_z(\xi, \theta) = 0, \qquad \text{at} \quad \xi = \xi_2, \qquad \text{for all } \theta \tag{6.4-6}$$

$$v_z(\xi, \theta) = v_z(\xi, \theta + 2\pi), \qquad \text{for all } \xi, \theta \tag{6.4-7}$$

The boundary conditions suggest that we look for a solution independent of θ, and we find then the Newtonian solution

$$\frac{v_z}{V} = \frac{\xi - \xi_2}{\xi_1 - \xi_2} \tag{6.4-8}$$

and

$$p_N = p_0 \tag{6.4-9}$$

where p_0 is a constant. This constant hydrostatic pressure does not produce any net lateral force on the inner cylinder.

Now that we have solved the Newtonian flow problem, we may use the rectilinear flow theorem of Langlois, Rivlin, and Pipkin to conclude that for the second-order fluid the velocity field is still given by Eq. 6.4-8 with the pressure field given by Eq. 6.3-22. Our interest is, however, not in

the complete pressure field but only in the lateral force exerted on the moving cylinder, given by Eq. 6.3-28. In order to use this equation we need to "translate" it from the local rectangular coordinate system to the bipolar coordinate system used here. Since the bipolar coordinate system is an orthogonal coordinate system, and since $\boldsymbol{\delta}_\xi$ points into the inner cylinder and $\boldsymbol{\delta}_z$ is in the direction of flow we see that $\boldsymbol{\delta}_2 = -\boldsymbol{\delta}_\xi$ and $\boldsymbol{\delta}_3 = \boldsymbol{\delta}_z$. In addition we calculate the rate-of-strain tensor as follows:

$$\dot{\boldsymbol{\gamma}} = \dot{\gamma}_{\xi z}(\boldsymbol{\delta}_\xi\boldsymbol{\delta}_z + \boldsymbol{\delta}_z\boldsymbol{\delta}_\xi) = \dot{\gamma}_{23}(\boldsymbol{\delta}_2\boldsymbol{\delta}_3 + \boldsymbol{\delta}_3\boldsymbol{\delta}_2) \tag{6.4-10}$$

where $\dot{\gamma}_{\xi z}$ can be obtained from Eq. U of Table A.7-4:

$$\dot{\gamma}_{\xi z} = \frac{X}{a}\frac{\partial v_z}{\partial \xi} = \frac{XV}{a(\xi_2 - \xi_1)} \tag{6.4-11}$$

With the above relations between the unit base vectors we see that $\dot{\gamma}_{23} = -\dot{\gamma}_{\xi z}$, and therefore that Eq. 6.3-28 in the bipolar coordinate system reads

$$\boldsymbol{\pi}_\xi|_{\xi=\xi_1} = [\boldsymbol{\delta}_\xi \cdot \boldsymbol{\pi}]_{\xi=\xi_1} = [p_0 - \Psi_{2,0}\tfrac{1}{2}(-\dot{\gamma}_{\xi z})^2]_{\xi=\xi_1}\boldsymbol{\delta}_\xi + [\eta_0(-\dot{\gamma}_{\xi z})]_{\xi=\xi_1}\boldsymbol{\delta}_z \tag{6.4-12}$$

To get the lateral component of the net transmitted force we form the dot product with $\boldsymbol{\delta}_x$:

$$(\boldsymbol{\delta}_x \cdot \boldsymbol{\pi}_\xi)_{\xi=\xi_1} = \left[(p_0 - \tfrac{1}{2}\Psi_{2,0}\dot{\gamma}_{\xi z}^2)\frac{1 + \cosh\xi\cos\theta}{X(\xi,\theta)}\right]_{\xi=\xi_1} \tag{6.4-13}$$

where we have used the result for $(\boldsymbol{\delta}_\xi \cdot \boldsymbol{\delta}_x)$, which can be obtained from §A.7 (see Eq. A.7-11 and Exercise 5). The net force exerted in the x-direction on a length L of the cylinder, F_x, is then

$$\begin{aligned} F_x &= \int_S (\boldsymbol{\delta}_x \cdot \boldsymbol{\pi}_\xi)_{\xi=\xi_1}\, dS \\ &= \int_0^L \int_0^{2\pi} (\boldsymbol{\delta}_x \cdot \boldsymbol{\pi}_\xi)_{\xi=\xi_1} \frac{a}{X(\xi_1,\theta)}\, d\theta\, dz \end{aligned} \tag{6.4-14}$$

where we have used the fact that the element of area of a surface ξ = constant in bipolar coordinates is $(a/X)\, d\theta\, dz$. We now substitute $(\boldsymbol{\delta}_x \cdot \boldsymbol{\pi}_\xi)$ from Eq. 6.4-13 into Eq. 6.4-14 to find

$$F_x = La\int_0^{2\pi}\left[\frac{p_0}{X^2(\xi_1,\theta)} - \frac{\Psi_{2,0}V^2}{2a^2(\xi_1 - \xi_2)^2}\right](1 + \cosh\xi_1\cos\theta)\, d\theta \tag{6.4-15}$$

It is now a bit tedious to show that the contribution from the p_0 term is zero as expected. To do this one makes use of the integrals in part (c) of Problem 1C.4. It is considerably easier to find the contribution from the $\Psi_{2,0}$ term to get, finally,

$$F_x = -\Psi_{2,0}\frac{\pi V^2}{a(\xi_1 - \xi_2)^2}L \tag{6.4-16}$$

where $a(R_1, R_2, \delta)$ is given in the caption of Fig. A.7-1. We see that if the second normal stress coefficient $\Psi_{2,0}$ is negative, the force F_x will be positive and the wire self-centering.

The use of the second-order fluid as the constitutive equation means that the analysis is limited to small Deborah number. This means that $\mathrm{De}(b_{11}/b_2) = -\Psi_{2,0}\dot{\gamma}/\eta_0 \ll 1$ where $\dot{\gamma}$ is a typical shear rate in the annular region. If $\mathrm{De}(b_{11}/b_2) \geq 1$ there will in addition to the axial velocity component be a secondary tangential velocity component. Tadmor and Bird[1] have made an analysis based on the CEF equation of §9.6 and the assumption that the secondary flow is negligible. Their

result for F_x is identical to Eq. 6.4-16 but with $\Psi_{2,0}$ replaced by $\Psi_2(\dot{\gamma})$, where $\dot{\gamma}$ is the shear rate in the annular region.

Many other physical phenomena may be important in wire coating, such as (a) phenomena associated with the wetting of the wire by the polymer, for instance entrainment of gas bubbles; and (b) phenomena associated with unsteady flow that could result from high coating speeds for which the flow is inherently unstable, or for which the lateral vibrations of the wire are significant.

EXAMPLE 6.4-2 Tangential Eccentric Annular Flow (Journal-Bearing Flow)[2]

In Problem 1C.4 the flow of a Newtonian fluid in a simplified journal-bearing system is discussed. Rework the same problem for the second-order fluid in order to assess the role of the normal stresses.

SOLUTION This is an example of a plane flow, and we may then use the plane flow theorem of Tanner and Pipkin to conclude that the flow field in the second-order fluid is the same as that found in Problem 1C.4 for the Newtonian fluid, and that the pressure field is given by Eq. 6.3-13. Again our interest is just in the forces exerted on the inner cylinder given by Eq. 6.3-19. In the use of this equation we may identify $\boldsymbol{\delta}_1$ with $\boldsymbol{\delta}_X$ and $\boldsymbol{\delta}_2$ with $\boldsymbol{\delta}_Y$ of Fig. 1C.4. Equation 6.3-19 then gives the following expression for the local force per unit area exerted by the fluid on the inner cylinder $\boldsymbol{\pi}_{-Y} = [-\boldsymbol{\delta}_Y \cdot \boldsymbol{\pi}]_w$:

$$\boldsymbol{\pi}_{-Y} = \left[p_N + \tfrac{1}{2}\Psi_{1,0}\left(-\frac{1}{\eta_0} W_1 r_1 \frac{d}{dX} p_N + \frac{1}{2}\left(\frac{\partial v_X}{\partial Y}\right)^2 \right) \right]_w (-\boldsymbol{\delta}_Y) + \left[\eta_0 \left(\frac{\partial v_X}{\partial Y}\right) - \tfrac{1}{2}\Psi_{1,0} W_1 r_1 \frac{\partial}{\partial X}\left(\frac{\partial v_X}{\partial Y}\right) \right]_w \boldsymbol{\delta}_X \tag{6.4-17}$$

where p_N, dp_N/dX, and $\partial v_X/\partial Y$ are given in Eqs. 1C.4-21, 1C.4-3, and 1C.4-5. When these expressions are used in Eq. 6.4-17 we may write the result in the notation of Problem 1C.4 as

$$\boldsymbol{\pi}_{-Y} = -\pi_{YX}\boldsymbol{\delta}_X - \pi_{YY}\boldsymbol{\delta}_Y \tag{6.4-18}$$

where

$$\pi_{YX} = \left[\eta_0 W_1 r_1 \left(\frac{4}{B} - \frac{3B_0}{B^2}\right) - \tfrac{1}{2}\Psi_{1,0} W_1^2 r_1 \frac{d}{d\theta}\left(\frac{4}{B} - \frac{3B_0}{B^2}\right) \right]_w \tag{6.4-19}$$

$$\pi_{YY} = \left[p_N + \tfrac{1}{2}\Psi_{1,0} W_1^2 r_1^2 \left(\frac{1}{B} - \frac{3B_0}{B^2}\right) \right]_w \tag{6.4-20}$$

and B_0 is defined below Eq. 1C.4-2.

Equations 6.4-18 to 20 are the result of the application of the Tanner–Pipkin theorem locally. The force expression may now be regarded as a function of θ to find the total torque and force on the inner cylinder. The developments given below are straightforward but somewhat tedious. They involve the use of the integrals in part **(c)** of Problem 1C.4.

[2] This example is based on the publication of J. M. Davies and K. Walters, *Rheology of Lubricants*, Elsevier Applied Science, London (1973). In this paper results are also given for the third-order fluid and for the Oldroyd model. See also R. I. Tanner, *Aust. J. Appl. Sci.*, **14**, 129–136 (1963); A. B. Metzner, *Rheol. Acta*, **10**, 434–444 (1971); R. I. Tanner, *Engineering Rheology*, Oxford University Press (1985), §6.3; and Example 7.5-1.

We now calculate the torque $\mathscr{T}$ on the inner cylinder which is defined to be positive in the direction of increasing θ:

$$\begin{aligned}\mathscr{T} &= L\int_0^{2\pi}(\boldsymbol{\delta}_X\cdot\boldsymbol{\pi}_{-Y})r_1^2\,d\theta\\ &= -L\int_0^{2\pi}\pi_{YX}r_1^2\,d\theta\\ &= -\frac{2\pi\eta_0 LW_1r_1^3(c^2+2a^2)}{\sqrt{c^2-a^2}\,(c^2+\frac{1}{2}a^2)}\end{aligned}\tag{6.4-21}$$

Notice that the term involving $\Psi_{1,0}$ vanishes when the integration is performed. Hence the expression for the torque is the same found for a Newtonian fluid.

The force in the y-direction is defined by

$$\begin{aligned}F_y &= L\int_0^{2\pi}(\boldsymbol{\delta}_y\cdot\boldsymbol{\pi}_{-Y})r_1\,d\theta = -L\int_0^{2\pi}(\pi_{YX}\cos\theta+\pi_{YY}\sin\theta)r_1\,d\theta\\ &= L\eta_0W_1r_1^3\int_0^{2\pi}\left[\frac{1}{r_1}\left(-\frac{4}{B}+\frac{6B_0}{B^2}\right)-\underline{6\left(\frac{1}{B^2}-\frac{B_0}{B^3}\right)}\right]\cos\theta\,d\theta\\ &\doteq -\frac{6\pi\eta_0LW_1r_1^3a}{\sqrt{c^2-a^2}\,(c^2+\frac{1}{2}a^2)}\end{aligned}\tag{6.4-22}$$

In going from the first to the second line of this equation, products that are odd on the interval $[0, 2\pi]$—and therefore vanish in the integration—have been omitted. In addition the term involving p_N has been integrated by parts, for simplicity. In going from the second to the third line, only the dashed underlined term has been retained since it will be the leading term for small eccentricities.

The force in the x-direction is given by

$$\begin{aligned}F_x &= L\int_0^{2\pi}(\boldsymbol{\delta}_x\cdot\boldsymbol{\pi}_{-Y})r_1\,d\theta = L\int_0^{2\pi}(\sin\theta\,\pi_{YX}-\cos\theta\,\pi_{YY})r_1\,d\theta\\ &\doteq -L\Psi_{1,0}W_1^2r_1^3\int_0^{2\pi}\left(\frac{1}{B}-\frac{3B_0}{B^2}\right)^2\cos\theta\,d\theta\\ &= \frac{2\pi\Psi_{1,0}LW_1^2r_1^3a(c^4-\frac{1}{8}a^2c^2+\frac{1}{4}a^4)}{(c^2-a^2)^{3/2}(c^2+\frac{1}{2}a^2)^2}\end{aligned}\tag{6.4-23}$$

Here again, in going from the first to the second line terms that are odd on the interval $[0, 2\pi]$ have been omitted. As before, only the leading term in the eccentricity has been retained.

The results of this example show that the magnitude of the force $F = (F_x^2 + F_y^2)^{1/2}$ for the second-order fluid is greater than the resultant force for the corresponding Newtonian fluid. This has been interpreted by Davies and Walters[2] to mean that lubricants with polymeric additives will support greater loads and therefore result in reduced wear. Keep in mind that this conclusion can be challenged, inasmuch as the analysis was done for a second-order fluid and is hence restricted to small values of $\mathrm{De} = \Psi_{10}W_1r_1/2\eta_0B_0$; furthermore viscous heating effects and "shear thinning" of the viscosity may be far more imporant than the normal stress effects.

§6.5 PERTURBATION TECHNIQUE FOR CREEPING FLOWS

The governing partial differential equations for the flow of fluids described by the retarded-motion expansion are nonlinear in the velocity field. This may be seen specifically for the second-order fluid from Eqs. 6.3-1 and 2. In the previous two sections we presented some techniques that may be used for constructing exact analytical flow solutions for second-order fluids for certain special classes of flows. For most problems we cannot find exact analytical solutions, so we turn in this section to a perturbation technique that can be used to develop solutions to flow problems for the retarded-motion expansion for small Deborah numbers. Inasmuch as the retarded-motion expansion is itself restricted to small De, no significant new limitations are imposed by the use of the perturbation procedure.

To introduce the technique we use the Deborah number $\mathrm{De} = -(b_2/b_1)\kappa = (\Psi_{1,0}/2\eta_0)\kappa$ introduced in connection with Eq. 6.2-12. Recall that κ is a characteristic strain rate in the flow, and that the Deborah number is a dimensionless strain rate that determines the importance of the various nonlinear terms in the retarded-motion expansion. Since the retarded-motion expansion is designed specifically to describe fluids in the limit of small Deborah number, it seems natural to expand the velocity and pressure fields for creeping motion as follows:

$$\boldsymbol{v} = \boldsymbol{v}_0 + \mathrm{De}\,\boldsymbol{v}_1 + \cdots \quad \text{or} \quad \boldsymbol{v}^* = \boldsymbol{v}_0^* + \mathrm{De}\,\boldsymbol{v}_1^* + \cdots \tag{6.5-1}$$

$$p = p_0 + \mathrm{De}\,p_1 + \cdots \quad \text{or} \quad p^* = p_0^* + \mathrm{De}\,p_1^* + \cdots \tag{6.5-2}$$

in which $\boldsymbol{v}^* = \boldsymbol{v}/V$ and $p^* = p/b_1\kappa$; here V is a characteristic velocity for the flow system. For illustrative purposes the expansion is carried only to first order in De here, but the technique may in principle be extended to any order. We then insert the expansion in Eq. 6.5-1 into Eq. 6.2-12 for the stress tensor, which gives

$$\begin{aligned}\boldsymbol{\tau}^* = &-[\boldsymbol{\gamma}^*_{(1)0} + \mathrm{De}\,\boldsymbol{\gamma}^*_{(1)1} - \cdots] \\ &+ \mathrm{De}\,[\boldsymbol{\gamma}^*_{(2)0} + \cdots] \\ &+ \mathrm{De}\,B_{11}[\{\boldsymbol{\gamma}^*_{(1)0}\cdot\boldsymbol{\gamma}^*_{(1)0}\} + \cdots]\end{aligned} \tag{6.5-3}$$

in which $\boldsymbol{\gamma}^*_{(n)k} = \boldsymbol{\gamma}_{(n)k}/\kappa^n$, where $\boldsymbol{\gamma}_{(n)k}$ is the nth rate-of-strain tensor evaluated using $\boldsymbol{v}_k$ of Eq. 6.5-1.

Next we have to write the equations of continuity and motion in dimensionless form. The expression for $\boldsymbol{v}^*$ in Eq. 6.5-1 must be inserted into the equation $(\nabla\cdot\boldsymbol{v}) = 0$ in appropriate dimensionless form; and the above expression for $\boldsymbol{\tau}^*$ must be substituted into the equation of motion for creeping flow, which in dimensionless form is

$$\mathbf{0} = -\nabla^* p^* - [\nabla^*\cdot\boldsymbol{\tau}^*] + \boldsymbol{g}^* \tag{6.5-4}$$

in which $\nabla^* = (V/\kappa)\nabla$ and $\boldsymbol{g}^* = (V/b_1\kappa^2)\rho\boldsymbol{g}$. These substitutions lead to sets of equations of change obtained by equating the coefficients of De^0, De^1, De^2, and so on:

Zero Order:

$$(\nabla^*\cdot\boldsymbol{v}_0^*) = 0 \tag{6.5-5}$$

$$\nabla^{*2}\boldsymbol{v}_0^* - \nabla^*\mathscr{P}_0^* = 0 \tag{6.5-6}$$

First Order:

$$(\nabla^*\cdot\boldsymbol{v}_1^*) = 0 \tag{6.5-7}$$

$$\nabla^{*2}\boldsymbol{v}_1^* - \nabla^* p_1^* = [\nabla^*\cdot\boldsymbol{\gamma}^*_{(2)0}] + B_{11}[\nabla^*\cdot\boldsymbol{\gamma}^{*2}_{(1)0}] \tag{6.5-8}$$

in which $B_{11} = b_{11}/b_2$ and $\mathscr{P}^* = \mathscr{P}/b_1\kappa$. Second- and higher-order sets of equations can be written down by the same procedure. Each set has the same form, but the equation of motion for $\boldsymbol{v}_k^*$ (with $k \geq 1$) has nonhomogeneous terms on the right side, and these are known from the solution of the $(k-1)$th-order problem. The right side of Eq. 6.5-8 can be put into an alternative form by using the Giesekus equation, Eq. 6.3-6:

$$[\nabla^* \cdot \gamma^*_{(2)0} + B_{11}\nabla^* \cdot \gamma^{*2}_{(1)0}] = \nabla^*\left(\frac{D}{Dt^*}\mathscr{P}^*_0 + \tfrac{1}{4}\gamma^*_{(1)0} : \gamma^*_{(1)0}\right) + (B_{11} - 1)[\nabla^* \cdot \gamma^{*2}_{(1)0}] \tag{6.5-9}$$

The velocity field that enters into the substantial derivative D/Dt^* is $\boldsymbol{v}_0^*$, and $D/Dt^* = (D/Dt)/\kappa$.

It is now possible to put Eq. 6.5-8 into a slightly different form,

$$\nabla^{*2}\boldsymbol{v}_1^* - \nabla^*\tilde{p}_1^* + \boldsymbol{f}^* = \boldsymbol{0} \tag{6.5-10}$$

in which $\boldsymbol{f}^* = (V/b_1\kappa^2)\boldsymbol{f}$ (see Table 1.4-1) is given by

$$\boldsymbol{f}^* = (1 - B_{11})(\nabla^* \cdot \gamma^{*2}_{(1)0}) \tag{6.5-11}$$

and

$$\tilde{p}_1^* = p_1^* - \frac{D}{Dt^*}\mathscr{P}^*_0 - \tfrac{1}{4}(\gamma^*_{(1)0} : \gamma^*_{(1)0}) \tag{6.5-12}$$

Then Eq. 6.5-7 (continuity) and Eq. 6.5-10 (motion) are solved to get $\boldsymbol{v}_1^*$ and $\tilde{p}_1^*$, so that the final expressions for $\boldsymbol{v}^*$ and $\mathscr{P}^*$ become

$$\boldsymbol{v}^* = \boldsymbol{v}_0^* + \mathrm{De}\,\boldsymbol{v}_1^* + \cdots \tag{6.5-13}$$

$$\mathscr{P}^* = \mathscr{P}^*_0 + \mathrm{De}\left[\tilde{p}_1^* + \frac{D}{Dt^*}\mathscr{P}^*_0 + \tfrac{1}{4}(\gamma^*_{(1)0} : \gamma^*_{(1)0})\right] + \cdots \tag{6.5-14}$$

The zero-order functions $\boldsymbol{v}_0^*$ and p_0^* must satisfy the physical boundary conditions prescribed for the given problem. The perturbation fields $\boldsymbol{v}_k^*$ and p_k^* $(k \geq 1)$ must be subject to boundary conditions such that the functions $\boldsymbol{v}$ and p satisfy the boundary conditions of the stated problem for any value of De.

The simplest type of boundary condition arises when the velocity is specified on the entire boundary. Then the perturbation fields $\boldsymbol{v}_k$ for $k \geq 1$ must be zero on the entire boundary; an example of this situation is illustrated in Example 6.5-1. A different situation arises when a stress component is specified on part of the boundary. Then it is in fact necessary to evaluate $\gamma_{(2)0}$ in connection with the formulation of the boundary condition for the perturbation fields, as illustrated in Example 6.5-2. Note that in both examples the perturbation fields satisfy the Newtonian fluid creeping flow equations augmented by a nonhomogeneous term. Hence we expect that the physical boundary conditions will be sufficient to determine all $\boldsymbol{v}_k^*$ and p_k^*.

Similar perturbation techniques have been developed for other types of models such as the differential models considered in Chapter 7. However, when these other models are

TABLE 6.5-1

Some Flow Systems That May be Used to Measure Second-Order Retarded-Motion Constants[a]

Flow System	Combination Evaluated	Comments
Plane flow (e.g., transverse slot)	Ψ_1	§6.4[b]
Translating bubble	$\Psi_1 + \frac{4}{7}\Psi_2$	Example 6.5-2
Rotating sphere	$\Psi_1 + 2\Psi_2$	Example 6.5-1
Rod-climbing	$\Psi_1 + 4\Psi_2$	Problem 6B.6
Rectilinear flow (e.g., tilted trough)	Ψ_2	§6.4[c]
Radial flow	$\Psi_1 - 3\Psi_2$	[a]

[a] A. Co and R. B. Bird, *Appl. Sci. Res.*, **33**, 385–404 (1977).
[b] R. I. Tanner and A. C. Pipkin, *Trans. Soc. Rheol.*, **13**, 471–484 (1964).
[c] A. C. Pipkin and R. I. Tanner, *Mech. Today*, **1**, 262–321 (1972); R. I. Tanner, *Trans. Soc. Rheol.*, **14**, 483–507 (1970); L. Sturges and D. D. Joseph, *Arch. Rat. Mech. Anal.*, **59**, 359–387 (1976).

used, the perturbation results are equivalent to those obtained from the retarded-motion expansion, as explained in connection with Fig. 6.2-2. In addition, although the models described in Chapters 7 and 8 are really designed to give a reasonable description over a wide range of strain rates, some of them are not complete at third order, and sometimes not even at second order. Therefore the perturbation technique based on the retarded-motion expansion is the simplest and safest method to obtain flow solutions at low Deborah number.

Table 6.5-1 lists some of the flow systems for which perturbation solutions are available. The remainder of this section is devoted to two examples that serve to illustrate the technique. The first concerns the determination of the first-order perturbation of a velocity field, and it is illustrated how this perturbation may be obtained in an efficient manner with the use of a stream function. The second example is somewhat more lengthy since the first-order perturbations in the pressure and stress fields are also required.

EXAMPLE 6.5-1 Flow Near a Rotating Sphere[1]

In Example 1.4-3 we considered the flow around a sphere rotating with angular velocity W in a Newtonian liquid of infinite extent. It was shown that inertial effects produce a secondary flow away from the sphere in the equatorial plane and towards the sphere along the axis of rotation. By contrast, the secondary flow around a sphere rotating slowly in a polymeric fluid goes in the opposite direction, as shown in Fig. 2.4-1; the fluid is drawn inward toward the sphere in the equatorial plane and then ejected along the axis of rotation. It is desired to obtain the secondary velocity field predicted by the second-order fluid by a perturbation analysis.

[1] H. Giesekus, *Rheol. Acta*, **3**, 59–71 (1963). In this landmark publication results are given complete through third order for the flow near a simultaneously rotating and translating sphere. Results for a rotating but not translating sphere are given complete through fourth order by R. L. Fosdick and B. G. Kao, *Rheol. Acta*, **19**, 675–697 (1980).

SOLUTION We take the origin of the coordinate system to be at the center of the sphere, with the z-axis along the axis of rotation of the sphere. We work in spherical coordinates, r, θ, ϕ, and we anticipate that the velocity and pressure fields will be independent of ϕ. We let the characteristic velocity V be WR so that $\boldsymbol{v}^* = \boldsymbol{v}/WR$, and we take the characteristic shear rate κ to be W so that $\boldsymbol{\gamma}^*_{(n)} = \boldsymbol{\gamma}_{(n)}/W^n$, $p^* = p/b_1W$, $\mathscr{P}^* = \mathscr{P}/b_1W$, $\boldsymbol{f}^* = \boldsymbol{f}R/b_1W^2$, and $\mathrm{De} = -(b_2/b_1)W$. These definitions enable us to take over the general analysis in the introduction to this section.

The boundary conditions for this problem are

$$\text{At } r = R, \qquad \boldsymbol{v} = WR \sin\theta\, \boldsymbol{\delta}_\phi \tag{6.5-15}$$

$$\text{As } r \to \infty, \qquad \boldsymbol{v} \to \boldsymbol{0} \tag{6.5-16}$$

$$\text{As } r \to \infty, \qquad \mathscr{P} \to \text{constant} \tag{6.5-17}$$

As we know from Example 1.4-3, the solution to the *zero-order* equations of Eqs. 6.5-5 and 6 satisfying the above boundary conditions is

$$\boldsymbol{v}_0 = WR\,(R/r)^2 \sin\theta\, \boldsymbol{\delta}_\phi \tag{6.5-18}$$

$$\mathscr{P}_0 = \text{constant} \tag{6.5-19}$$

Next we have to solve the *first-order* equations with the boundary conditions

$$\text{At } r = R, \qquad \boldsymbol{v}_1 = \boldsymbol{0} \tag{6.5-20}$$

$$\text{As } r \to \infty, \qquad \boldsymbol{v}_1 \to \boldsymbol{0} \tag{6.5-21}$$

$$\text{As } r \to \infty, \qquad p_1 \to 0 \text{ at } \theta = \pi/2 \tag{6.5-22}$$

Obtaining the solution of the first-order equations in Eqs. 6.5-7 and 10 is a lengthy task, which is the main business of the remainder of this example.

Our first task is to work out the expression for $\boldsymbol{f}$ in Eq. 6.5-10. From the expression for $\boldsymbol{v}_0$ in Eq. 6.5-18 we first get

$$\boldsymbol{\gamma}_{(1)0} = -3W(R/r)^3 \sin\theta\, \{\boldsymbol{\delta}_r\boldsymbol{\delta}_\phi + \boldsymbol{\delta}_\phi\boldsymbol{\delta}_r\} \tag{6.5-23}$$

From this we obtain

$$\boldsymbol{\gamma}^2_{(1)0} = \{\boldsymbol{\gamma}_{(1)0} \cdot \boldsymbol{\gamma}_{(1)0}\} = 9W^2(R/r)^6 \sin^2\theta\, \{\boldsymbol{\delta}_r\boldsymbol{\delta}_r + \boldsymbol{\delta}_\phi\boldsymbol{\delta}_\phi\} \tag{6.5-24}$$

$$[\boldsymbol{\nabla} \cdot \boldsymbol{\gamma}^2_{(1)0}] = -9(W^2/R)(R/r)^7 \sin\theta\, (5\sin\theta\, \boldsymbol{\delta}_r + \cos\theta\, \boldsymbol{\delta}_\theta) \tag{6.5-25}$$

Therefore Eq. 6.5-10 becomes for the rotating-sphere problem:

$$b_1\boldsymbol{\nabla}^2\boldsymbol{v}_1 - \boldsymbol{\nabla}\tilde{p}_1 = -\left(\frac{b_{11}}{b_2} - 1\right)9 \sin\theta\, (W/R)b_1(R/r)^7\, (5\sin\theta\, \boldsymbol{\delta}_r + \cos\theta\, \boldsymbol{\delta}_\theta) \tag{6.5-26}$$

This has to be solved with the boundary conditions mentioned above (note that at $\theta = \pi/2$ and as $r \to \infty$, we have $\tilde{p}_1 \to 0$, since $\mathscr{P}_0 = \text{constant}$ and $\boldsymbol{\gamma}_{(1)0} \to \boldsymbol{0}$).

Because the flow is axisymmetric and because $\boldsymbol{v}$ and $\mathscr{P}$ do not depend on ϕ, it is expedient to use the stream-function method of §1.4. Use of Eq. E of Table 1.4-1 gives (with $-\boldsymbol{f}$ designating the right side of Eq. 6.5-26)

$$E^4\psi = E^2(E^2\psi) = -(r/b_1)\sin\theta\,[\nabla \times \boldsymbol{f}]_\phi$$

$$= \left(\frac{b_{11}}{b_2} - 1\right)144\,(W/R)(R/r)^7 \sin^2\theta\cos\theta \tag{6.5-27}$$

in which

$$E^2 = \frac{\partial^2}{\partial r^2} + \frac{\sin\theta}{r^2}\frac{\partial}{\partial\theta}\left(\frac{1}{\sin\theta}\frac{\partial}{\partial\theta}\right) \tag{6.5-28}$$

If we now postulate a solution to Eq. 6.5-27 of the form $\psi(r, \theta) = WR^3\, g(r)\sin^2\theta\cos\theta$, we get

$$\left(\frac{d^2}{dr^2} - \frac{6}{r^2}\right)\left(\frac{d^2}{dr^2} - \frac{6}{r^2}\right)g = \frac{144}{R^2}\left(\frac{b_{11}}{b_2} - 1\right)\left(\frac{R}{r}\right)^7 \tag{6.5-29}$$

This is a fourth-order, nonhomogeneous ordinary differential equation, for which we have to find the "complementary function," containing four constants of integration and a "particular integral." The *complementary function* is obtained by trying a solution of the form $g(r) = (r/R)^n$; substitution of this trial function into Eq. 6.5-29 with the right side set equal to zero leads to a quartic equation for n, and the latter has roots -2, 0, 3, and 5. Therefore, the complementary function is

$$[g(r)]_{\text{C.F.}} = c_1(R/r)^2 + c_2 + c_3(r/R)^3 + c_4(r/R)^5 \tag{6.5-30}$$

As $r \to \infty$, the function g must not be allowed to become infinite, and therefore c_3 and c_4 must both be zero. The *particular integral* is obtained by trying a function of the form $g(r) = c_0(r/R)^m$; insertion of this into the nonhomogeneous equation in Eq. 6.5-29 gives the values of c_0 and m. The particular integral is thus found to be

$$[g(r)]_{\text{P.I.}} = \left(\frac{b_{11}}{b_2} - 1\right)\left(\frac{R}{r}\right)^3 \tag{6.5-31}$$

The complete solution is given by the sum of these last two expressions. The two constants c_1 and c_2 are determined from

$$\text{At } r = R, \qquad v_{1r} = -(1/r^2\sin\theta)\,\partial\psi/\partial\theta = 0, \qquad \text{which implies that } g(R) = 0 \tag{6.5-32}$$

$$\text{At } r = R, \qquad v_{1\theta} = +(1/r\sin\theta)\,\partial\psi/\partial r = 0 \qquad \text{which implies that } g'(R) = 0 \tag{6.5-33}$$

These conditions give

$$c_1 = -\frac{3}{2}\left(\frac{b_{11}}{b_2} - 1\right); \quad c_2 = +\frac{1}{2}\left(\frac{b_{11}}{b_2} - 1\right) \tag{6.5-34}$$

and with these results $\psi(r, \theta)$ is now known completely. From $\psi(r, \theta)$ we can now obtain v_{1r} and $v_{1\theta}$, and hence $\boldsymbol{v}_1$. The velocity is then

$$\begin{aligned} \boldsymbol{v} = {} & WR(R/r)^2 \sin\theta\, \boldsymbol{\delta}_\phi \\ & - \mathrm{De}\, WR\left(\frac{b_{11}}{b_2} - 1\right)\left[\left(\frac{1}{2}\left(\frac{R}{r}\right)^2 - \frac{3}{2}\left(\frac{R}{r}\right)^4 + \left(\frac{R}{r}\right)^5\right)(3\cos^2\theta - 1)\,\boldsymbol{\delta}_r \right. \\ & \left. - 3\left(\left(\frac{R}{r}\right)^4 - \left(\frac{R}{r}\right)^5\right)\sin\theta\cos\theta\,\boldsymbol{\delta}_\theta\right] \\ & + O(\mathrm{De}^2) \end{aligned} \tag{6.5-35}$$

or in terms of the zero-shear-rate viscometric functions

$$\begin{aligned} \boldsymbol{v} = {} & WR(R/r)^2 \sin\theta\, \boldsymbol{\delta}_\phi \\ & + W^2R\left(\frac{\Psi_{1,0} + 2\Psi_{2,0}}{2\eta_0}\right)\left[\left(\frac{1}{2}\left(\frac{R}{r}\right)^2 - \frac{3}{2}\left(\frac{R}{r}\right)^4 + \left(\frac{R}{r}\right)^5\right)(3\cos^2\theta - 1)\,\boldsymbol{\delta}_r \right. \\ & \left. - 3\left(\left(\frac{R}{r}\right)^4 - \left(\frac{R}{r}\right)^5\right)\sin\theta\cos\theta\,\boldsymbol{\delta}_\theta\right] + \cdots \end{aligned} \tag{6.5-36}$$

Note that the primary velocity field has only a ϕ-component and is proportional to W, whereas the secondary flow field has only r- and θ-components and is proportional to W^2. If $\Psi_{1,0} + 2\Psi_{2,0} > 0$ the secondary flow far from the sphere will be toward the sphere near the equator and away from the sphere near the axis, with the two zones being separated by conical surfaces given by $3\cos^2\theta - 1 = 0$, or $\theta = \arccos(1/\sqrt{3}) \doteq 54°44'$ or $125°16'$. This behavior is in qualitative agreement with the flow pattern observed experimentally.[2]

The velocity field in Eq. 6.5-35 may be used to calculate the torque needed to maintain the angular velocity W. The result, $\mathscr{T} = 8\pi b_1 R^3 W$, is identical to that for a Newtonian fluid. Walters and Waters[3] have performed a perturbation calculation for third-order fluids, and they have included the inertial terms as well (i.e., the $[\boldsymbol{v}\cdot\nabla\boldsymbol{v}]$-term in the equation of motion). Their result for the torque is

$$\begin{aligned} \mathscr{T} = {} & 8\pi b_1 R^3 W\left[1 + \frac{\mathrm{Re}^2}{1200} + \frac{\mathrm{ReDe}}{140}\left(1 + \frac{b_{11}}{b_2}\right)\right. \\ & \left. - \frac{2\mathrm{De}^2}{15}\left(1 + \frac{b_{11}}{b_2}\right)^2 - \frac{24\mathrm{De}^2}{5}\frac{b_1(b_{12} - b_{1:11})}{b_2^2}\right] + \cdots \end{aligned} \tag{6.5-37}$$

in which $\mathrm{Re} = R^2 W\rho/b_1$ and $\mathrm{De} = -(b_2/b_1)W$. Note that the two dimensionless groups, Re and De, can be varied independently of one another. Note further that the third-order constant b_3 does not appear in this expression.

EXAMPLE 6.5-2 Flow Near a Translating Bubble[4]

In Example 1.4-2 we considered the flow around a spherical bubble rising slowly in an incompressible Newtonian fluid of density ρ. It is desired to extend this analysis to a bubble rising slowly in a second-order fluid as follows:

[2] K. Walters and J. G. Savins, *Trans. Soc. Rheol.*, **9**:1, 407-416 (1965); Y. Ide and J. L. White, *J. Appl. Polym. Sci.*, **18**, 2997-3018 (1974).

[3] K. Walters and N. D. Waters, *Br. J. Appl. Phys.*, **14**, 667-671 (1963); **15**, 989-991 (1964); *Rheol. Acta*, **3**, 312-315 (1964).

[4] O. Hassager in K. Østergaard and Aa. Fredenslund, eds., *Chemical Engineering with Per Søltoft*, Teknisk Forlag, Copenhagen (1977). The slow motion of a bubble in an Oldroyd fluid was studied by O. O. Ajayi, *J. Eng. Math.*, **9**, 273-280 (1975), through terms of first order, and by G. F. Tiefenbruck and L. G. Leal, *J. Non-Newtonian Fluid Mech.*, **7**, 257-264 (1980), through terms of second order in the Deborah number. The corresponding drop motion was first studied by M. G. Wagner and J. L. Slattery, *AIChE J.*, **17**, 1198-1207 (1971).

a. First, assume that the bubble remains spherical, and find the velocity perturbation in the fluid, the pressure and stress distributions on the surface of the bubble, and the velocity of rise of the bubble to first order in the Deborah number.

b. Second, use the pressure and stress distributions calculated above to estimate the shape of the bubble in the limit that it is only slightly deformed from spherical shape.

SOLUTION **(a)** This example differs from the preceding example in that the velocity is not completely specified on the entire boundary. On the surface of the bubble we specify that the normal component of velocity must be zero and that the shear stress must be zero. That is, if we describe the flow in the spherical coordinate system shown in Fig. 1.4-1 with origin at the center of the bubble we have the conditions

$$\text{At } r = R_0, \qquad v_r = 0; \qquad \tau_{r\theta} = 0 \tag{6.5-38}$$

$$\text{At } r = \infty \text{ and } \theta = \pi/2, \qquad p = p_\infty \tag{6.5-39}$$

Here R_0 is the radius of the undeformed sphere. We then expand the velocity and pressure according to Eqs. 6.5-1 and 2. For this problem the characteristic strain rate is $\kappa = V/R_0$, where V is the rise velocity of the bubble; this means that the dimensionless quantities used in the introduction to this section are: $\text{De} = -(b_2/b_1)(V/R_0)$, $\gamma^*_{(n)} = \gamma_{(n)}(R_0/V)^n$, $p^* = pR_0/b_1V$, $\tau^* = \tau R_0/b_1V$, and $f^* = fR_0^2/b_1V$. When Eq. 6.5-1 is inserted into Eq. 6.5-38 we find

$$\text{At } r = R_0, \qquad v_{0r} = 0 \quad v_{1r} = 0 \tag{6.5-40}$$

We also use Eq. 6.5-3 to reformulate the shear-stress condition in Eq. 6.5-38 to

$$\text{At } r = R_0, \qquad \gamma_{(1)0r\theta} = 0; \quad \gamma_{(1)1r\theta} = \frac{R_0}{V}(\gamma_{(2)0r\theta} + (b_{11}/b_2)\{\boldsymbol{\gamma}_{(1)0} \cdot \boldsymbol{\gamma}_{(1)0}\}_{r\theta}) \tag{6.5-41}$$

Notice that the boundary conditions specify values of the $r\theta$-component of the $\boldsymbol{\gamma}_{(1)}$ tensor constructed from $\boldsymbol{v}_0$ and $\boldsymbol{v}_1$, respectively. The $\boldsymbol{\gamma}_{(2)}$ tensor enters the boundary conditions for $\boldsymbol{v}_1$ only in $\boldsymbol{\gamma}_{(2)0}$, with the $\boldsymbol{v}_0$ field known from the solution of the unperturbed flow problem.

The perturbation solution now proceeds in the same way as in the preceding example and some detail will be omitted in the following. First we need the solution for the unperturbed velocity field and pressure distribution from Example 1.4-2:

$$\boldsymbol{v}_0 = V[-(1 - (R_0/r))\cos\theta\,\boldsymbol{\delta}_r + (1 - \tfrac{1}{2}(R/r))\sin\theta\,\boldsymbol{\delta}_\theta] \tag{6.5-42}$$

$$p_0 = (b_1VR_0r^{-2} - \rho gr)\cos\theta + p_\infty \tag{6.5-43}$$

From Eq. 6.5-42 we find

$$\boldsymbol{\gamma}_{(1)0} = VR_0r^{-2}\cos\theta\,(-2\boldsymbol{\delta}_r\boldsymbol{\delta}_r + \boldsymbol{\delta}_\theta\boldsymbol{\delta}_\theta + \boldsymbol{\delta}_\phi\boldsymbol{\delta}_\phi) \tag{6.5-44}$$

Then we calculate $\boldsymbol{\gamma}_{(2)0}$ and $\{\boldsymbol{\gamma}_{(1)0} \cdot \boldsymbol{\gamma}_{(1)0}\}$. These tensors turn out to have a vanishing $r\theta$-component at $r = R_0$, so that the boundary condition for $\boldsymbol{v}_1$ in Eq. 6.5-41 reduces to

$$\text{At } r = R_0, \qquad \gamma_{(1)1r\theta} = 0 \tag{6.5-45}$$

Next we need to calculate the expression for $\boldsymbol{f}$ in Eq. 6.5-11, which gives

$$\boldsymbol{f} = 2((b_{11}/b_2) - 1)\,b_1VR_0^3r^{-5}(5\cos^2\theta\boldsymbol{\delta}_r + \sin\theta\cos\theta\,\boldsymbol{\delta}_\theta) \tag{6.5-46}$$

We now may solve Eqs. 6.5-7, 10, and 46 with the use of a stream function with the help of Table 1.4-1. The results are

$$v_{1r} = [1 - (b_{11}/b_2)](VR_0^2/10)[-3r^{-2} + 5R_0r^{-3} - 2R_0^2r^{-4}](3\cos^2\theta - 1) \tag{6.5-47}$$

$$v_{1\theta} = [1 - (b_{11}/b_2)](VR_0^2/10)[+5R_0r^{-3} - 4R_0^2r^{-4}]\sin\theta\cos\theta \tag{6.5-48}$$

$$\tilde{p}_1 = b_1[1 - (b_{11}/b_2)](VR_0^2/10)[-6r^{-3}(3\cos^2\theta - 1) + 5R_0r^{-4}(8\cos^2\theta - 1)] \tag{6.5-49}$$

The solution of the equation for the stream function provides just $\boldsymbol{v}_1$. Subsequently the known expressions for $\boldsymbol{v}_1$ and f must be introduced in the equation of motion in Eq. 6.5-10 and the resulting equation is then solved for $\tilde{p}_1$. In this last step we use the condition that $\tilde{p}_1 \to 0$ for $r \to \infty$ and $\theta = \pi/2$.

The complete solution for the velocity and pressure fields for the flow around a spherical bubble through terms of first order in the Deborah number may now be obtained from Eqs. 6.5-13 and 14 as

$$\boldsymbol{v} = \boldsymbol{v}_0 - (b_2/b_1)(V/R_0)\boldsymbol{v}_1 + \cdots \tag{6.5-50}$$

$$p = p_0 - (b_2/b_1)(V/R_0)\tilde{p}_1 + b_2V^2R_0[(3\cos^2\theta - 1)r^{-3} - \tfrac{1}{2}(2\cos^2\theta - 1)R_0r^{-4}] + \cdots \tag{6.5-51}$$

where $\boldsymbol{v}_0$, $\boldsymbol{v}_1$, p_0, and $\tilde{p}_1$ are given above.

The normal stress distribution at the surface of the bubble may now be obtained through terms of first order in De from Eq. 6.5-3 as

$$\begin{aligned}[\pi_{rr}]_{r=R_0} &= \left[p - b_1\left\{\gamma_{(1)0} + \mathrm{De}\left(\gamma_{(1)1} - \frac{R_0}{V}\gamma_{(2)0}\right.\right.\right. \\ &\qquad \left.\left.\left. -(b_{11}R_0/b_2V)\{\gamma_{(1)0}\cdot\gamma_{(1)0}\}_{rr}\right)\right\}\right]_{r=R_0} \\ &= p_\infty + [3b_1(V/R_0) - \rho gR_0]\cos\theta \\ &\qquad + \frac{b_2}{10}(V/R_0)^2[(42 - 12(b_{11}/b_2))\cos^2\theta - 14 - (b_{11}/b_2)]\end{aligned} \tag{6.5-52}$$

Now we may parallel the treatment in Example 1.4-2 to find the following expression for the total force in the z-direction on the bubble:

$$\begin{aligned}F_z &= \int_0^{2\pi}\int_0^{\pi}[-\pi_{rr}\cos\theta]_{r=R_0}R_0^2\sin\theta\,d\theta\,d\phi \\ &= -4\pi b_1R_0V + \frac{4}{3}\pi R_0^3\rho g\end{aligned} \tag{6.5-53}$$

We see that the bubble will rise with the steady-state velocity

$$V = \tfrac{1}{3}\rho gR_0^2/b_1 \tag{6.5-54}$$

and that the normal stresses developed in the fluid do not affect the rise velocity at first order in the Deborah number. When Eq. 6.5-54 is introduced into the expression for the normal stress in Eq. 6.5-52, we see that the coefficient in front of $\cos\theta$ vanishes and we may rewrite the equation as

$$[\pi_{rr}]_{r=R_0} = p_m - \frac{2b_1V}{5R_0}\left(7 - 2\frac{b_{11}}{b_2}\right)\mathrm{De}\,P_2(C) \tag{6.5-55}$$

with

$$p_m = p_\infty - \tfrac{1}{2} b_{11} (V/R_0)^2 \tag{6.5-56}$$

Here $P_2(C) = \frac{1}{2}(3C^2 - 1)$ is the second Legendre polynomial and $C = \cos\theta$. If one integrates Eq. 6.5-55 over the entire surface then the term involving $P_2(C)$ vanishes, so that p_m represents a mean pressure on the bubble.

(b) To describe the deformation of the bubble we need to know the velocity field and pressure distribution around the deformed bubble. We assume here that the bubble is deformed only so slightly from the spherical shape that the velocity field and pressure distribution for flow around the spherical bubble calculated in part **(a)** remain valid in a first approximation.

We now need to introduce the surface tension σ. This property will appear in the dimensionless group $\text{Ca} = b_1 V/\sigma$ called the *capillary number*. Small values of the capillary number correspond to situations with dominant surface tension. In particular at zero capillary number there can be no deformation of the bubble from the spherical shape for any Deborah number. Conversely at zero Deborah number we see from Eq. 6.5-55 that only a normal stress independent of θ remains, and there will be no deformation of the spherical bubble independent of the capillary number. Consequently the leading term in a series approximation for the deformation of the bubble in powers of De and Ca will be linear in both De and Ca. That is, we consider that the bubble is deformed from a sphere of radius R_0 to a shape described by $R(\theta)$ as

$$R(\theta)/R_0 = 1 + \text{Ca De}\, \zeta(\theta) + \cdots \tag{6.5-57}$$

where we wish to determine $\zeta(\theta)$ subject to the conditions that $\text{De} < O(1)$ and $\text{Ca} < O(1)$. Now that we have the additional unknown function $\zeta(\theta)$ we need one more equation. This extra equation is furnished by the normal stress boundary condition at the surface of the bubble, which has so far been ignored. The condition states that at the surface of the bubble the gas pressure inside the bubble p_g equals the sum of the normal stress exerted by the fluid π_{rr} and the surface tension force:

$$p_g = \pi_{rr} + \sigma\left(\frac{1}{R_1} + \frac{1}{R_2}\right) \tag{6.5-58}$$

Here R_1 and R_2 are the principal radii of curvature of the surface. This boundary condition should really be applied at $r = R(\theta)$. However, in agreement with our assumption that the deformation is small, we now substitute $[\pi_{rr}]_{r=R_0}$ from Eq. 6.5-55 for π_{rr} into Eq. 6.5-58. Also for the small deformations from the spherical shape considered in Eq. 6.5-57 the surface tension terms may be linearized as follows:[5]

$$\frac{1}{R_1} + \frac{1}{R_2} = \frac{2}{R_0} - \frac{\text{Ca De}}{R_0}\left\{2\zeta + \frac{d}{dC}\left[(1 - C^2)\frac{d\zeta}{dC}\right]\right\} + O((\text{Ca De})^2) \tag{6.5-59}$$

where $C = \cos\theta$. When Eqs. 6.5-55 and 59 are substituted into Eq. 6.5-58 one obtains the following differential equation for $\zeta(\theta)$:

$$(\text{Ca De})\left\{\frac{d}{dC}\left[(1 - C^2)\frac{d\zeta}{dC}\right] + 2\zeta\right\} = \left[2 + \frac{R_0}{\sigma}(p_m - p_g)\right] - \tfrac{2}{5}\left(7 - 2\frac{b_{11}}{b_2}\right)\text{Ca De}\, P_2(C) \tag{6.5-60}$$

The function ζ has to satisfy the two conditions

$$\int_{-1}^{1} \zeta dC = 0; \quad \int_{-1}^{1} \zeta C dC = 0 \tag{6.5-61}$$

These equations are linearizations of the conditions that the volume of the bubble must remain equal to $(4\pi/3)R_0^3$ and that the "center of mass" of the bubble must remain at the origin of coordinates,

[5] L. D. Landau and E. M. Lifshitz, *Fluid Mechanics*, Addison-Wesley, Reading, MA (1959), pp. 238–239.

respectively. The condition that there is no kink in the surface at the poles, that is, that $d\zeta/d\theta$ is zero for $\theta = 0$ and π, is replaced by a condition that $d\zeta/dC$ is finite at $\theta = 0$ and π.

From a solution of Eq. 6.5-60 subject to the stated conditions one finds that $R(\theta)$ is

$$R/R_0 = 1 + \text{Ca}\,(V/20R_0)(7\Psi_{1,0} + 4\Psi_{2,0})P_2(\cos\theta) + \cdots \tag{6.5-62}$$

where the Deborah number has been rewritten in terms of the zero-shear-rate normal stress coefficients. Note that the second normal stress coefficient plays a relatively minor role in this expression, so that the deformation is primarily determined by the first normal stress coefficient. Since $\Psi_{1,0} \geq 0$ the calculation shows that the bubble is deformed into the shape of an ellipsoid elongated at the poles (a "prolate" ellipsoid). In the process of obtaining this solution we have applied the boundary conditions not at $R(\theta)$ but at R_0. To see that this approximation is consistent with the solution obtained let us consider the velocity perturbation to first order in the product of the Deborah number and capillary number. We call the velocity solution obtained in part (**a**) $\boldsymbol{v}^{(0)}$ and consider then a disturbance Ca De $\boldsymbol{v}^{(1)}$ due to the deformation in Eq. 6.5-57 such that the altered velocity field is

$$\boldsymbol{v} = \boldsymbol{v}^{(0)} + \text{Ca De}\,\boldsymbol{v}^{(1)} + \cdots \tag{6.5-63}$$

Now we expand this velocity field in a Taylor series in R around R_0 to obtain

$$\boldsymbol{v}(R, \theta) = \boldsymbol{v}^{(0)}(R_0, \theta) + \text{Ca De}\,[\zeta R_0(\partial \boldsymbol{v}^{(0)}/\partial R) + \boldsymbol{v}^{(1)}]_{R_0,\theta} + \cdots \tag{6.5-64}$$

Now we see that it is indeed consistent to apply the boundary conditions for $\boldsymbol{v}^{(0)}$ at R_0 rather than at R. Furthermore Eq. 6.5-64 gives a procedure for the construction of boundary conditions for $\boldsymbol{v}^{(1)}$ given the solution $\boldsymbol{v}^{(0)}$. However we are interested in the deformation just to first order in the capillary number, and for this purpose $\boldsymbol{v}^{(0)}$ is all that is needed.

§6.6 LIMITATIONS OF THE RETARDED-MOTION EXPANSION AND RECOMMENDATIONS FOR ITS USE

When the retarded-motion expansion was introduced in §6.2 it was described as a constitutive equation restricted to small Deborah number. An appreciation of the origin of this restriction may be obtained in Chapter 9 where a formal derivation of the expansion is given. At this point we merely summarize some of the difficulties that one may encounter if one tries to apply the retarded-motion expansion outside its range of validity:

- **i.** One may predict a shear stress vs. shear rate curve with a maximum, or even negative, viscosity or elongational viscosity (as discussed in Example 6.2-1 and in the text immediately following the example).
- **ii.** One may predict that the second-order fluid is unstable in the rest state unless one chooses some unrealistic values of the retarded-motion constants (see Problem 6C.1).
- **iii.** One may need additional boundary conditions due to the appearance of higher-order derivatives in terms such as $\{\boldsymbol{v} \cdot \nabla \boldsymbol{\gamma}_{(1)}\}$. However if the retarded-motion expansion is used in a perturbation expansion then the higher-order derivatives always appear in the nonhomogeneous terms (as explained in §6.5) and no additional boundary conditions are needed.
- **iv.** One cannot describe even qualitatively the stress relaxation experiments discussed in Chapter 3.

There may be more difficulties, but this list is sufficient to emphasize that the restriction to small De should be taken seriously. Any solution to a flow problem with a retarded-motion expansion where the second-order terms are not small corrections to the Newtonian terms (and the third-order terms small corrections to the second-order terms,

and so on) must be regarded with suspicion and is likely to be a mathematical curiosity with no physical relevance.

Unfortunately, for flows in some geometries it is not possible to construct a solution where the second-order terms are everywhere small corrections to the Newtonian terms. Examples of such problems are flow around a sharp corner (where the second-order terms dominate the Newtonian terms close to the corner; see Problem 6C.2) and flow into a line sink (where the second-order terms dominate the Newtonian terms close to the sink; see Problem 6B.5). Consequently for flows that involve sharp corners, sinks, or sources the retarded-motion expansion should never be used.

Even when the retarded-motion expansion is used correctly, however, it is important to note that the use of more than the second-order terms in perturbation solutions often results in series with "diminishing returns." By this we mean that while retention of second-order terms gives a qualitative and quantitative description of the departure from Newtonian behavior, the inclusion of third- and higher-order terms provides only very minor additional improvements to the solution. This should be compared with the fact that the second-order terms may usually be obtained at a moderate analytical effort, but the higher-order terms require increasingly tedious and lengthy algebraic developments.

With the above restrictions in mind, then, we recommend that the retarded motion expansion be used primarily just through second-order terms for analytical investigations of the departure from Newtonian behavior. The purpose of such investigations could be:

- **i.** To investigate qualitative behavior of polymer flow phenomena, such as the direction of secondary flows.
- **ii.** To compare with numerical (or approximate) solutions of more realistic constitutive equations in limiting situations.
- **iii.** To compare with experimental data in order to characterize polymeric fluids by their values of η_0, $\Psi_{1,0}$, and $\Psi_{2,0}$.
- **iv.** To explore the nature of the motions of orientable or deformable particles in suspensions with a polymeric suspending fluid.

When experiments are performed to determine η_0, $\Psi_{1,0}$, and $\Psi_{2,0}$ from comparison with retarded-motion solutions it is often difficult to obtain data at sufficiently slow deformation rates that the fluid behaves as a second-order fluid and still retain sufficient sensitivity to enable accurate determinations of $\Psi_{1,0}$ and $\Psi_{2,0}$. Consequently for this purpose we would presently recommend the use of geometries in which no pressure transducers are required and the fluid acts as its own "manometer" as in the development of secondary flow or in deformation of a free surface (the rotating sphere, the rod climbing effect, the tilted trough, or the translating bubble). Keep in mind that these kinds of experimentally observed phenomena cannot be described by using the generalized Newtonian models of Chapter 4 or the linear viscoelastic models of Chapter 5.

The second-, third-, and higher-order fluid models have been used to examine flows in a wide variety of systems; we mention some of them here: secondary flow in curved tubes[1] and in conduits of noncircular cross section;[2–4] flow in eccentric annuli, both

[1] H. A. Barnes and K. Walters, *Proc. Roy. Soc. Ser. A*, **314**, 85–109 (1969).

[2] R. S. Rivlin in M. Reiner and D. Abir, eds., *Second Order Effects in Elasticity, Plasticity, and Fluid Dynamics*, Macmillan, New York (1964), pp. 668–677.

[3] R. S. Rivlin and W. E. Langlois, *Rend. Mat.*, **22**, 169–185 (1963).

[4] A. C. Pipkin, *Proceedings of the 4th International Congress on Rheology*, Vol. 1, Wiley-Interscience, New York (1965), pp. 213–222.

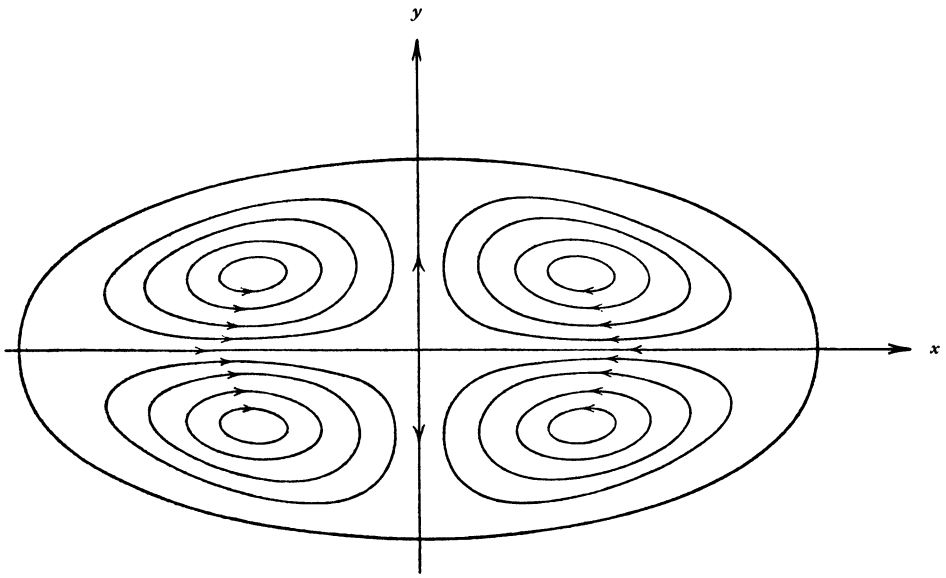

FIGURE 6.6-1. Secondary flow of a fourth-order fluid flowing in the z-direction through a straight pipe of elliptical cross section. [R. S. Rivlin in R. J. Seeger and G. Temple, eds., *Research Frontiers in Fluid Dynamics*, Wiley, New York (1965), Chapt. 5.]

tangential[5] and axial;[6] secondary flow in the disk and cylinder system[7] and in the cone-and-plate viscometer;[8–10] flow near a translating sphere;[11–13] flow in a converging tube;[14,15] radial flow between parallel disks;[16–18] climbing of a fluid near a rotating rod (Weissenberg effect);[19–21] boundary layer flows;[22–24] extrudate swell;[25] the hole pressure

[5] J. M. Davies and K. Walters in T. C. Davenport, ed., *Rheology of Lubricants*, Wiley, New York (1973), pp. 65–80.
[6] J. Y. Kazakia and R. S. Rivlin, *J. Non-Newtonian Fluid Mech.*, **8**, 311–317 (1981).
[7] D. F. Griffiths, D. T. Jones, and K. Walters, *J. Fluid Mech.*, **36**, 161–175 (1969).
[8] H. Giesekus, *Rheol. Acta*, **6**, 339–353 (1967).
[9] D. F. Griffiths and K. Walters, *J. Fluid Mech.*, **42**, 379–399 (1970).
[10] K. Walters and N. D. Waters in R. E. Wetton and R. W. Whorlow, eds., *Polymer Systems, Deformation and Flow*, Macmillan, London (1968), Chapt. 17, pp. 211–235.
[11] B. Caswell and W. H. Schwarz, *J. Fluid Mech.*, **13**, 417–426 (1962).
[12] H. Giesekus, *Rheol. Acta*, **3**, 59–71 (1963).
[13] M. G. Wagner and J. C. Slattery, *AIChE J.*, **17**, 1198–1207 (1971).
[14] E. B. Adams, J. C. Whitehead, and D. C. Bogue, *AIChE J.*, **11**, 1026–1032 (1965).
[15] P. Schümmer, *Rheol. Acta*, **6**, 192–200 (1967).
[16] W. H. Schwarz and C. Bruce, *Chem. Eng. Sci.*, **24**, 399–413 (1969).
[17] J. M. Piau and M. Piau, *C. R. Acad. Sci. Ser. A*, **270**, 159–161 (1970).
[18] A. Co and R. B. Bird, *Appl. Sci. Res.*, **33**, 385–404 (1977).
[19] A. Kaye, *Rheol. Acta*, **12**, 207–211 (1973).
[20] D. D. Joseph, G. S. Beavers, and R. L. Fosdick, *Arch. Rat. Mech. Anal.*, **49**, 381–401 (1973).
[21] D. D. Joseph and R. L. Fosdick, *Arch. Rat. Mech. Anal.*, **49**, 321–380 (1973).
[22] D. W. Beard and K. Walters, *Proc. Camb. Phil. Soc.*, **60**, 667–674 (1964).
[23] M. H. Davies, *Z. Angew. Math. Phys.*, **17**, 189–191 (1966).
[24] M. M. Denn, *Chem. Eng. Sci.*, **22**, 394–405 (1967).
[25] M. Zidan, *Rheol. Acta*, **8**, 89–123 (1969).

effect;[26–28] and motions of suspended, orientable particles.[29] One of the oldest of the ordered-fluid calculations is that for noncircular tubes,[30] in which purely axial flow is in general not possible if terms of fourth order are retained; the axial flow must then be accompanied by secondary flows. An illustration of this is given in Fig. 6.6-1.

In some of the flow systems listed above the retarded-motion expansion has been used outside its range of applicability. An example of this is the extrudate swell problem, where the retarded-motion expansion should not be used because of the presence of the sharp corner.

PROBLEMS

6B.1 Kinematic Tensors for Shear and Shearfree Flows

a. Verify the matrix displays for $\nabla \boldsymbol{v}$, $\gamma_{(1)}$, and $\gamma_{(2)}$ for shear flows and for shearfree flows given in Table C.1.

b. Show that $\gamma_{(n)} = \mathbf{0}$ for $n \geqslant 3$ for *steady-state* shear flow.

c. Show that

$$\gamma_{(n)} = (-1)^{n+1}\gamma_{(1)}^{n} \tag{6B.1-1}$$

for *steady-state* shearfree flows.

6B.2 Eccentric-Disk Rheometer Flow

In the eccentric-disk rheometer shown in Fig. 3B.1, the velocity distribution is given by

$$v_x = -W(y - Az); \quad v_y = Wx; \quad v_z = 0 \tag{6B.2-1}$$

in which W is the angular velocity of both disks (rotating in the same direction), and $A = a/b$, where a is the distance between the axes of rotation, and b is the spacing between the disks.

a. For this flow display the following tensors in matrix form: $\nabla \boldsymbol{v}$, $(\nabla \boldsymbol{v})^{\dagger}$, $\gamma_{(1)}$, $\gamma_{(2)}$, $\gamma_{(3)}$, $\{\gamma_{(1)} \cdot \gamma_{(1)}\}$, and $\{\gamma_{(1)} \cdot \gamma_{(2)} + \gamma_{(2)} \cdot \gamma_{(1)}\}$.

b. Use the third-order fluid to find τ_{xz} and τ_{yz}, which can be measured in the eccentric-disk rheometer.

c. Next show that

$$\lim_{A \to 0}\left(-\frac{\tau_{xz}}{AW}\right) = b_1 - b_3 W^2 \tag{6B.2-2}$$

$$\lim_{A \to 0}\left(-\frac{\tau_{yz}}{AW}\right) = -b_2 W \tag{6B.2-3}$$

Compare these results with Eqs. 6B.3-2.

[26] E. A. Kearsley, *Trans. Soc. Rheol.*, **14**, 419–424 (1970).
[27] R. I. Tanner and A. C. Pipkin, *Trans. Soc. Rheol.*, **13**, 471–484 (1969).
[28] S. A. Trogdon and D. D. Joseph, *J. Non-Newtonian Fluid Mech.*, **10**, 185–213 (1982).
[29] L. G. Leal, *J. Fluid Mech.*, **69**, 305–338 (1975); *Ann. Rev. Fluid Mech.*, **12**, 435–476 (1976); P. C. Chan and L. G. Leal, *J. Fluid Mech.*, **82**, 549–559 (1977).
[30] P. Brunn, *J. Non-Newtonian Fluid Mech.*, **7** 271–288 (1980); *Rheol. Acta*, **18**, 229–243 (1979); *J. Fluid Mech.*, **82**, 529–547 (1977).

6B.3 Complex Viscosity for Third-Order Fluid

a. Show that for the third-order fluid

$$\eta^*(\omega) = b_1 + b_2 i\omega - b_3\omega^2 \tag{6B.3-1}$$

b. Then obtain

$$\eta'(\omega) = b_1 - b_3\omega^2; \quad \eta''(\omega) = -b_2\omega \tag{6B.3-2}$$

Compare these equations with some data of Chapter 3 to assess the usefulness of these results.

c. From the results in **(b)** and the results in Eqs. 6.2-5 and 6, show that

$$\lim_{\omega\to 0} \frac{\eta''/\omega}{\eta'} = \lim_{\dot\gamma\to 0} \frac{\Psi_1}{2\eta} \tag{6B.3-3}$$

See Table 5.3-1, where this relation is given.

d. Can the relation in **(c)** be obtained from *linear* viscoelasticity?

6B.4 Shearfree Flows for Third-Order Fluid

a. Show that the functions $\bar\eta_1$ and $\bar\eta_2$ of Eqs. 3.5-1 and 2 are for the third-order fluid

$$\bar\eta_1 = b_1(3+b) + (b_{11} - b_2)(3 - 2b - b^2)\dot\varepsilon + [(8 + (1+b)^3)(b_3 - 2b_{12}) + (3+b)(6+2b^2)b_{1:11}]\dot\varepsilon^2 \tag{6B.4-1}$$

$$\bar\eta_2 = 2b_1 b - 4(b_{11} - b_2)b\dot\varepsilon + [2(b_3 - 2b_{12})(3b + b^3) + 4b_{1:11}b(3+b^2)]\dot\varepsilon^2 \tag{6B.4-2}$$

b. For elongational flow, with $b = 0$, it is known experimentally that $\bar\eta$ increases with $\dot\varepsilon$. What does this tell us about the quantity $(b_{11} - b_2)$? Is this consistent with the molecular-theory results given in Table 6.2-1?

6B.5 Flow into a Line Sink (or out of a Line Source) for a Third-Order Fluid

A third-order fluid is flowing into a line sink (or from a line source) whose strength is given by a constant $C = Q/2\pi L$where Q is the volume flow rate out of the sink and L is its length. For sink flow $Q < 0$ and for source flow $Q > 0$. Assume that the flow is purely radial and that there is no θ-dependence of the velocity v_r.

a. Obtain an expression for $v_r(r)$ in terms of the sink (or source) strength C by using the equation of continuity.

b. Show that the normal stresses are given by

$$\tau_{rr} = b_1\frac{2C}{r^2} - b_{11}\frac{4C^2}{r^4} + b_{1:11}\frac{8C^3}{r^6} \tag{6B.5-1}$$

$$\tau_{\theta\theta} = -b_1\frac{2C}{r^2} + (2b_2 - b_{11})\frac{4C^2}{r^4} - (6b_3 - 4b_{12} + b_{1:11})\frac{8C^3}{r^6} \tag{6B.5-2}$$

c. Obtain the pressure distribution in the fluid relative to the pressure far from the sink (or source), p_∞:

$$p_\infty - p(r) = \frac{\rho C^2}{2r^2} - (2b_{11} - b_2)\frac{2C^2}{r^4} - (3b_3 - 2b_{12} - 2b_{1:11})\frac{8C^3}{3r^6} \tag{6B.5-3}$$

Sketch the pressure distribution qualitatively for a typical polymer melt or solution. *Note*: Sufficiently near the line sink the third-order terms will dominate the second-order terms, which in turn will dominate the Newtonian terms. Hence in this problem the retarded-motion expansion is used outside of its range of validity.

6B.6 Rod-Climbing of Second-Order Fluids[1]

A vertical rod of radius R is rotating with angular velocity W in a fluid with a free surface. At small values of W the height of the free surface $h(r, W)$ (relative to the level far from the rod) as function of the radial coordinate r may be expanded as

$$h(r, W) = \frac{R^4}{gr^2}\left[\frac{2\beta}{\rho r^2} - \frac{1}{2}\right]W^2 + O(W^4) \tag{6B.6-1}$$

where ρ is the density of the fluid, g the gravitational acceleration, and $\beta = (2b_{11} - b_2)$ the "climbing constant." Surface tension has been neglected in this expression.

a. Show that when W is so small that terms of $O(W^4)$ can be neglected the fluid will climb the rod if and only if

$$\beta = \frac{1}{2}(\Psi_{1,0} + 4\Psi_{2,0}) > 0 \quad \text{and} \quad R^2 < 4\beta/\rho \tag{6B.6-2}$$

b. Show that for the Curtiss-Bird model of Table 6.2-1 we mus require that the parameter ε be greater than 1/8 to describe "rod-climbing" at second order. In particular deduce that the Doi-Edwards model ($\varepsilon = 0$) incorrectly shows "rod-dipping" at second order.

6B.7 Radial Flow between Parallel Disks

The flow of Problem 4B.3 has been studied for the third-order fluid. It has been found[2] that the stress $p + \tau_{zz}$ exerted on the disks is

$$\frac{\Delta(p + \tau_{zz})}{\Delta(p + \tau_{zz})_N} = 1 + \frac{3}{10}\frac{(R_2/r)^2 - 1}{(R_2/h)\ln(R_2/r)}\left[2\left(1 + \frac{3}{2}\frac{b_{11}}{b_2}\right)\mathrm{De} - \frac{6}{7}\mathrm{Re} - 9\left(\frac{R_2}{h}\right)\left(\frac{b_1(b_{12} - b_{1:11})}{b_2^2}\right)\mathrm{De}^2 + \cdots\right] \tag{6B.7-1}$$

Here $\mathrm{Re} = \rho Vh/b_1$, $\mathrm{De} = (-b_2/b_1)(V/h)$, $V = Q/4\pi R_2 h$, and $h = B/2$. In addition, we let $\Delta(p + \tau_{zz}) = (p + \tau_{zz})|_r - (p + \tau_{zz})|_{R_2}$, and $\Delta(p + \tau_{zz})_N = 3(R_2/h)\ln(R_2/r)$ is the Newtonian creeping flow solution.

a. Interpret the solution.

b. Obtain the coefficient of the De term in Eq. 6B.7-1.

[1] This problem is based on G. S. Beavers and D. D. Joseph, *J. Fluid Mech.*, **69**, 475-511 (1975), who included the effect of surface tension in the special situation where the contact angle at the rod is 90°. The first analysis of rod-climbing in second-order fluids is that of H. Giesekus, *Rheol. Acta*, **1**, 403-413 (1961), who neglected both inertia and surface tension. See also A. S. Lodge, *Elastic Liquids*, Academic Press, New York (1964), pp. 193-194, 231-236, and O. Hassager, *J. Rheol.*, **29**, 361-364 (1985).

[2] A. Co and R. B. Bird, *Appl. Sci. Res.*, **33**, 385-404 (1977).

6B.8 Total Normal Stress on Spherical Bubble

Verify the following intermediate results needed to obtain Eq. 6.5-52:

a. $$[p]_{r=R_0} = p_0 + [b_1(V/R_0) - \rho g R_0]\cos\theta + \frac{b_2}{10}(V/R_0)^2[(-2 + 22B_{11})\cos^2\theta - 6 + B_{11}] \tag{6B.8-1}$$

b. $$[-b_1\gamma_{(1)0rr}]_{r=R_0} = 2b_1(V/R_0)\cos\theta \tag{6B.8-2}$$

c. $$[-b_1 \mathrm{De}\,\gamma_{(1)1rr}]_{r=R_0} = \frac{b_2}{10}(V/R_0)^2[(-6 + 6B_{11})\cos^2\theta + 2 - 2B_{11}] \tag{6B.8-3}$$

d. $$[b_1 \mathrm{De}(R_0/V)\gamma_{(2)0rr}]_{r=R_0} = \frac{b_2}{10}(V/R_0)^2[50\cos^2\theta - 10] \tag{6B.8-4}$$

e. $$[b_1 \mathrm{De}(B_{11}R_0/V)\{\boldsymbol{\gamma}_{(1)0}\cdot\boldsymbol{\gamma}_{(1)0}\}_{rr}]_{r=R_0} = \frac{b_2}{10}(V/R_0)^2[-40B_{11}\cos^2\theta] \tag{6B.8-5}$$

where $B_{11} = b_{11}/b_2$.

6B.9 Bubble Deformation Equation

a. Derive Eqs. 6.5-61 as boundary conditions for the bubble deformation equation in Eq. 6.5-60.

b. Solve Eq. 6.5-60 to obtain

$$p_g = p_m + 2\frac{\sigma}{R_0} \tag{6B.9-1}$$

$$\zeta = -\frac{1}{4}P_2 \tag{6B.9-2}$$

Hint: The Legendre polynomials $P_n(x)$ are solutions of the equation:

$$\frac{d}{dx}\left[(1 - x^2)\frac{dP_n}{dx}\right] + n(n+1)P_n = 0 \tag{6B.9-3}$$

6B.10 Rectilinear Flow

a. Use the definition in Eq. 6.3-20 to show that for rectilinear flow:

$$\{(\nabla\boldsymbol{v})\cdot(\nabla\boldsymbol{v})\} = \mathbf{0}, \qquad \{(\nabla\boldsymbol{v})^\dagger\cdot(\nabla\boldsymbol{v})^\dagger\} = \mathbf{0} \tag{6B.10-1}$$

b. Also for rectilinear flow show that:

$$[\nabla\cdot\{(\nabla\boldsymbol{v})^\dagger\cdot(\nabla\boldsymbol{v})\}] = \mathbf{0} \tag{6B.10-2}$$

c. Then use the above results to show that

$$[\nabla\cdot\{\boldsymbol{\gamma}_{(1)}\cdot\boldsymbol{\gamma}_{(1)}\}] = [(\nabla\boldsymbol{v})\cdot\nabla^2\boldsymbol{v}] + \tfrac{1}{2}\nabla((\nabla\boldsymbol{v}):(\nabla\boldsymbol{v})^\dagger) \tag{6B.10-3}$$

d. Finally show that if $\boldsymbol{v}$ satisfies Eq. 6.3-3 of the text, then

$$[\nabla \cdot \{\boldsymbol{\gamma}_{(1)} \cdot \boldsymbol{\gamma}_{(1)}\}] = \nabla\left(\frac{1}{b_1}(\boldsymbol{v} \cdot \nabla \mathscr{P}_N) + \tfrac{1}{2}((\nabla \boldsymbol{v}):(\nabla \boldsymbol{v})^{\dagger})\right) \tag{6B.10-4}$$

6B.11 Flow of a Second-Order Fluid into a Slit Located in a Wedge[3]

A polymeric fluid is flowing into a thin slit located at the bottom of a wedge, in steady, creeping flow. In the cylindrical coordinate system shown in Fig. 6B.11, the wedge is described by the planes $\theta = \pm\theta_0$. Let Q be the volume flow rate in the positive r-direction through a section of the slit extending a distance W in the z-direction. In the following the slit is replaced by a line sink of strength Q/W located at the intersection of the planes $\theta = \pm\theta_0$. For a Newtonian fluid the velocity distribution is known to be

$$v_r(r, \theta) = \frac{\alpha}{r}(\cos 2\theta - \cos 2\theta_0); \quad v_\theta = 0; \quad v_z = 0 \tag{6B.11-1}$$

where

$$\alpha = \frac{-Q/W}{\sin 2\theta_0 - 2\theta_0 \cos 2\theta_0} \tag{6B.11-2}$$

a. For a Newtonian fluid with viscosity η_0, show that the equation of motion for creeping flow gives

$$p(r, \theta) = p_\infty + \frac{2\alpha\eta_0}{r^2}\cos 2\theta \tag{6B.11-3}$$

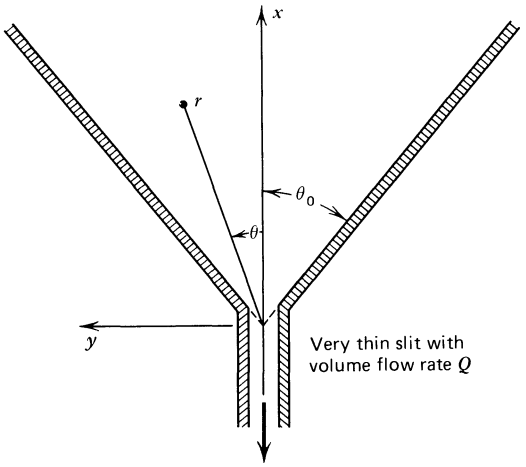

FIGURE 6B.11. Flow from a wedge into a thin slit. The flow is described in a cylindrical (r, θ, z) coordinate system. The z-axis is pointing outward from the plane of the paper.

[3] R. I. Tanner, *Phys. Fluids*, **9**, 1246–1247 (1968).

b. Now use Eq. 6.3-19 to show that the force per unit area exerted by a second-order fluid on the wedge at $\theta = \theta_0$ is

$$[\boldsymbol{\delta}_\theta \cdot \boldsymbol{\pi}]_{\theta=\theta_0} = \left(p_\infty + \frac{2\alpha}{r^2}\eta_0 \cos 2\theta_0 + \frac{\alpha^2}{r^4}\Psi_{1,0}\sin^2 2\theta_0\right)\boldsymbol{\delta}_\theta + \frac{2\alpha}{r^2}\eta_0 \sin 2\theta_0 \boldsymbol{\delta}_r \qquad \text{(6B.11-4)}$$

where $\boldsymbol{\delta}_\theta$ and $\boldsymbol{\delta}_r$ are evaluated at $\theta = \theta_0$.

c. Would it be possible to distinguish between a Newtonian fluid and a second-order fluid by measuring total normal thrust on the surface $\theta = \theta_0$ when $\theta_0 = \pi/2$ with flush-mounted pressure transducers?

Note: In the vicinity of the slit, the second-order terms associated with $\Psi_{1,0}$ are large compared to the Newtonian terms. Hence the second-order fluid is used outside its range of applicability, and the expression in Eq. 6B.11-4 may be devoid of physical significance.

6B.12 The Second-Order Fluid and the "Turntable Experiment"

Suppose that we decided to construct a constitutive equation as follows: We let $\boldsymbol{\tau}$ be a function of $\boldsymbol{\gamma}_{(1)}$ and all of its partial time derivatives $\partial^n\boldsymbol{\gamma}_{(1)}/\partial t^n$. A possibly useful expansion would then be

$$\begin{aligned}\boldsymbol{\tau} = -[&b_1\boldsymbol{\gamma}_{(1)} + b_2\partial\boldsymbol{\gamma}_{(1)}/\partial t + b_{11}\{\boldsymbol{\gamma}_{(1)}\cdot\boldsymbol{\gamma}_{(1)}\} \\ &+ b_3\partial^2\boldsymbol{\gamma}_{(1)}/\partial t^2 + b_{12}\{\boldsymbol{\gamma}_{(1)}\cdot\partial\boldsymbol{\gamma}_{(1)}/\partial t \\ &+ (\partial\boldsymbol{\gamma}_{(1)}/\partial t)\cdot\boldsymbol{\gamma}_{(1)}\} + b_{1:11}(\boldsymbol{\gamma}_{(1)}:\boldsymbol{\gamma}_{(1)})\boldsymbol{\gamma}_{(1)} + \cdots]\end{aligned} \qquad \text{(6B.12-1)}$$

This has the same form as Eq. 6.2-1; in the latter $\boldsymbol{\gamma}_{(n)}$ appears whereas $\partial^{n-1}\boldsymbol{\gamma}_{(1)}/\partial t^{n-1}$ appears in Eq. 6B.12-1. We now study both of these equations in terms of the turntable experiment in Example 5.5-1. We make this comparison using only the terms containing b_1, b_2, and b_{11} (i.e., the second-order fluid).

a. Use the velocity distribution in Eqs. 5.5-3 and 4 to verify the matrix display of $\boldsymbol{\gamma}_{(1)}$ given in Eq. 5.5-5, and then obtain the matrix display for $\{\boldsymbol{\gamma}_{(1)}\cdot\boldsymbol{\gamma}_{(1)}\}$. Next write both of these matrices for $t = 0$ (the time at which the parallel-plate system is lined up with the x-axis).

b. Evaluate $\partial\boldsymbol{\gamma}_{(1)}/\partial t$ and $\boldsymbol{\omega}$ for the flow field in Eqs. 5.5-3 and 4; display in matrix form.

c. Next show that the kinematic tensor $\boldsymbol{\gamma}_{(2)}$ can be written as

$$\boldsymbol{\gamma}_{(2)} = \frac{D}{Dt}\boldsymbol{\gamma}_{(1)} - \{\boldsymbol{\gamma}_{(1)}\cdot\boldsymbol{\gamma}_{(1)}\} + \tfrac{1}{2}\{\boldsymbol{\omega}\cdot\boldsymbol{\gamma}_{(1)} - \boldsymbol{\gamma}_{(1)}\cdot\boldsymbol{\omega}\} \qquad \text{(6B.12-2)}$$

where $\boldsymbol{\omega}$ is the vorticity tensor of Eq. 6.1-3.

d. Use the results of (**b**) and (**c**) to get $\boldsymbol{\gamma}_{(2)}$ at $t = 0$.

e. Display the expression for the stress tensor of a second-order fluid in matrix form for the flow field in Eqs. 5.5-3 and 4 at time $t = 0$. Compare with the second-order fluid terms in Eq. 6.2-4.

f. Do the same for the corresponding terms in Eq. 6B.12-1. Compare the result with that in (**e**). Discuss.

6B.13 Tangential Annular Flow Device for Determining the First Normal Stress Coefficient

Figure 6B.13 shows a flow device that has been suggested for measuring Ψ_1, the first normal stress coefficient. Geiger and Winter[4] list these assumptions in their analysis of the device:

[4] H. R. Osmers and P. F. Lobo, *Trans. Soc. Rheol.*, **20**, 239–252 (1976); K. Geiger and H. H. Winter, *Rheol. Acta*, **17**, 264–273 (1978).

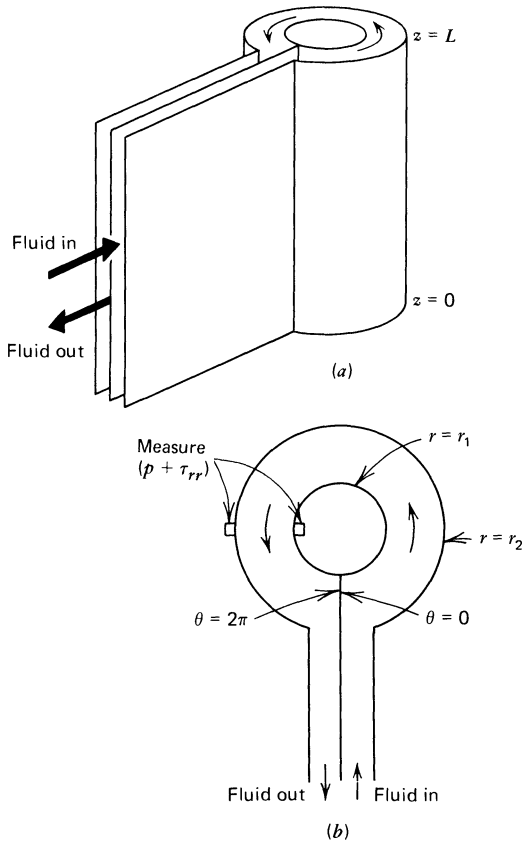

FIGURE 6B.13. Tangential annular flow device for measuring Ψ_1: (*a*) view of exterior of apparatus; (*b*) top view.

- **i.** The centrifugal force in the r-component of the equation of motion can be neglected.
- **ii.** Entrance and exit effects are neglected (i.e., near $\theta = 0$ and $\theta = 2\pi$).
- **iii.** Top and bottom effects are neglected (i.e., near $z = 0$, L).
- **iv.** $\partial p/\partial\theta$ is independent of r, and can be set equal to $-(p_0 - p_{2\pi})/2\pi \equiv -\Delta p/2\pi$.
- **v.** The system is isothermal.
- **vi.** The rheological properties are pressure-independent.
- **vii.** The fluid is incompressible.
- **viii.** There is no fluid slip at the solid surfaces.

It is postulated that $v_\theta = v_\theta(r)$, $v_r = 0$, $v_z = 0$, and $p = p(r, \theta)$. In the flow experiment one measures the tangential pressure drop Δp, the volume rate of flow Q, and the difference in "pressure readings" across the gap $\Delta\pi_{rr} = (p + \tau_{rr})|_{r=r_1} - (p + \tau_{rr})|_{r=r_2}$.

Geiger and Winter give an elaborate analysis for any kind of viscoelastic fluid. Here for the sake of simplicity, we analyze the apparatus for a second-order fluid.

a. For the postulated velocity profile write out the second-order fluid in matrix form (with components in the order r, θ, z).

b. From (**a**) obtain the expressions for the shear stress $\tau_{r\theta}$ and the first normal stress difference $\tau_{\theta\theta} - \tau_{rr}$.

c. Integrate the appropriately simplified r-component of the equation of motion from $r = r_1$ (inner cylinder) to $r = r_2$ (outer cylinder). Show that this leads to an expression for $\Delta\pi_{rr}$ as an integral involving $\tau_{\theta\theta} - \tau_{rr}$.

d. Substitute $\tau_{\theta\theta} - \tau_{rr}$ from (**b**) into the integral in (**c**) and obtain

$$\Delta\pi_{rr} = 2b_2 \int_{r_1}^{r_2} \left[r \frac{\partial}{\partial r}\left(\frac{v_\theta}{r}\right)\right]^2 \frac{dr}{r} \tag{6B.13-1}$$

e. Combine $\tau_{r\theta}$ from (**b**) and the θ-component of the equation of motion to get an ordinary differential equation for $v_\theta(r)$. Show that this can be integrated to give

$$\frac{v_\theta}{r} = \frac{\Delta p}{4\pi b_1}\left[\frac{\kappa^2 \ln \kappa}{\kappa^2 - 1}\left[1 - \left(\frac{r_2}{r}\right)^2\right] - \ln\frac{r}{r_2}\right] \tag{6B.13-2}$$

where $\kappa = r_1/r_2$.

f. By combining the results of (**d**) and (**e**) and performing the integration, obtain an expression for b_2 in terms of the measurable quantities $\Delta\pi_{rr}$ and Δp, the cylinder radii r_1 and r_2, and the zero-shear-rate viscosity b_1.

g. Finally, derive an equation for the volume flow rate from which b_1 may be determined.

6B.14 Centripetal Pumping between Parallel Disks[5]

Two disks are separated by a fixed distance H, and the upper disk is joined to a circular tube (see Fig. 6B.14). The upper disk is rotated with a constant angular velocity $W_0\delta_z$. For a Newtonian fluid the rotation of the upper disk would cause a centrifugal force that would tend to suck the fluid downward out of the tube. For viscoelastic fluids, on the other hand, the normal stresses may cause the fluid to flow inward through the space between the disks and upward through the tube.

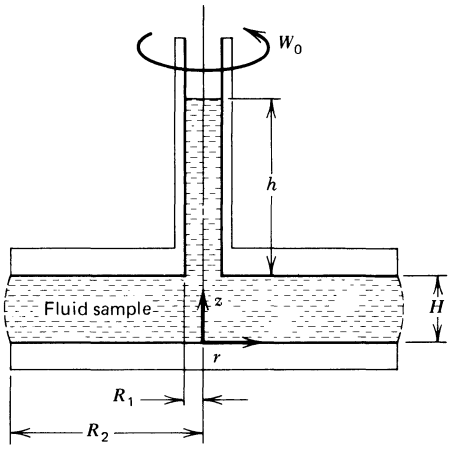

FIGURE 6B.14. Centripetal pumping in a disk-tube assembly. The viscoelastic fluid is pumped radially inward and up into the tube because of the action of normal stresses.

[5] Y. Tomita and H. Katō, *Trans. Jpn. Soc. Mech. Eng.* (*Nippon Kikai Gakkai Ronbunshū*), **32**, 241, 1399-1408 (Sept. 1966); B. Maxwell and A. J. Scalora, *Mod. Plast.*, **37**(2), 107 (1959); P. A. Good, A. J. Schwartz, and C. W. Macosko, *AIChE J.*, **20**, 67-73 (1974). Note that where we have 1/6 in Eq. 6B.14-7, a more detailed analysis gives 3/20 [K. Stewartson, *Proc. Camb. Phil. Soc.*, **49**, 333-341 (1953)]. For a discussion of tangential flow with slow superimposed radial flow see D. F. James, *Trans. Soc. Rheol.*, **19**, 67-80 (1975).

The complete calculation of the centripetal pumping is quite difficult, inasmuch as it is not a viscometric flow. However, it is relatively easy to use Eq. 6.2-1 to find out what pressure difference must be maintained between "1" and "2" in order to prevent flow. Find the height to which the fluid will rise in the tube to balance the normal stresses tending to drive the fluid up the tube.

a. Before doing the viscoelastic fluid calculations, it is instructive to solve the problem for the Newtonian fluid, to find the pressure difference required to prevent radially outward flow because of centrifugal effects. Make the postulate that $v_\theta = zf(r)$, $v_r = v_z = 0$; then show that the r-, θ-, and z-components of the equation of motion become

$$-\rho\frac{z^2f^2}{r} = -\frac{\partial p}{\partial r} \tag{6B.14-1}$$

$$0 = \mu\frac{d}{dr}\left(\frac{1}{r}\frac{d}{dr}(rf)\right) \tag{6B.14-2}$$

$$0 = -\frac{\partial p}{\partial z} - \rho g \tag{6B.14-3}$$

The first of these describes the balance between the centrifugal force and the radial pressure gradient. Solve the second equation to get the velocity distribution

$$v_\theta = \frac{W_0 rz}{H} \tag{6B.14-4}$$

Insert this into Eq. 6B.14-1 to get

$$-\rho W_0^2 r\left(\frac{z}{H}\right)^2 = -\frac{\partial p}{\partial r} \tag{6B.14-5}$$

It can now be seen that Eqs. 6B.14-3 and 5 are inconsistent, since the two equations give different results for the mixed second derivative $\partial^2 p/\partial r\partial z$. This means that the assumption made prior to Eq. 6B.14-1 regarding the velocity field is incorrect, and that strictly speaking secondary flows must be allowed for. To get an approximate expression for the radial pressure gradient, however, take an average of Eq. 6B.14-5 in the z-direction to get

$$-\frac{\rho W_0^2 r}{3} = -\frac{d\bar{p}}{dr} \tag{6B.14-6}$$

where $\bar{p} = (\int_0^H p dz)/H$. Then integrate this equation to get

$$\bar{p}_2 - \bar{p}_1 = \tfrac{1}{6}\rho W_0^2(R_2^2 - R_1^2) \tag{6B.14-7}$$

We see that we have to push harder at "2" than at "1" to keep the fluid from being thrown out of the gap.

b. Next rework the problem for the second-order fluid. For the velocity distribution in Eq. 6B.14-4 show that the stress tensor may be displayed in matrix form:

$$\boldsymbol{\tau} = -b_1\begin{pmatrix}0&0&0\\0&0&1\\0&1&0\end{pmatrix}\frac{W_0 r}{H} + 2b_2\begin{pmatrix}0&0&0\\0&1&0\\0&0&0\end{pmatrix}\frac{W_0^2 r^2}{H^2} - b_{11}\begin{pmatrix}0&0&0\\0&1&0\\0&0&0\end{pmatrix}\frac{W_0^2 r^2}{H^2} \tag{6B.14-8}$$

Show that the second-order fluid analog to Eq. 6B.14-7 is

$$\bar{p}_2 - \bar{p}_1 = \frac{1}{6}\rho W_0^2(R_2^2 - R_1^2) + (2b_2 - b_{11})\frac{W_0^2}{2H^2}(R_2^2 - R_1^2) \tag{6B.14-9}$$

and finally that the height of rise of the fluid in the tube is

$$h = -\frac{W_0^2}{6g}(R_2^2 - R_1^2) - \frac{W_0^2}{2\rho g H^2}(2b_2 - b_{11})(R_2^2 - R_1^2) \tag{6B.14-10}$$

Interpret the result. The centripetal pumping has been observed experimentally and it has been used in plastics processing.[6]

6B.15 The Hole Pressure for Creeping Flow of a Second-Order Fluid Across a Transverse Slot[7]

Consider a plane flow across the deep, transverse slot shown in Fig. 2.3-4. Sufficiently far upstream and downstream from the slot, the fluid is flowing in the x-direction. It is desired to obtain an expression for the hole pressure p^* defined in §2.3c, for the pressure-driven, creeping flow of an incompressible, second-order fluid. Assume that the slot is so deep that the shear rate is zero at the bottom of the slot. Assume also that the presence of the slot does not significantly alter the flow near the plane $y = B$ so that the shear rate at the wall $y = B$, denoted by $\dot{\gamma}_w$, is a constant, independent of x.

a. Show that the plane $x = 0$ is a plane of symmetry for creeping flow of an incompressible Newtonian fluid, and that consequently $\partial\tau_{yx}/\partial x = 0$ along the line $x = 0$.

b. Then show from the y-component of the equation of motion that $\partial(\mathscr{P} + \tau_{yy})/\partial y = 0$ along the line $x = 0$, and that consequently $p^* = 0$ for plane creeping flow of an incompressible Newtonian fluid.

c. Finally use the expression in Eq. 6.3-19 to show that:

$$p^* = (1/4)\Psi_{1,0}\dot{\gamma}_w^2 \tag{6B.15-1}$$

for plane, creeping flow of an incompressible second-order fluid across a deep transverse slot.

6C.1 Stability of Second-Order Fluids[8]

Consider a second-order fluid of density ρ that fills the gap between two fixed plates of separation H as shown in Fig. 6C.1. Prior to time $t = 0$ the fluid is at rest. Then at $t = 0$ the fluid is subjected to a small velocity disturbance of the form $v_x = U(y)$, $v_y = v_z = 0$.

a. Assume that the velocity field for $t \geq 0$ is of the form $v_x = v_x(y, t)$, $v_y = v_z = 0$ with the conditions that $v_x(0, t) = v_x(H, t) = 0$. Show that v_x must satisfy

$$\rho\frac{\partial v_x}{\partial t} = b_1\left[\underbrace{\frac{\partial^2 v_x}{\partial y^2}}_{(1)} + \underbrace{\frac{b_2}{b_1}\frac{\partial}{\partial t}\frac{\partial^2 v_x}{\partial y^2}}_{(2)}\right] \tag{6C.1-1}$$

where term (2) on the right-hand side must be a small correction to term (1) for the constitutive equation to apply.

[6] Z. Tadmor and C. G. Gogos, *Principles of Polymer Processing*, Wiley, New York, (1979), p. 372.

[7] R. I. Tanner and A. C. Pipkin, *Trans. Soc. Rheol.*, **13**, 471-484 (1969).

[8] A. C. Pipkin, *Lectures in Viscoelasticity Theory*, Springer Verlag, New York (1972).

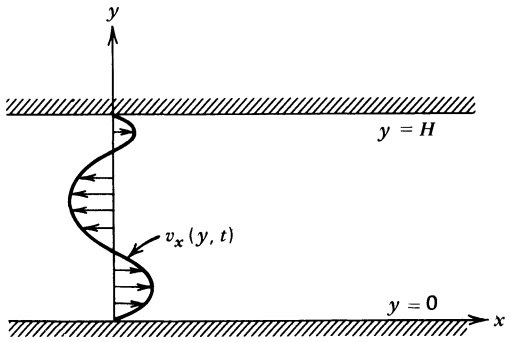

FIGURE 6C.1. A second-order fluid is contained in the gap between two parallel plates. At time $t = 0$ the velocity field is of the form $v_x = U(y), v_y = v_z = 0$ with the conditions that $U(0) = U(H) = 0$. The plates are fixed at all times $t \geq 0$, and there is no pressure gradient other than that due to gravity.

b. Solve this equation by separation of variables to obtain formally

$$v_x(y, t) = \sum_{n=1}^{\infty} A_n \sin(n\pi y/H) \exp(\alpha_n t) \tag{6C.1-2}$$

where

$$A_n = \frac{2}{H} \int_0^H U(y) \sin(n\pi y/H)\, dy \tag{6C.1-3}$$

and

$$\alpha_n = -\left(\frac{b_2}{b_1} + \frac{\rho H^2}{b_1 n^2 \pi^2}\right)^{-1} \tag{6C.1-4}$$

where the α_n must be negative for the disturbances to die out.

c. Assume that the above solution must remain valid for all Fourier components, that is all values of n, and show that this results in the following necessary condition for the second-order fluid to be stable at rest

$$b_2/b_1 \geq 0 \quad \text{or} \quad \Psi_{1,0} \leq 0 \tag{6C.1-5}$$

d. Show that the condition for term (2) in Eq. 6C.1-1 to be small compared to term (1) may be formulated as

$$|\alpha_n(b_2/b_1)| \ll 1 \tag{6C.1-6}$$

for each Fourier mode n of the initial disturbance.

e. Finally show that if the initial disturbance is sufficiently smooth so that condition 6C.1-6 holds for all n with non-zero A_n then the corresponding α_n are all negative. Conclude that the condition in Eq. 6C.1-5 is then no longer necessary and that, within the range of validity of the solution and the assumed form of the velocity field, the disturbance will die out irrespective of the sign of $\Psi_{1,0}$.

6C.2 Flow of a Second-Order Fluid near a Corner

a. Review Problem 1C.3 for the plane flow of a Newtonian fluid near a sharp corner. Show that the stresses near the corner have the following dependence on the radial coordinate

$$\tau_{ij} \sim A_{ij} r^{\lambda_1 - 2} \qquad (r \to 0) \tag{6C.2-1}$$

where the A_{ij} are bounded functions of θ.

b. Use the plane-flow theorem of Tanner and Pipkin to show that the equations for plane flow of an incompressible second-order fluid are satisfied by the same velocity field, and that the stresses near the corner are

$$\tau_{ij} \sim B_{ij} r^{\lambda_1 - 2} \qquad (r \to 0) \tag{6C.2-2}$$

where the B_{ij} are bounded functions of θ.

c. Compare the Newtonian and second-order contributions to the stresses, and conclude that the retarded-motion expansion should not be used unless $\lambda_1 \geq 2$.

d. Compare this value with those in Table 1C.3, and give examples of flow situations where the retarded-motion expansion can be used, and examples where it definitely should not be used.

CHAPTER 7

DIFFERENTIAL CONSTITUTIVE EQUATIONS

In Chapters 4, 5, and 6 we have encountered constitutive equations that are useful in three different flow regimes and for three different groups of people. The generalized Newtonian fluid model of Chapter 4 is restricted to steady-state shear flows and has been primarily used by engineers; the material information in the generalized Newtonian fluid model is contained in the viscosity $\eta(\dot{\gamma})$. In Chapter 5 we presented the linear viscoelastic fluid model which is restricted to small-displacement-gradient flows and has been primarily useful to chemists; the material information in this model is given by the relaxation modulus $G(t)$. Then in Chapter 6, the retarded-motion expansion, valid for slow, slowly varying flows, was presented. The retarded-motion expansion is of interest mostly to applied mathematicians and physicists; the material information is contained in the constants $b_1, b_2, b_{11}, \ldots$. Up to this point we have made no connection between $\eta(\dot{\gamma})$, $G(t)$, and the b's, except for $b_1 = \eta(0) = \int_0^\infty G(t)dt$.

In this chapter we first seek more general constitutive equations that can be used for arbitrary flows. It should be possible, of course, to simplify these more general constitutive equations to include the special models of Chapters 4, 5, and 6, but we also want to describe, at least qualitatively, as much additional nonlinear rheological material behavior in Chapter 3 as possible. Second, we want to focus attention on applying these constitutive equations to solving polymer fluid flow problems.

We begin the task of constructing more general, "admissible" constitutive equations by modifying the linear viscoelastic models of Chapter 5, which are valid for any time-dependent flow with small displacement gradients. In this chapter we modify these in their differential forms by replacing the time derivatives by convected derivatives as introduced in Chapter 6. In the next chapter we show how to get admissible equations by starting with the integral forms of the models. Constitutive equations obtained by reformulating the linear viscoelastic models are called *quasi-linear models.*

Once we see the kinds of rheological properties that can be predicted by the quasi-linear models, we will explore several ways in which they can be altered in order to obtain better agreement with the material functions presented in Chapter 3. This leads to the discussion of *nonlinear models* in §§7.3 and 8.3. Several of these nonlinear models describe, at least qualitatively, a wide variety of the material functions of Chapter 3; in particular, they show the well-known decrease of η and Ψ_1 with increasing $\dot{\gamma}$.

Once the rheological models have been presented, we turn to the primary task of solving fluid flow problems. For the most part these are solved here with the quasi-linear models so that we can illustrate the methods without becoming overcome with tedious algebra or numerical analysis; however, we do show some results for nonlinear models to

emphasize the influence of differences in choice of constitutive equations on the calculated flow fields.

The illustration of problem solving is broken down into two sections: the first for problems involving one spatial variable (and possibly time) and the second for problems involving two or three spatial variables (and possibly time). As will be clear from the discussion and examples in these sections, success in obtaining analytical solutions to viscoelastic flow problems has been limited to situations in which the problem is either one-dimensional or can be reduced to one dimension by means of similarity or periodic solutions.

Finally in the last section we point out the limitations of the differential models and give recommendations for situations in which the different constitutive equations should be used.

§7.1 THE CONVECTED DERIVATIVE OF THE STRESS TENSOR

In Chapter 6 we introduced the convected time derivatives of the rate-of-strain tensor. In this chapter we introduce the *convected time derivative of the stress tensor*[1,2] $\boldsymbol{\tau}_{(1)}$ defined by (cf. Eq. 6.1-6)

$$\begin{aligned}\boldsymbol{\tau}_{(1)} &= \frac{D}{Dt}\boldsymbol{\tau} - \{(\nabla \boldsymbol{v})^{\dagger}\cdot\boldsymbol{\tau} + \boldsymbol{\tau}\cdot(\nabla \boldsymbol{v})\} \\ &= \frac{D}{Dt}\boldsymbol{\tau} - \{\boldsymbol{\tau}\cdot\nabla \boldsymbol{v}\}^{\dagger} - \{\boldsymbol{\tau}\cdot\nabla \boldsymbol{v}\} \quad \text{(for symmetric } \boldsymbol{\tau}\text{)}\end{aligned} \tag{7.1-1}$$

In Chapter 9 we will show that $\boldsymbol{\tau}_{(1)}$ is a time derivative of stress that has a significance independent of superposed rotations. We can thus construct admissible constitutive equations from the differential linear viscoelastic models of Chapter 5 by replacing $\partial\boldsymbol{\tau}/\partial t$ by $\boldsymbol{\tau}_{(1)}$ and $\partial^n\dot{\boldsymbol{\gamma}}/\partial t^n$ by $\boldsymbol{\gamma}_{(n+1)}$.

In evaluating the quantities $\boldsymbol{\tau}_{(1)}$ and $\boldsymbol{\gamma}_{(n)}$ in differential constitutive equations it is convenient to use expressions for these that are tabulated in Appendix C for time-dependent

[1] In Chapter 9 this is referred to as the *contravariant convected time derivative* to distinguish it from the covariant convected time derivative denoted by a superscript (1). In this chapter we use only the former, and "contravariant" is implied in the phrase "convected time derivative."

[2] The method we use in this chapter for generating admissible equations is not unique. Instead of using convected time derivatives of the stress and rate-of-strain tensors in constitutive equations we could use the corotational or Jaumann derivative $\mathscr{D}/\mathscr{D}t$ defined by

$$\begin{aligned}\frac{\mathscr{D}}{\mathscr{D}t}\boldsymbol{\tau} &= \frac{D}{Dt}\boldsymbol{\tau} + \tfrac{1}{2}\{\boldsymbol{\omega}\cdot\boldsymbol{\tau} - \boldsymbol{\tau}\cdot\boldsymbol{\omega}\} \\ &= \boldsymbol{\tau}_{(1)} + \tfrac{1}{2}\{\dot{\boldsymbol{\gamma}}\cdot\boldsymbol{\tau} + \boldsymbol{\tau}\cdot\dot{\boldsymbol{\gamma}}\}\end{aligned} \tag{7.1-1a}$$

The second line of Eq. 7.1-1a makes it clear that constitutive equations written with the corotational derivative can easily be rewritten in terms of the convected derivative and vice versa. The idea of the corotational derivative is quite old. See, for example, S. Zaremba, *Bull. Int. Acad. Sci. Cracovie*, 594–614, 614–621 (1903); G. Jaumann, *Grundlagen der Bewegungslehre*, Leipzig (1905), *Sitzungsberichte Akad. Wiss. Wien IIa*, **120**, 385–530 (1911); H. Fromm, *Z. Angew. Math. Mech.*, **25/27**, 146–150 (1947); **28**, 43–54 (1948); J. G. Oldroyd, *Proc. Roy. Soc.*, **A245**, 278–297 (1958); and J. D. Goddard and C. Miller, *Rheol. Acta*, **5**, 177–184 (1966). The first edition of *Dynamics of Polymeric Liquids* (Volume 1) contains an extensive discussion of the corotational derivative and corotational models. In addition, see H. Giesekus, *Rheol. Acta*, **3**, 59–71 (1963); *Zeits. f. angew. Math. u. Mech.*, **42**, 32–61 (1962).

shear and shearfree flows. In addition the contributions needed to evaluate $\boldsymbol{\tau}_{(1)}$ and $\boldsymbol{\gamma}_{(n)}$ are given in Appendix A for several orthogonal, curvilinear coordinate systems.

EXAMPLE 7.1-1 The Convected Derivative of the Stress Tensor for Simple Shear Flow

Show how the entry for $\boldsymbol{\tau}_{(1)}$ in Appendix C is obtained for a time-dependent simple shear flow $v_x = \dot{\gamma}_{yx}(t)y$, $v_y = v_z = 0$.

SOLUTION For simple shear flow the stress tensor is given in Eq. 3.2-1 and the velocity gradient and its transpose are shown in Eq. 6.1-7. To evaluate $\boldsymbol{\tau}_{(1)}$ we insert these into Eq. 7.1-1 and perform the indicated matrix multiplications. In this way we obtain

$$\begin{aligned}
\boldsymbol{\tau}_{(1)} &= \frac{\partial}{\partial t}\begin{pmatrix} \tau_{xx} & \tau_{yx} & 0 \\ \tau_{yx} & \tau_{yy} & 0 \\ 0 & 0 & \tau_{zz} \end{pmatrix} + \underline{v_x \frac{\partial}{\partial x}\begin{pmatrix} \tau_{xx} & \tau_{yx} & 0 \\ \tau_{yx} & \tau_{yy} & 0 \\ 0 & 0 & \tau_{zz} \end{pmatrix}} \\
&\quad - \begin{pmatrix} 0 & \dot{\gamma}_{yx} & 0 \\ 0 & 0 & 0 \\ 0 & 0 & 0 \end{pmatrix}\begin{pmatrix} \tau_{xx} & \tau_{yx} & 0 \\ \tau_{yx} & \tau_{yy} & 0 \\ 0 & 0 & \tau_{zz} \end{pmatrix} - \begin{pmatrix} \tau_{xx} & \tau_{yx} & 0 \\ \tau_{yx} & \tau_{yy} & 0 \\ 0 & 0 & \tau_{zz} \end{pmatrix}\begin{pmatrix} 0 & 0 & 0 \\ \dot{\gamma}_{yx} & 0 & 0 \\ 0 & 0 & 0 \end{pmatrix} \\
&= \frac{\partial}{\partial t}\begin{pmatrix} \tau_{xx} & \tau_{yx} & 0 \\ \tau_{yx} & \tau_{yy} & 0 \\ 0 & 0 & \tau_{zz} \end{pmatrix} - \dot{\gamma}_{yx}\begin{pmatrix} 2\tau_{yx} & \tau_{yy} & 0 \\ \tau_{yy} & 0 & 0 \\ 0 & 0 & 0 \end{pmatrix}
\end{aligned} \tag{7.1-2}$$

Note that the dashed-underline term arising in the substantial derivative is zero because the flow is homogeneous (i.e., the shear rate is independent of position) so that the stress tensor components do not depend on x, y, and z.

EXAMPLE 7.1-2 Calculation of $\boldsymbol{\tau}_{(1)}$ for Flow between Parallel Disks

A viscoelastic fluid is undergoing time-dependent torsional flow between parallel disks; the velocity field is assumed to be axisymmetric so that we write $v_r = v_r(r, z, t)$, $v_\theta = v_\theta(r, z, t)$, and $v_z = v_z(r, z, t)$. Determine $\boldsymbol{\tau}_{(1)}$ for this flow.

SOLUTION From the definition of the convected derivative in Eq. 7.1-1 (second line) we see that it is necessary to evaluate $\{\boldsymbol{v}\cdot\nabla\boldsymbol{\tau}\}$ and $\{\boldsymbol{\tau}\cdot\nabla\boldsymbol{v}\}$. The components of $\{\boldsymbol{v}\cdot\nabla\boldsymbol{\tau}\}$ are listed in cylindrical coordinates in Table A.7-2, Eqs. BB through JJ; we take those results over here by discarding terms involving $\partial/\partial\theta$ and by using the symmetry of $\boldsymbol{\tau}$. Similarly, we take the components of $\nabla\boldsymbol{v}$ from Eqs. S through AA of Table A.7-2, with $\partial(\cdot)/\partial\theta = 0$. When the matrix formed from these components is premultiplied by the matrix for $\boldsymbol{\tau}$ in cylindrical coordinates we obtain a matrix representation of $\{\boldsymbol{\tau}\cdot\nabla\boldsymbol{v}\}$. Adding this to its transpose gives, for example

$$[\{\boldsymbol{\tau}\cdot\nabla\boldsymbol{v}\}^\dagger + \{\boldsymbol{\tau}\cdot\nabla\boldsymbol{v}\}]_{rr} = 2\left[\tau_{rr}\frac{\partial v_r}{\partial r} + \tau_{r\theta}\left(-\frac{v_\theta}{r}\right) + \tau_{rz}\frac{\partial v_r}{\partial z}\right] \tag{7.1-3}$$

$$[\{\boldsymbol{\tau}\cdot\nabla\boldsymbol{v}\}^\dagger + \{\boldsymbol{\tau}\cdot\nabla\boldsymbol{v}\}]_{r\theta} = \left[\tau_{rr}\frac{\partial v_\theta}{\partial r} + \tau_{r\theta}\left(\frac{v_r}{r} + \frac{\partial v_r}{\partial r}\right) + \tau_{rz}\frac{\partial v_\theta}{\partial z} - \tau_{\theta\theta}\frac{v_\theta}{r} + \tau_{\theta z}\frac{\partial v_r}{\partial z}\right] \tag{7.1-4}$$

In a similar way the rz-, $\theta\theta$-, θz-, and zz-components can be obtained. When the various contributions to $\boldsymbol{\tau}_{(1)}$ are put together we obtain:

$$\tau_{(1)rr} = \frac{\partial \tau_{rr}}{\partial t} + v_r \frac{\partial}{\partial r}\tau_{rr} + v_z \frac{\partial}{\partial z}\tau_{rr} - 2\tau_{rr}\frac{\partial v_r}{\partial r} - 2\tau_{rz}\frac{\partial v_r}{\partial z} \tag{7.1-5}$$

$$\tau_{(1)r\theta} = \frac{\partial \tau_{r\theta}}{\partial t} + v_r \frac{\partial}{\partial r}\tau_{r\theta} + v_z \frac{\partial}{\partial z}\tau_{r\theta} + \tau_{rr}\left(\frac{v_\theta}{r} - \frac{\partial v_\theta}{\partial r}\right) - \tau_{r\theta}\left(\frac{v_r}{r} + \frac{\partial v_r}{\partial r}\right) - \tau_{rz}\frac{\partial v_\theta}{\partial z} - \tau_{\theta z}\frac{\partial v_r}{\partial z} \tag{7.1-6}$$

$$\tau_{(1)rz} = \frac{\partial \tau_{rz}}{\partial t} + v_r \frac{\partial}{\partial r}\tau_{rz} + v_z \frac{\partial}{\partial z}\tau_{rz} - \tau_{rr}\frac{\partial v_z}{\partial r} - \tau_{rz}\left(\frac{\partial v_z}{\partial z} + \frac{\partial v_r}{\partial r}\right) - \tau_{zz}\frac{\partial v_r}{\partial z} \tag{7.1-7}$$

$$\tau_{(1)\theta\theta} = \frac{\partial \tau_{\theta\theta}}{\partial t} + v_r \frac{\partial}{\partial r}\tau_{\theta\theta} + v_z \frac{\partial}{\partial z}\tau_{\theta\theta} - 2\tau_{\theta\theta}\frac{v_r}{r} + 2\tau_{r\theta}\left(\frac{v_\theta}{r} - \frac{\partial v_\theta}{\partial r}\right) - 2\tau_{\theta z}\frac{\partial v_\theta}{\partial z} \tag{7.1-8}$$

$$\tau_{(1)\theta z} = \frac{\partial \tau_{\theta z}}{\partial t} + v_r \frac{\partial}{\partial r}\tau_{\theta z} + v_z \frac{\partial}{\partial z}\tau_{\theta z} + \tau_{rz}\left(\frac{v_\theta}{r} - \frac{\partial v_\theta}{\partial r}\right) - \tau_{\theta z}\left(\frac{v_r}{r} + \frac{\partial v_z}{\partial z}\right) - \tau_{r\theta}\frac{\partial v_z}{\partial r} - \tau_{zz}\frac{\partial v_\theta}{\partial z} \tag{7.1-9}$$

$$\tau_{(1)zz} = \frac{\partial \tau_{zz}}{\partial t} + v_r \frac{\partial}{\partial r}\tau_{zz} + v_z \frac{\partial}{\partial z}\tau_{zz} - 2\tau_{rz}\frac{\partial v_z}{\partial r} - 2\tau_{zz}\frac{\partial v_z}{\partial z} \tag{7.1-10}$$

We will need Eqs. 7.1-5 through 10 in working Example 7.5-2.

EXAMPLE 7.1-3 Evaluation of $\boldsymbol{\tau}_{(1)}$ for Steady Shear Flow Plus Superposed Rotation

Find the components of $\boldsymbol{\tau}_{(1)}$ in the fixed coordinate system (i.e., $\tau_{(1)xx}$, $\tau_{(1)yy}$, and $\tau_{(1)yx}$) for the "turntable flow" described in Example 5.5-1. These components are to be evaluated at the instant $t = 0$, when the $\bar{x}$- and $\bar{y}$-axes coincide with the x- and y-axes.

SOLUTION At any time t the components of the tensor $\boldsymbol{\tau}$ in the xyz-system are related to those in the $\bar{x}\bar{y}\bar{z}$-system by a coordinate transformation

$$\tau_{mn} = \sum_{\bar{m}}\sum_{\bar{n}} \Omega_{m\bar{m}}\Omega_{n\bar{n}}\tau_{\bar{m}\bar{n}} \tag{7.1-11}$$

in which the $\Omega_{m\bar{m}}$ are the elements of a rotation matrix that accounts for the fact that the $\bar{x}\bar{y}\bar{z}$-system is "tilted" with respect to the xyz-system in Fig. 5.5-1

$$(\Omega_{m\bar{m}}) = \begin{pmatrix} \cos Wt & -\sin Wt & 0 \\ \sin Wt & \cos Wt & 0 \\ 0 & 0 & 1 \end{pmatrix} \tag{7.1-12}$$

Let us now obtain expressions for the various terms that make up $\boldsymbol{\tau}_{(1)}$ in Eq. 7.1-1.

First we get $\partial\boldsymbol{\tau}/\partial t$ at $t = 0$. This is done by using Eq. 7.1-12 in Eq. 7.1-11, differentiating the latter with respect to t, and then setting t equal to zero. This gives

$$\frac{\partial}{\partial t}\begin{pmatrix}\tau_{xx} & \tau_{xy} & \tau_{xz}\\ \tau_{yx} & \tau_{yy} & \tau_{yz}\\ \tau_{zx} & \tau_{zy} & \tau_{zz}\end{pmatrix} = \begin{pmatrix}-2\tau_{\bar{y}\bar{x}} & \tau_{\bar{x}\bar{x}} - \tau_{\bar{y}\bar{y}} & 0\\ \tau_{\bar{x}\bar{x}} - \tau_{\bar{y}\bar{y}} & 2\tau_{\bar{y}\bar{x}} & 0\\ 0 & 0 & 0\end{pmatrix}_{t=0} W \tag{7.1-13}$$

Note that $\partial\boldsymbol{\tau}/\partial t$ depends on the rate of rotation of the turntable, and therefore $\partial\boldsymbol{\tau}/\partial t$ is not admissible in a constitutive equation. The term $\{\boldsymbol{v}\cdot\nabla\boldsymbol{\tau}\}$ is zero, because the flow is homogeneous.

Next the $\nabla\boldsymbol{v}$ tensor must be calculated using the velocity profile in Eqs. 5.5-3 and 4. This gives

$$\nabla\boldsymbol{v} = \begin{pmatrix}-\dot{\gamma}\sin Wt\cos Wt & -\dot{\gamma}\sin^2 Wt + W & 0\\ \dot{\gamma}\cos^2 Wt - W & \dot{\gamma}\sin Wt\cos Wt & 0\\ 0 & 0 & 0\end{pmatrix} \xrightarrow{t=0} \begin{pmatrix}0 & W & 0\\ \dot{\gamma} - W & 0 & 0\\ 0 & 0 & 0\end{pmatrix} \tag{7.1-14}$$

Therefore, at $t = 0$

$$-\{\boldsymbol{\tau}\cdot\nabla\boldsymbol{v}\} = \begin{pmatrix}(W-\dot{\gamma})\tau_{\bar{y}\bar{x}} & -W\tau_{\bar{x}\bar{x}} & 0\\ (W-\dot{\gamma})\tau_{\bar{y}\bar{y}} & -W\tau_{\bar{y}\bar{x}} & 0\\ 0 & 0 & 0\end{pmatrix} \tag{7.1-15}$$

and $-\{(\nabla\boldsymbol{v})^\dagger\cdot\boldsymbol{\tau}\}$ is given by the transpose of this matrix.

If we now combine the various contributions to $\boldsymbol{\tau}_{(1)}$ above, we get at $t = 0$

$$\begin{pmatrix}\tau_{(1)xx} & \tau_{(1)xy} & \tau_{(1)xz}\\ \tau_{(1)yx} & \tau_{(1)yy} & \tau_{(1)yz}\\ \tau_{(1)zx} & \tau_{(1)zy} & \tau_{(1)zz}\end{pmatrix} = -\begin{pmatrix}2\tau_{yx} & \tau_{yy} & 0\\ \tau_{yy} & 0 & 0\\ 0 & 0 & 0\end{pmatrix}\dot{\gamma} \tag{7.1-16}$$

Here we have made use of the fact that $\tau_{\bar{m}\bar{n}} = \tau_{mn}$ at $t = 0$. It is thus seen that $\boldsymbol{\tau}_{(1)}$ does not contain W, the angular velocity of the turntable, and this is consistent with our assertion that it is admissible in a constitutive equation. It should be noted that the matrix in Eq. 7.1-16 is identical to that appearing in Eq. 7.1-2 for steady shear flow. We can think of $\boldsymbol{\tau}_{(1)}$ as being a special kind of time derivative which, unlike $\partial\boldsymbol{\tau}/\partial t$, "filters out" the effect of local rotation of the fluid.

If we calculate τ_{yx} at $t = 0$ in the system in Fig. 5.5-1 using the *linear Maxwell model* of Eq. 5.2-2, we find that $\tau_{yx}(t=0) = -\eta_0\dot{\gamma}/(1 + 4\lambda_1^2 W^2)$; this result shows (incorrectly) that the shear stress depends on the rate of rotation of the turntable. If, on the other hand, we replace $\partial\boldsymbol{\tau}/\partial t$ by $\boldsymbol{\tau}_{(1)}$ to get the *convected Maxwell model*, as we do in the next section, we will get $\tau_{yx}(t=0) = -\eta_0\dot{\gamma}$, with no dependence on W.

§7.2 QUASI-LINEAR DIFFERENTIAL MODELS

In this section we illustrate the construction of admissible constitutive equations by the procedure described in the preceding section. Because the Jeffreys model of Eq. 5.2-9 is known to describe linear viscoelastic behavior qualitatively, we use it to generate a quasi-linear model. This is done by replacing the partial time derivatives in the differential form of the Jeffreys model with the convected time derivatives to obtain the *convected Jeffreys model*[1] or *Oldroyd's fluid B*:[2]

$$\boxed{\boldsymbol{\tau} + \lambda_1\boldsymbol{\tau}_{(1)} = -\eta_0(\boldsymbol{\gamma}_{(1)} + \lambda_2\boldsymbol{\gamma}_{(2)})} \tag{7.2-1}$$

[1] In Chapter 9 this will be referred to as the "contravariant convected Jeffreys model" to distinguish it from the "covariant convected Jeffreys model" or Oldroyd's fluid A.

[2] J. G. Oldroyd, *Proc. Roy. Soc.*, **A200**, 523-541 (1950).

This constitutive equation contains three parameters: η_0, the zero-shear-rate viscosity; λ_1, the relaxation time; and λ_2, the retardation time. The kinematic tensors are those defined in §6.1 and used in the retarded-motion expansion. The convected Jeffreys model contains several other models as special cases:

- **a.** If $\lambda_2 = 0$, the model reduces to the "convected Maxwell model."[3] The convected Maxwell model has been widely used for viscoelastic flow calculations, because of its simplicity.
- **b.** If $\lambda_1 = 0$, the model simplifies to a second-order fluid with a vanishing second normal stress coefficient (see Eq. 6.2-1 with only the constants b_1 and b_2 nonzero).
- **c.** If $\lambda_1 = \lambda_2$, the model reduces to a Newtonian fluid with viscosity η_0.

Although we know that the convected Jeffreys model is admissible, we do not know a priori whether or not it describes the kinds of material functions shown in Chapter 3 for typical polymeric liquids.[4] Hence it is very important (as it is for any model) to test it in as many different rheometric experiments as possible.

EXAMPLE 7.2-1 Time-Dependent Shearing Flows of the Convected Jeffreys Model

(a) Show how the convected Jeffreys model simplifies for a general time-dependent, simple shearing flow with velocity gradient $\partial v_x/\partial y = \dot{\gamma}_{yx}(t)$. Then use this result to evaluate the material functions for **(b)** steady shear flow, **(c)** small-amplitude oscillatory shearing flow, **(d)** start-up of steady shear flow, and **(e)** stress relaxation following steady shear flow.

SOLUTION **(a)** We start by writing out the various tensors that enter into the constitutive equation. Appendix C gives the matrix representations for $\boldsymbol{\tau}_{(1)}$, $\boldsymbol{\gamma}_{(1)}$, and $\boldsymbol{\gamma}_{(2)}$ for an unsteady shearing flow. When these are substituted into the constitutive equation for the convected Jeffreys model we obtain the following matrix equation:

$$\begin{pmatrix} \tau_{xx} & \tau_{yx} & 0 \\ \tau_{yx} & \tau_{yy} & 0 \\ 0 & 0 & \tau_{zz} \end{pmatrix} + \lambda_1 \frac{d}{dt}\begin{pmatrix} \tau_{xx} & \tau_{yx} & 0 \\ \tau_{yx} & \tau_{yy} & 0 \\ 0 & 0 & \tau_{zz} \end{pmatrix} - \begin{pmatrix} 2\tau_{yx} & \tau_{yy} & 0 \\ \tau_{yy} & 0 & 0 \\ 0 & 0 & 0 \end{pmatrix}\lambda_1\dot{\gamma}_{yx}$$
$$= -\eta_0\left[\begin{pmatrix} 0 & 1 & 0 \\ 1 & 0 & 0 \\ 0 & 0 & 0 \end{pmatrix}\dot{\gamma}_{yx} + \lambda_2\begin{pmatrix} 0 & 1 & 0 \\ 1 & 0 & 0 \\ 0 & 0 & 0 \end{pmatrix}\frac{d\dot{\gamma}_{yx}}{dt} - 2\begin{pmatrix} 1 & 0 & 0 \\ 0 & 0 & 0 \\ 0 & 0 & 0 \end{pmatrix}\lambda_2\dot{\gamma}_{yx}^2\right] \tag{7.2-2}$$

From this matrix equation we can now obtain a set of coupled differential equations for the stress tensor components:

$$\left(1 + \lambda_1\frac{d}{dt}\right)\tau_{xx} - 2\tau_{yx}\lambda_1\dot{\gamma}_{yx}(t) = 2\eta_0\lambda_2\dot{\gamma}_{yx}^2(t) \tag{7.2-3}$$

$$\left(1 + \lambda_1\frac{d}{dt}\right)\tau_{yy} = 0 \tag{7.2-4}$$

[3] The convected Maxwell model was first obtained from a molecular model by M. S. Green and A. V. Tobolsky, *J. Chem. Phys.*, **14**, 80-92 (1946).

[4] The convected Jeffreys model is derived in Chapter 13 from the kinetic theory of dilute solutions of elastic dumbbells.

$$\left(1 + \lambda_1 \frac{d}{dt}\right)\tau_{zz} = 0 \tag{7.2-5}$$

$$\left(1 + \lambda_1 \frac{d}{dt}\right)\tau_{yx} - \underline{\tau_{yy}\lambda_1\dot{\gamma}_{yx}(t)} = -\eta_0\left(1 + \lambda_2 \frac{d}{dt}\right)\dot{\gamma}_{yx}(t) \tag{7.2-6}$$

From these equations it can be seen that the normal stresses τ_{yy} and τ_{zz} are zero for all simple, time-dependent shearing flows. Thus we can drop the dashed underlined term in Eq. 7.2-6. We now use Eqs. 7.2-3 through 6 to calculate specific material functions.

(b) For steady shear flow the differential equations in Eqs. 7.2-3 and 6 simplify to algebraic equations. The two equations for τ_{xx} and τ_{yx} are easily solved to give the viscometric functions:

$$\begin{aligned} \tau_{yx} &= -\eta_0\dot{\gamma}_{yx} && \text{or} \quad \eta = \eta_0 \\ \tau_{xx} - \tau_{yy} &= -2\eta_0(\lambda_1 - \lambda_2)\dot{\gamma}_{yx}^2 && \text{or} \quad \Psi_1 = 2\eta_0(\lambda_1 - \lambda_2) \\ \tau_{yy} - \tau_{zz} &= 0 && \text{or} \quad \Psi_2 = 0 \end{aligned} \tag{7.2-7}$$

The convected Jeffreys model thus gives a constant viscosity and first normal stress coefficient. The second normal stress coefficient is zero.

(c) To get the small amplitude oscillatory shearing properties, we take the shear strain to be $\gamma_{yx}(0, t) = \int_0^t \dot{\gamma}_0 \cos \omega t' dt' = \gamma_0 \sin \omega t$, in which $\gamma_0 = \dot{\gamma}_0/\omega$ is the amplitude of the shear strain, and seek solutions to Eqs. 7.2-3 and 6 in the limit of small γ_0. For this flow the differential equation for the shear stress is

$$\left(1 + \lambda_1 \frac{d}{dt}\right)\tau_{yx} = -\eta_0\gamma_0\omega(\cos \omega t - \lambda_2\omega \sin \omega t) \tag{7.2-8}$$

Since we seek a steady periodic solution, the nonhomogeneous part of the first-order, linear, ordinary differential equation suggests we try a solution for τ_{yx} of the form

$$\tau_{yx} = A \cos \omega t + B \sin \omega t \tag{7.2-9}$$

By substituting Eq. 7.2-9 into Eq. 7.2-8 we can see that A and B must be given by (cf. Eqs. 3.4-3b)

$$A = -\eta_0\left(\frac{1 + \lambda_1\lambda_2\omega^2}{1 + \lambda_1^2\omega^2}\right)\gamma_0\omega = -\eta'(\omega)\gamma_0\omega \tag{7.2-10}$$

$$B = -\eta_0 \frac{(\lambda_1 - \lambda_2)\gamma_0\omega^2}{1 + \lambda_1^2\omega^2} = -\eta''(\omega)\gamma_0\omega \tag{7.2-11}$$

Note that η' and η'' are the same as for the linear viscoelastic Jeffreys model.

To show that the convected Jeffreys model gives identical predictions to the Jeffreys model in the linear viscoelastic limit is a little more complicated than the calculation of η' and η''. It is also necessary to demonstrate that as $\gamma_0 \to 0$ the normal stresses become negligible compared with the shear stress (see Problem 7B.1). Notice that $\dot{\gamma}_0$ can be large in the linear viscoelastic limit so that the demand above on $\gamma_0 \to 0$ is more restrictive than simply requiring τ_{xx} to be small compared with τ_{yx} as $\dot{\gamma}_0 \to 0$. The latter is easily seen to hold by inspection of the governing differential equations, Eqs. 7.2-3 and 6.

(d) For start-up of steady shear flow we let $\dot{\gamma}_{yx} = \dot{\gamma}_0 H(t)$, where H is the Heaviside unit step function. The stresses τ_{xx} and τ_{yx} are then given by the differential equations

$$\left(1 + \lambda_1 \frac{d}{dt}\right)\tau_{xx} - 2\lambda_1 \dot{\gamma}_0 \tau_{yx} = +2\eta_0 \lambda_2 \dot{\gamma}_0^2 \tag{7.2-12}$$

$$\left(1 + \lambda_1 \frac{d}{dt}\right)\tau_{yx} = -\eta_0 \dot{\gamma}_0 (1 + \lambda_2 \delta(t)) \tag{7.2-13}$$

where the Dirac delta function has been introduced as the derivative of the step function $dH/dt = \delta(t)$ (see Eqs. 5.2-10a through c). Equation 7.2-13 is then multiplied by the integrating factor e^{t/λ_1} and integrated from $t = 0^-$ (where $\tau_{yx} = 0$) to an arbitrary time $t > 0$ to give (cf. Table 3.4-1)

$$\begin{aligned} \tau_{yx} &= -\eta_0 \dot{\gamma}_0 \frac{\lambda_2}{\lambda_1} - \eta_0 \dot{\gamma}_0 \left(1 - \frac{\lambda_2}{\lambda_1}\right)(1 - e^{-t/\lambda_1}) \\ &= -\eta^+(t, \dot{\gamma}_0)\dot{\gamma}_0 \end{aligned} \tag{7.2-14}$$

When this last result is combined with Eq. 7.2-12 we obtain for τ_{xx}

$$\begin{aligned} \tau_{xx} &= -2\eta_0(\lambda_1 - \lambda_2)\dot{\gamma}_0^2 \left[1 - \left(1 + \frac{t}{\lambda_1}\right)e^{-t/\lambda_1}\right] \\ &= -\Psi_1^+(t, \dot{\gamma}_0)\dot{\gamma}_0^2 \end{aligned} \tag{7.2-15}$$

From Eqs. 7.2-14 and 15, it can be seen that the shear stress and first normal stress growth functions do not depend on shear rate as is found for the polymer solution and melt data in Chapter 3. Moreover, the stresses grow monotonically to the steady-state values, so that the convected Jeffreys model does not predict the stress overshoot observed experimentally in polymeric liquids. Finally, there is a jump in the shear stress at $t = 0$, following which the shear stress grows monotonically to steady state. This sudden jump is associated with the retardation time λ_2 in the model, but does not seem to be observed experimentally. However, as a result of the jump, the shear stress is predicted to grow more rapidly than the normal stress, in qualitative agreement with data.

(e) For stress relaxation following steady shear flow we take the shear rate to be $\dot{\gamma}(t) = \dot{\gamma}_0\{1 - H(t)\}$. When this is inserted into Eq. 7.2-6 we obtain the following differential equation for the shear stress:

$$\left(1 + \lambda_1 \frac{d}{dt}\right)\tau_{yx} = \eta_0 \lambda_2 \dot{\gamma}_0 \delta(t) \tag{7.2-16}$$

This equation is integrated from $t = 0^-$ (where the shear stress is the steady-state value $-\eta_0 \dot{\gamma}_0$) to time $t > 0$ to give the shear stress relaxation function (cf. Table 3.4-1)

$$\begin{aligned} \tau_{yx} &= -\eta_0 \dot{\gamma}_0 \left(1 - \frac{\lambda_2}{\lambda_1}\right)e^{-t/\lambda_1} \\ &= -\eta^-(t, \dot{\gamma}_0)\dot{\gamma}_0 \end{aligned} \tag{7.2-17}$$

To find the normal stress relaxation we note from Eq. 7.2-3 that for $t \geq 0$ when the shear rate is zero, the normal stress τ_{xx} relaxes like e^{-t/λ_1} from its steady-state shear flow value. Thus,

$$\begin{aligned} \tau_{xx} &= -2\eta_0(\lambda_1 - \lambda_2)\dot{\gamma}_0^2 e^{-t/\lambda_1} \\ &= -\Psi_1^-(t, \dot{\gamma}_0)\dot{\gamma}_0^2 \end{aligned} \tag{7.2-18}$$

As we found for the stress growth material functions, the rate of stress relaxation does not depend on the shear rate. In addition, there is again a discontinuity in the shear stress at $t = 0$, whereas the normal stresses are continuous. The jump in τ_{yx} results in the fact that the shear stress relaxes to zero more rapidly than the normal stress, in qualitative agreement with experiments.

EXAMPLE 7.2-2 Time-Dependent Shearfree Flows of the Convected Jeffreys Model

(a) Show how the convected Jeffreys model simplifies for an arbitrary, time-dependent shearfree flow. **(b)** Then use this result to find the model response to start-up of steady planar and elongational flow. **(c)** What are the steady-state material functions for the convected Jeffreys model in these flows?

SOLUTION **(a)** We again turn to Appendix C where the various tensors in the convected Jeffreys model are displayed in matrix form for shearfree flows. When these are inserted into the constitutive equation, Eq. 7.2-1, we obtain the following uncoupled, ordinary differential equations for the stress components:

$$\tau_{xx} + \lambda_1 \frac{d\tau_{xx}}{dt} + \lambda_1(1+b)\tau_{xx}\dot{\varepsilon}(t) = +\eta_0\left[(1+b)\dot{\varepsilon}[1+(1+b)\lambda_2\dot{\varepsilon}] + \lambda_2(1+b)\frac{d\dot{\varepsilon}}{dt}\right] \tag{7.2-19}$$

$$\tau_{zz} + \lambda_1 \frac{d\tau_{zz}}{dt} - 2\lambda_1\tau_{zz}\dot{\varepsilon}(t) = -\eta_0\left[2\dot{\varepsilon}[1-2\lambda_2\dot{\varepsilon}] + 2\lambda_2\frac{d\dot{\varepsilon}}{dt}\right] \tag{7.2-20}$$

The equation for τ_{yy} is the same as for τ_{xx} except that $+b$ is replaced by $-b$.

(b) In start-up of steady shearfree flow, the elongation rate is given by the Heaviside unit step function $\dot{\varepsilon}(t) = \dot{\varepsilon}_0 H(t)$ where $\dot{\varepsilon}_0$ is constant. When the differential equation for τ_{xx}, for example, is specialized to this strain rate function we obtain

$$\left(1 + (1+b)\lambda_1\dot{\varepsilon}_0 + \lambda_1\frac{d}{dt}\right)\tau_{xx} = \eta_0(1+b)\dot{\varepsilon}_0[1+(1+b)\lambda_2\dot{\varepsilon}_0 + \lambda_2\delta(t)] \tag{7.2-21}$$

which is to be solved subject to the initial condition that $\tau_{xx}(0^-) = 0$. Integrating Eq. 7.2-21 from $t = 0^-$ to t gives

$$\tau_{xx} = \eta_0(1+b)\dot{\varepsilon}_0\frac{1+(1+b)\lambda_2\dot{\varepsilon}_0}{1+(1+b)\lambda_1\dot{\varepsilon}_0} - \eta_0\left(1-\frac{\lambda_2}{\lambda_1}\right)\frac{(1+b)\dot{\varepsilon}_0 e^{-t(1+(1+b)\lambda_1\dot{\varepsilon}_0)/\lambda_1}}{1+(1+b)\lambda_1\dot{\varepsilon}_0} \tag{7.2-22}$$

Similarly we find that τ_{yy} is identical to τ_{xx} with b replaced by $-b$ and τ_{zz} is given by

$$\tau_{zz} = -2\eta_0\dot{\varepsilon}_0\frac{1-2\lambda_2\dot{\varepsilon}_0}{1-2\lambda_1\dot{\varepsilon}_0} + 2\eta_0\left(1-\frac{\lambda_2}{\lambda_1}\right)\frac{\dot{\varepsilon}_0 e^{-t(1-2\lambda_1\dot{\varepsilon}_0)/\lambda_1}}{1-2\lambda_1\dot{\varepsilon}_0} \tag{7.2-23}$$

An interesting result of the above formulas is that no steady state is attained if

$$\lambda_1\dot{\varepsilon}_0 > \tfrac{1}{2} \quad \text{or} \quad \lambda_1\dot{\varepsilon}_0 < \frac{-1}{(1+b)} \quad \text{or} \quad \lambda_1\dot{\varepsilon}_0 < \frac{-1}{(1-b)} \tag{7.2-24}$$

Since we specify shearfree flows with b in the range $0 \le b \le 1$, the first two of these conditions determine which shearfree flows of the convected Jeffreys model will approach a steady state in the start-up experiment.

For $-1/(1+b) < \lambda_1\dot{\varepsilon}_0 < 1/2$ we find the stress growth material functions (Table 3.5-1):

$$\begin{aligned}\bar{\eta}_1^+ &= -\frac{\tau_{zz}-\tau_{xx}}{\dot{\varepsilon}_0} \\ &= (3+b)\eta_0\frac{\lambda_2}{\lambda_1} + \frac{(3+b)\eta_0(1-(\lambda_2/\lambda_1))}{(1+(1+b)\lambda_1\dot{\varepsilon}_0)(1-2\lambda_1\dot{\varepsilon}_0)} \\ &\quad - \eta_0(1+b)\left(1-\frac{\lambda_2}{\lambda_1}\right)\frac{e^{-t(1+(1+b)\lambda_1\dot{\varepsilon}_0)/\lambda_1}}{(1+(1+b)\lambda_1\dot{\varepsilon}_0)} \\ &\quad - 2\eta_0\left(1-\frac{\lambda_2}{\lambda_1}\right)\frac{e^{-t(1-2\lambda_1\dot{\varepsilon}_0)/\lambda_1}}{(1-2\lambda_1\dot{\varepsilon}_0)}\end{aligned} \tag{7.2-25}$$

$$\begin{aligned}\bar{\eta}_2^+ &= -\frac{\tau_{yy}-\tau_{xx}}{\dot{\varepsilon}_0} \\ &= 2b\eta_0\frac{\lambda_2}{\lambda_1} + \frac{2b\eta_0(1-(\lambda_2/\lambda_1))}{(1+(1+b)\lambda_1\dot{\varepsilon}_0)(1+(1-b)\lambda_1\dot{\varepsilon}_0)} \\ &\quad - \eta_0(1+b)\left(1-\frac{\lambda_2}{\lambda_1}\right)\frac{e^{-t(1+(1+b)\lambda_1\dot{\varepsilon}_0)/\lambda_1}}{(1+(1+b)\lambda_1\dot{\varepsilon}_0)} \\ &\quad + \eta_0(1-b)\left(1-\frac{\lambda_2}{\lambda_1}\right)\frac{e^{-t(1+(1-b)\lambda_1\dot{\varepsilon}_0)/\lambda_1}}{(1+(1-b)\lambda_1\dot{\varepsilon}_0)}\end{aligned} \tag{7.2-26}$$

(c) For steady-state shearfree flows, the governing differential equations, Eqs. 7.2-19 and 20, reduce to algebraic equations that are easily solved for the stresses. These are then combined with the material function definitions to give for any $\dot{\varepsilon}_0$:

$$\bar{\eta}_1 = (3+b)\eta_0\frac{\lambda_2}{\lambda_1} + \frac{(3+b)\eta_0(1-(\lambda_2/\lambda_1))}{(1+(1+b)\lambda_1\dot{\varepsilon}_0)(1-2\lambda_1\dot{\varepsilon}_0)} \tag{7.2-27}$$

$$\bar{\eta}_2 = 2b\eta_0\frac{\lambda_2}{\lambda_1} + \frac{2b\eta_0(1-(\lambda_2/\lambda_1))}{(1+(1+b)\lambda_1\dot{\varepsilon}_0)(1+(1-b)\lambda_1\dot{\varepsilon}_0)} \tag{7.2-28}$$

Note that the steady material functions become infinite at the critical strain rates given by Eq. 7.2-24.

§7.3 NONLINEAR DIFFERENTIAL MODELS

In the preceding section we wrote down an admissible constitutive equation that is capable of describing time-dependent flows. However, the model is not able to portray well the rheological properties that are observed in typical polymer solutions and melts. For example, we noted previously the deficiencies of constant viscosity and normal stress coefficients in steady shear flow and the infinite elongational viscosity at finite elongation rates. In this section we illustrate some of the methods that have been used to generate constitutive equations that more accurately represent real material data. In each of the approaches, it is necessary to give up the starting point of a linear model that we used in §7.2.

TABLE 7.3-1

Material Functions for the White-Metzner Model (Eq. 7.3-1)[a]

Steady shear flow	$\eta = \eta(\dot\gamma)$ $\Psi_1 = 2\eta(\dot\gamma)\lambda(\dot\gamma)$ $\Psi_2 = 0$	(A)
Small-amplitude oscillatory shearing	η', η'' not defined[b]	
Start-up of steady shear flow	$\eta^+(t, \dot\gamma) = \eta(\dot\gamma)[1 - e^{-t/\lambda(\dot\gamma)}]$ $\Psi_1^+(t, \dot\gamma) = 2\eta(\dot\gamma)\lambda(\dot\gamma)\left[1 - \left(1 + \frac{t}{\lambda(\dot\gamma)}\right)e^{-t/\lambda(\dot\gamma)}\right]$	(B)
Steady shearfree flow $(\dot\gamma \equiv \sqrt{\frac{1}{2}II}$ $= \sqrt{(3 + b^2)\,\lvert\dot\varepsilon\rvert})$	$\bar\eta_1 = \frac{(3 + b)\eta(\dot\gamma)}{(1 + (1 + b)\lambda\dot\varepsilon)(1 - 2\lambda\dot\varepsilon)}$ $\bar\eta_2 = \frac{2b\eta(\dot\gamma)}{(1 + (1 - b)\lambda\dot\varepsilon)(1 + (1 + b)\lambda\dot\varepsilon)}$	(C)

[a] The time "constant" $\lambda(\dot\gamma) = \eta(\dot\gamma)/G$.

[b] The White-Metzner model has no unique limit as strain amplitude approaches zero. For small shear rate amplitudes, the oscillatory shearing behavior is identical to that of the convected Maxwell model.

a. Inclusion of Invariants

We saw in Chapter 4 that for the generalized Newtonian fluid the viscosity was allowed to depend on the second invariant of the rate-of-strain tensor and that this led to a useful constitutive equation. It seems reasonable then to modify Eq. 7.2-1 to include dependence on $\dot\gamma = \sqrt{\frac{1}{2}(\boldsymbol{\gamma}_{(1)} : \boldsymbol{\gamma}_{(1)})}$. An example of this change is the *White-Metzner model*[1] which is the following modification of the convected Maxwell model:

$$\boxed{\boldsymbol{\tau} + \frac{\eta(\dot\gamma)}{G}\boldsymbol{\tau}_{(1)} = -\eta(\dot\gamma)\boldsymbol{\gamma}_{(1)}} \tag{7.3-1}$$

where G is a constant modulus. A few material functions for this model are summarized in Table 7.3-1. This model has the advantage of being relatively simple and yet still giving reasonable shapes for the shear-rate dependent viscosity and first normal stress coefficient. It can also be used in fast time-dependent motions, although its predictions are not completely realistic in these problems. This stems from its lack of a linear viscoelastic limit for small displacement gradients. In steady shearfree flows the model gives infinite elongational viscosities $\bar\eta_1$ and $\bar\eta_2$ in the same way as the convected Maxwell model; the exact value of elongation rate at which these viscosities become infinite depends on the particular form of $\eta(\dot\gamma)$. The model has been found useful in exploratory hydrodynamic calculations aimed at assessing the interaction of shear thinning and memory on flow fields.[2]

There are of course other ways in which invariants could be introduced into the model. There is no reason, other than for preserving simplicity, to include the invariant II of

[1] J. L. White and A. B. Metzner, *J. Appl. Polym. Sci.*, **7**, 1867-1889 (1963).

[2] A. Beris, R. C. Armstrong, and R. A. Brown, *J. Non-Newtonian Fluid Mech.*, **13**, 109-148 (1983).

$\dot{\gamma}$ but not *III* in the model. Similarly, we could include invariants of stress. The molecularly based Phan-Thien–Tanner and the FENE-P models both include tr $\boldsymbol{\tau}$, with a certain amount of success. These are listed in §7.6 and discussed in Chapters 20 and 13, respectively.

b. Inclusion of Quadratic Terms in Velocity Gradient

Oldroyd realized that models like the convected Jeffreys model have included terms that are quadratic in velocity gradient, but that their inclusion has not been systematic. He thus suggested that a possibly useful generalization of the convected Jeffreys model could be obtained by adding to the latter all possible quadratic terms involving products of $\boldsymbol{\tau}$ with $\boldsymbol{\gamma}_{(1)}$ and of $\boldsymbol{\gamma}_{(1)}$ with itself. Thus Oldroyd suggested[3]

$$\begin{aligned}\boldsymbol{\tau} + \underline{\lambda_1 \boldsymbol{\tau}_{(1)}} + \tfrac{1}{2}\lambda_3\{\boldsymbol{\gamma}_{(1)}\cdot\boldsymbol{\tau} + \boldsymbol{\tau}\cdot\boldsymbol{\gamma}_{(1)}\} + \tfrac{1}{2}\lambda_5(\mathrm{tr}\,\boldsymbol{\tau})\boldsymbol{\gamma}_{(1)} + \tfrac{1}{2}\lambda_6(\boldsymbol{\tau}:\boldsymbol{\gamma}_{(1)})\boldsymbol{\delta} \\ = \underline{-\eta_0[\boldsymbol{\gamma}_{(1)} + \lambda_2\boldsymbol{\gamma}_{(2)}]} + \lambda_4\{\boldsymbol{\gamma}_{(1)}\cdot\boldsymbol{\gamma}_{(1)}\} + \tfrac{1}{2}\lambda_7(\boldsymbol{\gamma}_{(1)}:\boldsymbol{\gamma}_{(1)})\boldsymbol{\delta}]\end{aligned} \tag{7.3-2}$$

The dashed-underlined terms belong to the convected Jeffreys model. Several simplified versions of this model, in which special values are assigned to some of the constants, have been used extensively in the literature; these are summarized in Table 7.3-2.

Some sample material functions for the Oldroyd 8-constant model are given in Table 7.3-3. In order that these material functions agree at least qualitatively with experimental data, there are some restrictions on the choice of the constants that have to be imposed:

1. Since η' is known to decrease with increasing ω, we must impose the requirement that $0 < \lambda_2 < \lambda_1$.
2. Since viscosity is generally a monotone decreasing function of $\dot{\gamma}$, we must require that $0 < \sigma_2 < \sigma_1$ [where $\sigma_i = \lambda_i(\lambda_3 + \lambda_5) + \lambda_{i+2}(\lambda_1 - \lambda_3 - \lambda_5) + \lambda_{i+5}(\lambda_1 - \lambda_3 - \frac{3}{2}\lambda_5)$, with $i = 1, 2$].
3. Since $|\tau_{xy}|$ is to be a monotone increasing function of $\dot{\gamma}$ for steady shear flow, we have to require that $\sigma_2 \geq \frac{1}{9}\sigma_1$.
4. When $\eta(\dot{\gamma})$ and $\eta'(\omega)$ are plotted on the same graph with $\dot{\gamma} = \omega$, the η-curve generally lies above the η'-curve. For this to be true in the region of moderate $\dot{\gamma}$ and ω, we must require that $\sigma_1 - \sigma_2 < \lambda_1(\lambda_1 - \lambda_2)$.
5. For the elongational viscosity to be bounded for positive and negative $\dot{\varepsilon}$ it is necessary for $\lambda_1 - \lambda_3$ to be between $\frac{2}{3}(\lambda_5 + \lambda_6) \pm \frac{1}{3}[4\lambda_6^2 - 11\lambda_5\lambda_6 + 4\lambda_5^2]^{1/2}$.

Consideration of additional material functions and additional flow patterns will in general provide further inequalities.

With eight constants and all the extra terms, considerably more variety in rheological response is possible than for the convected Jeffreys equation. Although we cannot obtain

[3] J. G. Oldroyd, *Proc. Roy. Soc.*, **A245**, 278–297 (1958); *Rheol. Acta*, **1**, 337–344 (1961). The parameters in Eq. 7.3-2 are related to the original constants used by Oldroyd as follows:

Eq. 7.3-2:	η_0	λ_1	λ_2	λ_3	λ_4	λ_5	λ_6	λ_7
Oldroyd:	η_0	λ_1	λ_2	$\lambda_1 - \mu_1$	$\lambda_2 - \mu_2$	μ_0	ν_1	ν_2

the kind of quantitative fit of the viscosity and first normal stress coefficient that is possible with the White-Metzner model, a wider range of properties can be correctly described qualitatively. For example, by suitable choice of the constants, stress overshoot in start-up of steady shear flow and a bounded elongational viscosity can be obtained. Also the algebraic form in which nonlinear terms have been included makes it generally easier to obtain analytical solutions than for the White-Metzner model. Thus, the Oldroyd 8-constant model has been found to be a useful and relatively simple constitutive equation for making exploratory fluid flow calculations.

The calculation of the material functions for the Oldroyd 8-constant model follows the same pattern that was illustrated in §7.2 for the convected Jeffreys model. For convenience we have tabulated in Table C.2 of Appendix C, the governing differential equations for the stresses in time-dependent shear and shearfree flows. The shapes of the material functions are illustrated in Figs. 7.3-1 through 4 for the special case of the Oldroyd 4-constant model. The model describes many of the rheological properties at least qualitatively correctly. In order to obtain more quantitative fits with data it is probably necessary to include a spectrum of relaxation times instead of the single λ_1. This is similar to the improvement found by use of the generalized Maxwell model in place of the Maxwell model in linear viscoelasticity. A defect in the Oldroyd 8-constant model that is not so easily removed is the presence of singularities in $\bar{\eta}_1$ and $\bar{\eta}_2$ for $\dot{\varepsilon} < 0$ and $0 < b < 1$. These arise from the polynomial nature of the Oldroyd 8-constant model[4] and are illustrated in Fig. 7.3-4.

c. Inclusion of Nonlinear Terms in Stress

There appear to be no rheological reasons why a constitutive equation must be restricted to terms linear in stress as Oldroyd has required. In this subsection we use the *Giesekus model*[5] as an example of a constitutive equation with nonlinear stress terms:

$$\boxed{\begin{aligned} &\boldsymbol{\tau} = \boldsymbol{\tau}_s + \boldsymbol{\tau}_p \\ &\boldsymbol{\tau}_s = -\eta_s \dot{\boldsymbol{\gamma}} \\ &\boldsymbol{\tau}_p + \lambda_1 \boldsymbol{\tau}_{p(1)} - \alpha \frac{\lambda_1}{\eta_p} \{\boldsymbol{\tau}_p \cdot \boldsymbol{\tau}_p\} = -\eta_p \dot{\boldsymbol{\gamma}} \end{aligned}} \tag{7.3-3}$$

Here the model is written as a superposition of solvent and polymer contributions, $\boldsymbol{\tau}_s$ and $\boldsymbol{\tau}_p$, to the stress tensor, which is the form in which constitutive equations derived by kinetic theory arise naturally for polymer solutions (see for example, Eqs. 13.3-1 and 13.4-4).

The Giesekus model contains four parameters: a relaxation time λ_1; the solvent and polymer contributions to the zero-shear-rate viscosity, η_s and η_p; and the dimensionless "mobility factor" α. The origin of the term involving α can be associated with anisotropic Brownian motion and/or anisotropic hydrodynamic drag on the constituent polymer molecules[6] (see §13.7).

[4] The shearfree flow properties of the Oldroyd 8-constant model are discussed in C. J. S. Petrie, *J. Non-Newtonian Fluid Mech.*, **14**, 189-202 (1984).

[5] H. Giesekus, *J. Non-Newtonian Fluid Mech.*, **11**, 69-109 (1982); **12**, 367-374 (1983); *Rheol. Acta*, **21**, 366-375 (1982).

[6] R. B. Bird and J. M. Wiest, *J. Rheol.*, **29**, 519-532 (1985).

TABLE 7.3-2

Models Included in the Oldroyd 8-Constant Model (Eq. 7.3-2)

Name of Model	Number of Constants	Values of Time Constants							Steady-State Shear Flow Material Functions[a]	Elongational Viscosity[b]	References
		λ_1	λ_2	λ_3	λ_4	λ_5	λ_6	λ_7			
Oldroyd 6-constant model	6						0	0	η depends on $\dot{\gamma}$ Ψ_1 depends on $\dot{\gamma}$ Ψ_2 not simply related to Ψ_1	See Table 7.3-3 Eq. F	Problem 14B.4 Table 6.2-2 See footnote[f]
Oldroyd 4-constant model	4			0	0		0	0	η depends on $\dot{\gamma}$ Ψ_1 depends on $\dot{\gamma}$ $\Psi_2 = 0$	See Table 7.3-3 Eq. F	
Oldroyd fluid A	3			$2\lambda_1$	$2\lambda_2$	0	0	0	$\eta = \eta_0$ $\Psi_1 = 2\eta_0(\lambda_1 - \lambda_2)$ $\Psi_2 = -\Psi_1$	$3\eta_0 \dfrac{1 + \lambda_2\dot{\varepsilon} - 2\lambda_1\lambda_2\dot{\varepsilon}^2}{1 + \lambda_1\dot{\varepsilon} - 2\lambda_1^2\dot{\varepsilon}^2}$	Problem 7B.4
Oldroyd fluid B (Convected Jeffreys)	3			0	0	0	0	0	$\eta = \eta_0$ $\Psi_1 = 2\eta_0(\lambda_1 - \lambda_2)$ $\Psi_2 = 0$	$3\eta_0 \dfrac{1 - \lambda_2\dot{\varepsilon} - 2\lambda_1\lambda_2\dot{\varepsilon}^2}{1 - \lambda_1\dot{\varepsilon} - 2\lambda_1^2\dot{\varepsilon}^2}$	§7.2; Eq. 13.4-5

Corotational Jeffreys model	3			λ_1	λ_2	0	0	0	η depends on $\dot{\gamma}$ Ψ_1 depends on $\dot{\gamma}$ $\Psi_2 = -\frac{1}{2}\Psi_1$	$3\eta_0$	
Second-order fluid[c]	3	0		0		0	0	0	$\eta = \eta_0$ $\Psi_1 = -2\eta_0\lambda_2$ $\Psi_2 = \eta_0\lambda_4$	$3\eta_0(1 - (\lambda_2 - \lambda_4)\dot{\varepsilon})$	Chapter 6; Table 6.2-1
Convected Maxwell model	2		0	0	0	0	0	0	$\eta = \eta_0$ $\Psi_1 = 2\eta_0\lambda_1$ $\Psi_2 = 0$	$3\eta_0 \frac{1}{(1 + \lambda_1\dot{\varepsilon})(1 - 2\lambda_1\dot{\varepsilon})}$	
Gordon–Schowalter	3	$\frac{\eta_s\lambda_1}{\eta_0}$	$\xi\lambda_1$	$\frac{\xi\eta_s\lambda_1}{\eta_0}$	0	0	0	0	η depends on $\dot{\gamma}$ Ψ_1 depends on $\dot{\gamma}$ $\Psi_2 < 0$	Becomes infinite at finite $\dot{\varepsilon}$	See footnote[d] $\eta_0 = (1 - \xi)\eta_p + \eta_s$ Problem 13B.2
Johnson–Segalman	3	$\frac{\eta_s\lambda_1}{\eta_0}$	$\xi\lambda_1$	$\frac{\xi\eta_s\lambda_1}{\eta_0}$	0	0	0	0	η depends on $\dot{\gamma}$ Ψ_1 depends on $\dot{\gamma}$ $\Psi_2 < 0$	Becomes infinite at finite $\dot{\varepsilon}$	See footnote[e] $\eta_0 = \eta_p + n_s$

[a] See Table 7.3-3, Eqs. A, B, and C for general expressions.

[b] See Table 7.3-3, Eq. F for general expression.

[c] For the relation of the Oldroyd model to the third-order fluid see Problem 7B.6.

[d] R. J. Gordon and W. R. Schowalter, *Trans. Soc. Rheol.*, **16**, 79–97 (1972). This equation is derived from a kinetic theory of dilute polymer solutions in which η_s is the solvent viscosity; $(1 - \xi)\eta_p$ is the polymer contribution to the viscosity, and ξ is a slip parameter. The zero-shear-rate viscosity is given by $\eta_0 = (1 - \xi)\eta_p + \eta_s$.

[e] M. W. Johnson, Jr. and D. Segalman, *J. Non-Newtonian Fluid Mech.*, **2**, 255–270 (1977); **9**, 33–56 (1981); *Mech. Today*, **5**, 129–137 (1980).

[f] R. B. Bird and J. M. Wiest, *J. Rheol.*, **29**, 519–532 (1985), Table 1; J. M. Wiest and R. B. Bird, *J. Non-Newtonian Fluid Mech.*, **22**, 115–119 (1986).

TABLE 7.3-3

Material Functions for the Oldroyd 8-Constant Model (Eq. 7.3-2)

Steady shear flow:

$$\frac{\eta}{\eta_0} = \frac{1 + \sigma_2\dot{\gamma}^2}{1 + \sigma_1\dot{\gamma}^2} \tag{A}$$

$$\frac{\Psi_1}{2\eta_0\lambda_1} = \frac{\eta(\dot{\gamma})}{\eta_0} - \frac{\lambda_2}{\lambda_1} \tag{B}$$

$$\frac{\Psi_2}{\eta_0\lambda_1} = -\frac{\Psi_1}{2\eta_0\lambda_1} + \frac{(\lambda_1 - \lambda_3)}{\lambda_1}\frac{\eta}{\eta_0} - \frac{(\lambda_2 - \lambda_4)}{\lambda_1} \tag{C}$$

where $\sigma_i = \lambda_i(\lambda_3 + \lambda_5) + \lambda_{i+2}(\lambda_1 - \lambda_3 - \lambda_5) + \lambda_{i+5}(\lambda_1 - \lambda_3 - \frac{3}{2}\lambda_5)$

Small-amplitude oscillatory shearing:

$$\frac{\eta'}{\eta_0} = \frac{1 + \lambda_1\lambda_2\omega^2}{1 + \lambda_1^2\omega^2} \tag{D}$$

$$\frac{\eta''}{\omega\eta_0} = \frac{(\lambda_1 - \lambda_2)}{1 + \lambda_1^2\omega^2} \tag{E}$$

Steady elongational flow:

$$\frac{\bar{\eta}}{3\eta_0} = \frac{1 - (\lambda_2 - \lambda_4)\dot{\varepsilon} + (\frac{3}{2}\lambda_5 - \lambda_1 + \lambda_3)(2\lambda_2 - 2\lambda_4 - 3\lambda_7)\dot{\varepsilon}^2}{1 - (\lambda_1 - \lambda_3)\dot{\varepsilon} + (\frac{3}{2}\lambda_5 - \lambda_1 + \lambda_3)(2\lambda_1 - 2\lambda_3 - 3\lambda_6)\dot{\varepsilon}^2} \tag{F}$$

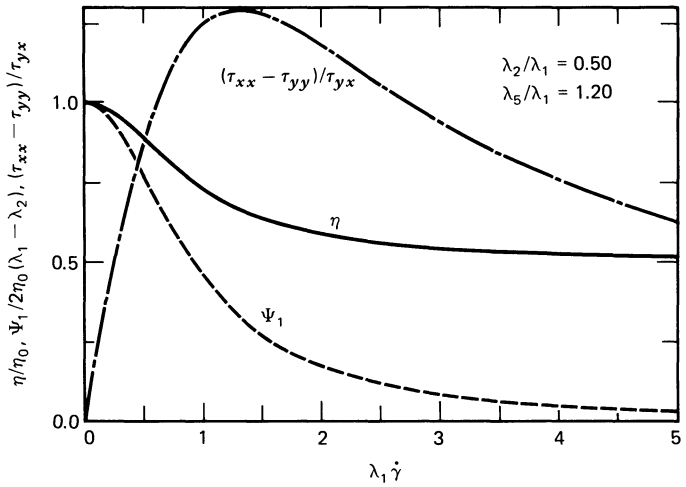

FIGURE 7.3-1. Dimensionless viscosity (——), first normal stress coefficient (- - - -), and stress ratio (— — —) as functions of dimensionless shear rate for the Oldroyd 4-constant model defined in Table 7.3-2. The second normal stress coefficient is zero. The shear thinning in η and Ψ_1 is in qualitative agreement with experimental observations, but experimental data show a monotone increasing stress ratio (cf. Fig. 3.3-8) in disagreement with the model predictions.

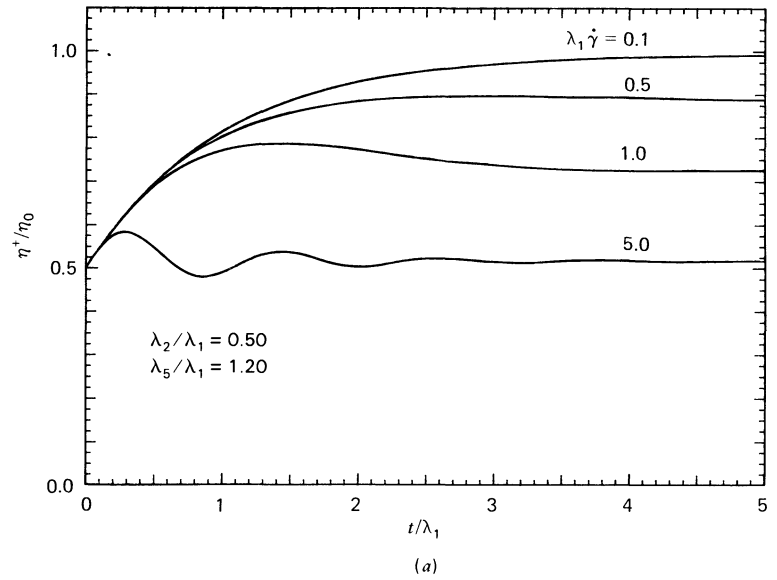

(*a*)

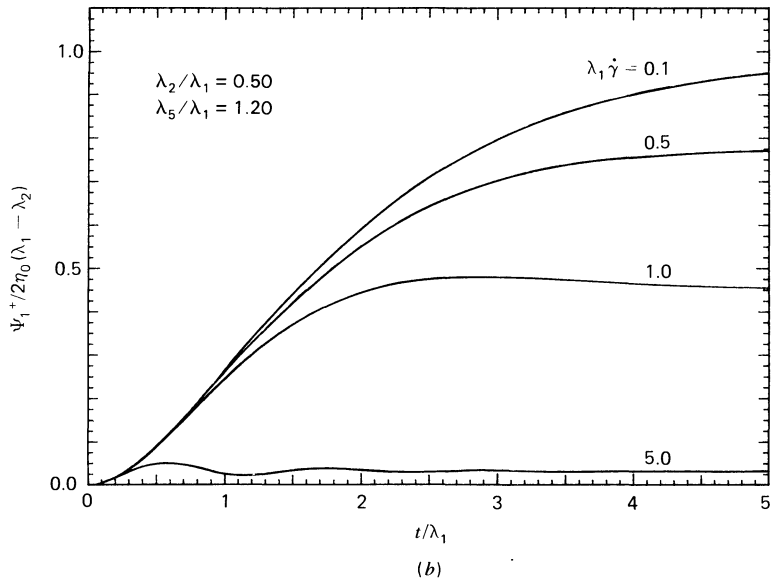

(*b*)

FIGURE 7.3-2. Stress growth material functions for start-up of steady shear flow for the Old 4-constant model defined in Table 7.3-2. These curves should be compared with the data in 3.4-7 through 3.4-10.

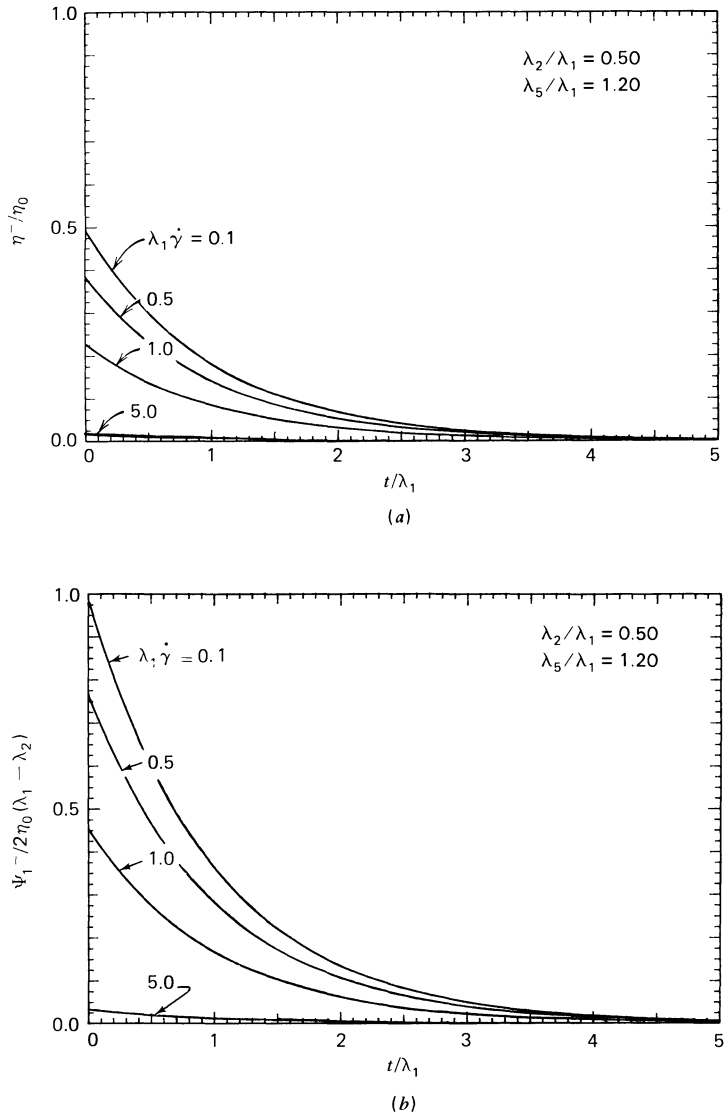

FIGURE 7.3-3. Stress relaxation material functions for cessation of steady shear flow of the Oldroyd 4-constant model defined in Table 7.3-2. These curves should be compared with the data in Figs. 3.4-11 through 3.4-13.

Equations 7.3-3 can be rewritten as a single constitutive equation by replacing τ_p in the last equation with $\tau - \tau_s = \tau + \eta_s\dot{\gamma}$. This leads to

$$\boxed{\begin{aligned}\tau + \lambda_1\tau_{(1)} - a\frac{\lambda_1}{\eta_0}\{\tau\cdot\tau\} - a\lambda_2\{\gamma_{(1)}\cdot\tau + \tau\cdot\gamma_{(1)}\} \\ = -\eta_0[\gamma_{(1)} + \lambda_2\gamma_{(2)} - a\frac{\lambda_2^2}{\lambda_1}\{\gamma_{(1)}\cdot\gamma_{(1)}\}]\end{aligned}} \tag{7.3-4}$$

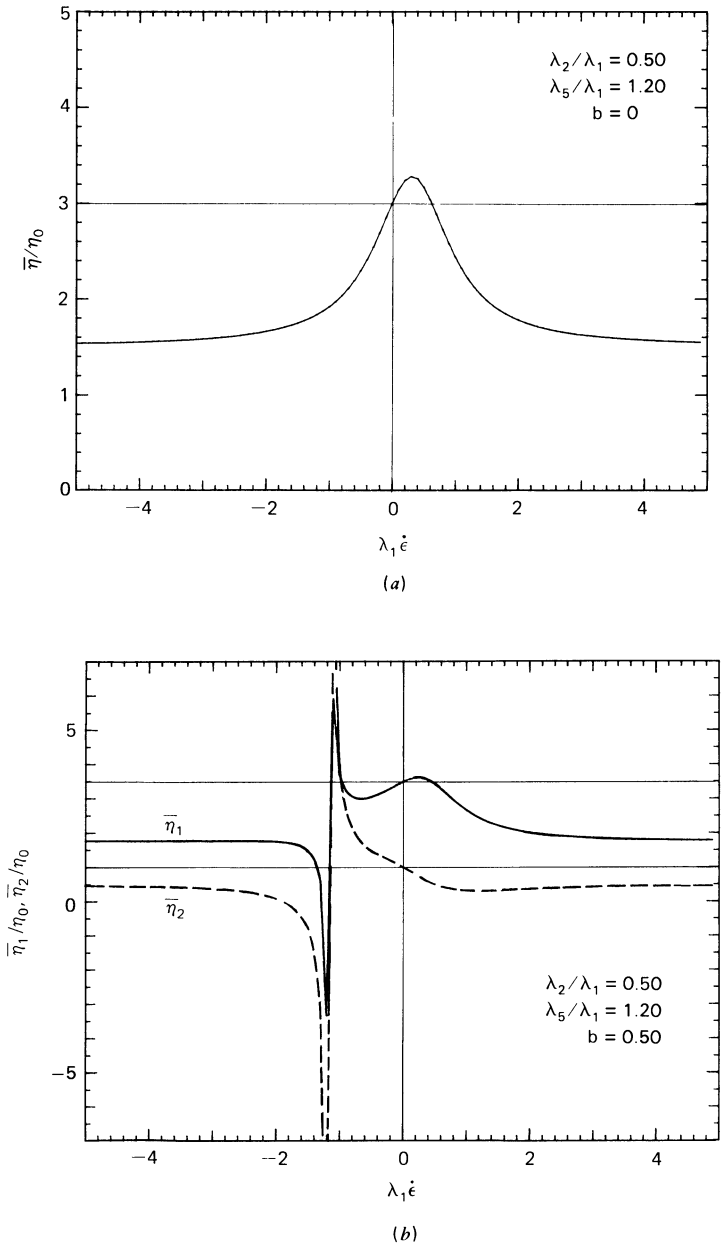

FIGURE 7.3-4. Steady shearfree flow material functions for the Oldroyd 4-constant model defined in Table 7.3-2 with $\lambda_2/\lambda_1 = 0.5$ and $\lambda_5/\lambda_1 = 1.2$ for several choices of the kinematic constant b: (*a*) $\bar{\eta}$ for elongational ($\dot{\epsilon} > 0$) and biaxial stretching ($\dot{\epsilon} < 0$) flow ($b = 0$); (*b*) $\bar{\eta}_1$ (——) and $\bar{\eta}_2$ (- - -) for $b = 0.5$. Note in part (*b*) that $\bar{\eta}_1$ and $\bar{\eta}_2$ are singular at a small negative value of $\dot{\epsilon}$. Although there are no steady-state experimental data for $b = 0.5$, this singular behavior does not seem realistic.

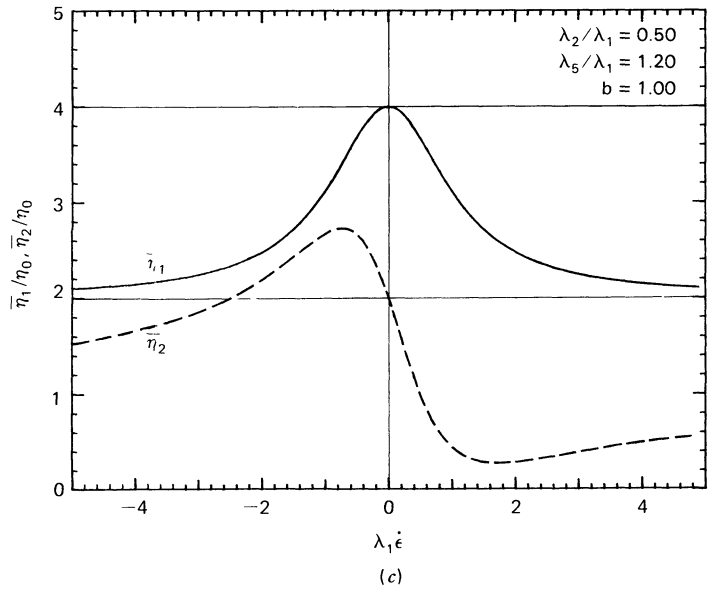

FIGURE 7.3-4. (*c*) $\bar{\eta}_1$ (——) and $\bar{\eta}_2$ (- - -) for planar elongational flow ($b = 1$).

where the zero-shear-rate viscosity η_0, the retardation time λ_2, and the modified mobility parameter a, are given in terms of η_s, η_p, and α as follows:

$$\eta_0 = \eta_s + \eta_p; \quad \lambda_2 = \lambda_1 \frac{\eta_s}{\eta_p}; \quad a = \frac{\alpha}{1 - (\lambda_2/\lambda_1)} \tag{7.3-5}$$

As given in Eq. 7.3-4, the Giesekus model is a special case of the Oldroyd 8-constant model to which a term involving $\{\boldsymbol{\tau} \cdot \boldsymbol{\tau}\}$ is added. Note that if $a = 0$ the convected Jeffreys model is recovered; thus the convected Jeffreys model can be written as the superposition in Eq. 7.3-3 with $\alpha = 0$ (cf. Eqs. 7.5-60). A number of equations used in the literature to which the Giesekus model can be reduced are listed in Table 7.3-4. Thus considerable diversity in the rheological predictions of the model is possible.

The inclusion of the $\{\boldsymbol{\tau} \cdot \boldsymbol{\tau}\}$ term in Eq. 7.3-3 gives material functions that are much more realistic than those obtained for the Oldroyd 8-constant model. For example, large decreases in the viscosity and normal stress coefficients with increasing shear rate are possible. For all $\alpha \neq 0$ or 1 the power-law slope of the viscosity is -1 when $\lambda_2 = 0$; this is unrealistically steep. However, by adding a small retardation term (e.g., $\lambda_2/\lambda_1 = 10^{-3}$), the value of $d \log \eta / d \log \dot{\gamma}$ can be kept larger than -1 so that the magnitude of the shear stress is always increasing with increasing shear rate. The second normal stress coefficient is non-zero and can be varied in size relative to the first normal stress coefficient; for example $\Psi_{2,0} = -(\alpha/2)\Psi_{1,0}$. Provided $\alpha \neq 0$ the elongational viscosity is bounded and reaches a constant value at large strain rates. Graphs of several steady and transient, shear and shearfree flow material functions are shown in Figs. 7.3-5 through 8 for the special choice $\alpha = 1/3$. In general we must require $0 < \alpha < 1/2$ for realistic properties.[7]

[7] In §7.6 we present a multimode Giesekus model which is a superposition of contributions to the stress tensor, each given by an equation like Eq. 7.3-3 with $\eta_s = 0$. There it is seen that the multimode model is capable of nearly quantitative fits of η, Ψ_1, η^+, and $\bar{\eta}^+$ for low-density polyethylene (cf. Figs. 7.6-1 through 3).

TABLE 7.3-4

Models Included in the Giesekus Model (Eq. 7.3-3 or 4) (see also Eqs. 13.7-10 and 11)

Name of Model	Values of Constants			Remarks
	$\lambda_1 \geq 0$	λ_2	$0 \leq \alpha \leq 1$	
Newtonian	0, λ	0, λ	0	Eq. 1.2-2
Second-order fluid	0	$\lambda_2 < 0$		Eq. 6.2-1
Convected Maxwell		0	0	Eq. 7.2-1 (with $\lambda_2 = 0$)
Convected Jeffreys		$\lambda_2 > 0$	0	Eq. 7.2-1
"Leonov-like"		0	1/2	Reduces to Leonov[a] model for steady shear and shearfree flows
"Corotational Maxwell-like"		0	1	Reduces to corotational Maxwell model[b] for shearfree flow

[a] A. I. Leonov, *Rheol. Acta*, **15**, 85-98 (1976); A. I. Leonov, E. H. Lipkina, E. D. Paskhin, and A. N. Prokunin, *Rheol. Acta*, **15**, 411-426 (1976).

[b] S. Zaremba, *Bull. Int. Acad. Sci. Cracovie*, 594-614 (1903); 614-621 (1903); H. Fromm, *Z. Angew. Math. Mech.*, **25/27**, 146-150 (1947); **28**, 43-54 (1948); and T. W. DeWitt, *J. Appl. Phys.*, **26**, 889-894 (1955). The corotational Maxwell model is sometimes called the ZFD model.

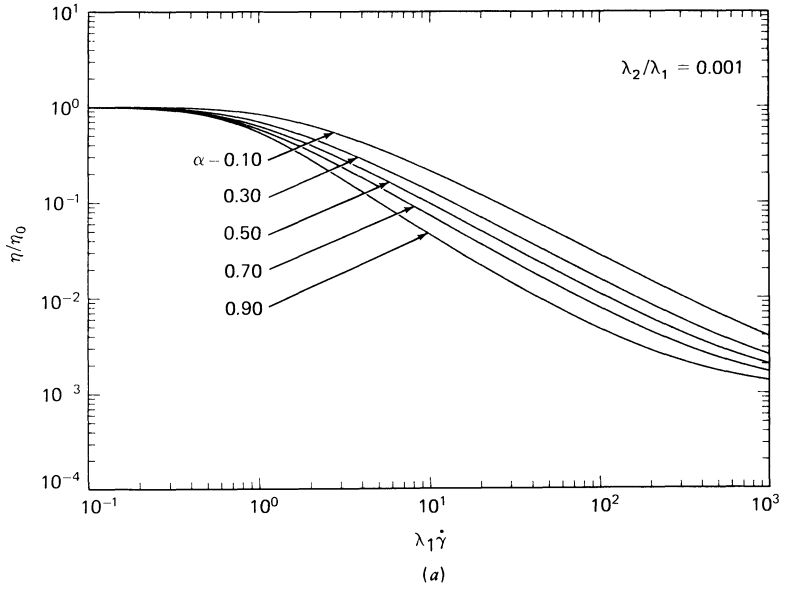

FIGURE 7.3-5. Dimensionless steady shear flow material functions for the Giesekus model with $\lambda_2/\lambda_1 = 10^{-3}$ and various values of α: (*a*) viscosity.

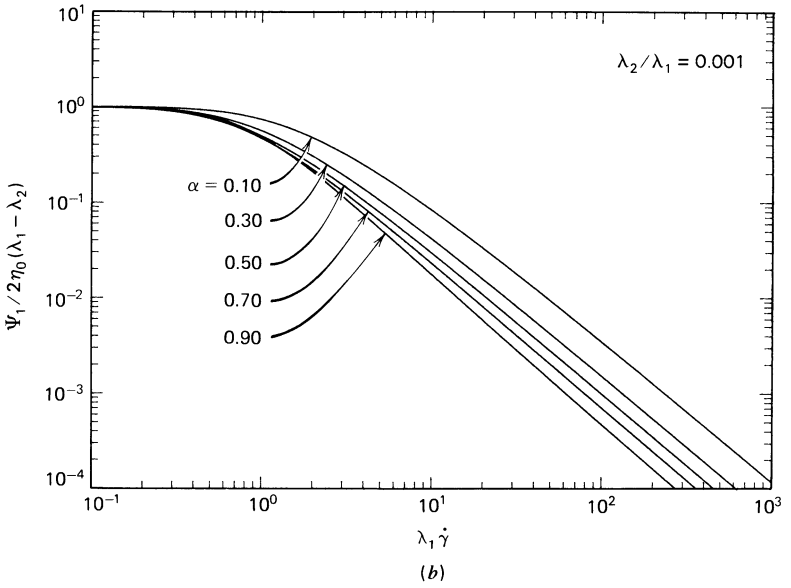

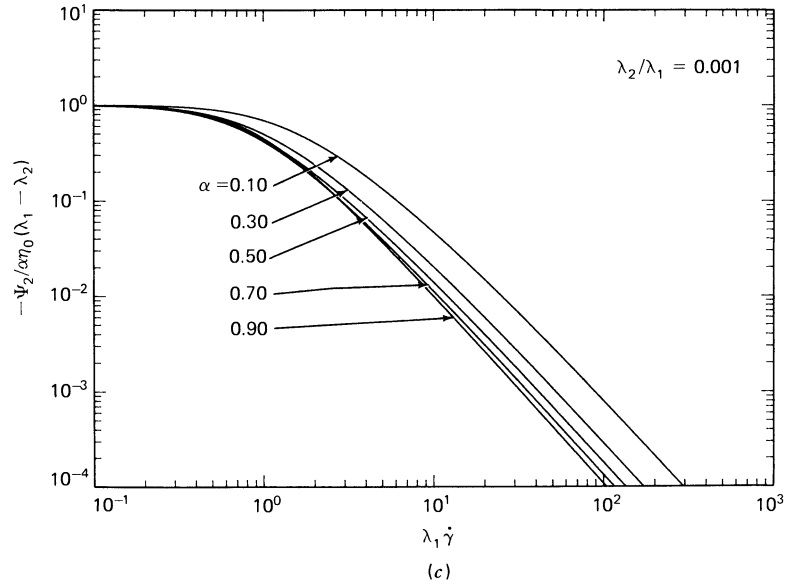

GURE 7.3-5. (*b*) first normal stress coefficient, (*c*) second normal stress coeffic

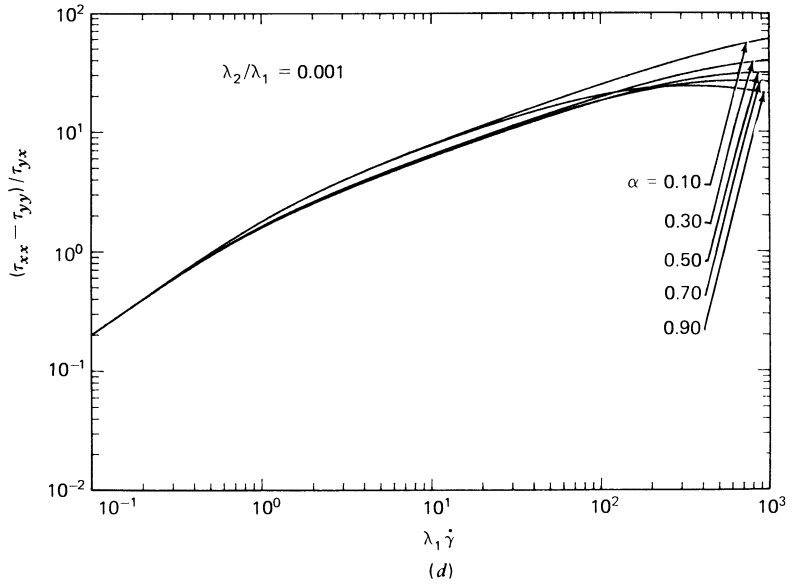

FIGURE 7.3-5. (*d*) stress ratio. The shear thinning of the viscometric functions is in good qualitative agreement with experimental data on polymer melts and solutions. The maximum in the stress ratio at high shear rates is probably unrealistic (cf. Fig. 3.3-8).

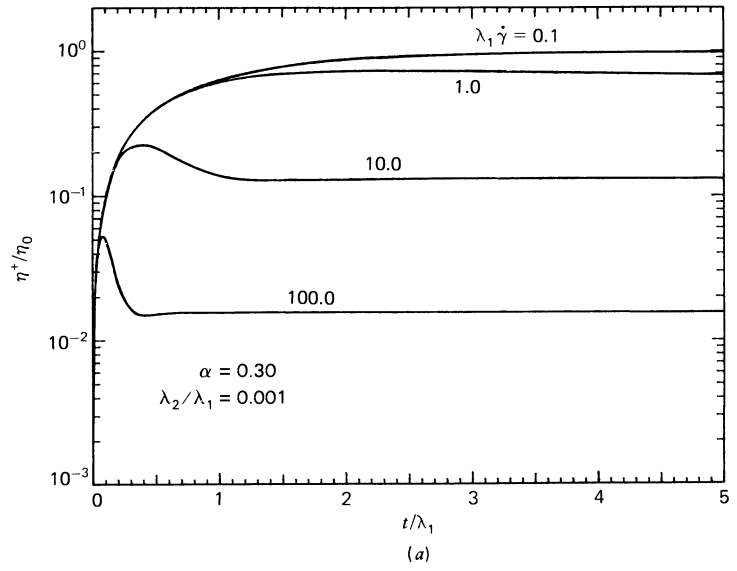

FIGURE 7.3-6. Dimensionless stress growth material functions for the Giesekus model with $\alpha = 0.3$ and $\lambda_2/\lambda_1 = 10^{-3}$. (*a*) η^+.

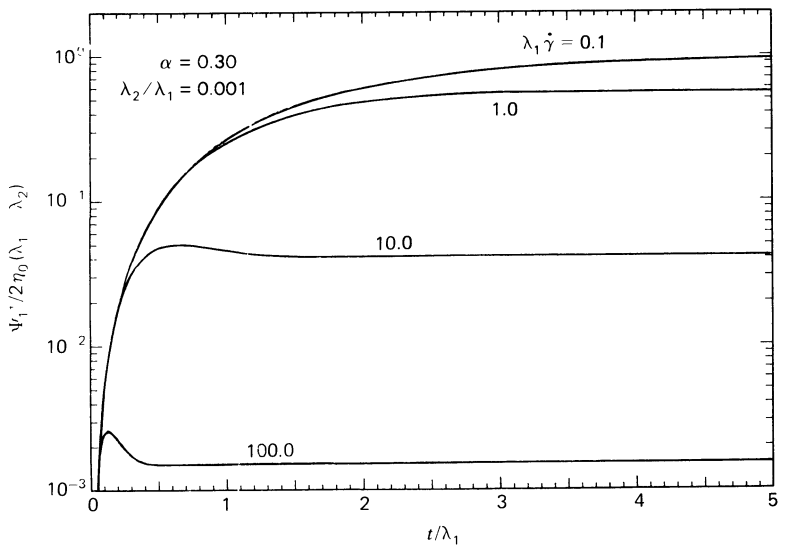

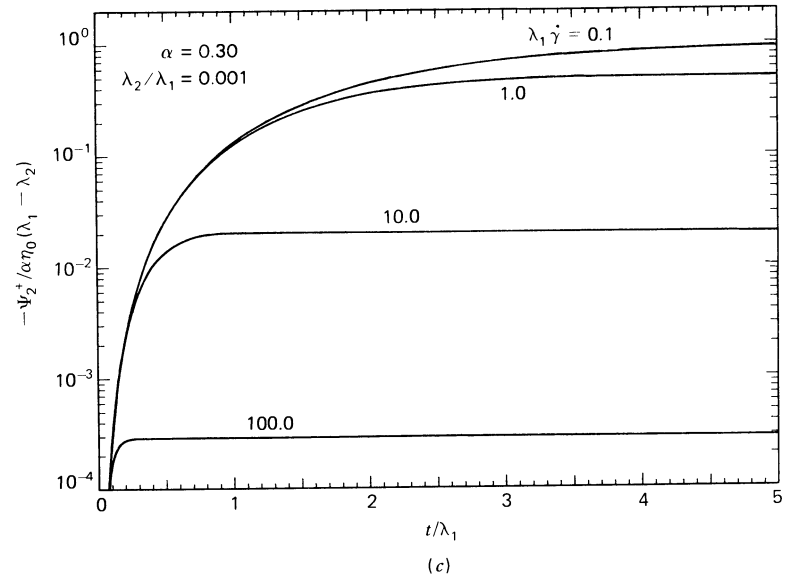

FIGURE 7.3-6. Dimensionless stress growth material functions for the Giesekus model with $\alpha = 0.3$ and $\lambda_2/\lambda_1 = 10^{-3}$. (*b*) Ψ_1^+, (*c*) Ψ_2^+. The stress overshoot in η^+ and Ψ_1^+ is in good agreement with experimental data on polymer melts and solutions (cf. Figs. 3.4-7–3.4-10).

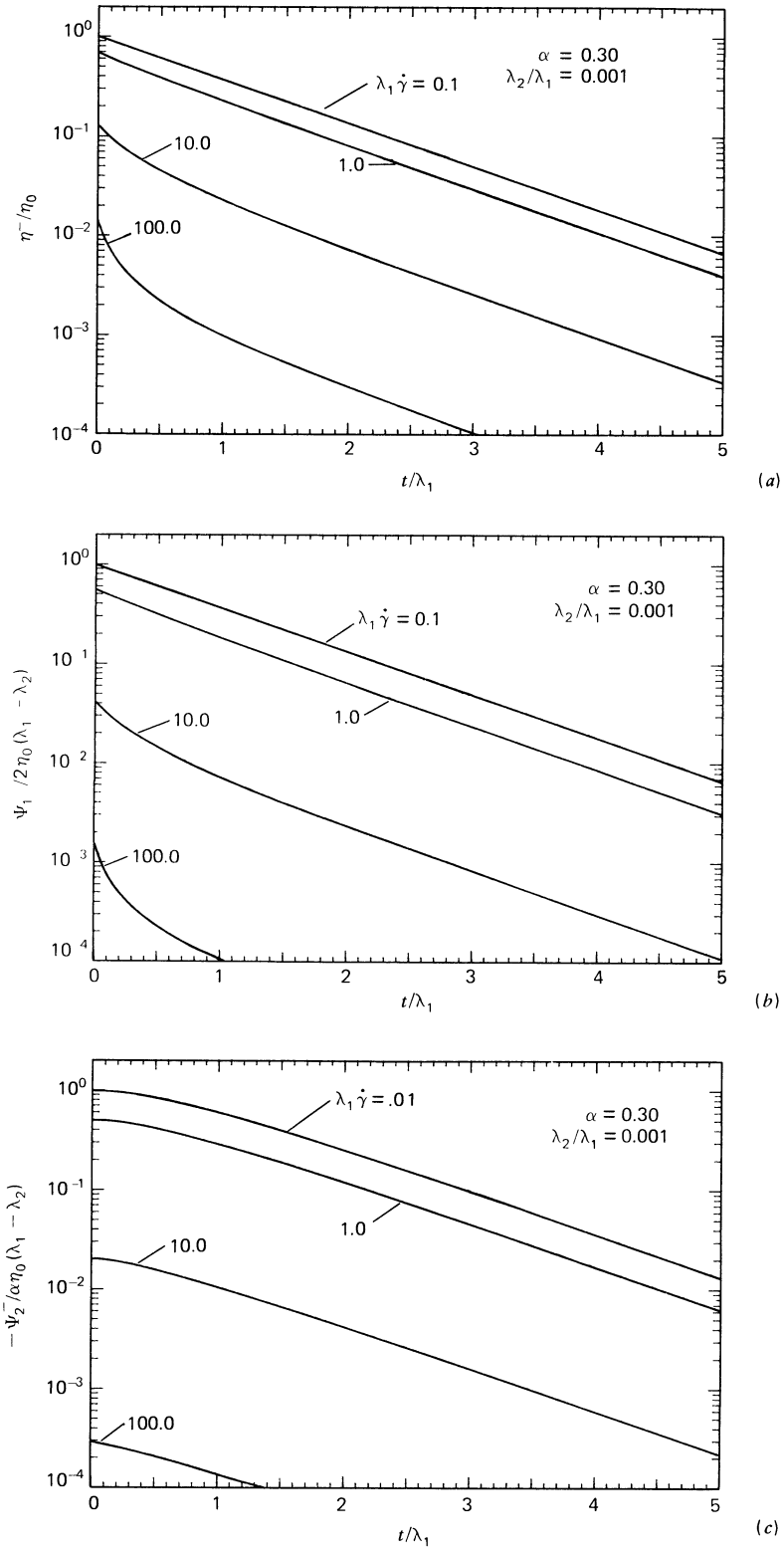

FIGURE 7.3-7. Dimensionless stress relaxation material functions for the Giesekus model with $\alpha = 0.3$ and $\lambda_2/\lambda_1 = 10^{-3}$. The increase in rate of relaxation with increasing shear rate for η^- and Ψ_1^- is in agreement with experimental data for polymer melts and solutions (cf. Figs. 3.4-11–3.4-13).

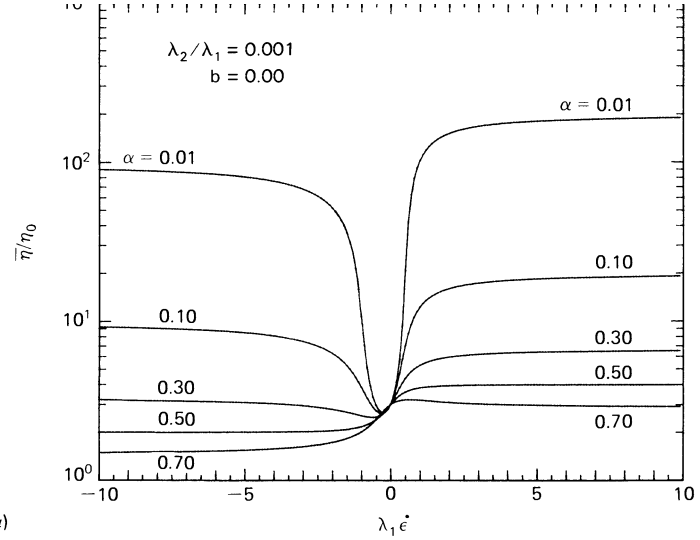
λ2/λ1 = 0.001
b = 0.00
α = 0.01
α = 0.01
0.10
0.10
0.30
0.50
0.70
0.30
0.50
0.70
η̄1/η0
λ1ε̇

(a)

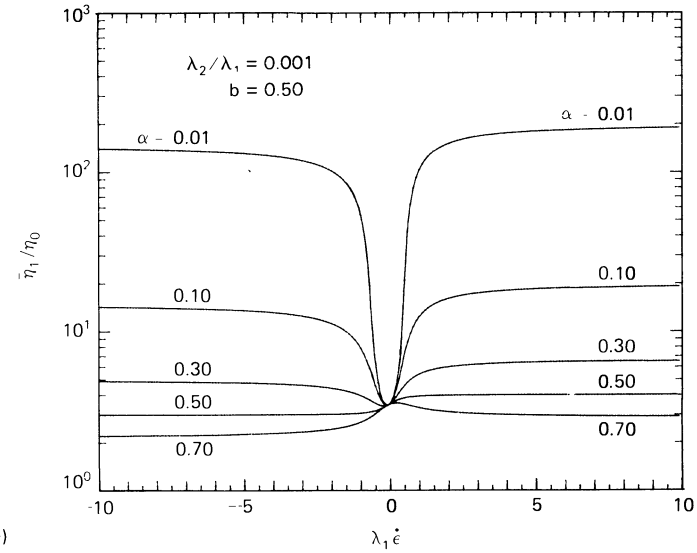
λ2/λ1 = 0.001
b = 0.50
α = 0.01
α = 0.01
0.10
0.10
0.30
0.50
0.70
0.30
0.50
0.70
η̄1/η0
λ1ε̇

(b)

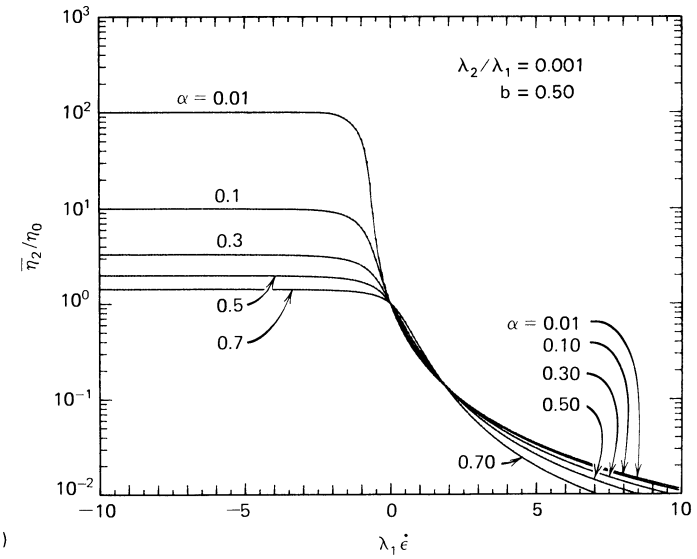
λ2/λ1 = 0.001
b = 0.50
α = 0.01
0.1
0.3
0.5
0.7
α = 0.01
0.10
0.30
0.50
0.70
η̄2/η0
λ1ε̇

(b)

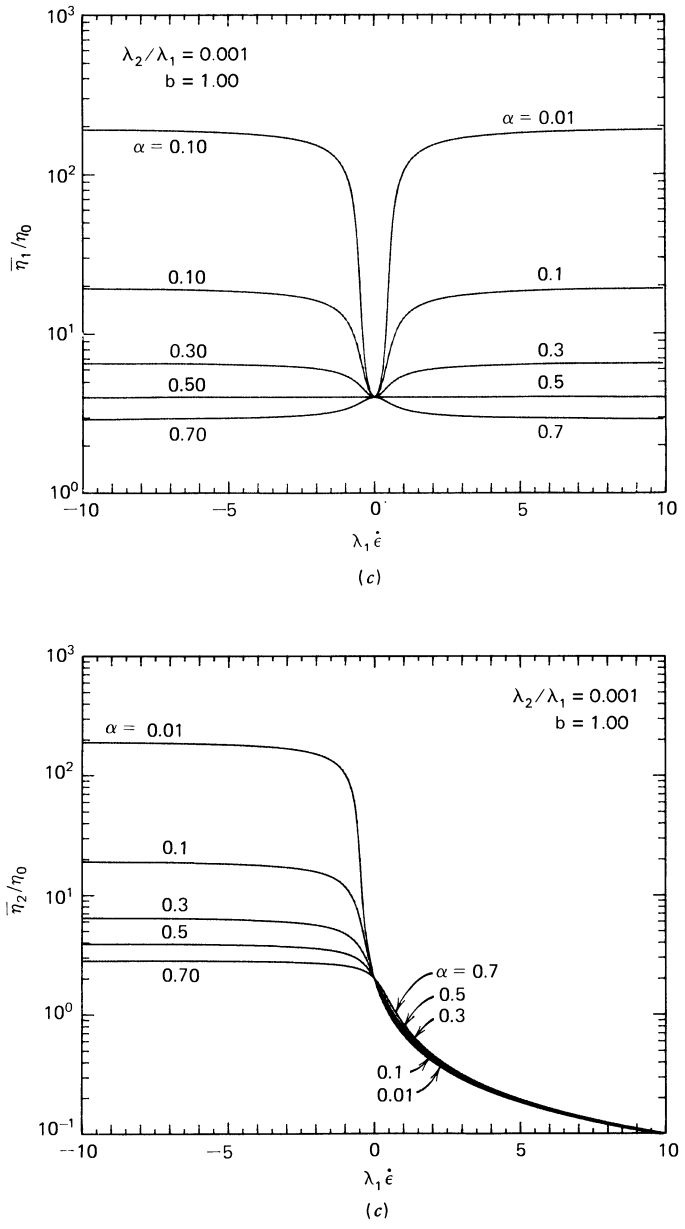

FIGURE 7.3-8. Dimensionless shearfree flow material functions for the Giesekus model with $\lambda_2/\lambda_1 = 10^{-3}$ and various values of α for several choices of the kinematic parameter b: (*a*) $\bar{\eta}$ for elongational ($\dot{\varepsilon} > 0$) and biaxial elongational ($\dot{\varepsilon} < 0$) flow for $b = 0$; (*b*) $\bar{\eta}_1$ and $\bar{\eta}_2$ for $b = 0.5$; and (*c*) $\bar{\eta}_1$ and $\bar{\eta}_2$ for planar elongational flow where $b = 1$.

TABLE 7.3-5

Material Functions for the Giesekus Model (Eq. 7.3-3)

Steady shear flow:

$$\frac{\eta}{\eta_0} = \frac{\lambda_2}{\lambda_1} + \left(1 - \frac{\lambda_2}{\lambda_1}\right)\frac{(1-f)^2}{1+(1-2\alpha)f} \tag{A}$$

$$\frac{\Psi_1}{2\eta_0(\lambda_1 - \lambda_2)} = \frac{f(1-\alpha f)}{(\lambda_1\dot{\gamma})^2\alpha(1-f)} \tag{B}$$

$$\frac{\Psi_2}{\eta_0(\lambda_1 - \lambda_2)} = \frac{-f}{(\lambda_1\dot{\gamma})^2} \tag{C}$$

where

$$f = \frac{1-\chi}{1+(1-2\alpha)\chi}; \quad \chi^2 = \frac{(1+16\alpha(1-\alpha)(\lambda_1\dot{\gamma})^2)^{1/2} - 1}{8\alpha(1-\alpha)(\lambda_1\dot{\gamma})^2}$$

For $\lambda_2 = 0$ and $\alpha \neq 0, 1$ the following asymptotic formulas are available:

$$\eta \sim \sqrt{(1-\alpha)/\alpha}\,\frac{\eta_0}{\lambda_1\dot{\gamma}} \qquad (\dot{\gamma} \to \infty) \tag{D}$$

$$\Psi_1 \sim \frac{\sqrt{2}}{\alpha}(\alpha(1-\alpha))^{1/4}\frac{\eta_0\lambda_1}{(\lambda_1\dot{\gamma})^{3/2}} \qquad (\dot{\gamma} \to \infty) \tag{E}$$

$$\Psi_2 \sim -\frac{\eta_0\lambda_1}{(\lambda_1\dot{\gamma})^2} \qquad (\dot{\gamma} \to \infty) \tag{F}$$

Small-amplitude oscillatory shear flow:

$$\frac{\eta'}{\eta_0} = \frac{1+\lambda_1\lambda_2\omega^2}{1+\lambda_1^2\omega^2} \tag{G}$$

$$\frac{\eta''}{\eta_0\omega} = \frac{(\lambda_1 - \lambda_2)}{1+\lambda_1^2\omega^2} \tag{H}$$

Steady elongational flow ($\alpha \neq 0$):

$$\frac{\bar{\eta}}{3\eta_0} = \frac{\lambda_2}{\lambda_1} + \left(1 - \frac{\lambda_2}{\lambda_1}\right)\frac{1}{6\alpha}\left[3 + \frac{1}{\lambda_1\dot{\varepsilon}}\{[1 - 4(1-2\alpha)\lambda_1\dot{\varepsilon} + 4\lambda_1^2\dot{\varepsilon}^2]^{1/2} - [1 + 2(1-2\alpha)\lambda_1\dot{\varepsilon} + \lambda_1^2\dot{\varepsilon}^2]^{1/2}\}\right] \tag{I}$$

For $\lambda_2 = 0$ and $\alpha \neq 0$ the following asymptotic formula holds:

$$\bar{\eta} \sim \frac{2\eta_0}{\alpha}, \qquad (\dot{\varepsilon} \to \infty) \tag{J}$$

The nonlinear stress term does make it more difficult to obtain analytical solutions for the material functions; a few of these are given in Table 7.3-5. For the transient material functions, numerical methods must be used. As a convenience, we provide in Table C.2 of Appendix C the governing equations to be used in finding these material functions.

§7.4 FLOW PROBLEMS IN ONE SPATIAL VARIABLE

In this section we illustrate the solution of one dimensional flow problems with the differential constitutive equations described in the previous two sections. The first two examples illustrate time-dependent effects in unsteady shearing flows, whereas the third example deals with elongational flow behavior.

EXAMPLE 7.4-1 The Rayleigh Problem for a Convected Jeffreys Fluid[1]

A semi-infinite body of viscoelastic liquid with constant density ρ is bounded at $y = 0$ by a flat solid surface (the xz-plane). Before $t = 0$ the fluid and the solid surface are at rest; after $t = 0$ the surface moves with constant velocity V in the positive x-direction. Find the velocity distribution if the fluid is described by a convected Jeffreys model. (See Problem 1B.6 for the analogous Newtonian fluid problem, and Problem 4C.3 for the power-law model.)

SOLUTION We postulate a solution of the form $v_x = v_x(y, t)$, that is, the flow is a nonhomogeneous shear flow with the shear rate a function of y and t. Then the equation of continuity is satisfied identically and the three components of the equation of motion are

$$\rho \frac{\partial v_x}{\partial t} = -\frac{\partial \tau_{yx}}{\partial y} \tag{7.4-1}$$

$$0 = -\frac{\partial p}{\partial y} - \frac{\partial \tau_{yy}}{\partial y} \tag{7.4-2}$$

$$0 = -\frac{\partial p}{\partial z} + \rho g \tag{7.4-3}$$

Since the shear rate depends on y and t we also expect $\tau_{ij} = \tau_{ij}(y, t)$. The $\{\boldsymbol{v}\cdot\nabla\boldsymbol{\tau}\}$ and $\{\boldsymbol{v}\cdot\nabla\boldsymbol{\gamma}_{(1)}\}$ contributions to $\boldsymbol{\tau}_{(1)}$ and $\boldsymbol{\gamma}_{(2)}$ are both zero since the velocity is perpendicular to the direction of the gradients. This means that the convected Jeffreys model will be the same as for homogeneous shear flow, which is given in Eqs. 7.2-3 through 6, with $\dot{\gamma}_{yx}(y, t) = \partial v_x/\partial y$ and with all d/dt replaced by $\partial/\partial t$.

From Eq. 7.2-4 we obtain immediately

$$\tau_{yy} = A(y)e^{-t/\lambda_1} \tag{7.4-4}$$

where $A(y)$ is an arbitrary function of y. But τ_{yy} is zero for $t \leq 0$, so $A(y)$ must be zero. Then the τ_{yy} term in Eq. 7.2-6 can be omitted (as it was for homogeneous flows) and Eqs. 7.4-1 and 7.2-6 can be combined to give:

$$\rho\left(\frac{\partial v_x}{\partial t} + \lambda_1 \frac{\partial^2 v_x}{\partial t^2}\right) = \eta_0\left(\frac{\partial^2 v_x}{\partial y^2} + \lambda_2 \frac{\partial}{\partial t}\frac{\partial^2 v_x}{\partial y^2}\right) \tag{7.4-5}$$

[1] This example is patterned after R. I. Tanner, *Z. Angew. Math. Phys.*, **13**, 573-580 (1962). Y. Mochimaru, *J. Non-Newtonian Fluid Mech.*, **12**, 135-152 (1983), has done start-up of steady shear flow between parallel plates.

It is convenient to introduce the following dimensionless quantities:

$$\phi = \frac{v_x}{V} \qquad T = \frac{t}{\lambda_1}$$
$$Y = \left(\frac{\rho}{\eta_0 \lambda_1}\right)^{1/2} y \qquad \Lambda = \frac{\lambda_2}{\lambda_1} \tag{7.4-6}$$

Note that y is scaled by the viscous diffusion penetration length for time λ_1. The mathematical problem that we have to solve then consists of the linear partial differential equation

$$\frac{\partial \phi}{\partial T} + \frac{\partial^2 \phi}{\partial T^2} = \frac{\partial^2 \phi}{\partial Y^2} + \Lambda \frac{\partial^3 \phi}{\partial T \partial Y^2} \tag{7.4-7}$$

along with the following boundary and initial conditions:

$$\phi = H(T), \qquad \text{at } Y = 0 \tag{7.4-8}$$

$$\phi \to 0, \qquad \text{as } Y \to \infty \tag{7.4-9}$$

$$\frac{\partial \phi}{\partial T} = \frac{\partial^2 \phi}{\partial T^2} = 0, \qquad \text{for } T \leq 0 \tag{7.4-10}$$

where $H(T)$ is the Heaviside unit step function.

Tanner solved the problem by taking the Laplace transform of Eq. 7.4-7 and using the initial condition; this gives

$$(s + s^2)\bar{\phi} = (1 + \Lambda s)\frac{d^2 \bar{\phi}}{dY^2} \tag{7.4-11}$$

where s is the Laplace transform variable. This ordinary differential equation can be solved with the boundary conditions that $\bar{\phi}$ approaches zero as $Y \to \infty$, and $\bar{\phi} = 1/s$ at $Y = 0$. The result is

$$\bar{\phi} = \frac{1}{s} \exp\left(-\left(\frac{s(1 + s)}{1 + \Lambda s}\right)^{1/2} Y \right) \tag{7.4-12}$$

Tanner inverted Eq. 7.4-12 by performing a contour integral in the complex plane to obtain the solution

$$\phi(Y, T) = \frac{1}{2} + \frac{1}{\pi} \int_0^\infty \exp\left[-\left(\frac{u}{2}\right)^{1/2} M(\cos\theta - \sin\theta) Y \right]$$
$$\cdot \sin\left[uT - \left(\frac{u}{2}\right)^{1/2} M(\cos\theta + \sin\theta) Y \right] \frac{du}{u} \tag{7.4-13}$$

in which $M(u)$ and $\theta(u)$ are defined by:

$$M(u) = \left(\frac{1 + u^2}{1 + \Lambda^2 u^2}\right)^{1/4}; \quad \theta(u) = \frac{1}{2}(\arctan u - \arctan \Lambda u) \tag{7.4-14}$$

We see that for this very idealized problem and simplified constitutive equation, an analytical solution can be obtained. For the special case of $\Lambda = 1$ (both time constants equal), in which case the convected

Jeffreys model reduces to the Newtonian fluid, Tanner showed that the solution simplifies correctly to the error function expression given in Problem 1B.6 for the Newtonian fluid. For the limit $\Lambda = 0$ (the convected Maxwell model), Tanner showed that the solution reduced to

$$\phi(Y, T) = e^{-Y/2}H(T - Y) + \frac{Y}{2}\int_0^T \frac{e^{-u/2}}{\sqrt{u^2 - Y^2}} I_1\left(\tfrac{1}{2}\sqrt{u^2 - Y^2}\right)H(u - Y)du \tag{7.4-15}$$

where I_1 is the modified Bessel function of the first kind. Thus the convected Maxwell model is seen to give a wave that propagates away from the plate at constant speed $\sqrt{\eta_0/\rho\lambda_1}$.

To show how the character of the solution changes as Λ goes from 0 (the "damped wave equation") to 1 (the "diffusion equation"), we have performed the integral in Eq. 7.4-13 numerically. Figure 7.4-1 illustrates the results of these calculations; the velocity is shown there as a function of position for different times and Λ. Note that for a given time t, small velocity disturbances are felt at larger distances y from the moving plate for larger values of Λ. That is, the retardation term which adds Newtonian character to the convected Jeffreys fluid produces more diffusivelike behavior, as expected. For the smallest value of $\Lambda = 0.01$ in Fig. 7.4-1, the wave front associated with elastic wave propagation is seen clearly in the rapid change in velocity over small distances (the flat regions). Comparison of the results for different values of Λ in this figure shows how the wave front is diffused as Λ increases.

EXAMPLE 7.4-2 Tube Flow of a White–Metzner Fluid with a Pulsatile Pressure Gradient[2,3]

Consider the unsteady flow of a viscoelastic fluid in a horizontal circular tube of radius R. Let the pressure gradient vary sinusoidally about some mean value $\Delta p_0/L$

$$\frac{\Delta p}{L} = \frac{\Delta p_0}{L}(1 + \varepsilon\, \mathscr{R}e\{e^{i\omega t}\}) \tag{7.4-16}$$

where Δp_0 is the time-averaged pressure drop over a length L of tube, ε is the *small* amplitude of the pressure gradient variation, and ω is the frequency of the fluctuations in the pressure drop. Assume that inertial effects are negligible. We wish to find the mean volume flow rate $\langle Q\rangle$ as a function of the mean pressure gradient and frequency of fluctuation. Of particular interest is the flow enhancement relative to the steady-state volume flow rate Q_0 given by

$$I = \frac{\langle Q\rangle - Q_0}{Q_0} \tag{7.4-17}$$

Since the volume flow rate for the base problem of steady tube flow can be given exactly by the White–Metzner model, we will use this model to describe the viscoelastic flow. Of course, for steady tube flow the White–Metzner model gives the same velocity field as the generalized Newtonian fluid.

[2] This example is patterned after J. M. Davies, S. Bhumiratana, and R. B. Bird, *J. Non-Newtonian Fluid Mech.*, **3**, 237–259 (1977/78) and N. Phan-Thien, *J. Non-Newtonian Fluid Mech.*, **4**, 167–176 (1978). Other discussions of this problem have been given by K. Walters and P. Townsend in S. Onogi, ed., *Proceedings of the Fifth International Congress on Rheology*, Vol. 4, University of Tokyo Press (1970), pp. 471–483, and H. A. Barnes, P. Townsend, and K. Walters, *Nature*, **224**, 585–587 (1969); *Rheol. Acta*, **10**, 517–527 (1971). A review article including the pulsatile flow problem as well as flow in a corrugated pipe, flow in a curved pipe, and flow in a noncircular pipe has been prepared by K. Walters in W. R. Schowalter, ed., *Progress in Heat and Mass Transfer*, Vol. 5, Pergamon Press, Elmsford, NY (1972), pp. 217–231.

[3] See Example 4.2-6 for pulsatile tube flow of a power-law fluid.

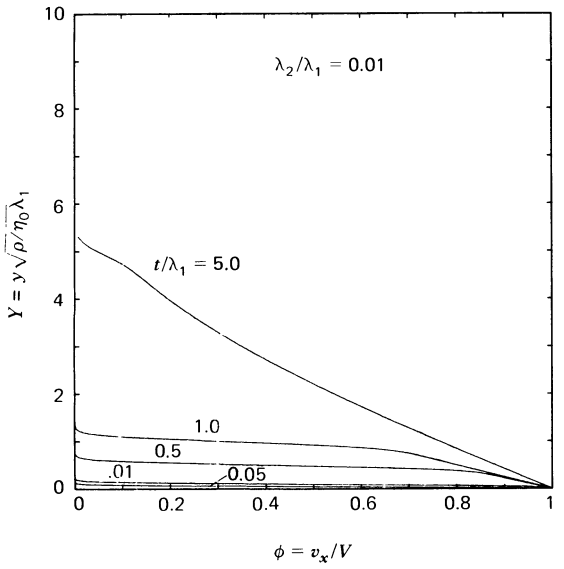

(*a*)

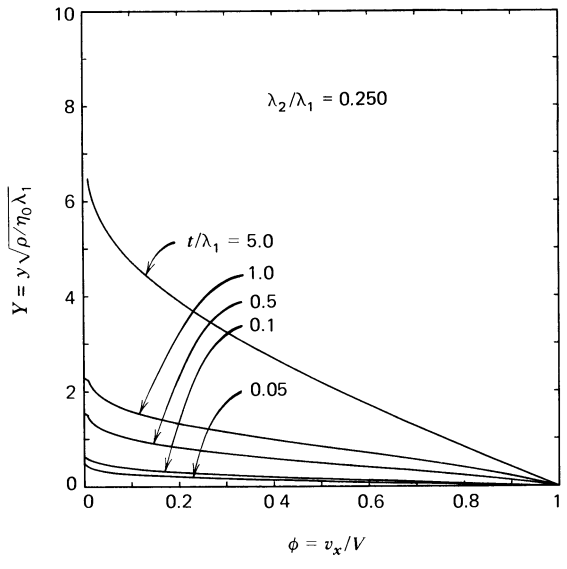

(*b*)

FIGURE 7.4-1. Calculated velocity profiles for the Rayleigh problem for a convected Jeffreys fluid. The curves show the velocity variation with position for a series of times $T = t/\lambda_1$. The influence of $\Lambda = \lambda_2/\lambda_1$ is illustrated by comparison of parts (*a*) through (*d*). As Λ decreases, the fluid becomes more

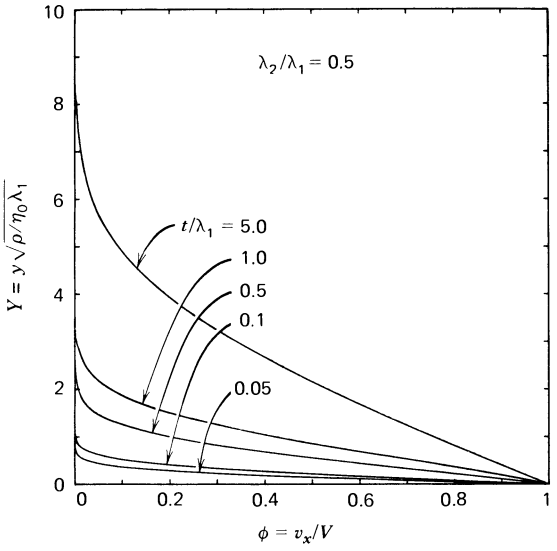

(c)

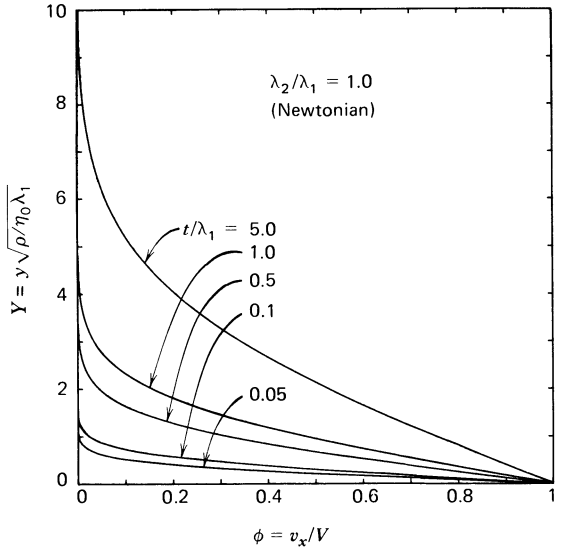

(d)

and more elastic (i.e., more solidlike). In the Newtonian limit ($\Lambda = 1$), the parameter λ_1 is an arbitrary constant.

SOLUTION It seems reasonable to assume that $v_z = v_z(r, t)$ and $v_r = v_\theta = 0$. For most polymer solutions and melts, the viscosity is so large that the inertial terms in the equation of motion can be neglected. The axial component of the equation of motion is then

$$0 = \frac{\Delta p_0}{L}(1 + \varepsilon\, \mathscr{R}e\{e^{i\omega t}\}) - \frac{1}{r}\frac{\partial}{\partial r}(r\tau_{rz}) \tag{7.4-18}$$

The shear stress is obtained by integrating with respect to r

$$\tau_{rz} = \frac{\Delta p_0 r}{2L}(1 + \varepsilon\, \mathscr{R}e\{e^{i\omega t}\}) \tag{7.4-19}$$

where we have required τ_{rz} to be finite at $r = 0$. This result must be combined with the constitutive equation to obtain an equation for the velocity field. The rz-component of the White-Metzner model gives (cf Eqs. 7.2-3 through 6)

$$\left(1 + \frac{\eta(\dot\gamma)}{G}\frac{\partial}{\partial t}\right)\tau_{rz} = -\eta(\dot\gamma)\dot\gamma_{rz} = \eta(\dot\gamma)\dot\gamma \tag{7.4-20}$$

In the second equality of Eq. 7.4-20, we have used the fact that since the amplitude of the pressure gradient oscillation ε is small and inertial effects are negligible, the axial velocity is expected to oscillate as shown in Fig. 7.4-2. This means that everywhere in the tube $\dot\gamma_{rz}$ will be negative and equal to $-\dot\gamma$. When Eqs. 7.4-19 and 20 are combined we obtain

$$\frac{\Delta p_0 r}{2L}\left[1 + \varepsilon\left(\mathscr{R}e\{e^{i\omega t}\} + \frac{\eta(\dot\gamma)}{G}\mathscr{R}e\{i\omega e^{i\omega t}\}\right)\right] = \eta(\dot\gamma)\dot\gamma \tag{7.4-21}$$

Solution of this algebraic equation for $\dot\gamma(r, t)$ is sufficient for obtaining the flow enhancement I, which is shown next.

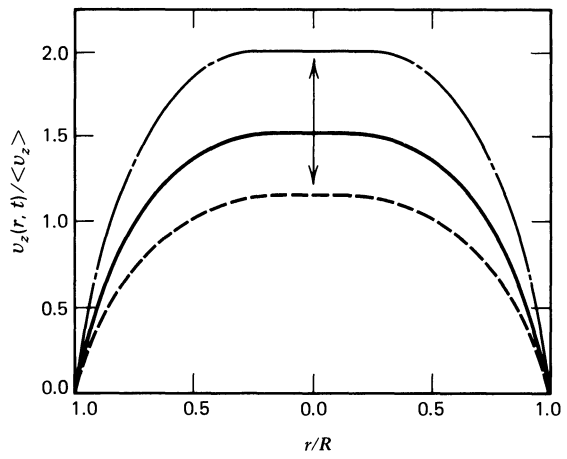

FIGURE 7.4-2. Schematic diagram illustrating the anticipated velocity profile $v_z(r, t)$ in pulsatile tube flow. The axial velocity at each time t is normalized by the average velocity $\langle v_z\rangle$ at that time. The solid curve (——) is the velocity at the average pressure drop Δp_0. The other two curves give the velocity for $\varepsilon = 0.1$: (—·—) corresponds to the maximum pressure drop, 1.1 Δp_0 and (– – –) corresponds to the minimum pressure drop 0.9 Δp_0.

The presence of the small parameter ε suggests that we develop a series solution for $\dot{\gamma}(r, t)$ of the form

$$\dot{\gamma}(r, t) = \dot{\gamma}_0 + \varepsilon[\dot{\gamma}_{10} + \mathscr{R}e\{\dot{\gamma}_{11}e^{i\omega t}\}] + \varepsilon^2[\dot{\gamma}_{20} + \mathscr{R}e\{\dot{\gamma}_{21}e^{i\omega t}\} + \mathscr{R}e\{\dot{\gamma}_{22}e^{2i\omega t}\}] + \cdots \quad (7.4\text{-}22)$$

in which the $\dot{\gamma}_{m0}(r)$ are real, the other $\dot{\gamma}_{mn}(r)$ are complex, and $\dot{\gamma}_0(r)$ is the shear rate distribution in steady tube flow. We now show that only $\dot{\gamma}_0$ and $\dot{\gamma}_{20}$ need to be found.

The time-averaged volume flow rate is given by

$$\langle Q\rangle = \frac{\omega}{2\pi}\int_0^{2\pi/\omega} 2\pi \int_0^R v_z(r, t) r dr dt \quad (7.4\text{-}23)$$

If this expression is integrated by parts and the no-slip boundary condition at the tube wall applied, then the result is

$$\langle Q\rangle = \pi \int_0^R \langle\dot{\gamma}\rangle r^2 dr \quad (7.4\text{-}24)$$

in which $\langle\cdot\rangle = (\omega/2\pi)\int_0^{2\pi/\omega}(\cdot)dt$. The steady-state flow rate corresponding to $\varepsilon = 0$ is

$$Q_0 = \pi \int_0^R \dot{\gamma}_0 r^2 dr \quad (7.4\text{-}25)$$

The enhancement is obtained by combining Eqs. 7.4-17, 22, 24, and 25:

$$I = \frac{\int_0^R[\varepsilon\dot{\gamma}_{10} + \varepsilon^2\dot{\gamma}_{20} + \cdots]r^2 dr}{\int_0^R \dot{\gamma}_0 r^2 dr} = \frac{\varepsilon^2\int_0^R \dot{\gamma}_{20} r^2 dr}{\int_0^R \dot{\gamma}_0 r^2 dr} + O(\varepsilon^4) \quad (7.4\text{-}26)$$

In writing down the last line of Eq. 7.4-26 we have set $\dot{\gamma}_{10} = 0$, since the volume flow rate must be an even function of ε. This will be verified in the subsequent development. Thus finding I requires only that we determine $\dot{\gamma}_0$ and $\dot{\gamma}_{20}$ from Eqs. 7.4-21 and 22.

We now return to the problem of solving Eq. 7.4-21. To develop the series solution to this equation, we need in addition to Eq. 7.4-22 an expansion for η in powers of ε. A Taylor expansion in ε gives

$$\begin{aligned}\eta(\dot{\gamma}) = \eta(\dot{\gamma}_0) &+ \varepsilon\eta_1(\dot{\gamma}_0)[\dot{\gamma}_{10} + \mathscr{R}e\{\dot{\gamma}_{11}e^{i\omega t}\}] \\ &+ \frac{\varepsilon^2}{2}\Big[\eta_2(\dot{\gamma}_0)[\dot{\gamma}_{10} + \mathscr{R}e\{\dot{\gamma}_{11}e^{i\omega t}\}]^2 + 2\eta_1(\dot{\gamma}_0)[\dot{\gamma}_{20} \\ &+ \mathscr{R}e\{\dot{\gamma}_{21}e^{i\omega t}\} + \mathscr{R}e\{\dot{\gamma}_{22}e^{2i\omega t}\}]\Big] + \cdots\end{aligned} \quad (7.4\text{-}27)$$

in which $\eta_j = d^j\eta/d\dot{\gamma}^j$. Also, by multiplying the expansions in Eqs. 7.4-22 and 27 we have

$$\begin{aligned}\eta(\dot{\gamma})\dot{\gamma} = \eta(\dot{\gamma}_0)\dot{\gamma}_0 &+ \varepsilon[\eta_1(\dot{\gamma}_0)\dot{\gamma}_0 + \eta(\dot{\gamma}_0)][\dot{\gamma}_{10} + \mathscr{R}e\{\dot{\gamma}_{11}e^{i\omega t}\}] \\ &+ \varepsilon^2\{(\eta(\dot{\gamma}_0)\dot{\gamma}_{20} + [\eta_1(\dot{\gamma}_0) + \tfrac{1}{2}\eta_2(\dot{\gamma}_0)\dot{\gamma}_0][\dot{\gamma}_{10}^2 + \tfrac{1}{2}\dot{\gamma}_{11}\bar{\dot{\gamma}}_{11}] \\ &+ \eta_1(\dot{\gamma}_0)\dot{\gamma}_0\dot{\gamma}_{20}) \\ &+ \text{terms involving } e^{i\omega t} \text{ and } e^{2i\omega t}\} + \cdots\end{aligned} \quad (7.4\text{-}28)$$

Since we seek only $\dot{\gamma}_0$ and $\dot{\gamma}_{20}$ we do not need the oscillatory terms at order ε^2. In obtaining the above we have made use of Eq. 4.2-56a, and we denote the complex conjugate by an overbar.

We now combine Eqs. 7.4-21, 27, and 28. Equating terms of equal order in ε and of the same frequency gives the following results:

$O(\varepsilon^0)$:

$$\frac{\Delta p_0 r}{2L} = \eta(\dot{\gamma}_0)\dot{\gamma}_0 \tag{7.4-29}$$

$O(\varepsilon)$:

Constant terms

$$0 = [\eta_1(\dot{\gamma}_0)\dot{\gamma}_0 + \eta(\dot{\gamma}_0)]\dot{\gamma}_{10} \tag{7.4-30}$$

$e^{i\omega t}$ *terms*

$$\frac{\Delta p_0 r}{2L}\left[1 + \frac{i\omega\eta(\dot{\gamma}_0)}{G}\right] = [\eta_1(\dot{\gamma}_0)\dot{\gamma}_0 + \eta(\dot{\gamma}_0)]\dot{\gamma}_{11} \tag{7.4-31}$$

$O(\varepsilon^2)$:

Constant terms

$$\eta(\dot{\gamma}_0)\dot{\gamma}_0 \frac{\eta_1(\dot{\gamma}_0)}{2G}\mathscr{R}e\{-i\omega\dot{\gamma}_{11}\} = \eta(\dot{\gamma}_0)\dot{\gamma}_{20} + \eta_1(\dot{\gamma}_0)\dot{\gamma}_0\dot{\gamma}_{20} + [\eta_1(\dot{\gamma}_0) + \tfrac{1}{2}\eta_2(\dot{\gamma}_0)\dot{\gamma}_0][\dot{\gamma}_{10}^2 + \tfrac{1}{2}\dot{\gamma}_{11}\bar{\dot{\gamma}}_{11}] \tag{7.4-32}$$

There is no need to consider the other terms at $O(\varepsilon^2)$, since the constant terms are sufficient to give $\dot{\gamma}_{20}$, and this is all that affects the enhancement I. To find $\dot{\gamma}_{20}$ we note that in general the viscosity function will not be such that the [ ] term in Eq. 7.4-30 is zero. This means $\dot{\gamma}_{10}$ must be zero. Equation 7.4-29 can be combined with Eq. 7.4-31, and $\dot{\gamma}_{11}$ can be solved for explicitly. Then combination of these results for $\dot{\gamma}_{10}$ and $\dot{\gamma}_{11}$ with Eq. 7.4-32 leads to the final result for $\dot{\gamma}_{20}$

$$\dot{\gamma}_{20} = -\frac{(\eta\dot{\gamma}_0)^2}{2(\eta + \eta_1\dot{\gamma}_0)^3}\left\{(\eta_1 + \tfrac{1}{2}\eta_2\dot{\gamma}_0)\left(1 + \left(\frac{\eta}{G}\right)^2\omega^2\right) - \frac{\eta\eta_1\omega^2}{G^2}(\eta + \eta_1\dot{\gamma}_0)\right\} \tag{7.4-33}$$

where it is understood that η, η_1, and η_2 are all evaluated at $\dot{\gamma}_0$ (this same convention is used below in Eq. 7.4-34).

To evaluate the enhancement it is convenient to change the integration variable in Eq. 7.4-26 from r to $\dot{\gamma}_0$ by using Eq. 7.4-29. This results in:

$$\frac{I}{\varepsilon^2} = \frac{\int_0^{\dot{\gamma}_{0w}} \dot{\gamma}_{20}\eta^2[\eta + \eta_1\dot{\gamma}_0]\dot{\gamma}_0^2\, d\dot{\gamma}_0}{\int_0^{\dot{\gamma}_{0w}} \dot{\gamma}_0^3\eta^2[\eta + \eta_1\dot{\gamma}_0]d\dot{\gamma}_0} + \cdots \tag{7.4-34}$$

in which $\dot{\gamma}_{0w}$ is the wall shear rate at steady state which is given by Eq. 7.4-29 written for $r = R$. To examine I/ε^2 we have chosen a Carreau viscosity equation for η given by Eq. 4.1-9 with $a = 2$. With this choice of viscosity expression, I/ε^2 is a function of the following dimensionless quantities:

n	power-law index
$\dfrac{\eta_\infty}{\eta_0 - \eta_\infty}$	dimensionless infinite-shear-rate viscosity
$\Omega = \lambda\omega$	dimensionless frequency
$\dfrac{R\langle\Delta p\rangle\lambda}{L(\eta_0 - \eta_\infty)}$	dimensionless mean pressure gradient

Equation 7.4-34 was then integrated numerically by Romberg's method combined with Neville's algorithm for extrapolating to zero mesh size.[4] In these calculations it is reasonable to take the Carreau time constant λ to be equal to $(\eta_0 - \eta_\infty)/G$. Figure 7.4-3 shows some sample calculations. These suggest that the pulsatile pressure gradient may either increase or decrease the volume rate of flow. They further suggest that there will be a "resonance" effect, with appreciable increase or decrease near a particular pressure gradient.

Figure 7.4-4 contains some sample experimental data of Barnes, Townsend, and Walters for aqueous polyacrylamide solutions. The shapes of the curves are similar to the low-pressure-gradient results for the White–Metzner model. Note that the experimentally observed maximum enhancement occurs at approximately a constant mean pressure gradient, independent of the frequency of oscillation; this observation agrees with the White–Metzner model predictions at low $\Delta p_0/L$. Moreover, the measured values of the enhancement reported in Fig. 7.4-4 fall in the range $1.4 < I/\varepsilon^2 < 6$, so that the magnitude of I is also correctly given by the White–Metzner model over the same frequency range. However, the value of $\Delta p_0/L$ at which the maximum occurs is underestimated somewhat by the White–Metzner model calculations. If we assume the viscosity of the polyacrylamide solution used in the experiments is the same as that in Fig. 3.3-3, then the calculated values for $\Delta p_0/L$ at the maximum are too low by a factor of about four. At high pressure gradients where shear thinning in the viscosity and time constants is important, the White–Metzner model predicts negative flow enhancement, whereas only positive values are seen in the experimental results. Other data by Phan-Thien and Dudek[5] also show strictly positive I values, with I sometimes increasing and sometimes decreasing with frequency.

Comparison of the results presented here for the White–Metzner model with literature results for other constitutive equations shows that the enhancement predictions are very sensitive to the model used. This is illustrated in Fig. 7.4-5 where the enhancement results[6] are given for the Tanner model.[7] The Tanner model is the same as the convected Maxwell model except that the zero-shear-rate viscosity η_0 is replaced by the shear-rate-dependent viscosity $\eta(\dot{\gamma})$. The shapes of the enhancement versus mean pressure gradient curves are more realistic for the Tanner model than for the White–Metzner model; notice that no negative enhancement is predicted at large pressure gradients. Also the $\Delta p_0/L$ at which the maximum I occurs is only underestimated by a factor of two for the Tanner model. However, the magnitude of the enhancement is overestimated by an order of magnitude or more. Definitive experimental data and calculations are both needed to resolve the issue of the mean pressure drop and frequency dependence of the flow enhancement.

EXAMPLE 7.4-3 Fiber Spinning of a White–Metzner Fluid[8]

A viscoelastic fluid is formed into a fiber by extruding it through a small, circular orifice known as a spinneret and winding the resulting filament on a spool (see Fig. 7.4-6). The velocity of the fiber at the wind-up spool is greater than the extrusion velocity, so that the fiber is under tension. In addition to being stretched during the travel between the spinneret and the take-up spool, the polymer may pass through a solidification bath, be cooled, experience solvent evaporation, or be coagulated. Here we want to model the stretching of the polymeric fluid before it is solidified. To keep the analysis

[4] W. H. Press, B. P. Flannery, S. Teukolsky, and W. T. Vetterling, *Numerical Recipes*, Cambridge University Press (1985).

[5] N. Phan-Thien and J. Dudek, *J. Non-Newtonian Fluid Mech.*, **11**, 147–161 (1982).

[6] N. Phan-Thien, *J. Non-Newtonian Fluid Mech.*, **4**, 167–176 (1978).

[7] R. I. Tanner, *ASLE Trans.*, **8**, 179–183 (1965); see Table 7.6-1.

[8] This example is based on R. J. Fisher and M. M. Denn, *AIChE J.*, **22**, 236–246 (1976). In addition to the steady-state analysis presented here, Fisher and Denn also analyze the stability of the fiber spinning. For more information on fiber spinning see A. Ziabicki, *Fundamentals of Fibre Formation*, Wiley, New York (1976); J. R. A. Pearson, *Mechanics of Polymer Processing*, Elsevier, London (1985), Chapt. 15; Z. Tadmor and C. G. Gogos, *Principles of Polymer Processing*, Wiley, New York (1979), Sect. 15.1; M. M. Denn, *Process Modeling*, Longman, New York (1986), Chap. 12, pp. 230–269; M. M. Denn in J. R. A. Pearson and S. M. Richardson, eds., *Computational Analysis of Polymer Processing*, Applied Science, London (1983), Chapter 6, pp. 179–216.

simple, we will ignore the temperature and/or concentration dependence of the rheological properties in the region prior to solidification and assume the process is steady state. We further assume that the viscoelastic fluid can be described by the White-Metzner model with $\eta = m\dot{\gamma}^{n-1}$.

Let us choose a cylindrical coordinate system with origin at the position where the axial velocity profile can first be assumed independent of radial position and where the radius R of the fiber is not changing rapidly, that is, $|dR/dz| \ll 1$ (Fig. 7.4-6). This point should occur just downstream from the point of maximum extrudate swell. At $z = 0$ the velocity and radius of the filament are v_0 and R_0, and the axial stress τ_{zz} is taken to be τ_0. It is, of course, not possible to measure τ_0, and its introduction is a consequence of not treating the flow problem all the way back into the spinneret where fully developed tube flow boundary conditions on velocity and stress could be specified. Fortuitously, it turns out that the downstream solution is not very sensitive to the value of τ_0 chosen. A distance L downstream from the origin, the polymer solidifies. For $z > L$ the velocity of the filament is assumed

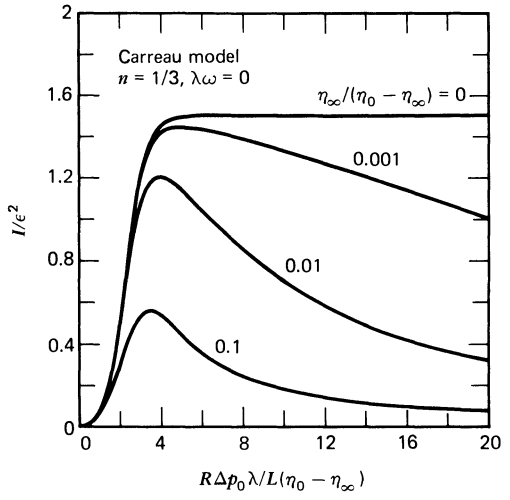

(a)

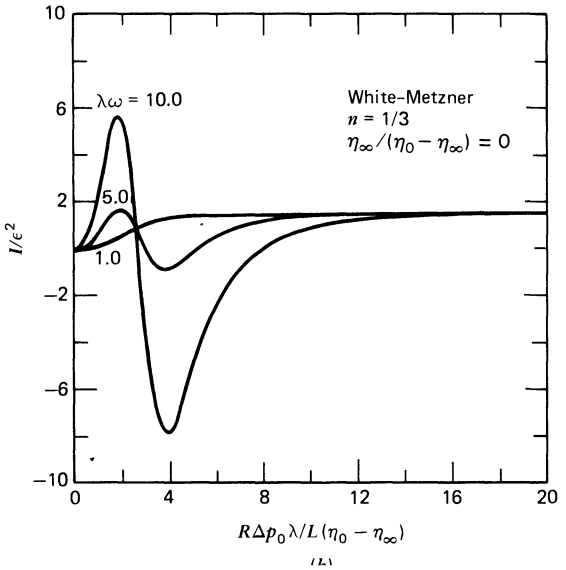

(b)

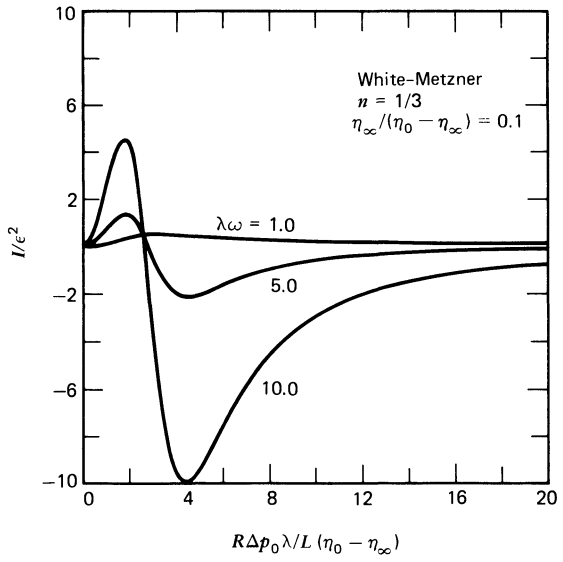

FIGURE 7.4-3. Flow enhancement I/ε^2 as a function of dimensionless pressure gradient $R\Delta p_0 \lambda/L(\eta_0 - \eta_\infty)$ for the White-Metzner model (Eq. 7.3-1) in which the viscosity is described by the Carreau equation (Eq. 4.1-9). All calculations assume a power-law index $n = \frac{1}{3}$. (*a*) $\lambda\omega = 0$ gives the generalized Newtonian fluid result; (*b*) and (*c*) show the influence of varying the dimensionless frequency $\lambda\omega$ and the dimensionless infinite-shear-rate viscosity given as $\eta_\infty/(\eta_0 - \eta_\infty)$. Here λ is the time constant in the Carreau equation.

constant (no further stretching occurs), so that the axial velocity v_L at $z = L$ is fixed by the speed at the wind-up spool. Find the velocity distribution in the filament and the tension F as functions of the "draw ratio" $D_R = v_L/v_0$.

SOLUTION In the region of interest it is reasonable to take $v_z = v_z(z)$ and $\tau_{ij} = \tau_{ij}(z)$. The continuity equation gives

$$\frac{v_z}{v_0} = \left(\frac{R_0}{R(z)}\right)^2 \tag{7.4-35}$$

where $R(z)$ is the local radius of the thread. In the thin filament[9] limit ($|dR/dz| \ll 1$), consideration of conservation of mass and momentum leads to (cf. Eq. 1C.5-2)

$$\frac{d}{dz}(\tau_{zz} - \tau_{rr}) = \frac{v_z'}{v_z}(\tau_{zz} - \tau_{rr}) \tag{7.4-36}$$

[9] The use of the thin filament approximation has been challenged by W. W. Schultz, "Slender Viscoelastic Fiber Flow," submitted to *J. Rheol.* A numerical simulation of the full fiber-spinning problem including flow in the capillary and the extrudate swell region by R. Keunings, M. J. Crochet, and M. M. Denn, *Ind. Eng. Chem. Fundam.*, **22**, 347-355 (1983) has been carried out for several viscoelastic fluid models including the convected Maxwell model. The results of this analysis support the use of the thin filament approximation for the region more than two spinneret diameters downstream from the spinneret and also downstream from the point of maximum extrudate swell. The results also indicate that the choice of the initial condition $T_0 = -1$ used in conjunction with Eq. 7.4-55 (see discussion after Eq. 7.4-64) is appropriate. Numerical results for the convected Maxwell model were obtained up to De $= \lambda_1 v_0/L = 0.025$ and for values of the tension F such that elastic effects were deemed to be important. The validity of the thin filament approximation at higher De is not known.

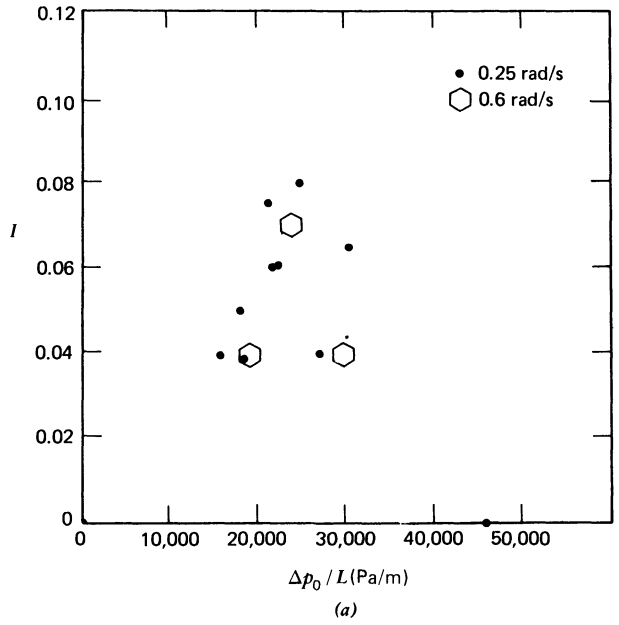

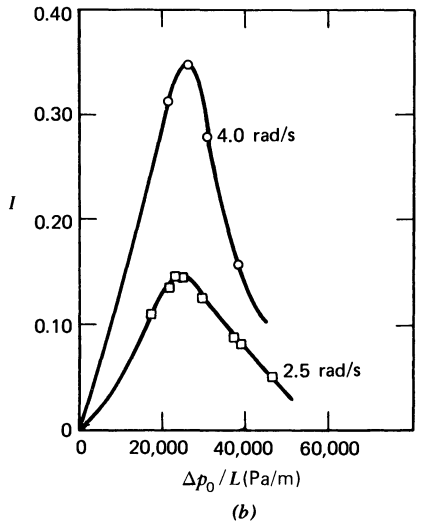

FIGURE 7.4-4. Experimental data on volume flow rate enhancement versus mean pressure gradient for a 1.75% aqueous polyacrylamide solution. In these experiments $\varepsilon = 0.25$ and $R = 0.16$ cm. (*a*) At low frequencies the flow enhancement is independent of frequency; (*b*) at higher frequencies the flow enhancement is seen to increase with increasing frequency. [H. A. Barnes, P. Townsend, and K. Walters, *Rheol. Acta*, **10**, 517–527 (1971).]

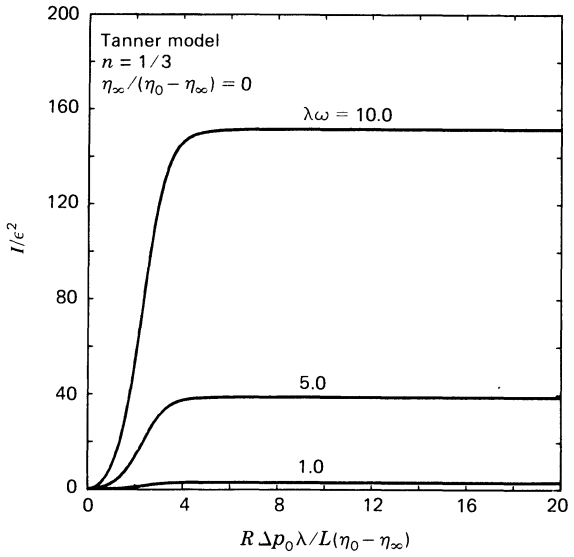

(*a*)

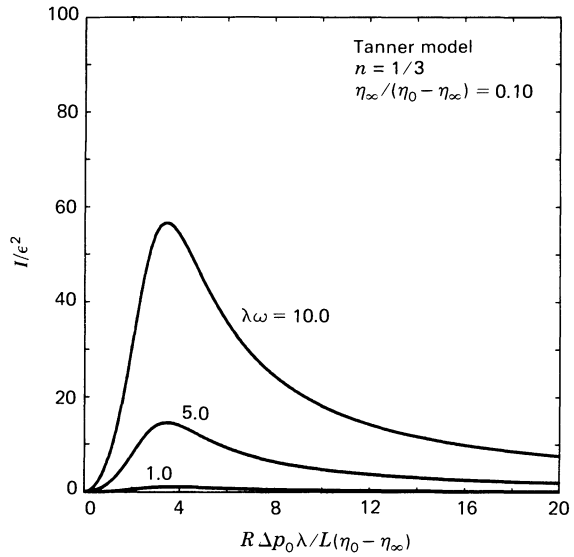

(*b*)

FIGURE 7.4-5. Flow enhancement I/ε^2 as a function of dimensionless pressure gradient $R\Delta p_0\lambda/L(\eta_0 - \eta_\infty)$ for the Tanner model in which the viscosity is described by the Carreau viscosity function (Eq. 4.1-9). The power-law index is $\frac{1}{3}$, and the dimensionless frequency is $\lambda\omega$ where λ is the time constant from the Carreau equation.

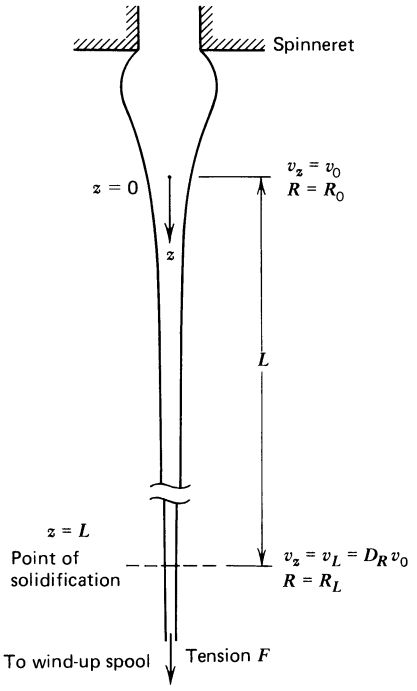

FIGURE 7.4-6. Schematic diagram of the fiber-spinning flow. The stretching of the polymer is modeled from a point $z = 0$ far enough from the spinneret for the axial velocity profile to be assumed flat to the point at $z = L$ where the polymer solidifies. From $x = L$ to the take-up spool no further stretching is assumed to occur. The draw ratio D_R is defined as v_L/v_0.

when we neglect inertia, gravitational forces, and surface tension; v_z' denotes dv_z/dz. Next, since $v_z = v_z(z)$, the continuity equation gives $v_r = -\frac{1}{2}r(dv_z/dz)$, and this leads to the following velocity gradient tensor:

$$\nabla \boldsymbol{v} = \begin{pmatrix} -\frac{1}{2}\frac{dv_z}{dz} & 0 & 0 \\ 0 & -\frac{1}{2}\frac{dv_z}{dz} & 0 \\ -\frac{1}{2}r\frac{d^2v_z}{dz^2} & 0 & \frac{dv_z}{dz} \end{pmatrix} \tag{7.4-37}$$

The three diagonal terms in $\nabla \boldsymbol{v}$ are all of order v_L/L, whereas the dashed-underlined term is of order $(v_L/L)(R_0/L)$. Since $R_0/L \ll 1$, we neglect this latter term. It is then straightforward to write the rr- and zz-components of the constitutive equation, Eq. 7.3-1, as

$$\tau_{rr} + \frac{\eta(\dot\gamma)}{G}\left[v_z\frac{d\tau_{rr}}{dz} + \frac{dv_z}{dz}\tau_{rr}\right] = \eta(\dot\gamma)\frac{dv_z}{dz} \tag{7.4-38}$$

$$\tau_{zz} + \frac{\eta(\dot\gamma)}{G}\left[v_z\frac{d\tau_{zz}}{dz} - 2\frac{dv_z}{dz}\tau_{zz}\right] = -2\eta(\dot\gamma)\frac{dv_z}{dz} \tag{7.4-39}$$

where $\dot{\gamma} = \sqrt{\frac{1}{2}(\boldsymbol{\gamma}_{(1)} : \boldsymbol{\gamma}_{(1)})} = \sqrt{3}\, dv_z/dz$. Equations 7.4-36 through 39 are solved subject to the boundary conditions

$$\text{At } z = 0, \qquad v_z = v_0 \tag{7.4-40}$$

$$\tau_{zz} - \tau_{rr} = -F/\pi R_0^2 \tag{7.4-41}$$

$$\text{At } z = L, \qquad v_z = v_L = D_R v_0 \tag{7.4-42}$$

The boundary condition on $\tau_{zz} - \tau_{rr}$ is written in terms of the tension F in the filament and the radius of the thread by means of a total force balance in the z-direction from the take-up reel to any position z. This balance requires the tension and atmospheric pressure acting along the axis of the fiber to be balanced by π_{zz}

$$\pi_{zz} \cdot \pi R^2 = -F + p_a \pi R^2 \tag{7.4-43}$$

where p_a is ambient pressure. Since a radial force balance gives $\pi_{rr} = p_a$ we get Eq. 7.4-41.

Next we recast the problem in terms of the following dimensionless variables:

$$\zeta = \frac{z}{L}; \quad \phi = \frac{v_z}{v_0}; \quad T_{ij} = \tau_{ij} \frac{\pi R_0^2}{F} \tag{7.4-44}$$

When these definitions are introduced, Eq. 7.4-36 and the two contributions from the constitutive equation become

$$\frac{d}{d\zeta}(T_{zz} - T_{rr}) = \frac{1}{\phi}\phi'(T_{zz} - T_{rr}) \tag{7.4-45}$$

$$T_{rr} + \text{De}\, \phi'^{(n-1)}\left[\phi \frac{dT_{rr}}{d\zeta} + \phi' T_{rr}\right] = N\phi'^n \tag{7.4-46}$$

$$T_{zz} + \text{De}\, \phi'^{(n-1)}\left[\phi \frac{dT_{zz}}{d\zeta} - 2\phi' T_{zz}\right] = -2N\phi'^n \tag{7.4-47}$$

where $\phi' = d\phi/d\zeta$. In writing the constitutive equations we have introduced two dimensionless groups: the Deborah number

$$\text{De} = \frac{\lambda_0 v_0}{L} = 3^{(n-1)/2}\left(\frac{m}{G}\right)\left(\frac{v_0}{L}\right)^n \tag{7.4-48}$$

in which the time constant $\lambda_0 = (m/G)(\sqrt{3}\, v_0/L)^{n-1}$ is given as a characteristic value for η/G, and a dimensionless group N defined by

$$N = \frac{m(\sqrt{3}v_0/L)^{n-1}(v_0/L)}{F/\pi R_0^2} \tag{7.4-49}$$

Thus N gives a ratio of the viscous stress in the threadline to the applied tensile stress. The dimensionless boundary conditions are

$$\text{At } \zeta = 0, \qquad \phi = 1 \tag{7.4-50}$$

$$T_{zz} - T_{rr} = -1 \tag{7.4-51}$$

$$\text{At } \zeta = 1, \qquad \phi = D_R \tag{7.4-52}$$

We now integrate Eq. 7.4-45 to get:

$$T_{zz} - T_{rr} = C\phi \tag{7.4-53}$$

The integration constant C is -1 from Eqs. 7.4-50 and 51. Next we subtract Eq. 7.4-46 from 47 and combine with Eq. 7.4-53 to find

$$T_{zz} = -\frac{\phi}{3\,\mathrm{De}\,\phi'^n} - \tfrac{2}{3}\phi + \frac{N}{\mathrm{De}} \tag{7.4-54}$$

The group N/De appearing in the above is equal to $G/(F/\pi R_0^2)$ so that it gives the ratio of a characteristic elastic stress in the fluid to the stress imposed at $z = 0$. Finally we can eliminate T_{zz} in Eq. 7.4-47 by means of Eq. 7.4-54 to find a single, nonlinear, ordinary differential equation for ϕ

$$\phi + (\mathrm{De}\,\phi - 3N)\phi'^n - 2\mathrm{De}^2\,\phi\phi'^{2n} - n\mathrm{De}\,\phi^2\phi''\phi'^{n-2} = 0 \tag{7.4-55}$$

with

$$\begin{aligned} &\text{At } \zeta = 0, \quad && \phi = 1 \\ &\text{At } \zeta = 1, \quad && \phi = D_R \end{aligned} \tag{7.4-56}$$

Equations 7.4-55 and 56 are easy to solve in the two limits $\mathrm{De} = 0$ and $N/\mathrm{De} = 0$.

In the first limit, namely $\mathrm{De} = 0$, the constitutive equation reduces to that for a generalized Newtonian fluid with a power-law viscosity function and we find[10]

$$\phi - 3N\phi'^n = 0 \tag{7.4-57}$$

which has as its solution

$$\phi = [1 + (3N)^{-s}(1 - s)\zeta]^{1/(1-s)} \tag{7.4-58}$$

where $s = 1/n$ and we have applied the boundary condition at $\zeta = 0$. Then we apply the second boundary condition on ϕ at $\zeta = 1$ and solve the result for N in order to have the dimensionless reciprocal tension in the filament as a function of the draw ratio

$$N = \frac{1}{3}\left[\frac{D_R^{1-s} - 1}{1 - s}\right]^{-1/s} \tag{7.4-59}$$

Finally, to get the stress in the filament we insert the solution for the velocity into Eq. 7.4-54:

$$T_{zz} = -\tfrac{2}{3}\phi \tag{7.4-60}$$

This result follows at once, since the first and last terms on the right side of Eq. 7.4-54 cancel for a velocity field that satisfies Eq. 7.4-57. For the generalized Newtonian fluid it was not necessary to specify the upstream axial stress $T_0 = \tau_0\pi R_0^2/F$ to solve for ϕ, and T_0 is found to be $-2/3$ for all draw ratios.

The second limit $N/\mathrm{De} = 0$ is of more interest in this chapter, since it corresponds to high Deborah number and a large amount of tension in the fiber. Here the $-3N\phi'^n$ term in Eq. 7.4-55 can be neglected and it is easy to verify that the resulting equation has the solution

$$\phi = 1 + \zeta/\mathrm{De}^s \tag{7.4-61}$$

[10] J. R. A. Pearson and Y. T. Shah, *Ind. Eng. Chem. Fundam.*, **13**, 134–138 (1974).

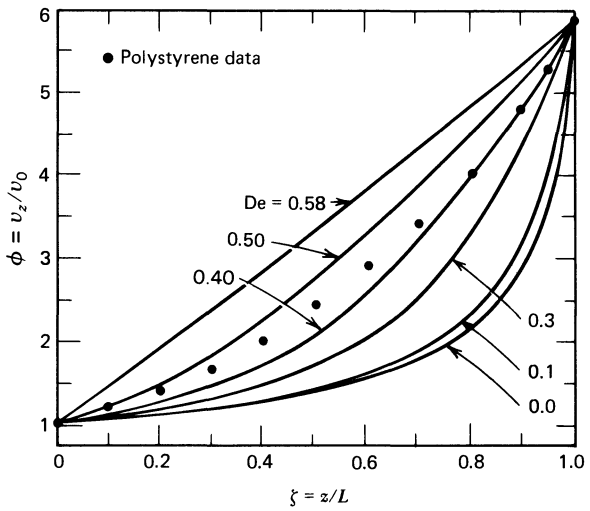

FIGURE 7.4-7. Comparison of calculated and measured dimensionless axial velocity profiles for different values of De $= 3^{(n-1)/2}(m/G)(v_0/L)^n$. The calculations are based on Eqs. 7.4-55 and 56 with $n = 1/3$ and $D_R = 5.85$. Data are for Dow Styron 666 at 443 K. [R. J. Fisher and M. M. Denn, *AIChE J.*, **22**, 236–246 (1976); data are from G. R. Zeichner, M.Ch.E. Thesis, University of Delaware, Newark (1973). Reproduced by permission of the American Institute of Chemical Engineers.]

Thus the velocity profile is linear and the strain rate in the fiber is uniform. Applying the second boundary condition at $\zeta = 1$ gives

$$D_R = 1 + \mathrm{De}^{-s} \tag{7.4-62}$$

Note that for arbitrary De, the limit being considered here corresponds to infinite tension, so that in order to have bounded stresses for finite De we require

$$D_R < 1 + \mathrm{De}^{-s} \tag{7.4-63}$$

This provides an upper limit on the operating range for a fiber-spinning process as modeled here. Finally we calculate the stress distribution from Eq. 7.4-54:

$$T_{zz} = -(1 + \zeta/\mathrm{De}^s) \tag{7.4-64}$$

so that the stress also grows linearly with distance down the threadline. As in the previous limit, it is not necessary here to specify an upstream stress T_0 in this case because the coefficient N involving the tension in the differential equation is dropped. As before T_0 is found to be independent of draw ratio, and in this limit it is equal to -1.

For other choices of De, Fisher and Denn have solved Eqs. 7.4-55 and 56 numerically. Calculations were done for a series of De; in all cases $n = 1/3$, $D_R = 5.85$, and $T_0 = -1$. The choices of n and D_R were made to correspond as closely as possible to the experiments.[11] The choice of T_0 is reasonable, since for the limiting cases of De $= 0$ and $N/\mathrm{De} = 0$, we have seen that T_0 is $-2/3$ and -1, respectively. In any case, Fisher and Denn report that the velocity field is insensitive to the choice of T_0. Solution of Eq. 7.4-55 requires that a value of N be given. However, specifying T_0 does not give a value of N directly but instead gives a combination of N and $\phi'(0)$ from Eq. 7.4-54. Thus the problem must be solved iteratively for different values of N until the solution for ϕ is found which gives $T_0 = -1$ in Eq. 7.4-54.

Results of the Fisher and Denn calculations for the velocity are compared in Fig. 7.4-7 to experimental data[11] on a polystyrene solution. The experimental data give $0.21 \leq \mathrm{De} \leq 0.31$ and

[11] G. R. Zeichner, M.Ch.E. Thesis, University of Delaware, Newark (1973).

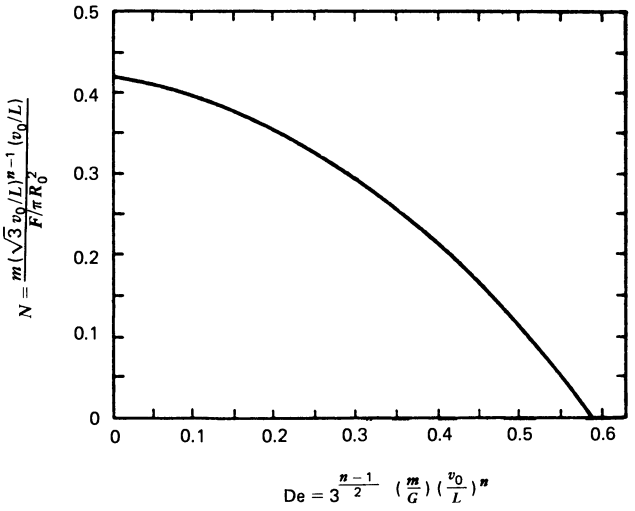

FIGURE 7.4-8. Dimensionless reciprocal tension N (Eq. 7.4-49) as a function of De (Eq. 7.4-48). The calculations are based on Eqs. 7.4-54, 55, and 56 with $n = 1/3$, $D_R = 5.85$, and $T_0 = -1$. [R. J. Fisher and M. M. Denn, *AIChE J.*, **22**, 236–246 (1976). Reproduced by permission of the American Institute of Chemical Engineers.]

$N \doteq 0.08$. Figure 7.4-7 shows that the inclusion of "elasticity" in the White–Metzner model improves the prediction of the velocity field relative to the power-law model. However, the model underestimates the velocity when the correct value of De is used. A good fit of the data is obtained with De between 0.4 and 0.5.

The solution for dimensionless reciprocal force as a function of De is shown in Fig. 7.4-8. There the force is seen to increase with increasing De as would be expected intuitively. Again the inclusion of elasticity improves the predictive ability of the model, but the calculated force is too small. To fit the measured value of $N = 0.08$, a value of De approximately equal to 5.2 must be chosen. This is somewhat higher than the De that best fits the velocity profiles.

§7.5 FLOW PROBLEMS IN TWO OR THREE SPATIAL VARIABLES

In this section we present two fairly lengthy examples illustrating how complex flows involving more than one spatial variable can be solved with differential constitutive equations. The first example, flow in a journal bearing, is important because it demonstrates how sensitive the calculated velocity, stress, and pressure fields are to the constitutive equation chosen to represent the fluid. We will see that constitutive equations which describe the memory of the fluid (e.g., the convected Maxwell and White–Metzner models) and a constitutive equation that describes only the shear thinning of the viscometric functions (the CEF model) differ markedly in predictions of (i) locations and presence of boundary layers in both the velocity and stress fields, (ii) direction of the force exerted by the fluid on the solid surfaces, and (iii) presence and location of separated flow regions.

The second example, flow of a convected Jeffreys model between parallel disks, is important because it shows the influence of the viscoelasticity on flow stability. We will see that even in creeping flow, the two-dimensional flow of the convected Jeffreys model is unstable above a critical Deborah number that is of order unity. Stability problems are important not only for viscometry but also for numerical simulations of viscoelastic flows.

EXAMPLE 7.5-1 Viscoelastic Flow in a Journal Bearing[1]

In Problem 1C.4 the flow of a Newtonian fluid in a simplified journal-bearing system (see Fig. 1C.4) is solved for small eccentricity, and in Example 6.4-2 the loads on the inner cylinder are calculated for the second-order fluid. Because of the Giesekus-Tanner-Pipkin theorem the velocity fields of the second-order and Newtonian fluids are identical. Here we examine the influence of viscoelasticity on both the velocity field and loads by considering the flow of a convected Maxwell model in the journal bearing.

As in the Newtonian and second-order fluid problems, we assume that both the gap and eccentricity are small; the small gap assumption is quite realistic, whereas small eccentricity is assumed simply to obtain analytical solutions. We will again approximate the local gap width $B(\theta)$ between the cylinders by

$$B(\theta) = c(1 + \varepsilon \cos \theta) \tag{7.5-1}$$

in which $c = r_2 - r_1$ is the average gap and $\varepsilon = a/c$ is the dimensionless eccentricity. Here, r_1 and r_2 are the radii of the inner and outer cylinders, respectively, and a is the distance between their axes. Whereas it is possible to solve exactly the lubrication equations for the Newtonian fluid with the approximate gap width given above, for more complicated constitutive equations such as the convected Maxwell model it is necessary to expand the velocity, stress, and pressure variables in powers of the small eccentricity ε. In order to develop consistent approximations in the description of the gap width, the equations of motion, and constitutive equations, and in order to organize the ordering of terms in the expansions, we use the domain perturbation approach of Joseph and Sturges.[2] Assume the flow is steady and two-dimensional.

SOLUTION **(a)** Equations to be Solved

If we neglect inertial and gravitational forces, then the continuity, momentum, and constitutive equations that govern the problem are

$$\begin{aligned} (\nabla \cdot \boldsymbol{v}) &= 0 \\ \nabla p + [\nabla \cdot \boldsymbol{\tau}] &= \mathbf{0} \\ \boldsymbol{\tau} + \lambda_1(\{\boldsymbol{v} \cdot \nabla \boldsymbol{\tau}\} - \{(\nabla \boldsymbol{v})^\dagger \cdot \boldsymbol{\tau}\}_s) &= -\eta_0 \dot{\boldsymbol{\gamma}} \end{aligned} \tag{7.5-2}$$

where the $\{\ \}_s$ symbol denotes $\{\ \} + \{\ \}^\dagger$. Since we take the flow to be two-dimensional, that is, $v_r = v_r(r, \theta)$, $v_\theta = v_\theta(r, \theta)$, and $v_z = 0$, then the necessary components of these equations are, in cylindrical coordinates

$$\frac{1}{r}\frac{\partial}{\partial r}(rv_r) + \frac{1}{r}\frac{\partial v_\theta}{\partial \theta} = 0 \tag{7.5-3}$$

$$\frac{\partial p}{\partial r} + \frac{\partial \tau_{rr}}{\partial r} + \left(\frac{\tau_{rr} - \tau_{\theta\theta}}{r}\right) + \frac{1}{r}\frac{\partial}{\partial \theta}\tau_{\theta r} = 0 \tag{7.5-4}$$

$$\frac{1}{r}\frac{\partial p}{\partial \theta} + \frac{1}{r}\frac{\partial}{\partial \theta}\tau_{\theta\theta} + \frac{\partial \tau_{r\theta}}{\partial r} + \frac{2}{r}\tau_{r\theta} = 0 \tag{7.5-5}$$

[1] This example is based on A. N. Beris, R. C. Armstrong, and R. A. Brown, *J. Non-Newtonian Fluid Mech.*, **13**, 109-148 (1983). In this paper solutions are presented for the second-order fluid, the CEF equation, the convected Maxwell model, and the White-Metzner model. For other viscoelastic calculations for this geometry see M. J. Davies and K. Walters in T. C. Davenport, ed., *Rheology of Lubricants*, Halsted Press, New York (1973); N. Phan-Thien and R. I. Tanner, *J. Non-Newtonian Fluid Mech.*, **9**, 107-117 (1981); B. Y. Ballal and R. S. Rivlin, *Trans. Soc. Rheol.*, **20**, 65-101 (1976); R. S. Rivlin, *J. Non-Newtonian Fluid Mech.*, **5**, 79-101 (1979); M. Reiner, M. Hanin, and A. Harnoy, *Israel J. Tech.*, **7**, 273-279 (1969).

[2] D. D. Joseph and L. Sturges, *J. Fluid Mech.*, **69**, 565-589 (1975).

$$\tau_{rr} + \lambda_1\left[v_r\frac{\partial}{\partial r}\tau_{rr} + \frac{v_\theta}{r}\frac{\partial}{\partial\theta}\tau_{rr} - 2\frac{v_\theta}{r}\tau_{r\theta} - 2(\kappa_{rr}\tau_{rr} + \kappa_{r\theta}\tau_{\theta r})\right] = -2\eta_0\frac{\partial v_r}{\partial r} \tag{7.5-6}$$

$$\tau_{r\theta} + \lambda_1\left[v_r\frac{\partial}{\partial r}\tau_{r\theta} + \frac{v_\theta}{r}\frac{\partial}{\partial\theta}\tau_{r\theta} + \frac{v_\theta}{r}(\tau_{rr} - \tau_{\theta\theta}) - (\kappa_{rr}\tau_{r\theta} + \kappa_{r\theta}\tau_{\theta\theta}) - (\kappa_{\theta r}\tau_{rr} + \kappa_{\theta\theta}\tau_{\theta r})\right]$$
$$= -\eta_0\left(\frac{\partial v_\theta}{\partial r} + \frac{1}{r}\frac{\partial v_r}{\partial\theta} - \frac{v_\theta}{r}\right) \tag{7.5-7}$$

$$\tau_{\theta\theta} + \lambda_1\left[v_r\frac{\partial}{\partial r}\tau_{\theta\theta} + \frac{v_\theta}{r}\frac{\partial}{\partial\theta}\tau_{\theta\theta} - 2\frac{v_\theta}{r}\tau_{r\theta} - 2(\kappa_{\theta r}\tau_{r\theta} + \kappa_{\theta\theta}\tau_{\theta\theta})\right] = -2\eta_0\left(\frac{1}{r}\frac{\partial v_\theta}{\partial\theta} + \frac{v_r}{r}\right) \tag{7.5-8}$$

where we have used the abbreviation $\boldsymbol{\kappa} = (\nabla\mathbf{v})^\dagger$. For the plane flow under consideration we have in cylindrical coordinates

$$\nabla\mathbf{v} = \boldsymbol{\kappa}^\dagger = \begin{pmatrix} \dfrac{\partial v_r}{\partial r} & \dfrac{\partial v_\theta}{\partial r} & 0 \\ \left(\dfrac{1}{r}\dfrac{\partial v_r}{\partial\theta} - \dfrac{v_\theta}{r}\right) & \left(\dfrac{1}{r}\dfrac{\partial v_\theta}{\partial\theta} + \dfrac{v_r}{r}\right) & 0 \\ 0 & 0 & 0 \end{pmatrix} \tag{7.5-9}$$

Because of the invariance of the flow with respect to z, we expect no momentum flux in the z-direction, so we have set τ_{rz}, $\tau_{\theta z}$, and τ_{zz} to zero and have eliminated the corresponding components of the constitutive equation. Also in writing down the components of the constitutive equation we have taken advantage of the expressions for $\{\mathbf{v}\cdot\nabla\boldsymbol{\tau}\}_{ij}$ in cylindrical coordinates given in Table A.7-2.

Equations 7.5-3 through 8 completely determine the velocity and stress fields in this problem when taken together with the boundary conditions that

$$\text{On } r = r_1: \qquad v_r = 0 \qquad v_\theta = V \tag{7.5-10}$$

$$\text{On } r = r_1 + B(\theta): \qquad v_r = 0 \qquad v_\theta = 0 \tag{7.5-11}$$

The linear velocity V of the inner cylinder is equal to $r_1 W_1$, where W_1 is the angular velocity of the inner cylinder. The only conditions on stress and pressure are those of periodicity:

$$\tau_{ij}(r, \theta) = \tau_{ij}(r, \theta + 2\pi)$$
$$p(r, \theta) = p(r, \theta + 2\pi) \tag{7.5-12}$$

We now solve these equations by the domain perturbation technique.

(b) The Domain Perturbation Method

The key idea in the domain perturbation solution is the mapping of the original domain onto a simpler, reference domain. In the present problem, it is convenient to choose the reference domain to be a concentric cylinder geometry with coordinates $(\bar{r}, \bar{\theta})$ (see Fig. 7.5-1). The mapping between eccentric and concentric cylinders is done by the linear transformation $(r, \theta) \rightarrow (\bar{r}, \bar{\theta})$:

$$r = r^{[0]}(\bar{r}, \bar{\theta}; \varepsilon) = r_1 + (\bar{r} - r_1)(1 + \varepsilon\cos\bar{\theta}) \qquad (r_1 \le \bar{r} \le r_2)$$
$$\theta = \theta^{[0]}(\bar{r}, \bar{\theta}; \varepsilon) = \bar{\theta} \qquad (0 \le \bar{\theta} < 2\pi) \tag{7.5-13}$$

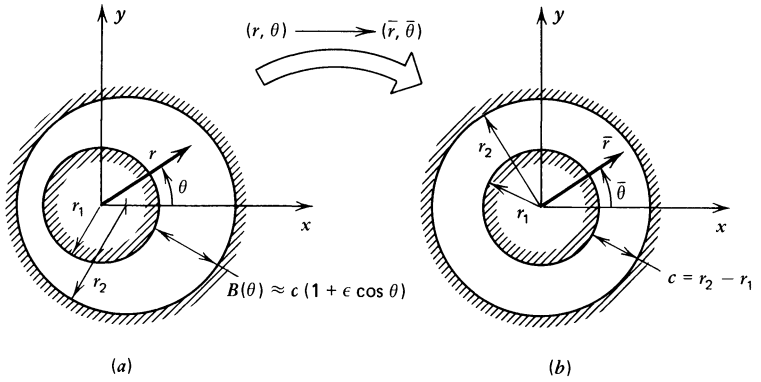

FIGURE 7.5-1. Mapping defined by Eq. 7.5-13 from the (*a*) eccentric cylinder geometry in which the coordinates are (r, θ) to a (*b*) reference (concentric cylinder) geometry with coordinates $(\bar{r}, \bar{\theta})$. The gap in the original problem is $c(1 + \varepsilon \cos \theta)$, whereas in the mapped problem it is a constant c.

where we have used a superscript square bracket $[\ ]$ to denote functions of the transformed, "concentric" coordinates $(\bar{r}, \bar{\theta})$. We will also use a superscript angular bracket $\langle\ \rangle$ to denote functions of the original coordinates (r, θ). A perturbation expansion in eccentricity for the original eccentric problem can be carried over to the concentric cylinder shape by a change of variables from (r, θ) to $(\bar{r}, \bar{\theta})$. Developing a perturbation expansion in either coordinate system involves taking partial derivatives of the dependent variables with respect to the small parameter ε. To get from the solution in the reference domain back to the original eccentric geometry requires knowing how to relate these two sets of partial derivatives. To illustrate these definitions and interrelations consider a function $u(r, \theta; \varepsilon) \equiv u^{\langle 0 \rangle}(r, \theta; \varepsilon) = u^{[0]}(\bar{r}, \bar{\theta}; \varepsilon)$. The two sets of partial derivatives are given by

$$u^{\langle n \rangle}(r, \theta; \varepsilon) \equiv \frac{\partial^n u^{\langle 0 \rangle}}{\partial \varepsilon^n}; \quad u^{[n]}(\bar{r}, \bar{\theta}; \varepsilon) \equiv \frac{\partial^n u^{[0]}}{\partial \varepsilon^n} \tag{7.5-14,15}$$

and they can be related through the chain rule, for example,

$$u^{[1]} = \frac{\partial u^{\langle 0 \rangle}}{\partial \varepsilon} + \frac{\partial r^{[0]}}{\partial \varepsilon} \frac{\partial u^{\langle 0 \rangle}}{\partial r} = u^{\langle 1 \rangle} + r^{[1]} \frac{\partial u^{\langle 0 \rangle}}{\partial r} \tag{7.5-16}$$

Equation 7.5-16 shows that $u^{[1]}$ can be regarded as a "substantial" derivative following the mapping. The factor $r^{[1]}$ in Eq. 7.5-16 arising from application of the chain rule can be evaluated from the mapping Eq. 7.5-13 as follows

$$r^{[1]} = \frac{\partial r^{[0]}}{\partial \varepsilon} = (\bar{r} - r_1) \cos \bar{\theta} \tag{7.5-17a}$$

$$r^{[1]}(\bar{r}, \bar{\theta}; 0) = (r - r_1) \cos \theta \tag{7.5-17b}$$

In Eq. 7.5-17b we have evaluated $r^{[1]}$ at $\varepsilon = 0$ and used the fact that $r = \bar{r}$ and $\theta = \bar{\theta}$ when the eccentricity is zero. Equation 7.5-17b is used in the subsequent expansions about $\varepsilon = 0$.

We now expand the dependent variables—velocity, stress, and pressure—in series in ε calculated in the reference domain, that is, with $\bar{r}$, $\bar{\theta}$ held constant:

$$\begin{pmatrix} \mathbf{v}(r, \theta; \varepsilon) \\ \boldsymbol{\tau}(r, \theta; \varepsilon) \\ p(r, \theta; \varepsilon) \end{pmatrix} = \sum_{n=0}^{\infty} \frac{\varepsilon^n}{n!} \begin{pmatrix} \mathbf{v}^{[n]}(\bar{r}, \bar{\theta}; \varepsilon) \\ \boldsymbol{\tau}^{[n]}(\bar{r}, \bar{\theta}; \varepsilon) \\ p^{[n]}(\bar{r}, \bar{\theta}; \varepsilon) \end{pmatrix}_{\varepsilon = 0} \tag{7.5-18}$$

The reason for choosing this expansion rather than one in the original eccentric geometry is that the boundary conditions are simpler. The price that is paid for simplicity in the boundary location is that equations for the "substantial" derivatives, $\boldsymbol{v}^{[1]}$, etc., are not easily obtained. This difficulty is overcome by expressing the $\boldsymbol{v}^{[n]}(\bar{r}, \bar{\theta}; 0) \ldots$ in terms of the $\boldsymbol{v}^{\langle n\rangle}(r, \theta; 0) \ldots$ by means of the chain rule as shown in Eqs. 7.5-15 through 17.

The equations for the $\boldsymbol{v}^{\langle n\rangle}(r, \theta; 0)$ are easily obtained by taking $\partial^n/\partial\varepsilon^n$ of the governing equation set, Eqs. 7.5-2, and then evaluating these at $\varepsilon = 0$. Keep in mind that in Eqs. 7.5-2 the $\boldsymbol{v}(r, \theta; \varepsilon)$, etc., are identical to the $\boldsymbol{v}^{\langle 0\rangle}(r, \theta; \varepsilon)$, etc. In this way we obtain

$$
\begin{aligned}
(\boldsymbol{\nabla} \cdot \boldsymbol{v}^{\langle n\rangle}) &= 0 \\
\boldsymbol{\nabla} p^{\langle n\rangle} + [\boldsymbol{\nabla} \cdot \boldsymbol{\tau}^{\langle n\rangle}] &= \mathbf{0} \\
\boldsymbol{\tau}^{\langle n\rangle} + \lambda_1(\{\boldsymbol{v} \cdot \boldsymbol{\nabla}\boldsymbol{\tau}\}^{\langle n\rangle} - \{(\boldsymbol{\nabla}\boldsymbol{v})^{\dagger} \cdot \boldsymbol{\tau}\}_s^{\langle n\rangle}) &= -\eta_0 \dot{\boldsymbol{\gamma}}^{\langle n\rangle}
\end{aligned}
\tag{7.5-19}
$$

in which all dependent variables are evaluated at $(r, \theta; 0)$. The specific forms of these equations for given values of n are conveniently obtained from Eqs. 7.5-2 by substituting power series in ε for the velocity, stress, and pressure with coefficients $\boldsymbol{v}^{\langle n\rangle}$, $p^{\langle n\rangle}$, and $\boldsymbol{\tau}^{\langle n\rangle}$ and equating equal orders in ε.

To obtain the boundary conditions for the $\boldsymbol{v}^{\langle n\rangle}(r, \theta; 0)$ we insert the expansion for $\boldsymbol{v}$ in Eqs. 7.5-18 into Eqs. 7.5-10 and 11. On $r = \bar{r} = r_1$ we have

$$
\begin{aligned}
v_r &= \sum_{n=0}^{\infty} \frac{1}{n!} v_r^{[n]}(\bar{r}, \bar{\theta}; 0)\varepsilon^n \Big|_{\bar{r}=r_1} \\
&= v_r^{\langle 0\rangle}(r_1, \theta; 0) + \varepsilon\left[v_r^{\langle 1\rangle}(r, \theta; 0) + (r - r_1)\cos\theta \frac{\partial v_r^{\langle 0\rangle}(r, \theta; 0)}{\partial r} \right]_{r=r_1} \\
&= v_r^{\langle 0\rangle}(r_1, \theta; 0) + \varepsilon v_r^{\langle 1\rangle}(r_1, \theta; 0) + \cdots \\
v_\theta &= v_\theta^{\langle 0\rangle}(r_1, \theta; 0) + \varepsilon v_\theta^{\langle 1\rangle}(r_1, \theta; 0) + \cdots
\end{aligned}
\tag{7.5-20}
$$

Since from here on all of the $v_i^{\langle n\rangle}$ are evaluated at $\varepsilon = 0$, we will drop this dependence from the arguments. For example, we abbreviate $v_\theta^{\langle 1\rangle}(r_1, \theta; 0)$ as $v_\theta^{\langle 1\rangle}(r_1, \theta)$. Comparing these equations with Eq. 7.5-10 gives

$$
\begin{aligned}
\text{On } r = r_1 \qquad & v_r^{\langle 0\rangle}(r_1, \theta) = 0 \quad v_\theta^{\langle 0\rangle}(r_1, \theta) = V \\
& v_r^{\langle 1\rangle}(r_1, \theta) = 0 \quad v_\theta^{\langle 1\rangle}(r_1, \theta) = 0 \\
& \vdots \qquad\qquad \vdots
\end{aligned}
\tag{7.5-21}
$$

Similarly for the outer boundary at $r = r_1 + B(\theta)$ or $\bar{r} = r_2$ we find

$$
\begin{aligned}
v_r(r_2, \theta) &= v_r^{\langle 0\rangle}(r_2, \theta) + \varepsilon[v_r^{\langle 1\rangle}(r, \theta) \\
&\qquad + (r - r_1)\cos\theta \frac{\partial v_r^{\langle 0\rangle}(r, \theta)}{\partial r}\Big]_{r=r_2} + \cdots \\
&= v_r^{\langle 0\rangle}(r_2, \theta) + \varepsilon\left[v_r^{\langle 1\rangle}(r_2, \theta) + c\cos\theta \frac{\partial v_r^{\langle 0\rangle}(r_2, \theta)}{\partial r} \right] + \cdots \\
v_\theta(r_2, \theta) &= v_\theta^{\langle 0\rangle}(r_2, \theta) + \varepsilon\left[v_\theta^{\langle 1\rangle}(r_2, \theta) + c\cos\theta \frac{\partial v_\theta^{\langle 0\rangle}(r_2, \theta)}{\partial r} \right] + \cdots
\end{aligned}
\tag{7.5-22}
$$

Comparing Eqs. 7.5-22 and 11 gives the conditions at $r = r_2$,

$$
\begin{aligned}
r = r_2 \qquad & v_r^{\langle 0\rangle}(r_2, \theta) = 0; \quad v_\theta^{\langle 0\rangle}(r_2, \theta) = 0 \\
& v_r^{\langle 1\rangle}(r_2, \theta) = -c \cos\theta \frac{\partial v_r^{\langle 0\rangle}(r_2, \theta)}{\partial r} \\
& v_\theta^{\langle 1\rangle}(r_2, \theta) = -c \cos\theta \frac{\partial v_\theta^{\langle 0\rangle}(r_2, \theta)}{\partial r} \\
& \vdots
\end{aligned}
\tag{7.5-23}
$$

(c) Solution of the Zeroth-Order Domain Perturbation Problem

We now solve the lowest-order problem given by Eqs. 7.5-19 with $n = 0$. Specifically,

$$
\begin{aligned}
(\nabla \cdot \boldsymbol{v}^{\langle 0\rangle}) &= 0 \\
\nabla p^{\langle 0\rangle} + [\nabla \cdot \boldsymbol{\tau}^{\langle 0\rangle}] &= \mathbf{0} \\
\boldsymbol{\tau}^{\langle 0\rangle} + \lambda_1(\{\boldsymbol{v}^{\langle 0\rangle} \cdot \nabla \boldsymbol{\tau}^{\langle 0\rangle}\} - \{(\nabla \boldsymbol{v}^{\langle 0\rangle})^\dagger \cdot \boldsymbol{\tau}^{\langle 0\rangle}\}_s) &= -\eta_0 \dot{\boldsymbol{\gamma}}^{\langle 0\rangle}
\end{aligned}
\tag{7.5-24}
$$

The component forms of these equations are given by Eqs. 7.5-3 through 8. The boundary conditions on $v_r^{\langle 0\rangle}$ and $v_\theta^{\langle 0\rangle}$ in Eqs. 7.5-21 and 23 suggest that we try $v_r^{\langle 0\rangle} = 0$, $v_\theta^{\langle 0\rangle} = v_\theta^{\langle 0\rangle}(r)$, $\tau_{ij}^{\langle 0\rangle} = \tau_{ij}^{\langle 0\rangle}(r)$, and $p^{\langle 0\rangle} = p^{\langle 0\rangle}(r)$. With this assumed solution the continuity equation is automatically satisfied.

The velocity gradient tensor is

$$
\nabla \boldsymbol{v}^{\langle 0\rangle} = \begin{pmatrix} 0 & \dfrac{\partial v_\theta^{\langle 0\rangle}}{\partial r} & 0 \\ -\dfrac{v_\theta^{\langle 0\rangle}}{r} & 0 & 0 \\ 0 & 0 & 0 \end{pmatrix} = \boldsymbol{\kappa}^{\langle 0\rangle\dagger}
\tag{7.5-25}
$$

When this is combined with the constitutive equations for $\tau_{rr}^{\langle 0\rangle}$, $\tau_{r\theta}^{\langle 0\rangle}$, and $\tau_{\theta\theta}^{\langle 0\rangle}$ we find

$$
\tau_{rr}^{\langle 0\rangle} = 0 \tag{7.5-26}
$$

$$
\tau_{r\theta}^{\langle 0\rangle} = -\eta_0 \left[\frac{\partial v_\theta^{\langle 0\rangle}}{\partial r} - \frac{v_\theta^{\langle 0\rangle}}{r} \right] = -\eta_0 \dot{\gamma}_{r\theta}^{\langle 0\rangle} \tag{7.5-27}
$$

$$
\tau_{\theta\theta}^{\langle 0\rangle} = 2\lambda_1 \left(\frac{\partial v_\theta^{\langle 0\rangle}}{\partial r} - \frac{v_\theta^{\langle 0\rangle}}{r} \right) \tau_{r\theta}^{\langle 0\rangle} = -2\eta_0 \lambda_1 \dot{\gamma}_{r\theta}^{\langle 0\rangle 2} \tag{7.5-28}
$$

Note that these results just give the viscometric properties of the convected Maxwell model at the shear rate $\dot{\gamma}_{r\theta}^{\langle 0\rangle}$.

The equations of motion now can be written as

r-component:
$$
\frac{dp^{\langle 0\rangle}}{dr} = \frac{\tau_{\theta\theta}^{\langle 0\rangle}}{r} \tag{7.5-29}
$$

θ-component:
$$
\frac{d}{dr}\tau_{r\theta}^{\langle 0\rangle} + \frac{2}{r}\tau_{r\theta}^{\langle 0\rangle} = 0 \tag{7.5-30}
$$

For use in the next order problem in the ε-series we develop solutions to the above equations as series in the small dimensionless gap μ defined as

$$\mu = c/r_1 \tag{7.5-31}$$

In this development it is convenient to use the following dimensionless variables and groups:

$$\begin{aligned}
\zeta &= \frac{(r - r_1)}{c} \\
T_{ij}^{\langle 0\rangle}(\zeta) &= \frac{\tau_{ij}^{\langle 0\rangle}(r)}{(\eta_0 V/c)} \\
P^{\langle 0\rangle}(\zeta) &= \frac{p^{\langle 0\rangle}(r)}{(\eta_0 V/c)} \\
\hat{v}_i^{\langle 0\rangle}(\zeta) &= \frac{v_i^{\langle 0\rangle}(r)}{V} \\
\mathrm{De} &= \mathrm{We}\mu = \lambda_1 V/r_1 \\
\mathrm{We} &= \lambda_1 V/c
\end{aligned} \tag{7.5-32}$$

The Weissenberg number We is a dimensionless shear rate, and for the small gap, concentric cylinder limit of the convected Maxwell model it is equal to $\Psi_1\dot{\gamma}/2\eta_0$. The Deborah number De is a ratio of the time constant for the convected Maxwell model to the time required for the fluid to move once around the journal bearing. Note that when μ is small, We $\gg$ De. We wish to develop solutions valid for De of order unity, so that memory of events in one part of the journal bearing is felt in other parts.

In terms of the dimensionless variables the θ-component of the equation of motion can be written for small μ as

$$\frac{d}{d\zeta} T_{r\theta}^{\langle 0\rangle} = -2\mu(1 - \mu\zeta + \cdots)T_{r\theta}^{\langle 0\rangle} \tag{7.5-33}$$

which has the solution

$$T_{r\theta}^{\langle 0\rangle} = c_0 + \mu(c_1 - 2c_0\zeta) + \cdots \tag{7.5-34}$$

where c_0 and c_1 are constants. When this is combined with the constitutive equation for $T_{r\theta}^{\langle 0\rangle}$, an ordinary differential equation for $\hat{v}_\theta^{\langle 0\rangle}$ is obtained. Solving this equation together with the boundary conditions that $\hat{v}_\theta^{\langle 0\rangle}(0) = 1$ and $\hat{v}_\theta^{\langle 0\rangle}(1) = 0$ leads to

$$\hat{v}_\theta^{\langle 0\rangle} = (1 - \zeta) + \frac{\mu}{2}(\zeta^2 - \zeta) + O(\mu^2) \tag{7.5-35}$$

In obtaining Eq. 7.5-35 we find the integration constants in Eq. 7.5-34 to be $c_0 = 1$ and $c_1 = 3/2$. It is then straightforward to develop the remaining series solutions, which have the leading behavior

$$\begin{aligned}
\hat{v}_r^{\langle 0\rangle} &= 0 \\
T_{rr}^{\langle 0\rangle} &= 0 \\
T_{r\theta}^{\langle 0\rangle} &= 1 + \mu(\tfrac{3}{2} - 2\zeta) + O(\mu^2) \\
T_{\theta\theta}^{\langle 0\rangle} &= -\frac{2\mathrm{De}}{\mu}(1 + O(\mu)) \\
P^{\langle 0\rangle} &= P_0 - 2\mathrm{De}\,\zeta + O(\mu)
\end{aligned} \tag{7.5-36}$$

The constant P_0 is an arbitrary reference pressure. We note in Eq. 7.5-36 that the normal stress $T_{\theta\theta}^{\langle 0\rangle}$ is singular and is thus the dominant term for $\mu \to 0$.

(d) Solution to the First-Order Domain Perturbation Problem

We now move to the next order in ε and solve Eqs. 7.5-19 for $n = 1$. The governing equations are

$$\begin{aligned} (\nabla \cdot \mathbf{v}^{\langle 1\rangle}) &= 0 \\ \nabla p^{\langle 1\rangle} + [\nabla \cdot \boldsymbol{\tau}^{\langle 1\rangle}] &= \mathbf{0} \\ \boldsymbol{\tau}^{\langle 1\rangle} + \lambda_1[\{\mathbf{v}^{\langle 0\rangle} \cdot \nabla \boldsymbol{\tau}^{\langle 1\rangle}\} + \{\mathbf{v}^{\langle 1\rangle} \cdot \nabla \boldsymbol{\tau}^{\langle 0\rangle}\} - \{(\nabla \mathbf{v}^{\langle 0\rangle})^\dagger \cdot \boldsymbol{\tau}^{\langle 1\rangle}\}_s - \{(\nabla \mathbf{v}^{\langle 1\rangle})^\dagger \cdot \boldsymbol{\tau}^{\langle 0\rangle}\}_s] &= -\eta_0 \dot{\boldsymbol{\gamma}}^{\langle 1\rangle} \end{aligned} \tag{7.5-37}$$

The boundary conditions on $v_r^{\langle 1\rangle}$ and $v_\theta^{\langle 1\rangle}$ are given by Eqs. 7.5-21 and 23 with Eq. 7.5-35 used to evaluate $\partial v_i^{\langle 0\rangle}/\partial r$ in Eq. 7.5-23. Including terms through order μ gives

$$\begin{aligned} \text{At } r = r_1, \quad & v_r^{\langle 1\rangle} = 0 \\ & v_\theta^{\langle 1\rangle} = 0 \\ \text{At } r = r_2, \quad & v_r^{\langle 1\rangle} = 0 \\ & v_\theta^{\langle 1\rangle} = V \cos\theta + O(\mu^2) \end{aligned} \tag{7.5-38}$$

The periodic nature of the boundary conditions suggests the use of a complex stream function $F(r)$:

$$\begin{aligned} v_r^{\langle 1\rangle} &= \mathscr{R}e\{iF(r)e^{i\theta}c/r\} \\ v_\theta^{\langle 1\rangle} &= \mathscr{R}e\{-F'(r)e^{i\theta}c\} \end{aligned} \tag{7.5-39}$$

The continuity equation is thus automatically satisfied. We note for later use the sizes of the following terms: $v_r^{\langle 1\rangle} \sim \mu V$, $v_\theta^{\langle 1\rangle} \sim V$, and $F \sim V$.

The rr-component of the constitutive equation given in Eq. 7.5-37 can be written down with the aid of Eq. 7.5-6

$$\tau_{rr}^{\langle 1\rangle} + \lambda_1\left[\frac{V(1-\zeta)}{r}\frac{\partial}{\partial\theta}\tau_{rr}^{\langle 1\rangle} - \frac{2}{r}\frac{\partial v_r^{\langle 1\rangle}}{\partial\theta}\eta_0\frac{V}{c}(1 + \mu(1-\zeta) + \cdots)\right] = -2\eta_0\frac{\partial v_r^{\langle 1\rangle}}{\partial r} \tag{7.5-40}$$

We next introduce dimensionless variables as defined in Eq. 7.5-32, and also a dimensionless stream function f defined by

$$f(\zeta) = F(r)/V \tag{7.5-41}$$

Also we assume periodic solutions for the stresses and pressure

$$\begin{aligned} \tau_{ij}^{\langle 1\rangle} &= \mathscr{R}e\{T_{ij}^{\langle 1\rangle}(\zeta)e^{i\theta}\}(\eta_0 V/c) \\ p^{\langle 1\rangle} &= \mathscr{R}e\{P^{\langle 1\rangle}(\zeta)e^{i\theta}\}(\eta_0 V/c) \end{aligned} \tag{7.5-42}$$

so that the stress and pressure, $\boldsymbol{T}^{\langle 1\rangle}$ and $P^{\langle 1\rangle}$, we seek at this order are functions of ζ alone. When Eq. 7.5-40 is rewritten with these new variables we obtain

$$T_{rr}^{\langle 1\rangle} + i\mathrm{De}(1-\zeta)(1 - \tfrac{3}{2}\mu\zeta + \cdots)T_{rr}^{\langle 1\rangle} = -2\mu(if' + \mathrm{De}f) + O(\mu^2) \tag{7.5-43}$$

where the prime denotes $d/d\zeta$. Clearly $T_{rr}^{\langle 1\rangle} \sim \mu$ so we can develop $T_{rr}^{\langle 1\rangle}$ as a series in μ with leading term

$$T_{rr}^{\langle 1\rangle} = -\frac{2(if' + \mathrm{De}f)}{[1 + i\mathrm{De}(1-\zeta)]}\mu + O(\mu^2) \tag{7.5-44}$$

Similarly we find

$$\begin{aligned} T_{r\theta}^{\langle 1\rangle}[1 + i\mathrm{De}(1-\zeta)] &= f'' + 2\mathrm{De}^2 f - \frac{\mathrm{De}}{\mu} T_{rr}^{\langle 1\rangle} \\ &= f'' + 2\mathrm{De}^2 f + \frac{2\mathrm{De}(if' + \mathrm{De}f)}{[1 + i\mathrm{De}(1-\zeta)]} + O(\mu) \end{aligned} \tag{7.5-45}$$

$$T_{\theta\theta}^{\langle 1\rangle}[1 + i\mathrm{De}(1-\zeta)] = \frac{2\mathrm{De}}{\mu}[2i\mathrm{De}f' - f'' - T_{r\theta}^{\langle 1\rangle}] + O(1) \tag{7.5-46}$$

We note that $T_{r\theta}^{\langle 1\rangle} \sim 1$ and $T_{\theta\theta}^{\langle 1\rangle} \sim 1/\mu$. Thus $T_{\theta\theta}^{\langle 1\rangle}$ is singular and dominant as $T_{\theta\theta}^{\langle 0\rangle}$ was at the previous order.

The constitutive equation must now be combined with the equations of motion. This leads to

r-component:
$$P^{\langle 1\rangle\prime} + T_{rr}^{\langle 1\rangle\prime} + \frac{\mu(T_{rr}^{\langle 1\rangle} - T_{\theta\theta}^{\langle 1\rangle})}{(1 + \mu\zeta)} + \frac{\mu}{(1 + \mu\zeta)} iT_{r\theta}^{\langle 1\rangle} = 0 \tag{7.5-47}$$

θ-component:
$$i\mu P^{\langle 1\rangle} + i\mu T_{\theta\theta}^{\langle 1\rangle} + (1 + \mu\zeta)T_{r\theta}^{\langle 1\rangle\prime} + 2\mu T_{r\theta}^{\langle 1\rangle} = 0 \tag{7.5-48}$$

From the θ-component of the equation of motion we can see that $P^{\langle 1\rangle}$ is of the same size as $T_{\theta\theta}^{\langle 1\rangle}$, that is $P^{\langle 1\rangle} \sim 1/\mu$, and from the radial component of the equation of motion we see that $P^{\langle 1\rangle\prime} \sim 1$. Thus the series for $P^{\langle 1\rangle}$ is

$$P^{\langle 1\rangle} = \frac{P_0^{\langle 1\rangle}}{\mu} + O(1) \tag{7.5-49}$$

so that the pressure is constant across the gap at lowest order in μ.

An equation for the stream function f can be obtained by first eliminating the pressure in Eq. 7.5-48 by taking $d/d\zeta$ of this equation. The leading behavior of the result is given by the dominant balance

$$i\mu T_{\theta\theta}^{\langle 1\rangle\prime} + T_{r\theta}^{\langle 1\rangle\prime\prime} = 0 \tag{7.5-50}$$

The stress coefficients $T_{r\theta}^{\langle 1\rangle}$ and $T_{\theta\theta}^{\langle 1\rangle}$ are then eliminated in favor of the stream function by means of Eqs. 7.5-45 and 46. After much tedious algebra this results in

$$(-2\xi + i(1-\xi^2))g^{(iv)} - (-2\xi^2 + 2i\xi)g''' + 2i\xi^2 g'' - 4i\xi g' + 4ig = 0 \tag{7.5-51}$$

where

$$\xi = \mathrm{De}(1-\zeta); \quad g(\xi) = f(\zeta); \quad g'(\xi) = -(1/\mathrm{De})f'(\zeta) \tag{7.5-52}$$

The general solution to Eq. 7.5-51 is

$$g(\xi) = Ae^{(1-i)\xi} + Be^{-(1+i)\xi} + C\xi^2 + D\xi \tag{7.5-53}$$

The constants A, B, C, and D are determined from the boundary conditions. The relevant boundary conditions are obtained by rewriting Eqs. 7.5-38 in terms of the stream function g and new independent variable ξ:

$$g(0) = g'(\mathrm{De}) = g(\mathrm{De}) = 0; \quad g'(0) = 1/\mathrm{De} \tag{7.5-54}$$

These conditions lead to

$$\begin{aligned} \frac{1}{A} &= \mathrm{De}\left\{\left(1 - i - \frac{2}{\mathrm{De}}\right)e^{(1-i)\mathrm{De}} + \left(1 + i + \frac{2}{\mathrm{De}}\right)e^{-(1+i)\mathrm{De}} + 2\right\} \\ B &= -A \\ C &= \mathrm{De}^{-2}\{A(2\mathrm{De} + e^{-(1+i)\mathrm{De}} - e^{(1-i)\mathrm{De}}) - 1\} \\ D &= -2A + \mathrm{De}^{-1} \end{aligned} \tag{7.5-55}$$

Once the stream function is known the stresses are readily calculated from Eqs. 7.5-44 through 46 and the pressure from Eq. 7.5-48.

(e) Discussion of Results for Velocity and Stress Fields

Solutions for the velocity and stress fields for the White-Metzner and CEF[3] models can be obtained in a similar fashion, although the differential equation for the stream function for the White-Metzner model is most conveniently solved numerically.[4] In the following we compare results for these two constitutive equations with those for the convected Maxwell model. In the White-Metzner and CEF models the viscosity is described by a power-law expression, the first normal stress coefficient is given by $2\eta^2(\dot\gamma)/G$, and $\Psi_2 = 0$. We do this to facilitate comparison between the models. The use of a power-law for η amounts to a Taylor expansion for the viscosity about the mean shear rate $\dot\gamma_0 = V/c$ in the small gap limit. The constant modulus G is related to λ_1 in the convected Maxwell model by $\lambda_1 = \eta(\dot\gamma_0)/G$. In scaling the stresses and pressure for the shear-thinning models the zero-shear-rate viscosity of the convected Maxwell model is replaced by $\eta^{\langle 0\rangle} = \eta(\dot\gamma_0)$.

Figure 7.5-2 shows the radial variation in the correction to the radial velocity $v_r^* = v_r^{\langle 1\rangle}/V\mu$ at an angular position of $\theta = 3\pi/2$. From Eq. 7.5-39 we see that at this position $v_r^{\langle 1\rangle}$ is proportional to the real part of the stream function F. Note that since $v_r^{\langle 0\rangle} = 0$, v_r^* gives the total radial velocity up through order ε in the expansion in Eq. 7.5-18. Differences in the various model predictions are dramatic. Whereas the inclusion of shear thinning does not greatly affect the De dependence of v_r^*, the absence of memory in the CEF equation allows the development of a boundary layer at the outer cylinder as De is increased. This is in contrast to the boundary layer in $dv_r^*/d\zeta$ that develops with increasing De at the inner cylinder for the convected Maxwell and White-Metzner models. This latter boundary layer results from the no-slip condition on v_θ and the interrelation of $v_r^{\langle 1\rangle}$ and $v_\theta^{\langle 1\rangle}$ through the stream function in Eq. 7.5-39.

The tangential velocity expansion in Eq. 7.5-18 has contributions from both $v_\theta^{[0]}$ and[5] $v_\theta^{[1]} = v_\theta^{\langle 1\rangle} - \zeta V \cos\theta$ and thus we plot the dimensionless total tangential velocity $v_\theta^* = v_\theta/V$ in Fig. 7.5-3. These contours of v_θ^* are shown for the three constitutive equations on the reference domain which has been cut at $\theta = 0$ and unwrapped. An eccentricity of $\varepsilon = 0.4$ has been used to emphasize

[3] The CEF model, mentioned briefly in §4.6, is developed in Example 9.6-3 (see Eq. 9.6-18). This model describes the stresses in viscometric flows exactly and thus is sufficient for the solution of the concentric cylinder problem. However, the CEF model, like the generalized Newtonian fluid, predicts that stress depends on the instantaneous value of the velocity gradient tensor. Thus the CEF equation is incapable of describing memory effects, and comparison of its predictions with those for the White-Metzner and convected Maxwell models allows us to assess the importance of fluid memory, as given by the Deborah number, in the journal-bearing problem.

[4] A. N. Beris, R. C. Armstrong, and R. A. Brown, *op cit.*

[5] The term $v_\theta^{[1]}$ is obtained from Eq. 7.5-16. It is given evaluated at $\bar r = r_2$ as the [ ] term in the last line of Eq. 7.5-22. Note also $\partial v_\theta^{\langle 0\rangle}/\partial r = -V/c$ at lowest order.

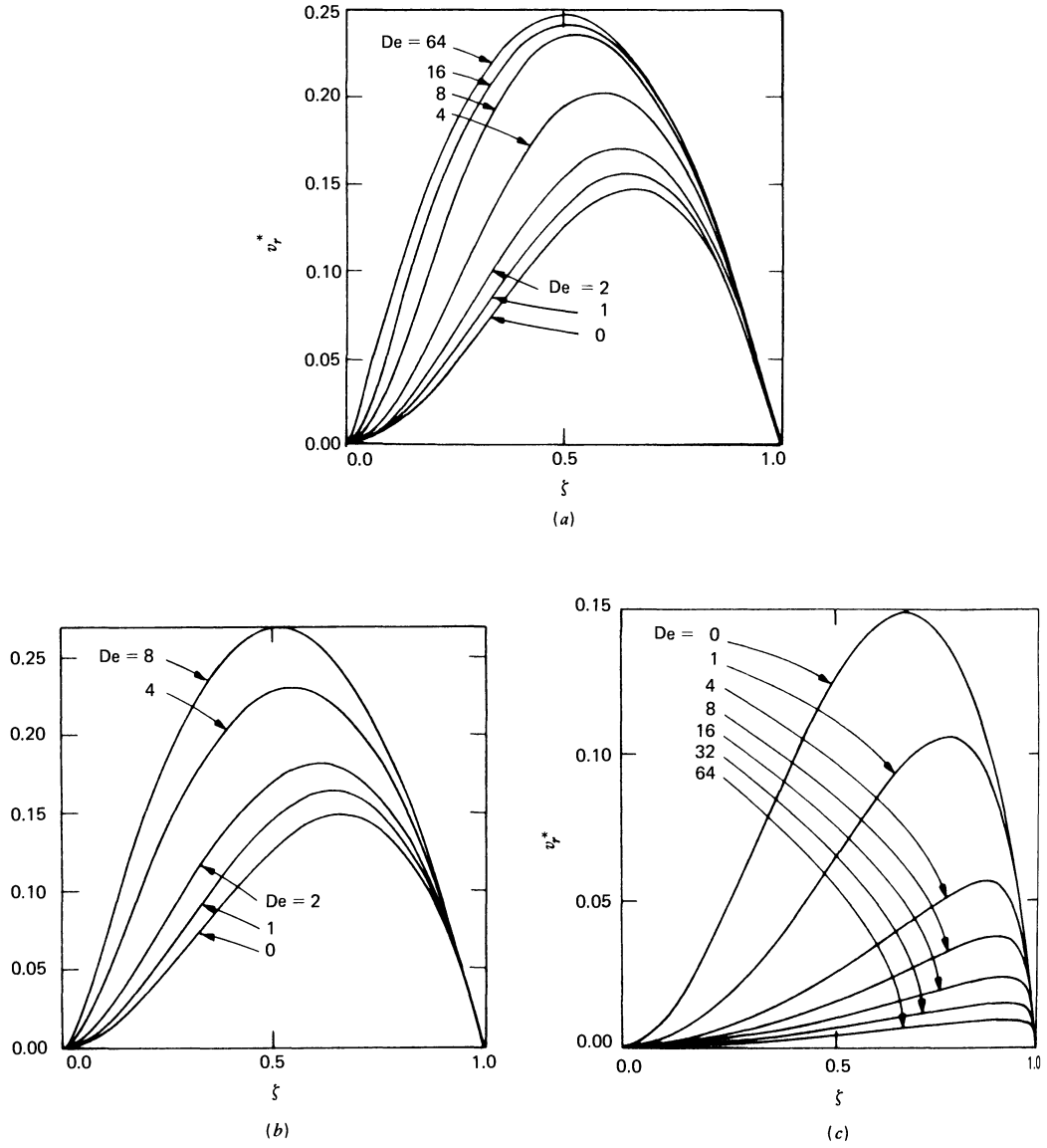

FIGURE 7.5-2. Dependence of the correction to the radial velocity $v_r^* = v_r^{\langle 1\rangle}/V\mu$ on the dimensionless radial coordinate $\zeta = (r - r_1)/c(1 + \varepsilon \cos\theta)$ at $\theta = 3\pi/2$ for (*a*) the convected Maxwell model, (*b*) the White-Metzner model with power-law index $n = 0.3$, and (*c*) the CEF model with $n = 0.3$. [A. N. Beris, R. C. Armstrong, and R. A. Brown, *J. Non-Newtonian Fluid Mech.*, **13**, 109-148 (1983).]

differences in the models. Note that at De = 0.01 there is flow separation at the outer cylinder at $\theta = 0$ as is predicted from the exact Newtonian solution. Increasing De in the convected Maxwell model causes this secondary flow to disappear, whereas in the White-Metzner model it shrinks slightly and is convected downstream. The CEF model again predicts very different results; for this constitutive equation the secondary flow regime grows with increasing De and stays centered on $\theta = 0$.

The tangential normal stress is shown in Fig. 7.5-4. Since the $\tau_{\theta\theta}^{[0]}$ term is constant at lowest order in μ, we show only the correction term in the dimensionless form $\tau_{\theta\theta}^* = \tau_{\theta\theta}^{\langle 1\rangle}\,\mu/(\eta^{\langle 0\rangle}V/c)\mathrm{De}$. Note that $\tau_{\theta\theta}^*$ contains all of the spatial dependence of $\tau_{\theta\theta}$ in the distinguished limit $0 < \mu \ll \varepsilon \ll 1$. A boundary layer near the outer wall is seen to develop in $\tau_{\theta\theta}^*$ in all of the models at large De. In the

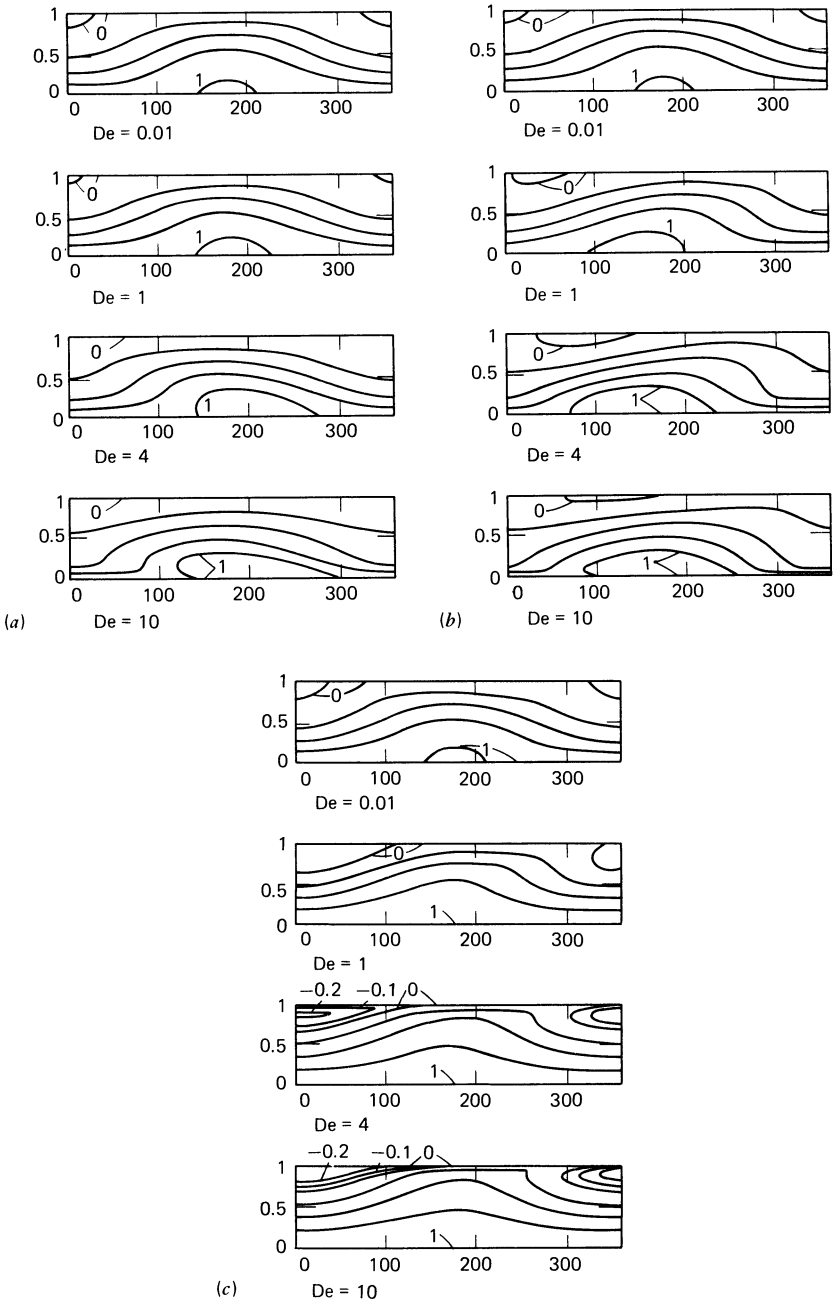

FIGURE 7.5-3. Contours of the tangential velocity $v_\theta^*(\zeta, \theta) = v_\theta(\zeta, \theta)/V$ at Deborah numbers ranging from 0.01 to 10 for the same models as in Fig. 7.5-2: (*a*) convected Maxwell; (*b*) White-Metzner ($n = 0.3$); (*c*) CEF ($n = 0.3$). The total tangential velocity is calculated from the perturbation results as $v_\theta = v_\theta^{\langle 0 \rangle} + \varepsilon(v_\theta^{\langle 1 \rangle} - \zeta\ V \cos\theta)$, and an eccentricity of $\varepsilon = 0.4$ was used. The contours are equally spaced between the minimum and maximum values. [A. N. Beris, R. C. Armstrong, and R. A. Brown, *J. Non-Newtonian Fluid Mech.*, **13**, 109–148 (1983).]

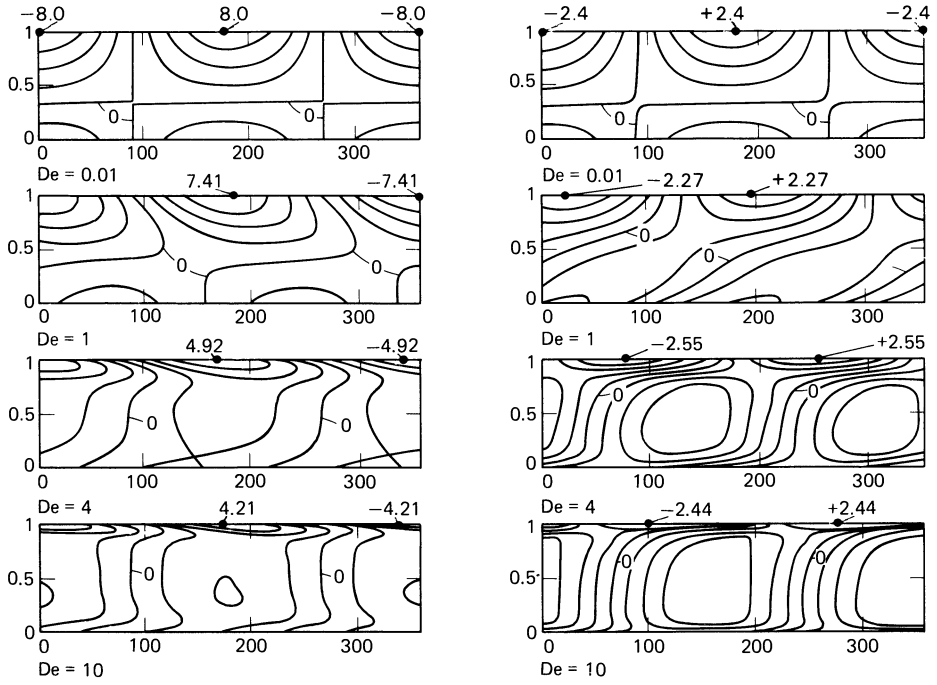

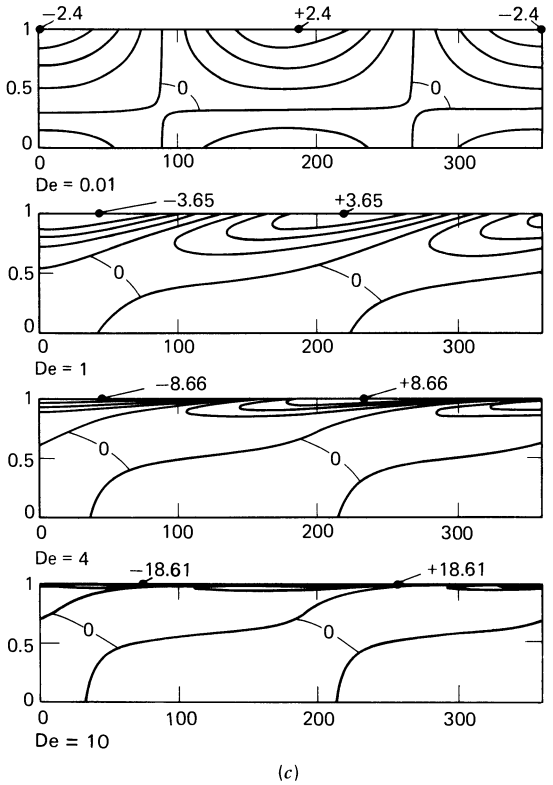

FIGURE 7.5-4. Contours of the correction to the tangential normal stress $\tau^*_{\theta\theta} = \tau^{\langle 1\rangle}_{\theta\theta}\mu/(\eta^{\langle 0\rangle}V/c)\mathrm{De}$ for the same three models as in Fig. 7.5-2: (*a*) convected Maxwell; (*b*) White-Metzner ($n = 0.3$); (*c*) CEF ($n = 0.3$). Contours are evenly spaced between the minimum and maximum values. [A. N. Beris, R. C. Armstrong, and R. A. Brown, *J. Non-Newtonian Fluid Mech.*, **13**, 109–148 (1983).]

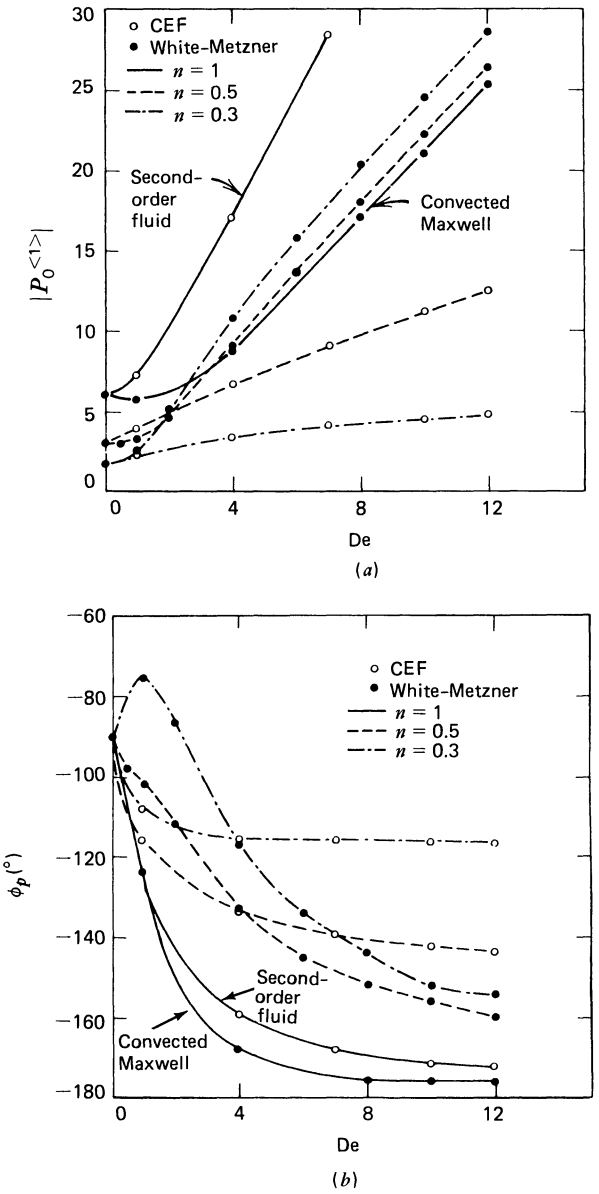

FIGURE 7.5-5. Dependence on $\mathrm{De} = \lambda_1 V/r_1$ of the amplitude $|P_0^{\langle 1\rangle}|$ and phase angle ϕ_p of the dimensionless correction to the pressure $p^* = p^{\langle 1\rangle}\mu/(\eta_0 V/c) = |P_0^{\langle 1\rangle}| \cos(\theta + \phi_p)$. Results are shown for the White-Metzner and CEF constitutive equations for several power-law indices. Note that the $n = 1$ curves for White-Metzner and CEF correspond to the convected Maxwell and second-order fluid results, respectively. [A. N. Beris, R. C. Armstrong, and R. A. Brown, *J. Non-Newtonian Fluid Mech.*, **13**, 109-148 (1983).]

models with memory, away from the outer wall $\tau^*_{\theta\theta}$ is nearly independent of ζ. For the CEF equation, however, the tangential normal stress is almost uniformly zero away from the outer wall; moreover, the stress gradient in the boundary layer is much more intense for this constitutive equation.

Finally in Fig. 7.5-5 we depict the dimensionless pressure. When the solutions to $p^{\langle 0\rangle}$ and $p^{\langle 1\rangle}$ are combined in the expansion for pressure we find that $p/(\eta_0 V/c) = (\varepsilon/\mu)|P_0^{\langle 1\rangle}| \cos(\theta + \phi_p) + O(1)$, that is, the largest contribution to p comes from the $P^{\langle 1\rangle}$ term. The dimensionless pressure is thus

defined as $p^* = p^{\langle 1\rangle}\mu/(\eta_0 V/c) = |P_0^{\langle 1\rangle}| \cos(\theta + \phi_p)$ where ϕ_p is the phase angle between the pressure and shape variations. The magnitude of the pressure oscillation governs the load-carrying capability of the journal bearing. In this regard it is interesting that at high De, increasing shear thinning increases $|P_0^{\langle 1\rangle}|$ for the models with memory and decreases it for the model without memory. The phase angle determines the steady-state position of the journal relative to the outer cylinder. For a Newtonian fluid $\phi_p = -90°$ and the offset direction is perpendicular to the load. The White-Metzner model with power-law index of 0.3 shows that the fluid pushes the inner cylinder toward the direction of the narrow part of the gap at moderate De. All other models show that the viscoelastic nature of the fluid causes the direction of the pressure force to shift toward the wide part of the gap.

Experimental observations[6] of a 1.5% polyacrylamide solution in a journal bearing with dimensionless gap μ of approximately 0.1 and $\varepsilon = 0.6$ show that the amplitude of the pressure oscillation decreases rapidly with increasing De and that the minimum in the pressure field shifts upstream, that is, the phase angle ϕ_p becomes less negative, as De increases. None of the models correctly predicts the pressure amplitude dependence and only the White-Metzner model gives the correct trend in ϕ_p (and then only for moderate De). The experiments also show that the separated flow region rapidly disappears with increasing De. This observation is consistent with the predictions of the convected Maxwell model, although the experiments show the recirculation to vanish at much lower De than those calculated here. The CEF model predicts the opposite trend of growth of the separated flow cell, whereas the White-Metzner model predicts first a shift downstream and then a small shrinkage at very high De (~ 10). Thus none of these models is completely satisfactory for this flow but the White-Metzner model seems to give the best overall, qualitative agreement with data. Numerical calculations with the Giesekus model[7] show better agreement than any of the models used here.

EXAMPLE 7.5-2. Torsional Flow of a Convected Jeffreys Fluid between Parallel Disks.[8]

A problem of considerable importance in the characterization of viscoelastic fluids is flow between parallel, coaxial disks, one of which is rotating. This problem was treated for Newtonian fluids in Problem 1B.5, and the geometry is shown in Fig. 1B.5. The disks are separated by a gap B; the bottom plate is fixed, and the upper one rotates with constant angular velocity W for $t \geq 0$. For $t < 0$ the fluid is at rest. Determine the time dependent velocity profiles in the gap for a convected Jeffreys fluid. Is the flow stable? Assume for this analysis that the disks are of infinite radius.

SOLUTION **(a)** Governing Equations

The fluid is taken to be incompressible and the flow is assumed to be axisymmetric: $v_i = v_i(r, z, t)$, $i = r, \theta, z$. The equation of continuity and equations of motion then give

$$\frac{1}{r}\frac{\partial}{\partial r}(rv_r) + \frac{\partial v_z}{\partial z} = 0 \tag{7.5-56}$$

$$\rho\left(\frac{\partial v_r}{\partial t} + v_r\frac{\partial v_r}{\partial r} - \frac{v_\theta^2}{r} + v_z\frac{\partial v_r}{\partial z}\right) = -\frac{\partial p}{\partial r} - \left[\frac{1}{r}\frac{\partial}{\partial r}(r\tau_{rr}) + \frac{\partial}{\partial z}\tau_{zr} - \frac{\tau_{\theta\theta}}{r}\right] \tag{7.5-57}$$

[6] J. V. Lawler, S. J. Muller, R. A. Brown, and R. C. Armstrong, *J. Non-Newtonian Fluid Mech.*, **20**, 51-92 (1986); R. C. Armstrong, R. A. Brown, J. V. Lawler, and S. J. Muller in *Proceedings of the Symposium on Viscoelasticity* (Mathematics Research Center, Madison, WI), Elsevier, New York (1985).

[7] A. N. Beris, R. C. Armstrong, and R. A. Brown, *J. Non-Newtonian Fluid Mech.*, **16**, 141-172 (1984); **19**, 323-347 (1986).

[8] This example is based on N. Phan-Thien, *J. Non-Newtonian Fluid Mech.*, **13**, 325-340 (1983). See also N. Phan-Thien, *J. Fluid Mech.*, **125**, 427-442 (1983); D. F. Griffiths, T. H. Jones, and K. Walters, *J. Fluid Mech.*, **36**, 161-176 (1969); R. K. Bhatnagar and M. G. N. Perera, *J. Rheol.*, **26**, 19-41 (1982).

$$\rho\left(\frac{\partial v_\theta}{\partial t}+v_r\frac{\partial v_\theta}{\partial r}-\frac{v_\theta v_r}{r}+v_z\frac{\partial v_\theta}{\partial z}\right)=-\left[\frac{1}{r^2}\frac{\partial}{\partial r}(r^2\tau_{r\theta})+\frac{\partial \tau_{z\theta}}{\partial z}\right] \tag{7.5-58}$$

$$\rho\left(\frac{\partial v_z}{\partial t}+v_r\frac{\partial v_z}{\partial r}+v_z\frac{\partial v_z}{\partial z}\right)=-\frac{\partial p}{\partial z}-\left[\frac{1}{r}\frac{\partial}{\partial r}(r\tau_{rz})+\frac{\partial \tau_{zz}}{\partial z}\right] \tag{7.5-59}$$

These equations must be solved together with the constitutive equation for the convected Jeffreys model, Eq. 7.2-1. The constitutive equation is somewhat simplified if we split the stress tensor into two parts $\boldsymbol{\tau}_s$ and $\boldsymbol{\tau}_p$ where $\boldsymbol{\tau}_s$ is a "Newtonian solvent" contribution and $\boldsymbol{\tau}_p$ is given by the convected Maxwell model:[9]

$$\boldsymbol{\tau}=\boldsymbol{\tau}_s+\boldsymbol{\tau}_p \tag{7.5-60a}$$

$$\boldsymbol{\tau}_s=-\eta_s\dot{\boldsymbol{\gamma}} \tag{7.5-60b}$$

$$\boldsymbol{\tau}_p+\lambda_1\boldsymbol{\tau}_{p(1)}=-\eta_p\dot{\boldsymbol{\gamma}} \tag{7.5-60c}$$

If we add Eq. 7.5-60b to λ_1 times the convected derivative of Eq. 7.5-60b and then add this sum to Eq. 7.5-60c, we see that the result is identical to the convected Jeffreys model of Eq. 7.2-1 if we require

$$\eta_0=\eta_s+\eta_p;\quad \lambda_2=(\eta_s/\eta_0)\lambda_1 \tag{7.5-61}$$

For the axisymmetric flow, the Newtonian part of the constitutive equation is readily evaluated (see Eqs. B.3-7 through 12 in Appendix B):

$$\boldsymbol{\tau}_s=-\eta_s\begin{pmatrix} 2\dfrac{\partial v_r}{\partial r} & r\dfrac{\partial}{\partial r}\left(\dfrac{v_\theta}{r}\right) & \dfrac{\partial v_r}{\partial z}+\dfrac{\partial v_z}{\partial r} \\ r\dfrac{\partial}{\partial r}\left(\dfrac{v_\theta}{r}\right) & 2\dfrac{v_r}{r} & \dfrac{\partial v_\theta}{\partial z} \\ \dfrac{\partial v_r}{\partial z}+\dfrac{\partial v_z}{\partial r} & \dfrac{\partial v_\theta}{\partial z} & 2\dfrac{\partial v_z}{\partial z} \end{pmatrix} \tag{7.5-62}$$

The six constitutive equations for $\boldsymbol{\tau}_p$ are written by combining the results for $\boldsymbol{\tau}_{p(1)}$ in Example 7.1-2, the rate-of-strain tensor on the right side of Eq. 7.5-62, and Eq. 7.5-60c.

The boundary conditions require no slip on the solid plates:

$$\begin{aligned} &\text{At } z=0, && v_r=v_\theta=v_z=0 \\ &\text{At } z=B, && v_r=v_z=0; \quad v_\theta=Wr \end{aligned} \tag{7.5-63}$$

These boundary conditions suggest we try[10]

$$v_\theta=G(z,t)r \tag{7.5-64}$$

If we let v_r and v_z depend on z through a second function $H(z,t)$ then the continuity equation requires that

$$v_z=-2H;\quad v_r=r\frac{\partial H}{\partial z} \tag{7.5-65}$$

We must then find G and H from the equations of motion and constitutive equations.

[9] This splitting of $\boldsymbol{\tau}$ was used in Eq. 7.3-3 for the Giesekus model.

[10] The velocity field in Eqs. 7.5-64 and 65 is the form of the classical solution due to von Karman for Newtonian fluids; T. von Kármán, *Z. Angew. Math. Mech.*, **1**, 233–252 (1921).

It is convenient to introduce dimensionless variables as follows:

$$\begin{gathered}\zeta = z/B; \quad \xi = r/B; \quad \tau = Wt \\ g(\zeta, \tau) = G/W; \quad h(\zeta, \tau) = H/WB \\ \mathbf{T} = \boldsymbol{\tau}/\eta_0 W = -\Lambda\dot{\boldsymbol{\Gamma}} + \boldsymbol{t} \\ \dot{\boldsymbol{\Gamma}} = \dot{\boldsymbol{\gamma}}/W; \quad \boldsymbol{t} = \boldsymbol{\tau}_p/\eta_0 W \\ P = p/\eta_0 W; \quad \Lambda = \eta_s/\eta_0 = \lambda_2/\lambda_1; \\ \mathrm{De} = \lambda_1 W; \quad \mathrm{Re} = \rho W B^2/\eta_0\end{gathered} \tag{7.5-66}$$

Note that De is the Deborah number for the problem and gives the relative importance of elasticity in the problem, and $\boldsymbol{t}$ is the dimensionless "polymer" contribution to the stress tensor. The dimensionless velocity field is given by

$$v_r/WB = \xi h_\zeta; \quad v_\theta/WB = \xi g; \quad v_z/WB = -2h \tag{7.5-67}$$

in which h_ζ denotes $\partial h(\zeta, \tau)/\partial\zeta$.

In terms of the functions g and h the dimensionless rate-of-strain tensor is

$$\dot{\boldsymbol{\Gamma}} = \begin{pmatrix} 2h_\zeta & 0 & \xi h_{\zeta\zeta} \\ 0 & 2h_\zeta & \xi g_\zeta \\ \xi h_{\zeta\zeta} & \xi g_\zeta & -4h_\zeta \end{pmatrix} \tag{7.5-68}$$

and the dimensionless components of the "polymer" contribution to the stress tensor are

$$t_{rr} + \mathrm{De}\left[\frac{\partial t_{rr}}{\partial\tau} + \xi h_\zeta \frac{\partial}{\partial\xi} t_{rr} - 2h \frac{\partial}{\partial\zeta} t_{rr} - 2h_\zeta t_{rr} - 2\xi h_{\zeta\zeta} t_{rz}\right] = -2(1-\Lambda)h_\zeta \tag{7.5-69}$$

$$t_{r\theta} + \mathrm{De}\left[\frac{\partial t_{r\theta}}{\partial\tau} + \xi h_\zeta \frac{\partial}{\partial\xi} t_{r\theta} - 2h \frac{\partial}{\partial\zeta} t_{r\theta} - 2h_\zeta t_{r\theta} - \xi g_\zeta t_{rz} - \xi h_{\zeta\zeta} t_{\theta z}\right] = 0 \tag{7.5-70}$$

$$t_{rz} + \mathrm{De}\left[\frac{\partial t_{rz}}{\partial\tau} + \xi h_\zeta \frac{\partial}{\partial\xi} t_{rz} - 2h \frac{\partial}{\partial\zeta} t_{rz} + h_\zeta t_{rz} - \xi h_{\zeta\zeta} t_{zz}\right] = -(1-\Lambda)\xi h_{\zeta\zeta} \tag{7.5-71}$$

$$t_{\theta\theta} + \mathrm{De}\left[\frac{\partial t_{\theta\theta}}{\partial\tau} + \xi h_\zeta \frac{\partial}{\partial\xi} t_{\theta\theta} - 2h \frac{\partial}{\partial\zeta} t_{\theta\theta} - 2h_\zeta t_{\theta\theta} - 2\xi g_\zeta t_{\theta z}\right] = -2(1-\Lambda)h_\zeta \tag{7.5-72}$$

$$t_{\theta z} + \mathrm{De}\left[\frac{\partial t_{\theta z}}{\partial\tau} + \xi h_\zeta \frac{\partial}{\partial\xi} t_{\theta z} - 2h \frac{\partial}{\partial\zeta} t_{\theta z} + h_\zeta t_{\theta z} - \xi g_\zeta t_{zz}\right] = -(1-\Lambda)\xi g_\zeta \tag{7.5-73}$$

$$t_{zz} + \mathrm{De}\left[\frac{\partial t_{zz}}{\partial\tau} + \xi h_\zeta \frac{\partial}{\partial\xi} t_{zz} - 2h \frac{\partial}{\partial\zeta} t_{zz} + 4h_\zeta t_{zz}\right] = 4(1-\Lambda)h_\zeta \tag{7.5-74}$$

The structure of the constitutive equations suggests we try power series solutions for the stress components:

$$t_{ij} = t_{ij}^0 + \xi t_{ij}^1 + \xi^2 t_{ij}^2 + \cdots = \sum_{k=0}^{\infty} \xi^k t_{ij}^k(\zeta, \tau) \tag{7.5-75}$$

Inserting these expansions into Eqs. 7.5-69 through 74 gives constitutive equations for the following nonzero t_{ij}^k:

$$t_{\theta z}^1 + \mathrm{De}\left[\frac{\partial t_{\theta z}^1}{\partial \tau} + 2h_\zeta t_{\theta z}^1 - 2h\frac{\partial}{\partial \zeta} t_{\theta z}^1 - g_\zeta t_{zz}^0\right] = -(1-\Lambda)g_\zeta \tag{7.5-76}$$

$$t_{zz}^0 + \mathrm{De}\left[\frac{\partial t_{zz}^0}{\partial \tau} - 2h\frac{\partial}{\partial \zeta} t_{zz}^0 + 4h_\zeta t_{zz}^0\right] = 4(1-\Lambda)h_\zeta \tag{7.5-77}$$

$$t_{rz}^1 + \mathrm{De}\left[\frac{\partial t_{rz}^1}{\partial \tau} - 2h\frac{\partial}{\partial \zeta} t_{rz}^1 + 2h_\zeta t_{rz}^1 - h_{\zeta\zeta} t_{zz}^0\right] = -(1-\Lambda)h_{\zeta\zeta} \tag{7.5-78}$$

$$t_{r\theta}^2 + \mathrm{De}\left[\frac{\partial t_{r\theta}^2}{\partial \tau} - 2h\frac{\partial t_{r\theta}^2}{\partial \zeta} - g_\zeta t_{rz}^1 - h_{\zeta\zeta} t_{\theta z}^1\right] = 0 \tag{7.5-79}$$

$$t_{rr}^0 + \mathrm{De}\left[\frac{\partial t_{rr}^0}{\partial \tau} - 2h\frac{\partial t_{rr}^0}{\partial \zeta} - 2h_\zeta t_{rr}^0\right] = -2(1-\Lambda)h_\zeta \tag{7.5-80a}$$

$$t_{rr}^2 + \mathrm{De}\left[\frac{\partial t_{rr}^2}{\partial \tau} - 2h\frac{\partial t_{rr}^2}{\partial \zeta} - 2h_{\zeta\zeta} t_{rr}^1\right] = 0 \tag{7.5-80b}$$

$$t_{\theta\theta}^0 + \mathrm{De}\left[\frac{\partial t_{\theta\theta}^0}{\partial \tau} - 2h\frac{\partial}{\partial \zeta} t_{\theta\theta}^0 - 2h_\zeta t_{\theta\theta}^0\right] = -2(1-\Lambda)h_\zeta \tag{7.5-81a}$$

$$t_{\theta\theta}^2 + \mathrm{De}\left[\frac{\partial t_{\theta\theta}^2}{\partial \tau} - 2h\frac{\partial}{\partial \zeta} t_{\theta\theta}^2 - 2g_\zeta t_{\theta z}^1\right] = 0 \tag{7.5-81b}$$

All other t_{ij}^k are zero. Note also that $t_{\theta\theta}^0 = t_{rr}^0$.

We can now return to the equation of motion and rewrite its components in terms of the assumed velocity field and the expansion coefficients for the stress components. At the same time we expand the pressure in a series in ξ:

$$P = P_0(\zeta, \tau) + \xi P_1(\zeta, \tau) + \xi^2 P_2(\zeta, \tau) + \cdots \tag{7.5-82}$$

From the r-component of the equation of motion we find that $P_1 = P_3 = P_4 \ldots = 0$ and that only P_0 and P_2 are nonzero. The r-, θ-, and z-components of the equation of motion then give, respectively,

$$\mathrm{Re}(h_{\zeta\tau} + h_\zeta^2 - g^2 - 2hh_{\zeta\zeta}) = 2P_2 + \Lambda h_{\zeta\zeta\zeta} - 3t_{rr}^2 + t_{\theta\theta}^2 - \frac{\partial t_{rz}^1}{\partial \zeta} \tag{7.5-83}$$

$$\mathrm{Re}(g_\tau + 2h_\zeta g - 2hg_\zeta) = \Lambda g_{\zeta\zeta} - 4t_{r\theta}^2 - \frac{\partial}{\partial \zeta} t_{\theta z}^1 \tag{7.5-84}$$

$$2\mathrm{Re}(h_\tau - 2hh_\zeta) = \frac{\partial}{\partial \zeta} P_0 + 2\Lambda h_{\zeta\zeta} + 2t_{rz}^1 + \frac{\partial}{\partial \zeta} t_{zz}^0 \tag{7.5-85a}$$

$$0 = \frac{\partial}{\partial \zeta} P_2 \tag{7.5-85b}$$

From the last equation we see that $P_2 = P_2(\tau)$. We can thus differentiate the r-component of the equation of motion with respect to ζ and thereby eliminate P_2:

$$\Lambda h_{\zeta\zeta\zeta\zeta} - 3\frac{\partial}{\partial\zeta}t^2_{rr} + \frac{\partial}{\partial\zeta}t^2_{\theta\theta} - \frac{\partial^2}{\partial\zeta^2}t^1_{rz} - \mathrm{Re}(h_{\zeta\zeta\tau} - 2gg_\zeta - 2hh_{\zeta\zeta\zeta}) = 0 \tag{7.5-86}$$

In order to solve for h, g, and the t^k_{ij} we use the above ζ-derivative of the r-component of the equation of motion together with the θ-component of the equation of motion and the constitutive equations, Eqs. 7.5-76 through 81. Once these are known we can find P_0 from the z-component of the equation of motion and P_2 from the r-component of the equation of motion. These equations are to be solved with the boundary conditions

$$\begin{aligned}
&\text{At } \zeta = 0, \qquad h = \frac{\partial h}{\partial\zeta} = g = 0\\
&\text{At } \zeta = 1, \qquad g = 1, h = \frac{\partial h}{\partial\zeta} = 0\\
&\text{At } \tau = 0, \qquad g = h = \frac{\partial h}{\partial\zeta} = t^k_{ij} = 0
\end{aligned} \tag{7.5-87}$$

(b) Small De, Re Expansion

We illustrate the solution to these equations for small Deborah and Reynolds numbers

$$0 < \mathrm{De} \ll \mathrm{Re} \ll 1 \tag{7.5-88}$$

The dependent variables are expanded as power series in De and Re. For example, for h we write

$$h = h_0 + \mathrm{Re}\, h_{01} + \mathrm{De}\, h_{10} + \mathrm{Re}^2 h_{02} + \mathrm{Re\,De}\, h_{11} + \cdots \tag{7.5-89}$$

At lowest order the constitutive equations give

$$\begin{aligned}
t^1_{\theta z0} &= -(1-\Lambda)g_{0\zeta}\\
t^0_{zz0} &= 4(1-\Lambda)h_{0\zeta}\\
t^1_{rz0} &= -(1-\Lambda)h_{0\zeta\zeta}\\
t^2_{r\theta0} &= 0\\
t^0_{rr0} &= -2(1-\Lambda)h_{0\zeta}; \qquad t^2_{rr0} = 0\\
t^k_{\theta\theta0} &= t^k_{rr0} \qquad (k = 0, 2)
\end{aligned} \tag{7.5-90}$$

Combining these with the equations of motion gives

$$h_{0\zeta\zeta\zeta\zeta} = 0; \quad g_{0\zeta\zeta} = 0 \tag{7.5-91}$$

which when solved with the boundary conditions leads directly to

$$h_0 = 0; \quad g_0 = \zeta \tag{7.5-92}$$

At lowest order the θ-component of velocity varies linearly from zero at the bottom disk to the rigid rotation at the top plate.

Continuing to higher order gives

$$\begin{aligned} h &= -\tfrac{1}{60}\,\mathrm{Re}(2\zeta^2 - 3\zeta^3 + \zeta^5) + \cdots \\ g &= \zeta + \tfrac{1}{30}(1-\Lambda)\mathrm{ReDe}(2\zeta^2 - 3\zeta^3 + \zeta^5) \\ &\quad + \tfrac{1}{30}\,\mathrm{Re}^2(-\tfrac{4}{105}\zeta - \tfrac{1}{6}\zeta^4 + \tfrac{3}{10}\zeta^5 - \tfrac{2}{21}\zeta^7) + \cdots \end{aligned} \tag{7.5-93}$$

These results can be used to show that the torques on the upper and lower disks are the same until order Re^2.

(c) Stability

Here we perform a linear stability analysis for the limit of creeping flow, $\mathrm{Re} = 0$, which is the limit of interest in most rheometer applications. The steady state solution in this limit is easily found to be

$$\begin{aligned} g &= \zeta \\ h &= 0 \\ t^1_{\theta z} &= -(1-\Lambda) \\ t^2_{\theta\theta} &= -2(1-\Lambda)\mathrm{De} \\ &\text{all other } t^k_{ij} = 0 \end{aligned} \tag{7.5-94}$$

This solution is valid for all De.

Now consider small disturbances about this flow. Let

$$\begin{aligned} g &= \zeta + g_1 \\ h &= h_1 \\ t^1_{\theta z} &= -(1-\Lambda) + \sigma_{\theta z} \\ t^2_{\theta\theta} &= -2(1-\Lambda)\mathrm{De} + \sigma_{\theta\theta} \\ t^2_{rr} &= \sigma_{rr};\quad t^0_{\theta\theta} = t^0_{rr} = \sigma_{rr,0} \\ t^1_{rz} &= \sigma_{rz};\quad t^0_{zz} = \sigma_{zz};\quad t^2_{r\theta} = \sigma_{r\theta} \end{aligned} \tag{7.5-95}$$

where h_1 and g_1 are the velocity disturbances and the σ_{ij} are the stress disturbances. When Eqs. 7.5-95 are substituted into the constitutive equations and the creeping flow equations of motion and the Laplace transforms of these equations taken, we obtain the following transformed constitutive equation and equations of motion:

$$\bar\sigma_{rr} + s\mathrm{De}\,\bar\sigma_{rr} = \mathrm{De}\,\sigma^0_{rr} \tag{7.5-96}$$

$$\bar\sigma_{zz} + s\mathrm{De}\,\bar\sigma_{zz} = \mathrm{De}\,\sigma^0_{zz} + 4(1-\Lambda)\bar h'_1 \tag{7.5-97}$$

$$\bar\sigma_{rz} + s\mathrm{De}\,\bar\sigma_{rz} = \mathrm{De}\,\sigma^0_{rz} - (1-\Lambda)\bar h''_1 \tag{7.5-98}$$

$$\bar\sigma_{r\theta} + s\mathrm{De}\,\bar\sigma_{r\theta} = \mathrm{De}\,(\sigma^0_{r\theta} + \bar\sigma_{rz} - (1-\Lambda)\bar h''_1) \tag{7.5-99}$$

$$\bar\sigma_{\theta\theta} + s\mathrm{De}\,\bar\sigma_{\theta\theta} = \mathrm{De}\,(\sigma^0_{\theta\theta} + 2\bar\sigma_{\theta z} - 2(1-\Lambda)\bar g'_1) \tag{7.5-100}$$

$$\bar\sigma_{\theta z} + s\mathrm{De}\,\bar\sigma_{\theta z} = \mathrm{De}\,(\sigma^0_{\theta z} + \bar\sigma_{zz} + 2(1-\Lambda)\bar h'_1) - (1-\Lambda)\bar g'_1 \tag{7.5-101}$$

$$\Lambda\bar g''_1 - 4\bar\sigma_{r\theta} - \bar\sigma'_{\theta z} = 0 \tag{7.5-102}$$

$$\Lambda\bar h^{(iv)}_1 - 3\bar\sigma'_{rr} + \bar\sigma'_{\theta\theta} - \bar\sigma''_{rz} = 0 \tag{7.5-103}$$

In these equations the overbar denotes the transformed variable, (e.g., $\mathscr{L}\{\sigma_{rr}\} = \bar{\sigma}_{rr}$), the initial conditions are denoted by the superscript zero (e.g., $\sigma_{rr}(\zeta, 0) = \sigma^0_{rr}(\zeta)$), the primes denote differentiation with respect to ζ (e.g., $d\bar{h}_1/d\zeta = \bar{h}'_1$), and s is the Laplace transform variable. We have not included a constitutive equation for $\sigma_{rr,0}$ inasmuch as this does not enter the equations of motion.

We now proceed to obtain a single ordinary differential equation for $\bar{h}$. This is done by first substituting the constitutive equations into the equations of motion, Eqs. 7.5-102 and 103. The equation that results from Eq. 7.5-102 is

$$\bar{g}''_1 - \frac{2(1-\Lambda)\,\mathrm{De}\,\bar{h}''_1}{(1+\Lambda s\mathrm{De})} = \frac{\mathrm{De}}{(1+\Lambda s\mathrm{De})}\left[4\sigma^0_{r\theta} + \sigma^{0\prime}_{\theta z} + \frac{\mathrm{De}(4\sigma^0_{rz} + \sigma^{0\prime}_{zz})}{(1+s\mathrm{De})}\right] \tag{7.5-104}$$

This result can be used to eliminate $\bar{g}_1$ from the equation obtained from Eq. 7.5-103 and the constitutive equations. The resulting equation for $\bar{h}$ is (after some lengthy algebra)

$$\begin{aligned}\bar{h}^{(\mathrm{iv})}_1 &+ \frac{4(1-\Lambda)\mathrm{De}^2(s^2\mathrm{De}^2 + 4s\mathrm{De} - 2\Lambda + 5)}{(1+\Lambda s\mathrm{De})^2(1+s\mathrm{De})^2}\,\bar{h}''_1 \\ &= \frac{\mathrm{De}}{(1+\Lambda s\mathrm{De})}\left[3\sigma^{0\prime}_{rr} - \sigma^{0\prime}_{\theta\theta} + \sigma^{0\prime\prime}_{rz} - \frac{2\,\mathrm{De}}{(1+s\mathrm{De})}\left(\frac{\mathrm{De}}{(1+s\mathrm{De})}\sigma^{0\prime}_{zz} + \sigma^{0\prime}_{\theta z}\right)\right. \\ &\quad \left. + \frac{2(1-\Lambda)(2+s\mathrm{De})\mathrm{De}}{(1+s\mathrm{De})(1+\Lambda s\mathrm{De})}\left(\frac{\mathrm{De}}{1+s\mathrm{De}}(4\sigma^{0\prime}_{rz} + \sigma^{0\prime}_{zz}) + 4\sigma^0_{r\theta} + \sigma^{0\prime}_{\theta z}\right)\right]\end{aligned} \tag{7.5-105}$$

For simplicity let us assume an initial disturbance in only one of the stress components, say $\sigma^0_{\theta\theta}$. That is, we take

$$\sigma^0_{\theta\theta} = \alpha_k \mathscr{R}e\{ie^{2\pi ik\zeta}\} \qquad (k = 1, 2\ldots) \tag{7.5-106}$$

where the amplitudes α_k are real and all other $\sigma^0_{ij} = 0$. Then,

$$\sigma^{0\prime}_{\theta\theta} = -2\pi k\alpha_k \mathscr{R}e\{e^{2\pi ik\zeta}\} \tag{7.5-107}$$

When these disturbances are substituted into Eq. 7.5-105, we see that $\bar{h}_1$ is of the form

$$\bar{h}_1 = \bar{\hbar}_1(s)e^{2\pi ik\zeta} \tag{7.5-108}$$

in which $\bar{\hbar}_1$ is given by

$$\begin{aligned}\bar{\hbar}_1 &= \frac{\alpha_k \mathrm{De}\,(1+\Lambda s\mathrm{De})(1+s\mathrm{De})^2}{8\pi k[\pi^2k^2(1+\Lambda s\mathrm{De})^2(1+s\mathrm{De})^2 - (1-\Lambda)\mathrm{De}^2(s^2\mathrm{De}^2 + 4s\mathrm{De} - 2\Lambda + 5)]} \\ &= \frac{\alpha_k \mathrm{De}(1+\Lambda s\mathrm{De})(1+s\mathrm{De})^2}{8\pi k[a_0(s\mathrm{De})^4 + a_1(s\mathrm{De})^3 + a_2(s\mathrm{De})^2 + a_3 s\mathrm{De} + a_4]}\end{aligned} \tag{7.5-109}$$

where the a_i's are

$$\begin{aligned} a_0 &= \pi^2k^2\Lambda^2 \\ a_1 &= 2\pi^2k^2\Lambda(1+\Lambda) \\ a_2 &= \pi^2k^2(\Lambda^2 + 4\Lambda - 11) - (1-\Lambda)\mathrm{De}^2 \\ a_3 &= 2\pi^2k^2(1+\Lambda) - 4(1-\Lambda)\mathrm{De}^2 \\ a_4 &= \pi^2k^2 + (1-\Lambda)(2\Lambda - 5)\mathrm{De}^2 \end{aligned} \tag{7.5-110}$$

To investigate the stability for $0 < \Lambda < 1$ we notice[11] that a *necessary* condition for stability is that all coefficients of the characteristic polynomial, $a_0, a_1, \ldots a_4$, be positive. This leads directly to the condition

$$\mathrm{De} < \mathrm{De}_c = \frac{\pi}{\sqrt{(1-\Lambda)(5-2\Lambda)}} \tag{7.5-111}$$

for stability, where De_c denotes the critical Deborah number. Note that the kth mode becomes unstable at a critical value $\mathrm{De}_{c,k} = \pi k/\sqrt{(1-\Lambda)(5-2\Lambda)}$. The stability of the flow is dictated by the smallest such number.

To show that Eq. 7.5-111 is also a sufficient condition for stability we must construct the Routh array:

$$\begin{array}{ll} a_0 & a_2 \quad a_4 \\ a_1 & a_3 \\ b_1 & b_2 \\ c_1 & \\ d_1 & \end{array} \tag{7.5-112}$$

where

$$\begin{aligned} b_1 &= (a_1a_2 - a_0a_3)/a_1; \qquad b_2 = a_4 \\ c_1 &= (b_1a_3 - a_1b_2)/b_1; \qquad d_1 = a_4 \end{aligned} \tag{7.5-113}$$

The necessary and sufficient condition for stability is that all coefficients in the first column of the Routh array are positive for $0 < \Lambda < 1$. Clearly a_0 and a_1 are positive. Also the condition that $d_1 > 0$ is given by Eq. 7.5-111. It is straightforward to show that b_1 and c_1 are also positive provided that Eq. 7.5-111 is satisfied. Therefore this equation is necessary and sufficient for $0 < \Lambda < 1$. Note that as $\Lambda \to 1$ the critical Deborah number in Eq. 7.5-111 goes to infinity, which is consistent with the fact that the creeping flow of a Newtonian fluid in this geometry is stable.

When $\Lambda = 0$ (the convected Maxwell model) the characteristic polynomial is only of second order, that is, the denominator of Eq. 7.5-109 is

$$8\pi k[a_0(s\mathrm{De})^2 + a_1 s\mathrm{De} + a_2] \tag{7.5-114}$$

in which

$$\begin{aligned} a_0 &= \pi^2k^2 - \mathrm{De}^2 \\ a_1 &= 2\pi^2k^2 - 4\mathrm{De}^2 \\ a_2 &= \pi^2k^2 - 5\mathrm{De}^2 \end{aligned} \tag{7.5-115}$$

[11] D. R. Coughanour and L. B. Koppel, *Process Systems Analysis and Control*, McGraw-Hill, New York (1965).

The Routh test results in the following possibilities:

De	a_0	a_1	a_2	Stability
$\mathrm{De}^2 < \frac{\pi^2 k^2}{5}$	+	+	+	Stable
$\frac{\pi^2 k^2}{5} < \mathrm{De}^2 < \frac{\pi^2 k^2}{2}$	+	+	−	Unstable
$\frac{\pi^2 k^2}{2} < \mathrm{De}^2 < \pi^2 k^2$	+	−	−	Unstable
$\pi^2 k^2 < \mathrm{De}^2$	−	−	−	Unstable

The critical Deborah number is then $\mathrm{De}_c = \pi/\sqrt{5}$. The fact that the kth mode becomes stable as De is increased beyond $\pi^2 k^2$ does not affect the overall stability of the flow, since as soon as $\mathrm{De} > \mathrm{De}_c$ there will always be a value of k large enough so that the mode is unstable.

§7.6 LIMITATIONS OF DIFFERENTIAL MODELS AND RECOMMENDATIONS FOR THEIR USE

The differential constitutive equations presented in this chapter are not limited to small deformation gradients as are the linear viscoelastic models of Chapter 5 or to small, slowly changing deformation rates as is the retarded-motion expansion of Chapter 6. Moreover, the quasi-linear and nonlinear models introduced in §§7.2 and 7.3 are simple enough to allow (barely!) analytical solutions to be obtained for some interesting flows. For this reason these constitutive equations have proven very useful in making exploratory fluid dynamical calculations to gain insight into the qualitative effects of viscoelasticity on complex flow fields. The price of simplicity in the constitutive equation is paid in the poor approximation to some of the material functions. The utility of one of these models in a specific flow problem depends on which material functions are most closely related to the flow and on how well the model describes those properties. Often, making this assessment must be based on experience. For example, in calculating flows where there is expected to be a strong elongational flow component, the Oldroyd models are not good choices, unless care is taken to ensure that the parameters are chosen to avoid an infinite elongational viscosity. Similarly, in flows that are primarily shearing and involve large shear rates, the Giesekus model should be used only if a retardation time is included so that the power-law region in which $\eta \propto \dot{\gamma}^{-1}$ is avoided.

There are many nonlinear differential models other than the ones we have chosen in §7.2 and 3 which can be found in the literature. We list some of these in Table 7.6-1. Note that these models contain no new types of terms.

All of the models presented here can be viewed as nonlinear generalizations of the linear viscoelastic Jeffreys model; all[1] have the same linear viscoelastic material functions as the Jeffreys model. The inability to describe linear viscoelasticity correctly is the result of having a single relaxation time and is the most serious defect of these models. There are two ways that we can remedy this problem. The first method, which can be used for only some of the nonlinear differential models, is to reformulate the model in integral form where it is

[1] Except for the White–Metzner model, which does not have a linear viscoelastic limit.

straightforward to include as many time constants as desired. The use of integral models with multiple time constants is discussed in Chapter 8. The connection between the differential and integral forms of the same model, for example, the convected Jeffreys model, is described in Chapter 9.

A second approach, which can be used for any of the nonlinear differential constitutive equations, is to superpose a series of models, each with a different time constant. This was done in Chapter 5 to construct the generalized Maxwell model of linear viscoelasticity. The corresponding generalized convected Maxwell model is

$$\boldsymbol{\tau} = \sum_i \boldsymbol{\tau}_i \tag{7.6-1}$$

$$\boldsymbol{\tau}_i + \lambda_i \boldsymbol{\tau}_{i(1)} = -\eta_i \boldsymbol{\gamma}_{(1)} \tag{7.6-2}$$

Here the constants η_i and λ_i are determined from linear viscoelasticity (see Example 5.3-7). Equations 7.6-1 and 2 are also known as the Rouse–Zimm model (see Chapter 15), which is obtained from the kinetic theory of a dilute solution of macromolecules modeled as freely jointed bead-spring units. The generalized convected Maxwell model is not any better than the convected Maxwell model at describing nonlinear material functions such as viscosity and normal stress coefficients. More successful data fitting can be achieved with superposition of nonlinear models, such as the Giesekus model, Eq. 7.3-4. To illustrate the improvement obtained by including additional modes we show a comparison in Figs. 7.6-1 through 3 of an 8-mode Giesekus model with experimental data in shear and elongational flow for a low-density polyethylene melt (see §§3.3–3.5). The time constants and viscosities, λ_i and η_i, are the same as those listed in Table 5.3-2. The α_i for each mode were chosen empirically to give a reasonable fit of the data. Clearly the fit can be made quite good. The drawback to using this, or any other multimode differential model, is that it is computationally impractical. In numerical simulations, the number of unknowns in a problem increases nearly linearly with the number of modes; with present computers, using more than two or possibly three modes is not reasonable.

Two other successful examples of multimode models are those of Acierno, La Mantia, Marrucci, and Titomanlio[2] and of Phan-Thien and Tanner;[3] these models are given in Table 7.6-1. Both models were derived from network theories[4] of concentrated polymer solutions and melts, and both have been shown to describe data on low-density polyethylene melts well.[3,5] Fitting data with the Phan-Thien–Tanner model is particularly straightforward, since the term involving ξ is most important in shear flows, and the parameter ε is most important in shearfree flows.

Still other superpositions are possible. In particular, Giesekus has pointed out that there is no reason a priori to assume the different time scale events are uncoupled.[6] This leads, however, to computationally cumbersome equations and is not recommended for fluid flow problem solving.

[2] D. Acierno, F. P. La Mantia, G. Marrucci, and G. Titomanlio, *J. Non-Newtonian Fluid Mech.*, **1**, 125–146 (1976); see also H. Janeschitz-Kriegl, *Polymer Melt Rheology and Flow Birefringence*, Springer, Berlin (1983), §2.5.5.

[3] N. Phan-Thien, *J. Rheol.*, **22**, 259–283 (1977); an alternative formulation of the nonlinear stress term involving ε is given by N. Phan-Thien and R. I. Tanner, *J. Non-Newtonian Fluid Mech.*, **2**, 353–365 (1977). A very similar model has been proposed by M. W. Johnson and D. Segalman, *J. Non-Newtonian Fluid Mech.*, **2**, 255–270 (1977).

[4] R. J. J. Jongschaap, *J. Non-Newtonian Fluid Mech.*, **8**, 183–190 (1981), has a clear discussion of the connection between the Acierno, La Mantia, Marrucci, and Titomanlio model and network theories. See also Chapter 20.

[5] D. Acierno, F. P. La Mantia, G. Marrucci, G. Rizzio, and G. Titomanlio, *J. Non-Newtonian Fluid Mech.*, **1**, 147–157 (1976); D. Acierno, F. P. La Mantia, and G. Marrucci, *J. Non-Newtonian Fluid Mech.*, **2**, 271–280 (1977).

[6] H. Giesekus, *Rheol. Acta*, **11**, 69–109 (1982); **12**, 367–374 (1983).

TABLE 7.6-1

Differential Constitutive Equations

Name	Reference	Constants or Functions	Equation for Model		Comments
Tanner	[a]	$\eta(\dot{\gamma})$, λ	$\boldsymbol{\tau} + \lambda\boldsymbol{\tau}_{(1)} = -\eta\boldsymbol{\gamma}_{(1)}$	(A)	Modification of Oldroyd B model (cf. Eq. 7.2-1) with $\lambda_2 = 0$.
FENE-P	[b]	η_s, η_p, λ_1, b $\varepsilon = 2/(b(b+2))$	$\boldsymbol{\tau} = -\eta_s\dot{\boldsymbol{\gamma}} + \boldsymbol{\tau}_p$ $Z\boldsymbol{\tau}_p + \lambda_1\boldsymbol{\tau}_{p(1)} - \lambda_1\left(\boldsymbol{\tau}_p - (1-\varepsilon b)\frac{\eta_p\boldsymbol{\delta}}{\lambda_1}\right)\frac{D\ln Z}{Dt}$ $= -(1-\varepsilon b)\eta_p\dot{\boldsymbol{\gamma}}$ $Z = 1 + \left(\frac{3}{b}\right)\left(1 - \lambda_1\frac{\operatorname{tr}\boldsymbol{\tau}_p}{3\eta_p}\right)$	(B)	Approximate constitutive equation for FENE dumbbells (cf. Eq. 13.5-56). The splitting of the stress tensor is similar to Eq. 7.3-3.
Nearly Hookean dumbbell	[c]	η_s, η_p, λ_1, b	$\boldsymbol{\tau} = -\eta_s\dot{\boldsymbol{\gamma}} + \boldsymbol{\tau}_p$ $\boldsymbol{\tau}_p = \eta_p\boldsymbol{\alpha}_{(1)}$ $\boldsymbol{\alpha} + \lambda_1\boldsymbol{\alpha}_{(1)} + \frac{1}{b}\{(\operatorname{tr}\boldsymbol{\alpha})\boldsymbol{\alpha} + 2\boldsymbol{\alpha}\cdot\boldsymbol{\alpha}\} = \boldsymbol{\delta}$	(C)	Derived for dilute suspension of nearly-Hookean dumbbells. (cf. Eqs. 13.5-56a–c)

Acierno, La Mantia, Marrucci, and Titomanlio [d]	$\eta_{i0}(=G_{i0}\lambda_{i0})$, λ_{i0}, a	$\boldsymbol{\tau} = \sum_i \boldsymbol{\tau}_i$ (D) $\left(1 - \lambda_i\right)\frac{\mathrm{D} \ln G_i}{Dt}\boldsymbol{\tau}_i + \lambda_i \boldsymbol{\tau}_{i(1)} = -\eta_i \dot{\boldsymbol{\gamma}}$ $G_i = G_{i0}x_i$; $\lambda_i = \lambda_{i0}x_i^{1.4}$; $\eta_i = G_i\lambda_i = \eta_{i0}x_i^{2.4}$ $\lambda_i \frac{dx_i}{dt} = (1 - x_i) - ax_i\sqrt{-(\mathrm{tr}\,\boldsymbol{\tau}_i)/2G_i}$	Derived from a network theory (see §20.5) The subscript '0' on the a_i, λ_i, and η_i denote values fit from linear viscoelastic data (see Example 5.3-7)
Phan-Thien and Tanner [e]	η_i, λ_i, ξ, ε	$\boldsymbol{\tau} = \sum_i \boldsymbol{\tau}_i$ (E) $Z(\mathrm{tr}\,\boldsymbol{\tau}_i)\boldsymbol{\tau}_i + \lambda_i \boldsymbol{\tau}_{i(1)} + \frac{\xi}{2}\lambda_i\{\dot{\boldsymbol{\gamma}} \cdot \boldsymbol{\tau}_i + \boldsymbol{\tau}_i \cdot \dot{\boldsymbol{\gamma}}\} = -\eta_i \dot{\boldsymbol{\gamma}}$ $Z = \begin{cases} 1 - \varepsilon\lambda_i\,\mathrm{tr}\,\boldsymbol{\tau}_i/\eta_i \\ \exp\left(-\varepsilon\lambda_i\,\mathrm{tr}\,\boldsymbol{\tau}_i/\eta_i\right) \end{cases}$	Derived from a network theory (Chapter 20). Two forms of $Z(\mathrm{tr}\,\boldsymbol{\tau}_i)$ have been used; the exponential form causes $\bar{\eta}$ to have a maximum.

[a] R. I. Tanner, *ASLE Trans.*, **8**, 179–183 (1965).

[b] R. I. Tanner, *Trans. Soc. Rheol.*, **19**, 37–65 (1975); R. B. Bird, *J. Non-Newtonian Fluid Mech.*, **5**, 1–12 (1979); R. B. Bird, P. J. Dotson, and N. L. Johnson, *J. Non-Newtonian Fluid Mech.*, **7**, 213–235 (1980); **8**, 193 (1981); X.-J. Fan, *J. Non-Newtonian Fluid Mech.*, **17**, 125–144 (1985).

[c] R. C. Armstrong and S. Ishikawa, *J. Rheol.*, **24**, 143–165 (1980); R. C. Armstrong, S. K. Gupta, and O. Basaran, *Polym. Eng. Sci.*, **20**, 466–472 (1980).

[d] D. Acierno, F. P. La Mantia, G. Marrucci, and G. Titomanlio, *J. Non-Newtonian Fluid Mech.*, **1**, 125–146 (1976).

[e] N. Phan-Thien, *J. Rheol.*, **22**, 259–283 (1977); an alternative formulation of the nonlinear stress term involving ε is given by N. Phan-Thien and R. I. Tanner, *J. Non-Newtonian Fluid Mech.*, **2**, 353–365 (1977). A very similar model has been proposed by M. W. Johnson and D. Segalman, *J. Non-Newtonian Fluid Mech.*, **2**, 255–270 (1977).

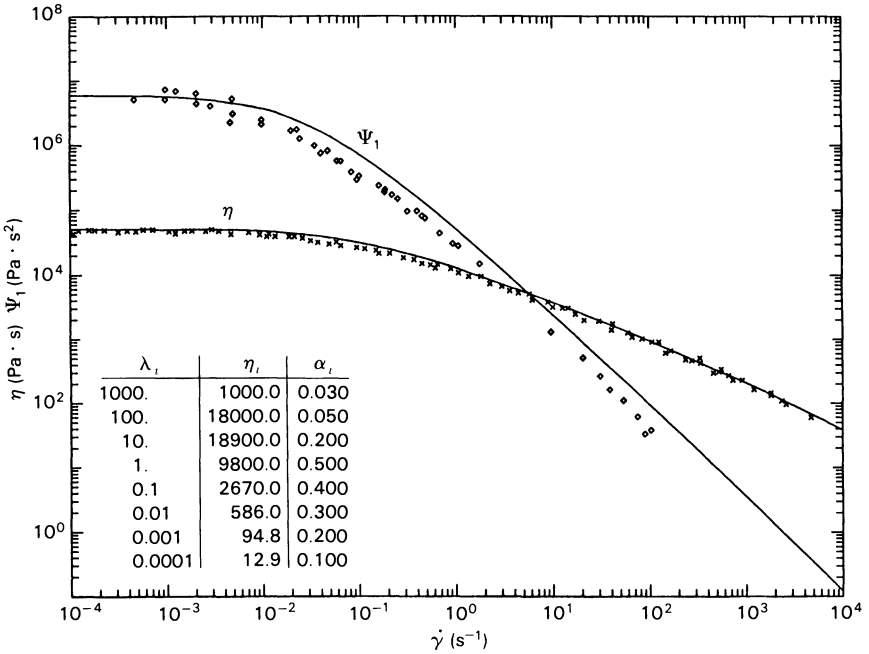

FIGURE 7.6-1. Viscosity and first normal stress coefficient for an 8-mode Giesekus model as compared to experimental data for a low-density polyethylene melt (cf. Fig. 3.3-2). The λ_i and η_i for the eight modes are listed in Table 5.3-2; the α_i were found empirically.

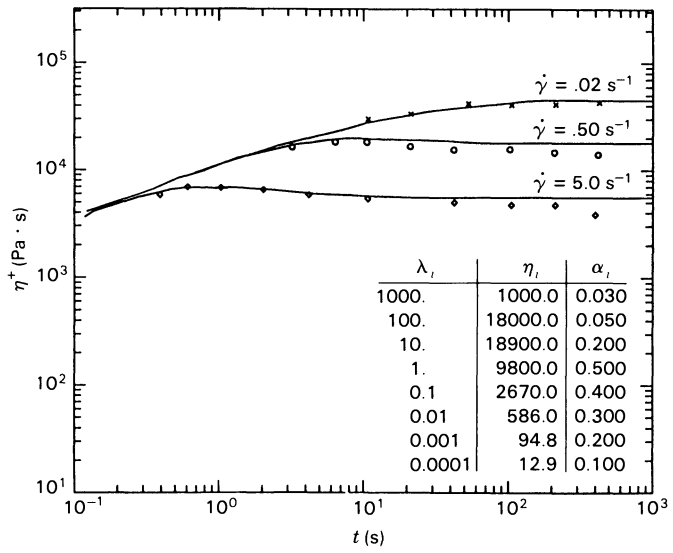

FIGURE 7.6-2. Comparison of η^+ calculated by an 8-mode Giesekus model with experimental data for a low-density polyethylene melt (cf. Fig. 3.4-7). The model parameters are given in Table 5.3-2 and in the figure.

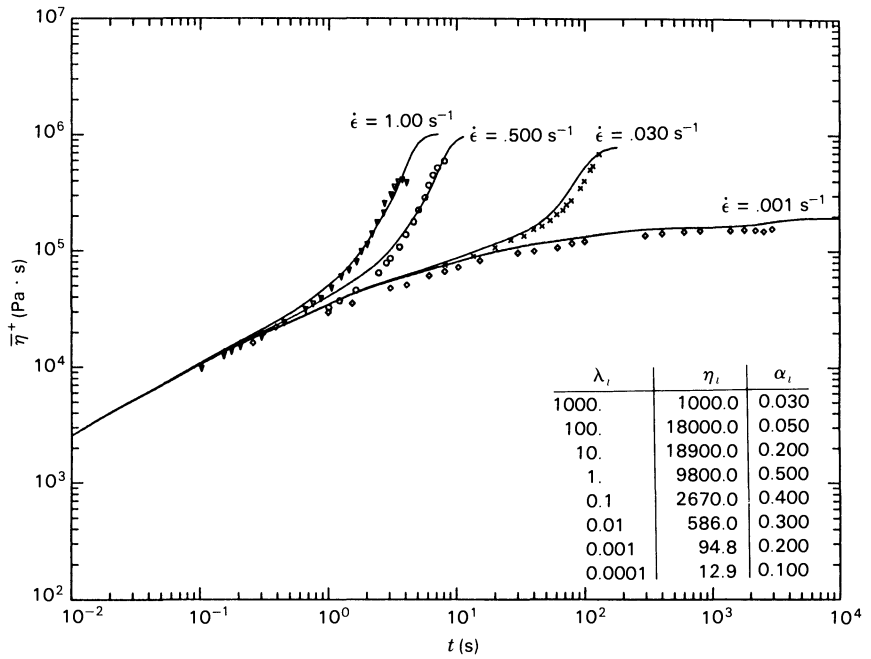

λ_i	η_i	α_i
1000.	1000.0	0.030
100.	18000.0	0.050
10.	18900.0	0.200
1.	9800.0	0.500
0.1	2670.0	0.400
0.01	586.0	0.300
0.001	94.8	0.200
0.0001	12.9	0.100

FIGURE 7.6-3. Comparison of $\bar{\eta}^+$ calculated by an 8-mode Giesekus model with experimental data for a low-density polyethylene melt (cf. Fig. 3.5-3). The model parameters are given in Table 5.3-2 and in the figure.

Finally, Leonov and co-workers have proposed a differential model based on nonequilibrium thermodynamics.[7] In this model the stress tensor τ is given in terms of an elastic potential function, an elastic strain tensor, and an irreversible rate-of-strain tensor. The constitutive equation is very closely related to nonlinear elasticity; at least for simple shear flow it is identical to the Giesekus model discussed in §7.3.

Clearly still other nonlinear differential models can be constructed by using the methods of §§7.1–7.3. It is, however, very difficult to decide what new kinds of terms should be added and time consuming to evaluate the resulting constitutive equations by comparison with experimental data. Helpful guidance in the selection of new terms can be obtained from molecular theory, which is the subject of Volume 2. It is interesting that many of the most successful models presented in this chapter have been obtained by molecular theory.

PROBLEMS

7A.1 Estimation of Oldroyd Model Parameters

Consider the 4-constant Oldroyd model obtained by setting $\lambda_3 = \lambda_4 = \lambda_6 = \lambda_7 = 0$ in Eq. 7.3-2. Obtain the numerical values of η_0, λ_1, λ_2, and λ_5 by using the data on $\eta(\dot{\gamma})$ and $\eta'(\omega)$ on 2% polyisobutylene in Primol (see Figs. 3.3-3 and 3.4-4). Having obtained the four parameters, plot the curve of Ψ_1 given by Eq. B of Table 7.3-3 and compare with the experimental data in Fig. 3.3-5. What conclusions do you draw from this comparison?

[7] A. I. Leonov, *Rheol. Acta*, **15**, 85–93 (1976); A. I. Leonov, E. H. Lipkina, E. D. Paskhin, and A. N. Prokunin, *Rheol. Acta*, **15**, 411–426 (1976). See also P. A. Dashner and W. E. Van Arsdale, *J. Non-Newtonian Fluid Mech.*, **8**, 59–67 (1981); **12**, 375–382 (1983).

7A.2 Deviation from Stokes' Law Because of Viscoelasticity of a Macromolecular Fluid.

Stokes' law for steady-state, creeping flow around a sphere was given in Example 1.4-1. The analogous problem of solving the equations of continuity and motion (with the inertial terms omitted) from the Oldroyd model of Eq. 7.3-2 was first done by Leslie.[1] In this work λ_3 and λ_4 were set equal to 0 and the abbreviations $\sigma_i = \lambda_i\lambda_5 + \lambda_{i+5}(\lambda_1 - \frac{3}{2}\lambda_5)$ were used (see the definition σ_i in Table 7.3-3). Leslie performed a perturbation analysis about the known Newtonian fluid solution, expanding in powers of the Deborah number $\mathrm{De} = v_\infty\lambda_1/R$. His solution is valid for

$$\mathrm{Re} \ll \mathrm{De} \ll 1 \tag{7A.2-1}$$

where $\mathrm{Re} = Rv_\infty\rho/\eta_0$ is the Reynolds number. Although the details of the derivation are tedious and lengthy, the final result for the drag force up through $O(\mathrm{De}^2)$ is rather simple. The result, as corrected by Giesekus[2] in a later publication, is

$$F_D = 6\pi\eta_0 Rv_\infty\left\{1 - \frac{1}{2275}\left[\left(\frac{401}{11} - 39\frac{\lambda_2}{\lambda_1}\right)\left(1 - \frac{\lambda_2}{\lambda_1}\right) - 471\left(\frac{\sigma_2 - \sigma_1}{\lambda_1^2}\right)\right]\mathrm{De}^2 + \cdots\right\} \tag{7A.2-2}$$

a. From Eq. 7A.2-1 show that in applying the above result for F_D to spheres falling in viscoelastic fluids, there is an upper limit to the radius of the sphere that can be used and an upper limit to the speed of descent of the sphere.

b. Design an experiment for testing Eq. 7A.2-2 for a fluid with the following properties:

$$\eta_0 = 1.05\ \mathrm{Pa\cdot s} \qquad \lambda_5 = 0.05\ \mathrm{s}$$
$$\lambda_1 = 0.1\ \mathrm{s} \qquad \lambda_6 = \lambda_7 = 0$$
$$\lambda_2 = 0.02\ \mathrm{s}$$

c. Find an expression for the terminal velocity of the falling sphere.

7B.1 Normal Stresses in Small Amplitude Oscillatory Shearing of the Convected Jeffreys Model

In Example 7.2-1 it was shown that η' and η'' for the convected Jeffreys model were identical to those for the Jeffreys model of linear viscoelasticity. Here we finish the task of showing that the two models also agree in predicting zero normal stresses in the limit of small strains.

a. Show that the normal stress τ_{xx} in small-amplitude oscillatory shear flow is the solution to

$$\left(1 + \lambda_1\frac{d}{dt}\right)\tau_{xx} = T(1 + \cos 2\omega t + \lambda_1\omega \sin 2\omega t) \tag{7B.1-1}$$

in which

$$T = -\frac{\eta_0\gamma_0^2\omega^2(\lambda_1 - \lambda_2)}{(1 + \lambda_1^2\omega^2)} \tag{7B.1-2}$$

[1] F. M. Leslie, *Q. J. Mech. Appl. Math.*, **14**, 36–48 (1961), with an appendix by R. I. Tanner.

[2] H. Giesekus, *Rheol. Acta*, **3**, 59–71 (1963), see footnote 16 on p. 69. In this paper the problem of simultaneous translation and rotation of a sphere in a viscoelastic liquid is studied. The effect of the container boundaries on the movement of a particle through a non-Newtonian fluid has been studied by B. Caswell, *Chem. Eng. Sci.*, **25**, 1167–1176 (1970).

b. Obtain a periodic solution to τ_{xx} of the form

$$\frac{\tau_{xx}}{T} = A \cos 2\omega t + B \sin 2\omega t + C \tag{7B.1-3}$$

where A, B, and C are functions of ω. Notice that the normal stress oscillates at a frequency 2ω about a non-zero mean value.

c. Use the results of part **(b)** together with Eqs. 7.2-9 through 11 to show that the ratio of the magnitude of τ_{xx} to the magnitude of τ_{xy} goes to zero as γ_0 approaches zero for all ω.

7B.2 Shearfree Flow for the White–Metzner Model

a. Show that the second invariant of the rate-of-deformation tensor is

$$\dot{\gamma} = \sqrt{(3 + b^2)}\,|\dot{\varepsilon}_0| \tag{7B.2-1}$$

where $\dot{\varepsilon}_0$ is the constant strain rate.

b. Derive Eqs. C in Table 7.3-1.

c. Suppose $\eta(\dot{\gamma})$ is given by the power-law function (Eq. 4.1-10). What is the maximum value of $\dot{\varepsilon}_0$ for which the results in part **(b)** are physically realistic. Is this an improvement on the convected Maxwell model?

7B.3 Step Strain Stress Relaxation for the Oldroyd 8-Constant Model

It is desired to determine the linear viscoelastic properties of the Oldroyd 8-constant model by finding its response to a step strain experiment, $\dot{\gamma}_{yx} = \gamma_0 \delta(t)$ where the shear strain amplitude γ_0 is small.

a. Show that in the limit $\gamma_0 \to 0$ if we retain only the terms first order in γ_0, all normal stresses are zero and the shear stress is given by

$$\tau_{yx} = \tau_{yx,1}\gamma_0 + O(\gamma_0^3) \tag{7B.3-1}$$

$$\left[1 + \lambda_1 \frac{d}{dt}\right]\tau_{yx,1} = -\eta_0\left[1 + \lambda_2 \frac{d}{dt}\right]\delta(t) \tag{7B.3-2}$$

where $\tau_{yx}(-\infty) = 0$.

b. Integrate Eq. 7B.3-1 to obtain

$$\tau_{yx,1} = 0 \qquad t < 0 \tag{7B.3-3a}$$

$$\tau_{yx,1} = \tau_0 e^{-t/\lambda_1} \qquad t > 0 \tag{7B.3-3b}$$

in which $\tau_0 = \tau_{yx,1}(0^+)$.

c. In order for the solution to be nontrivial it is clear that τ_0 must be singular. What form for τ_0 does the differential equation suggest?

d. Combine the results of **(b)** and **(c)** to obtain

$$\begin{aligned}\tau_{yx,1} &= -\frac{\eta_0\gamma_0}{\lambda_1}\left[\left(1 - \frac{\lambda_2}{\lambda_1}\right)H(t)e^{-t/\lambda_1} + \lambda_2\delta(t)\right] \\ &= -\frac{\eta_0\gamma_0}{\lambda_1}H(t)\left[\left(1 - \frac{\lambda_2}{\lambda_1}\right)e^{-t/\lambda_1} + 2\lambda_2\delta(t)\right]\end{aligned} \tag{7B.3-4}$$

What is the linear relaxation modulus $G(t)$?

7B.4 Elongational Viscosity for 8-Constant Oldroyd Fluid

a. Write out Eq. 7.3-2 in matrix form for steady-state elongational flow $v_z = \dot{\varepsilon}z$, $v_x = -(1/2)\dot{\varepsilon}x$, and $v_y = -(1/2)\dot{\varepsilon}y$, where $\dot{\varepsilon}$ is a constant.

b. From the matrix equation obtain a pair of equations for $\tau_{xx} - \tau_{zz}$ and $\text{tr}\,\boldsymbol{\tau} = \tau_{xx} + \tau_{yy} + \tau_{zz}$

$$(1 - (\lambda_1 - \lambda_3)\dot{\varepsilon})(\tau_{xx} - \tau_{zz}) - (\tfrac{3}{2}\lambda_5 - \lambda_1 + \lambda_3)\dot{\varepsilon}\,\text{tr}\,\boldsymbol{\tau} = 3\eta_0\dot{\varepsilon}(1 - (\lambda_2 - \lambda_4)\dot{\varepsilon}) \tag{7B.4-1}$$

$$(2(\lambda_1 - \lambda_3) - 3\lambda_6)\dot{\varepsilon}(\tau_{xx} - \tau_{zz}) + \text{tr}\,\boldsymbol{\tau} = 3\eta_0\dot{\varepsilon}^2(2(\lambda_2 - \lambda_4) - 3\lambda_7) \tag{7B.4-2}$$

c. Solve the equations in **(b)** for $\tau_{xx} - \tau_{zz}$ and find that the elongational viscosity $\bar{\eta}$ is given by Eq. F in Table 7.3-3. To what extent is this result in accord with known experimental facts?

7B.5 A 3-Constant Oldroyd Model[3]

The Oldroyd 8-constant model in §7.3 has often been used in simplified form by reducing the number of parameters. One simplification is to require that Ψ_2 be zero (this leads to $\lambda_3 = \lambda_4 = 0$) and to require arbitrarily that $\boldsymbol{\tau}$ be traceless (this leads to $\lambda_6 = \frac{2}{3}\lambda_1$, $\lambda_7 = \frac{2}{3}\lambda_2$).

a. Show that this leads to the following expressions for the steady shear flow functions:

$$\frac{\eta}{\eta_0} = \frac{1 + \frac{2}{3}\lambda_1\lambda_2\dot{\gamma}^2}{1 + \frac{2}{3}(\lambda_1\dot{\gamma})^2} \tag{7B.5-1}$$

$$\frac{\Psi_1}{2\eta_0\lambda_1} = \frac{1 - (\lambda_2/\lambda_1)}{1 + \frac{2}{3}(\lambda_1\dot{\gamma})^2} \tag{7B.5-2}$$

and that the small-amplitude oscillatory functions are given by Eqs. D and E in Table 7.3-3. What restrictions have to be placed on the time constants λ_1 and λ_2?

b. Show that $\eta(\dot{\gamma})$ is the same function as $\eta'(c\omega)$, and that $\Psi_1\dot{\gamma}/\sqrt{6}$ vs. $\dot{\gamma}$ is the same function as η'' vs. $c\omega$, with $c = \sqrt{3/2} = 1.24$. The constant c is called the "shift factor," and experimental values[4] lie between about 1.4 and 2.3.

c. An oft-quoted empiricism[3] known as the Cox–Merz rule (cf. §3.6) states that $\eta(\dot{\gamma})$ should be the same function as $|\eta^*|$ vs. ω. To what extent is the 3-constant Oldroyd model in agreement with this rule?

7B.6 Third-Order Retarded Motion Constants Corresponding to the Oldroyd 6-Constant Model

The Oldroyd and Giesekus models presented in §7.3 can easily be developed into a retarded-motion expansion by successive substitution. We illustrate the procedure here for the Oldroyd 6-constant model with $\lambda_6 = \lambda_7 = 0$.

a. Recognize that the first-order approximation to the stress in Eq. 7.3-2 is $\boldsymbol{\tau}_1 = -\eta_0\boldsymbol{\gamma}_{(1)}$ so that successive approximations to $\boldsymbol{\tau}$ are conveniently given by

$$\begin{aligned}\boldsymbol{\tau}_k = &-\eta_0[\boldsymbol{\gamma}_{(1)} + \lambda_2\boldsymbol{\gamma}_{(2)} + \lambda_4\boldsymbol{\gamma}_{(1)}^2] - \lambda_1\boldsymbol{\tau}_{k-1(1)} \\ &-\tfrac{1}{2}\lambda_3\{\boldsymbol{\tau}_{k-1}\cdot\boldsymbol{\gamma}_{(1)} + \boldsymbol{\gamma}_{(1)}\cdot\boldsymbol{\tau}_{k-1}\} - \tfrac{1}{2}\lambda_5(\text{tr}\,\boldsymbol{\tau}_{k-1})\boldsymbol{\gamma}_{(1)}\end{aligned} \tag{7B.6-1}$$

[3] M. C. Williams and R. B. Bird, *Phys. Fluids*, **5**, 1126–1127 (1962); the oscillatory normal stresses were given incorrectly in that publication, but were corrected in *Ind. Eng. Chem. Fundam.*, **3**, 42–49 (1964).

[4] See M. C. Williams, *Chem. Eng. Sci.*, **20**, 693–702 (1965), Figs. 4a and b.

b. Show then that τ_2 is

$$\tau_2 = -\eta_0[\gamma_{(1)} - (\lambda_1 - \lambda_2)\gamma_{(2)} - (\lambda_3 - \lambda_4)\gamma_{(1)}^2] \tag{7B.6-2}$$

c. Repeat the iteration to obtain the third-order expansion coefficients given in Table 6.2-2. In obtaining these coefficients it is necessary to use the Cayley-Hamilton theorem.

7B.7 Relation between Ψ_1 and η^-

The following equation has been found to be valid for a dilute suspension of rigid dumbbells as well as for dilute solutions of chainlike bead-spring models (see Example 15.4-1):

$$\Psi_1(\dot{\gamma}) = 2\int_0^\infty \eta^-(t, \dot{\gamma})dt \tag{7B.7-1}$$

Does this result hold for

a. The convected Jeffreys model?

b. The White-Metzner model?

c. The Oldroyd 4-constant model?

For part **(c)** you will need η^- from Problem 7D.1. What conclusions can you draw from these results?

7B.8 Steady Shearfree Flow of the Giesekus Model

a. Show that for the Giesekus model in a steady shearfree flow the three normal stresses are given by

$$aT_{pxx}^2 - (1 + (1 + b)\chi)T_{pxx} + (1 - \Lambda)(1 + b)\chi = 0 \tag{7B.8-1}$$

$$aT_{pyy}^2 - (1 + (1 - b)\chi)T_{pyy} + (1 - \Lambda)(1 - b)\chi = 0 \tag{7B.8-2}$$

$$aT_{pzz}^2 - (1 - 2\chi)T_{pzz} - 2(1 - \Lambda)\chi = 0 \tag{7B.8-3}$$

in which the following dimensionless quantities have been used: $\mathbf{T}_p = \tau_p/(\eta_0/\lambda_1)$, $\chi = \lambda_1\dot{\varepsilon}$, $\Lambda = \lambda_2/\lambda_1$, and $a = \alpha/(1 - \Lambda)$.

b. Solve these equations and obtain results for $\bar{\eta}_1$ and $\bar{\eta}_2$. In order to choose the correct roots from Eqs. 7B.8-1 through 3, require that the results simplify properly in the limit as $\alpha \to 0$.

c. Show that for steady elongational flow ($b = 0$) the following asymptotes hold when $\Lambda = 0$:

$$\frac{\bar{\eta}}{\eta_0} \sim \frac{2}{\alpha} \quad \text{as } \lambda_1\dot{\varepsilon} \to \infty \tag{7B.8-4}$$

$$\frac{\bar{\eta}}{\eta_0} \sim \frac{1}{\alpha} \quad \text{as } \lambda_1\dot{\varepsilon} \to -\infty \tag{7B.8-5}$$

7B.9 Eccentric-Disk Rheometer Flow

The eccentric-disk rheometer consists of two parallel disks, both of which rotate with a constant angular velocity W. The axes of rotation of the disks are separated by a distance a, and the gap between the disks is b (see Fig. 3B.1). The flow in this system may be reasonably well described by the velocity distribution

$$v_x = -W(y - Az); \quad v_y = Wx; \quad v_z = 0 \tag{7B.9-1}$$

in which $A = a/b$.

a. Find the tensors ∇v, $(\nabla v)^\dagger$, and $\gamma_{(1)}$ for this flow. Note that $\gamma_{(1)}$ is independent of position and time, so that it can be concluded that τ is constant throughout the gap; therefore $D\tau/Dt$ vanishes.

b. Display the convected Maxwell model in matrix form for this flow.

c. Show that this model gives

$$\left(-\frac{\tau_{xz}}{AW}\right) = \eta_0 \frac{1}{1 + \lambda_1^2 W^2} \tag{7B.9-2}$$

$$\left(-\frac{\tau_{yz}}{AW}\right) = \eta_0 \frac{\lambda_1 W}{1 + \lambda_1^2 W^2} \tag{7B.9-3}$$

d. Compare the results of **(c)** with Eqs. 7.2-10 and 11 with $\lambda_2 = 0$ (or Eqs. 5.3-8 and 9 with one term in the sum). What do you conclude? It is shown in Example 10.1-2 that a model-independent result of this sort can be obtained in the limit that $A \to 0$—that is, in the limit of small deformation gradients.

7B.10 Radial Flow between Two Lubricated Disks[5]

A high-viscosity polymer flows radially inward in the space between two parallel porous circular disks as shown in Fig. 7B.10. The disk surfaces are lubricated by injection of a small amount of low-viscosity liquid through the disks, so that the polymer fluid velocity profiles are roughly as shown in the figure. Find the relation between the volume flow rate and the pressure drop between the outer radius R_o and the inner radius R_i. Use the convected Maxwell model.

a. Use the continuity equation to get the velocity distribution $v_r = -C/r$, where $C = Q/2\pi B$ is a constant of integration.

b. Show next that the convected Maxwell model gives the following expressions for τ_{rr} and $\tau_{\theta\theta}$:

$$r\frac{d\tau_{rr}}{dr} - \left(\frac{r^2}{C\lambda_1} - 2\right)\tau_{rr} = \frac{2\eta_0}{\lambda_1} \tag{7B.10-1}$$

$$r\frac{d\tau_{\theta\theta}}{dr} - \left(\frac{r^2}{C\lambda_1} + 2\right)\tau_{\theta\theta} = -\frac{2\eta_0}{\lambda_1} \tag{7B.10-2}$$

Then rewrite these equations in terms of the dimensionless variables: $x = r^2/2\lambda_1 C$, $T_{rr} = \tau_{rr}\lambda_1/\eta_0$, $T_{\theta\theta} = \tau_{\theta\theta}\lambda_1/\eta_0$.

c. Solve the differential equations in **(b)**, with the boundary conditions $T_{rr} = T_{rr,o}$ and $T_{\theta\theta} = T_{\theta\theta,o}$ at $r = R_o$ (or $x = x_o$) to get

$$T_{rr} = -x^{-1} + C_1 x^{-1} e^x \tag{7B.10-3}$$

$$C_1 = x_o e^{-x_o}(T_{rr,o} + x_o^{-1}) \tag{7B.10-4}$$

$$T_{\theta\theta} = 1 - xe^x E_1(x) + C_2 x e^x \tag{7B.10-5}$$

$$C_2 = x_o^{-1} e^{-x_o}[T_{\theta\theta,o} - 1 + x_o e^{x_o} E_1(x_o)] \tag{7B.10-6}$$

in which C_1 and C_2 are constants of integration and $E_1(x) = -Ei(-x) = \int_x^\infty e^{-x} x^{-1}\, dx$.

d. Next use the r-component of the equation of motion in the form $r\,d(p + \tau_{rr})/dr = -(\tau_{rr} - \tau_{\theta\theta})$ to get

$$P + T_{rr} = \tfrac{1}{2}\{-x^{-1} + C_1[x^{-1}e^x - Ei(x)] - e^x E_1(x) + C_2 e^x\} + C_3 \tag{7B.10-7}$$

$$C_3 = P_o + \tfrac{1}{2}T_{rr,o}[1 + x_o e^{-x_o} Ei(x_o)] + \tfrac{1}{2}e^{-x_o} Ei(x_o) - \tfrac{1}{2}x_o^{-1} T_{\theta\theta,o} + \tfrac{1}{2}x_o^{-1} \tag{7B.10-8}$$

[5] D. K. Gartling, *J. Non-Newtonian Fluid Mech.*, **17**, 203-231 (1985).

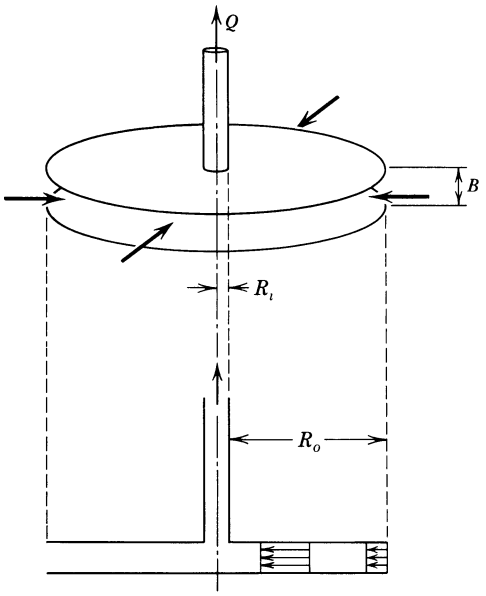

FIGURE 7B.10. Inward flow between two parallel porous circular disks through which a low-viscosity liquid lubricant is injected.

in which $Ei(x) = \int_{-\infty}^{x} e^x x^{-1}\, dx$ is the standard "exponential integral" function, $P = p\lambda_1/\eta_0$, and P_o is the dimensionless pressure at $r = R_o$.

e. The "pressure drop" desired now is $(P + T_{rr})_o - (P + T_{rr})_i$. However, when we obtain this expression, we find that it contains the unmeasurable quantities $T_{rr,o}$ and $T_{\theta\theta,o}$. Since, at the outer rim the flow is very slow, these quantities may at a lowest level of approximation be set equal to zero, and then P_o can be equated to $p_{\text{atm}}\lambda_1/\eta_o$. An improved approximation can be obtained by using the retarded-motion expansion equivalent to the Maxwell model (see Eq. 7B.6-2 with $\lambda_2 = \lambda_3 = \lambda_4 = 0$); since the flow field is known at $r = R_o$, the $\boldsymbol{\gamma}_{(1)}$ and $\boldsymbol{\gamma}_{(2)}$ in Eq. 7B.6-2 can be evaluated in terms of known quantities.

7C.1 Arbitrary Shearing and Shearfree Flows of the Convected Jeffreys Model

a. Show that the differential equations, Eqs. 7.2-3 and 6, for the stresses in a convected Jeffreys model undergoing arbitrary time-dependent shear flow can be integrated to give

$$\begin{aligned}\tau_{yx} &= -\eta_0 \frac{\lambda_2}{\lambda_1}\dot{\gamma}_{yx}(t) - \frac{\eta_0}{\lambda_1}\int_{-\infty}^{t}\left[\left(1-\frac{\lambda_2}{\lambda_1}\right)e^{-(t-t')/\lambda_1}\dot{\gamma}_{yx}(t')\right]dt' \\ &= -\eta_0 \frac{\lambda_2}{\lambda_1}\dot{\gamma}_{yx}(t) + \frac{\eta_0}{\lambda_1^2}\int_{-\infty}^{t}\left[\left(1-\frac{\lambda_2}{\lambda_1}\right)e^{-(t-t')/\lambda_1}\gamma_{yx}(t,t')\right]dt' \qquad \text{(7C.1-1)}\end{aligned}$$

$$\begin{aligned}\tau_{xx} &= -2\frac{\eta_0}{\lambda_1}\int_{-\infty}^{t}\int_{-\infty}^{t'}\left[\left(1-\frac{\lambda_2}{\lambda_1}\right)e^{-(t-t'')/\lambda_1}\dot{\gamma}_{yx}(t'')\dot{\gamma}_{yx}(t')\right]dt''\,dt' \\ &= -\frac{\eta_0}{\lambda_1^2}\int_{-\infty}^{t}\left[\left(1-\frac{\lambda_2}{\lambda_1}\right)e^{-(t-t')/\lambda_1}\gamma_{yx}^2(t,t')\right]dt' \qquad \text{(7C.1-2)}\end{aligned}$$

where $\gamma_{yx}(t,t') = \int_{t}^{t'}\dot{\gamma}_{yx}(t'')\,dt''$ is the shear strain and the stress tensor is taken to be zero at $t = -\infty$.

b. Use the integral results of part **(a)** to obtain the material functions η', η'', η^+, Ψ_1^+, η^-, and Ψ_1^- that were given in §7.2.

c. Assume that a convected Jeffreys fluid is at equilibrium prior to time $t = 0$. For $t \geq 0$ the fluid is subjected to a shearfree flow with arbitrary $\dot{\varepsilon}$ and b. Show that the differential equations that describe this problem, Eqs. 7.2-19 and 20 can be integrated to give

$$\tau_{xx} = \eta_0(1+b)\frac{\lambda_2}{\lambda_1}\dot{\varepsilon}(t) + \frac{\eta_0(1+b)}{\lambda_1}\left(1-\frac{\lambda_2}{\lambda_1}\right)\int_0^t e^{-(t-t')/\lambda_1}e^{+(1+b)\varepsilon(t,t')}\dot{\varepsilon}(t')dt' \tag{7C.1-3}$$

$$\tau_{zz} = -2\eta_0\frac{\lambda_2}{\lambda_1}\dot{\varepsilon}(t) - \frac{2\eta_0}{\lambda_1}\left(1-\frac{\lambda_2}{\lambda_1}\right)\int_0^t e^{-(t-t')/\lambda_1}e^{-2\varepsilon(t,t')}\dot{\varepsilon}(t')dt' \tag{7C.1-4}$$

in which $\varepsilon(t, t') = \int_t^{t'} \dot{\varepsilon}(t'')\,dt''$ is the Hencky strain between times t and t'. The normal stress τ_{yy} is given by Eq. 7C.1-3 with $(1 + b)$ replaced everywhere by $(1 - b)$.

d. Show how the results from part **(c)** can be used to obtain the shearfree flow material functions presented in Example 7.2-2.

7C.2 Tube Flow of an Oldroyd 8-Constant Fluid[6,7]

Obtain the expression for the volume flow rate vs. pressure drop for the flow of the Oldroyd 8-constant fluid through a circular pipe. Use the abbreviation σ_i for the groups of time constants as given in Table 7.3-3:

$$\sigma_i = \lambda_i(\lambda_3+\lambda_5) + \lambda_{i+2}(\lambda_1-\lambda_3-\lambda_5) + \lambda_{i+5}(\lambda_1-\lambda_3-\tfrac{3}{2}\lambda_5) \tag{7C.2-1}$$

Also use the following dimensionless quantities:

$$\Omega = \frac{3\sqrt{\sigma_1}Q}{\pi R^3} \tag{7C.2-2}$$

$$X = \sigma_1\dot{\gamma}_R^2 \qquad \left(\dot{\gamma}_R = -\left.\frac{dv_z}{dr}\right|_{r=R}\right) \tag{7C.2-3}$$

$$n = \frac{\sigma_2}{\sigma_1} \tag{7C.2-4}$$

Show that

$$\Omega = \left[1 - \frac{1}{2X^2}\left(\frac{1+X}{1+nX}\right)^3 f\right]\sqrt{X} \tag{7C.2-5}$$

in which

$$f = \tfrac{1}{2}n^3X^2 - 3n^2(n-1)X + 3n(n-1)(2n-1)\ln(1+X) - \tfrac{1}{2}X\left(\frac{n-1}{1+X}\right)^2[6n+(7n-1)X] \tag{7C.2-6}$$

[6] M. C. Williams and R. B. Bird, *AIChE J.*, **8**, 378–382 (1962).
[7] K. Walters, *Arch. Rat. Mech. Anal.*, **9**, 411–414 (1962).

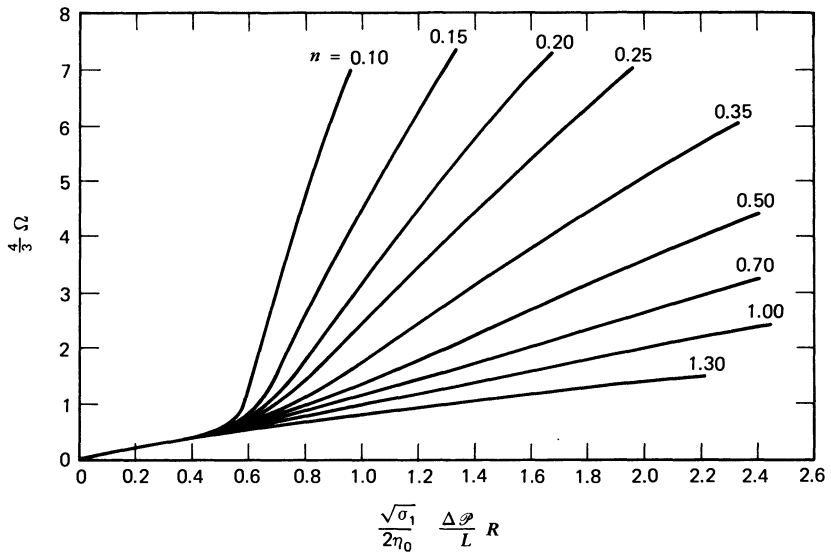

FIGURE 7C.2. Volumetric flow rate versus pressure difference for an 8-constant Oldroyd liquid in a cylindrical pipe, for various values of $n = \sigma_2/\sigma_1$. The quantities σ_i and Ω are defined in Eqs. 7C.2-1 and 2. [M. C. Williams and R. B. Bird, *AIChE J.*, **8**, 378–382 (1962).]

This gives us, in dimensionless form, the volume rate of flow in terms of the wall shear rate. Show further that the shear rate may be eliminated in favor of the pressure drop through the system by means of the relation

$$\frac{\sqrt{\sigma_1}}{2\eta_0}\frac{\Delta\mathscr{P}}{L}R = \left(\frac{1+nX}{1+X}\right)\sqrt{X} \tag{7C.2-7}$$

To get Ω in terms of $\Delta\mathscr{P}/L$, Eqs. 7C.2-5, 6, and 7 must be combined. When this is done numerically the plot in Fig. 7C.2 is obtained. To what extent does the result appear to be realistic?

7C.3 Spriggs-Bird Two Constant Model

Spriggs and Bird[8] considered the following nonlinear generalization of Eq. 5C.1-1:

$$\left(1 + \sum_{n=1}^{\infty} a_n \mathscr{F}^n\right)\boldsymbol{\tau} = -\eta_0\left(1 + \sum_{n=1}^{\infty} b_n \mathscr{F}^n\right)\dot{\boldsymbol{\gamma}} \tag{7C.3-1}$$

in which

$$\mathscr{F}\boldsymbol{\tau} = \boldsymbol{\tau}_{(1)} + \tfrac{1}{3}(\boldsymbol{\tau}:\dot{\boldsymbol{\gamma}})\boldsymbol{\delta} \tag{7C.3-2}$$

By choosing a_n and b_n in a certain way (see Eq. 5C.1-7), the linear viscoelastic material functions of the Rouse theory can be very nearly reproduced.

[8] T. W. Spriggs and R. B. Bird, *Ind. Eng. Chem. Fundam.*, **4**, 182–186 (1965). See also R. Roscoe, *Br. J. Appl. Phys.*, **15**, 1095–1101 (1964), for a somewhat more general model.

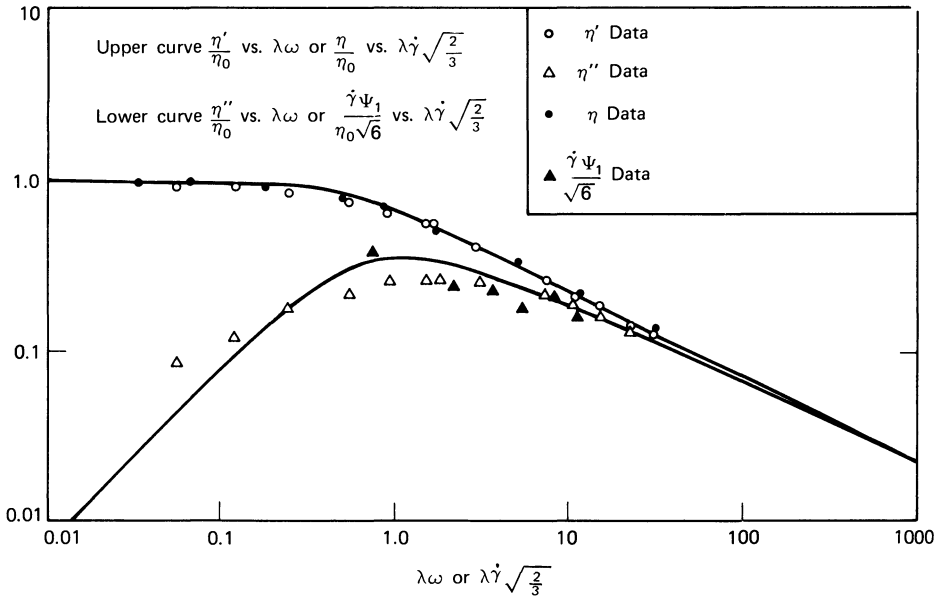

FIGURE 7C.3. Solid curves are functions obtained from the Spriggs-Bird model. The experimental data for η, η', and η'' for 5% polyisobutylene in decalin are taken from T. W. Dewitt, H. Markovitz, F. J. Padden, and L. J. Zapas, *J. Colloid Sci.*, **10**, 174–188 (1955), and the normal stress data are those of H. Markovitz and R. B. Williamson, *Trans. Soc. Rheol.*, **1**, 25–36 (1957). [Reprinted with permission from T. W. Spriggs and R. B. Bird, *Ind. Eng. Chem. Fundam.*, **4**, 182–186 (1965). Copyright by the American Chemical Society.]

Show that Eq. 7C.3-1 leads to the following expressions for η and Ψ_1

$$\frac{\eta}{\eta_0} = \frac{PR + QS}{R^2 + S^2} \tag{7C.3-3}$$

$$\frac{\Psi_1\dot{\gamma}}{\sqrt{6}\eta_0} = \frac{PS - QR}{R^2 + S^2} \tag{7C.3-4}$$

in which P, Q, R, and S are functions given in Eqs. 5C.1-3 to 6, except that the argument ω is replaced by $\sqrt{\frac{2}{3}}\dot{\gamma}$. This suggests that η and η' should superpose if a "shift factor" of $\sqrt{2/3}$ is applied, and that a similar superposition of η'' and $\Psi_1\dot{\gamma}/\sqrt{6}$ should be possible. One comparison with experimental data is given in Fig. 7C.3; there Eqs. 5C.1-9 and 10 are used for η' and η'', and the same equations with ω replaced by $\sqrt{2/3}\dot{\gamma}$ are used for η and $\Psi_1\dot{\gamma}\sqrt{6}$, respectively. The only parameters are the zero-shear-rate viscosity η_0 and the time constant λ.

7C.4 A Constitutive Equation Suggested from a Theory of Suspensions

From a kinetic theory study of a dilute suspension of nearly spherical rigid particles, Leal and Hinch[9] have deduced a constitutive equation of the form

$$\boldsymbol{\tau} = -c_1\dot{\boldsymbol{\gamma}} - c_2\boldsymbol{\alpha} - c_3\{\dot{\boldsymbol{\gamma}}\cdot\boldsymbol{\alpha} + \boldsymbol{\alpha}\cdot\dot{\boldsymbol{\gamma}} - \tfrac{2}{3}(\boldsymbol{\alpha}:\dot{\boldsymbol{\gamma}})\boldsymbol{\delta}\} \tag{7C.4-1}$$

[9] L. G. Leal and E. J. Hinch, *J. Fluid Mech.*, **55**, 745–765 (1972); Eqs. 7C.4-1 and 2 are a special case of a model by G. L. Hand, *J. Fluid Mech.*, **13**, 33–46 (1962). For an extended discussion of dilute suspension rheology and the Hand equation see D. Barthés-Biesel and A. Acrivos, *Int. J. Multiphase Flow*, **1**, 1–24 (1973).

in which $\boldsymbol{\alpha}$ is a "structure tensor" that obeys the relation

$$\boldsymbol{\alpha}_{(1)} + c_4\boldsymbol{\alpha} + \tfrac{1}{2}\{\dot{\boldsymbol{\gamma}}\cdot\boldsymbol{\alpha} + \boldsymbol{\alpha}\cdot\dot{\boldsymbol{\gamma}}\} = c_5\dot{\boldsymbol{\gamma}} \tag{7C.4-2}$$

The c_i are positive constants related to the particle shape and concentration. What properties does this constitutive equation have?

7D.1 Stress Growth and Stress Relaxation for the 4-Constant Oldroyd Model

a. For the stress relaxation after cessation of a steady shear flow with shear rate $\dot{\gamma}_0$, show that the constitutive equation, for $t > 0$, simplifies to

$$\tau_{xx} + \lambda_1 \frac{d}{dt}\tau_{xx} = 0 \tag{7D.1-1}$$

$$\tau_{yx} + \lambda_1 \frac{d}{dt}\tau_{yx} = -\eta_0\lambda_2 \frac{d}{dt}\dot{\gamma}_0[1 - H(t)] \tag{7D.1-2}$$

in which $H(t)$ is the Heaviside unit step function, and $dH/dt = \delta(t)$. Solve these equations using Laplace transforms; make use of the viscometric functions tabulated in Table 7.3-3 to supply the initial conditions for τ_{xx} and τ_{yx}. Obtain, finally,

$$\eta^- = \eta_0\left(\frac{1 + \lambda_2\lambda_5\dot{\gamma}_0^2}{1 + \lambda_1\lambda_5\dot{\gamma}_0^2} - \frac{\lambda_2}{\lambda_1}\right)e^{-t/\lambda_1} \tag{7D.1-3}$$

$$\Psi_1^- = 2\eta_0\left(\frac{\lambda_1 - \lambda_2}{1 + \lambda_1\lambda_5\dot{\gamma}_0^2}\right)e^{-t/\lambda_1} \tag{7D.1-4}$$

To what extent do these material functions describe the experimental data in Chapter 3?

b. Use Laplace transforms to do a similar analysis for stress growth, when a shear rate $\dot{\gamma}_0$ is suddenly applied at time $t = 0$. Show that

$$\eta^+ = \eta_0\left[\left(\frac{\lambda_2}{\lambda_1} - F\right)e^{-t/\lambda_1}\cos \Gamma t/\lambda_1 + (1 - F)\Gamma^{-1}e^{-t/\lambda_1}\sin \Gamma t/\lambda_1 + F\right] \tag{7D.1-5}$$

where $\Gamma = \sqrt{\lambda_1\lambda_5}\dot{\gamma}_0$ and $F = (1 + \lambda_2\lambda_5\dot{\gamma}_0^2)/(1 + \lambda_1\lambda_5\dot{\gamma}_0^2)$. How does η^+ behave as $t \to \infty$ and as $t \to 0$? Does the function η^+ as a function of t go through a maximum similar to that seen in the experimental data? Does the maximum shift to shorter times as $\dot{\gamma}_0$ increases?

CHAPTER 8

SINGLE-INTEGRAL CONSTITUTIVE EQUATIONS

In this chapter we turn our attention to single-integral constitutive equations. The starting point is the general linear viscoelastic model. Since this model is constructed specifically for flows with small displacement gradients, we need to generalize it to describe flows with large displacement gradients. Hence we start in §8.1 with a description of fluid particle paths and define the displacement functions that describe the motion of fluid particles in flow fields. Using the displacement functions we then define a set of finite strain tensors that can be used to formulate integral constitutive equations. Then in §8.2 we construct the general quasi-linear integral model with an arbitrary memory function. For a specific choice of the memory function the model is identical to the convected Jeffreys model (or Oldroyd-B model) presented in §7.2, but the form is such that the dependence of the stress at the present time on past configurations is illustrated more clearly. The proof of the equivalence of the two forms is postponed until Example 9.4-1. In §8.3 we modify the general quasi-linear model to obtain a nonlinear model providing an improved description of measured material functions In parallel with the previous chapter we consider in §8.4 flow problems in one spatial variable, and in §8.5 flow problems in two or three spatial variables. Finally in §8.6 we discuss the limitations of single-integral models and give recommendations for their use.

§8.1 THE FINITE STRAIN TENSORS

In §§6.1 and 7.1 where we introduced the tensors $\boldsymbol{\gamma}_{(n)}$ and $\boldsymbol{\tau}_{(1)}$, we described the fluid motion by means of the velocity field $\boldsymbol{v}(\boldsymbol{r}, t)$. In this section, where we introduce the finite strain tensors, we make use of an alternative description of the fluid motion in which the motions of fluid particles are given; that is, we select a fluid particle and then describe its trajectory through the three-dimensional space occupied by the fluid.

Consider a fluid particle moving as part of a fluid continuum. At some past time t' the particle has position $\boldsymbol{r}'$, and at the present time t the particle has position $\boldsymbol{r}$. The designation $\boldsymbol{r}, t$ (or $\boldsymbol{r}', t'$) then uniquely specifies the particle and is referred to as a "particle label." The motion of the particle may then be described by the functions

$$\boldsymbol{r}' = \boldsymbol{r}'(\boldsymbol{r}, t, t') \quad \text{or} \quad x_i' = x_i'(x, t, t') \tag{8.1-1}$$

which give the past position $\boldsymbol{r}'$ of the particle $\boldsymbol{r}, t$ as a function of time t', or by the functions

$$\boldsymbol{r} = \boldsymbol{r}(\boldsymbol{r}', t', t) \quad \text{or} \quad x_i = x_i(x', t', t) \tag{8.1-2}$$

which give the present position $\boldsymbol{r}$ of the particle $\boldsymbol{r}', t'$ as a function of time t. The equations have been given also in terms of the Cartesian coordinates (x_1, x_2, x_3) of $\boldsymbol{r}$ and (x'_1, x'_2, x'_3) of $\boldsymbol{r}'$; for the sake of brevity the sets of coordinates are denoted simply by x and x' respectively. The functions on the right side of Eqs. 8.1-1 and 2 are called the *displacement functions.* In these functions the first two arguments identify the particle and the last argument indicates the time dependence. The displacement functions for all particles and all times completely specify the motion of the fluid. Notice that in Eq. 8.1-1 the symbol $\boldsymbol{r}'$(or x'_i) appears with two different meanings: on the right the symbol denotes a function and on the left the symbol denotes the value of the function. Similar remarks apply to $\boldsymbol{r}$ (or x_i) in Eq. 8.1-2.

From a mathematical point of view $\boldsymbol{r}(\boldsymbol{r}', t', t)$ and $\boldsymbol{r}'(\boldsymbol{r}, t, t')$ are really the same function of the arguments in the indicated order. For this reason there is strictly speaking no reason to use separate symbols for the functions as long as the arguments are always included. However we shall keep the prime on the function $\boldsymbol{r}'(\boldsymbol{r}, t, t')$. This allows us to drop the list of arguments when no confusion can arise.

From the displacement functions we now define two *displacement gradient tensors* $\boldsymbol{\Delta}(\boldsymbol{r}, t, t')$ and $\mathbf{E}(\boldsymbol{r}, t, t')$. These are defined in terms of their Cartesian components $\Delta_{ij}(\boldsymbol{r}, t, t')$ and $E_{ij}(\boldsymbol{r}, t, t')$ by

$$\Delta_{ij}(\boldsymbol{r}, t, t') = \frac{\partial x'_i(x, t, t')}{\partial x_j} \tag{8.1-3}$$

$$E_{ij}(\boldsymbol{r}, t, t') = \frac{\partial x_i(x', t', t)}{\partial x'_j} \tag{8.1-4}$$

The Δ_{ij} are measures of the displacements at time t' relative to the positions at time t, whereas E_{ij} are measures of the displacements at time t relative to the positions at time t'. The tensors $\boldsymbol{\Delta}(\boldsymbol{r}, t, t')$ and $\mathbf{E}(\boldsymbol{r}, t, t')$ are inverse to each other; that is, in Cartesian coordinates[1]

$$\sum_m \Delta_{im} E_{mj} = \delta_{ij} \tag{8.1-5}$$

as may be seen from the definitions. In addition it may be shown (see Problem 8D.2) that for an incompressible fluid $\det(\Delta_{ij}) = \det(E_{ij}) = 1$. The displacement gradient tensors are generally not symmetrical and contain information about both deformation and rotation in the neighborhood of a given particle. They are therefore not immediately suitable for use in constitutive equations. In terms of the displacement gradient tensors, however, we can

[1]From the definitions in Eqs. 8.1-3 and 4 we could write $E_{ij}(\boldsymbol{r}, t, t') = \Delta_{ij}(\boldsymbol{r}', t', t)$ and $\Delta_{ij}(\boldsymbol{r}, t, t') = E_{ij}(\boldsymbol{r}', t', t)$ so that instead of having two separate symbols $\boldsymbol{\Delta}$ and $\mathbf{E}$ we could use just one symbol and then keep careful track of the order of the arguments. However, whenever we use $\boldsymbol{\Delta}$ and $\mathbf{E}$ we assume that the arguments are in the order given in the definitions in Eqs. 8.1-3 and 4 with t indicating the present state and t' a past state, and never in the reverse order. The use of two separate symbols enables us then to omit the arguments in situations when no confusion can occur, as we have done in Eq. 8.1-5; in other situations we retain the arguments t and t' but omit the $\boldsymbol{r}$.

We have used the term "displacement gradient tensors" here for both $\boldsymbol{\Delta}$ and $\mathbf{E}$ and, in Chapter 5, for $\nabla\boldsymbol{u}$. These three tensors are very closely related: $\boldsymbol{\Delta} = \mathbf{E}^{-1} = \nabla\boldsymbol{u} + \boldsymbol{\delta}$. Calling all three tensors by the same name will not cause confusion, since generally a specific symbol will be used. However, when we say that linear viscoelastic formulas are applicable "in the limit of vanishingly small displacement gradients," we are referring to $\nabla\boldsymbol{u}$, rather than $\boldsymbol{\Delta}$ or $\mathbf{E}$.

define two *finite strain tensors* suitable for this purpose. These are the *Cauchy strain tensor*, $\mathbf{B}^{-1}(\boldsymbol{r}, t, t')$:

$$\mathbf{B}^{-1}(\boldsymbol{r}, t, t') = \{\boldsymbol{\Delta}^{\dagger} \cdot \boldsymbol{\Delta}\} \quad \text{or} \quad B^{-1}_{ij}(\boldsymbol{r}, t, t') = \sum_m \frac{\partial x'_m}{\partial x_i} \frac{\partial x'_m}{\partial x_j} \tag{8.1-6}$$

and the *Finger strain tensor*, $\mathbf{B}(t, t')$:

$$\mathbf{B}(\boldsymbol{r}, t, t') = \{\mathbf{E} \cdot \mathbf{E}^{\dagger}\} \quad \text{or} \quad B_{ij}(\boldsymbol{r}, t, t') = \sum_m \frac{\partial x_i}{\partial x'_m} \frac{\partial x_j}{\partial x'_m} \tag{8.1-7}$$

From the properties of the displacement gradient tensors, we see that $\mathbf{B}$ and $\mathbf{B}^{-1}$ are indeed inverse to each other as implied by the notation, and further that for incompressible fluids their determinants are unity. Additional properties of $\mathbf{B}$ and $\mathbf{B}^{-1}$ are:

- **i.** They are symmetric (as seen from their definitions).
- **ii.** They are positive definite (Problem 8B.3).
- **iii.** They describe the deformation, from time t' to time t, of the material in the neighborhood of the given particle with a significance independent of superposed rigid rotations (Example 8.1-2 and §9.3).
- **iv.** They reduce to the unit tensor if the displacement from t' to t involves no deformation, that is, if it is a translation plus a rotation (Example 8.1-2).

The last property listed above leads us to define two closely related finite strain tensors $\boldsymbol{\gamma}^{[0]}$ and $\boldsymbol{\gamma}_{[0]}$, which are zero for a rigid body motion:

$$\boldsymbol{\gamma}^{[0]}(\boldsymbol{r}, t, t') = \{\boldsymbol{\Delta}^{\dagger} \cdot \boldsymbol{\Delta}\} - \boldsymbol{\delta}; \quad \gamma^{[0]}_{ij}(\boldsymbol{r}, t, t') = \sum_m \frac{\partial x'_m}{\partial x_i} \frac{\partial x'_m}{\partial x_j} - \delta_{ij} \tag{8.1-8}$$

$$\boldsymbol{\gamma}_{[0]}(\boldsymbol{r}, t, t') = \boldsymbol{\delta} - \{\mathbf{E} \cdot \mathbf{E}^{\dagger}\}; \quad \gamma_{[0]ij}(\boldsymbol{r}, t, t') = \delta_{ij} - \sum_m \frac{\partial x_i}{\partial x'_m} \frac{\partial x_j}{\partial x'_m} \tag{8.1-9}$$

To distinguish these tensors from those defined in Eqs. 8.1-6 and 7, we call $\boldsymbol{\gamma}^{[0]}$ and $\boldsymbol{\gamma}_{[0]}$ the *relative (finite) strain tensors.*[2] For small displacement gradients both of these tensors reduce to the infinitesimal strain tensor $\boldsymbol{\gamma}$ encountered in Chapter 5 (see Example 9.3-1).

The above component forms of the displacement gradient tensors and the strain tensors are valid in rectangular (Cartesian) coordinates only. In Table B.5 through B.7 of Appendix B, we give component forms of $\boldsymbol{\Delta}$, $\mathbf{E}$, $\boldsymbol{\gamma}^{[0]}$, $\boldsymbol{\gamma}_{[0]}$ for general deformations in rectangular, cylindrical, and spherical coordinate systems.[3] In addition in Appendix C we give expressions for $\boldsymbol{\Delta}$, $\mathbf{E}$, $\boldsymbol{\gamma}^{[0]}$ and $\boldsymbol{\gamma}_{[0]}$ in rectangular coordinates worked out specifically for simple shear flows and for shearfree flows. In Example 8.1-1 at the end of this section we illustrate the construction of some of the entries in Appendix C. Whenever components of $\boldsymbol{\Delta}$, $\mathbf{E}$, $\boldsymbol{\gamma}^{[0]}$, or $\boldsymbol{\gamma}_{[0]}$ are needed, the reader will find the tabulations in Appendices B and C helpful.

[2] J. G. Oldroyd, *J. Non-Newtonian Fluid Mech.*, **14**, 9–46 (1984), see Eq. 55.

[3] For the corresponding formulas for nonorthogonal coordinate systems, see footnote f of Table 9.3-1.

This completes the definition of the kinematic quantities needed in the chapter. Note that the finite strain tensors are defined in terms of the displacement functions and not in terms of the velocity field. Indeed the nonlinear integral models to be introduced in this chapter give explicit expressions for the stress tensor in terms of the displacement functions. Fluid mechanical problems with integral constitutive models may be formulated and solved just in terms of the displacement functions. One may then subsequently construct the velocity field if so desired. This is in contrast with all nonlinear models of Chapters 4, 6, and 7, in which the stresses are related directly to the velocity field, and for which one most naturally will formulate and solve flow problems for the velocity field. For completeness we now proceed to relate the displacement functions to (the history of) the velocity field.

Starting from the displacement functions in Eqs. 8.1-1 and 2 we define the velocity of a fluid particle at time t' and at time t by

$$\boldsymbol{w}'(\boldsymbol{r}, t, t') = \frac{\partial}{\partial t'} \boldsymbol{r}'(\boldsymbol{r}, t, t') \tag{8.1-10}$$

$$\boldsymbol{w}(\boldsymbol{r}', t', t) = \frac{\partial}{\partial t} \boldsymbol{r}(\boldsymbol{r}', t', t) \tag{8.1-11}$$

The spatial velocity field $\boldsymbol{v}$ at times t' and t is equal to the particle velocities at those instants, that is

$$\boldsymbol{v}'(\boldsymbol{r}', t') = \boldsymbol{w}'(\boldsymbol{r}, t, t') \tag{8.1-12}$$

where $\boldsymbol{r}'$ is given by Eq. 8.1-1 and

$$\boldsymbol{v}(\boldsymbol{r}, t) = \boldsymbol{w}(\boldsymbol{r}', t', t) \tag{8.1-13}$$

where $\boldsymbol{r}$ is given by Eq. 8.1-2. When use is made of the displacement function $\boldsymbol{r}'(\boldsymbol{r}, t, t')$ in Eq. 8.1-1, then Eqs. 8.1-10 and 12 give explicit recipes for the construction of the particle velocity field $\boldsymbol{w}'(\boldsymbol{r}, t, t')$ and the spatial velocity field $\boldsymbol{v}(\boldsymbol{r}', t')$. Similarly given the displacement function $\boldsymbol{r}(\boldsymbol{r}', t', t)$, then $\boldsymbol{w}(\boldsymbol{r}', t', t)$ and $\boldsymbol{v}(\boldsymbol{r}, t)$ are constructed from Eqs. 8.1-11 and 13. Here again note that there is only one particle velocity function, with the first two arguments denoting the particle dependence and the last argument denoting the time dependence, so that the prime on $\boldsymbol{w}'$ in Eq. 8.1-12 merely indicates the time dependence. Similar remarks hold for the prime on $\boldsymbol{v}'$.

We now turn the problem around to show how the displacement functions may be determined from a given spatial velocity field. For this purpose insert $\boldsymbol{v}(\boldsymbol{r}, t)$ into Eq. 8.1-11 to obtain the initial value problem

$$\frac{\partial}{\partial t} \boldsymbol{r}(\boldsymbol{r}', t', t) = \boldsymbol{v}(\boldsymbol{r}, t) \tag{8.1-14}$$

to be solved with the initial condition that $\boldsymbol{r} = \boldsymbol{r}'$ at $t = t'$. The initial value problem for $\boldsymbol{r}'$ is obtained by interchanging primed and unprimed quantities in Eq. 8.1-14 and in the initial condition. For simple flow fields these equations can sometimes be solved analytically (see Examples 8.1-1 and 8.1-4 as well as Problems 8B.5 and 9D.1). In general, however, numerical methods must be used.

EXAMPLE 8.1-1 Evaluation of Kinematic Tensors

It is desired to calculate the kinematic tensors $\boldsymbol{\Delta}$, $\mathbf{E}$, $\mathbf{B}^{-1}$, $\mathbf{B}$, $\boldsymbol{\gamma}^{[0]}$ and $\boldsymbol{\gamma}_{[0]}$ for **(a)** simple shear flow (Eq. 3.1-1) and **(b)** shearfree flows (Eq. 3.1-3).

SOLUTION **(a)** For the simple shear flow $v_x = \dot{\gamma}_{yx}(t)y$, Eq. 8.1-14 for the displacement functions reads

$$\frac{\partial x}{\partial t} = \dot{\gamma}_{yx}(t)y; \quad \frac{\partial y}{\partial t} = 0; \quad \frac{\partial z}{\partial t} = 0 \tag{8.1-15}$$

The solution to these three equations subject to the condition that $(x, y, z) = (x', y', z')$ at $t = t'$ is

$$x = x' - \gamma_{yx}(t, t')y'; \quad y = y'; \quad z = z' \tag{8.1-16}$$

where $\gamma_{yx}(t, t') = \int_t^{t'} \dot{\gamma}_{yx}(t'')dt''$, and $\dot{\gamma}_{yx}$ is the velocity gradient. Then the matrix representations are easily found for the following tensors

$$\mathbf{E} = \begin{pmatrix} 1 & -\gamma_{yx} & 0 \\ 0 & 1 & 0 \\ 0 & 0 & 1 \end{pmatrix}; \quad \boldsymbol{\Delta} = \begin{pmatrix} 1 & \gamma_{yx} & 0 \\ 0 & 1 & 0 \\ 0 & 0 & 1 \end{pmatrix} \tag{8.1-17}$$

As a check on the calculations at this point we may verify that $\mathbf{E}$ and $\boldsymbol{\Delta}$ are inverse to one another by performing a matrix multiplication. By matrix multiplication we also find

$$\mathbf{B} = \begin{pmatrix} 1 + \gamma_{yx}^2 & -\gamma_{yx} & 0 \\ -\gamma_{yx} & 1 & 0 \\ 0 & 0 & 1 \end{pmatrix}; \quad \mathbf{B}^{-1} = \begin{pmatrix} 1 & \gamma_{yx} & 0 \\ \gamma_{yx} & 1 + \gamma_{yx}^2 & 0 \\ 0 & 0 & 1 \end{pmatrix} \tag{8.1-18}$$

Again at this point we may check the calculations by performing a matrix multiplication to verify that $\mathbf{B}$ and $\mathbf{B}^{-1}$ are inverse to one another, and by showing that they have determinants equal to unity. Finally we may form $\boldsymbol{\gamma}^{[0]} = \mathbf{B}^{-1} - \boldsymbol{\delta}$ and $\boldsymbol{\gamma}_{[0]} = \boldsymbol{\delta} - \mathbf{B}$ by using Eqs. 8.1-8 and 9 to obtain the entries in Appendix C. Note that the finite strain tensors contain components that are nonlinear in the displacement gradients.

(b) For shearfree flows, $v_x = -\frac{1}{2}\dot{\varepsilon}(1 + b)x$, $v_y = -\frac{1}{2}\dot{\varepsilon}(1 - b)y$, $v_z = \dot{\varepsilon}z$, Eq. 8.1-14 for the displacement functions reads

$$\frac{\partial x}{\partial t} = -\tfrac{1}{2}(1 + b)\dot{\varepsilon}(t)x; \quad \frac{\partial y}{\partial t} = -\tfrac{1}{2}(1 - b)\dot{\varepsilon}(t)y; \quad \frac{\partial z}{\partial t} = \dot{\varepsilon}(t)z \tag{8.1-19}$$

The solution subject to the condition that $(x, y, z) = (x', y', z')$ at $t = t'$ may be written

$$x = x'\lambda_x; \quad y = y'\lambda_y; \quad z = z'\lambda_z \tag{8.1-20}$$

where we have defined

$$\lambda_x = \exp\left[\tfrac{1}{2}(1 + b)\varepsilon(t, t')\right] \tag{8.1-21}$$

$$\lambda_y = \exp\left[\tfrac{1}{2}(1 - b)\varepsilon(t, t')\right] \tag{8.1-22}$$

$$\lambda_z = \exp\left[-\varepsilon(t, t')\right] \tag{8.1-23}$$

and $\varepsilon(t, t') = \int_t^{t'} \dot{\varepsilon}(t'')dt''$; this quantity is called the *Hencky strain.* The quantities λ_x, λ_y, λ_z are called the *principal elongation ratios.* If we imagine for example, that the fluid at the past time t' has the shape of a cube with unit dimensions and faces perpendicular to the coordinate axes, then this cube becomes distorted into the shape of a rectangular box with dimensions given by the principal elongation ratios at the present time t (see Fig. 3.1-3). The displacement gradient tensors become

$$\mathbf{E} = \begin{pmatrix} \lambda_x & 0 & 0 \\ 0 & \lambda_y & 0 \\ 0 & 0 & \lambda_z \end{pmatrix}; \quad \boldsymbol{\Delta} = \begin{pmatrix} \lambda_x^{-1} & 0 & 0 \\ 0 & \lambda_y^{-1} & 0 \\ 0 & 0 & \lambda_z^{-1} \end{pmatrix} \tag{8.1-24}$$

We see that the condition that $\mathbf{E}$ and $\boldsymbol{\Delta}$ have determinants equal to unity requires that the product of the principal elongation ratios be unity, in agreement with Eqs. 8.1-21 through 23. This condition corresponds to the fact that the above-mentioned cube is distorted into a box of the same volume. The finite strain tensors become

$$\mathbf{B} = \begin{pmatrix} \lambda_x^2 & 0 & 0 \\ 0 & \lambda_y^2 & 0 \\ 0 & 0 & \lambda_z^2 \end{pmatrix}; \quad \mathbf{B}^{-1} = \begin{pmatrix} \lambda_x^{-2} & 0 & 0 \\ 0 & \lambda_y^{-2} & 0 \\ 0 & 0 & \lambda_z^{-2} \end{pmatrix} \tag{8.1-25}$$

Again from these we may construct $\boldsymbol{\gamma}^{[0]} = \mathbf{B}^{-1} - \boldsymbol{\delta}$ and $\boldsymbol{\gamma}_{[0]} = \boldsymbol{\delta} - \mathbf{B}$ by using Eqs. 8.1-8 and 9 to obtain the entries in Appendix C.

EXAMPLE 8.1-2 Evaluation of Strain Tensors for a Steady Shear Flow with a Superposed Rotation

It is desired to evaluate the strain tensors $\mathbf{B}(\boldsymbol{r}, t, t')$ and $\mathbf{B}^{-1}(\boldsymbol{r}, t, t')$ at time $t = 0$ for a typical particle in the shear flow with superposed rotation described in Example 5.5-1 and Problem 5C.2.

SOLUTION We use the same notation as in Example 5.5-1. Then the coordinates $\bar{x}$, $\bar{y}$ refer to the turntable on which we have a steady shear flow, $v_{\bar{x}} = \dot{\gamma}\bar{y}$, $v_{\bar{y}} = 0$, so that the displacement functions are

$$\begin{cases} \bar{x} = \bar{x}' - \dot{\gamma}\bar{y}'t' \\ \bar{y} = \bar{y}' \end{cases} \tag{8.1-26}$$

where the unprimed coordinates refer to the position of the particle at time $t = 0$, and the primed coordinates refer to the position at time t'. In addition we need transformation rules between the turntable coordinates and the space fixed coordinates. These are given by Eqs. 5.5-1 and 2 repeated here for $t = 0$ and $t = t'$ separately

At time 0:

$$\begin{cases} \bar{x} = x - x_0 \\ \bar{y} = y - y_0 \end{cases} \quad \text{or} \quad \begin{cases} x = \bar{x} + x_0 \\ y = \bar{y} + y_0 \end{cases} \tag{8.1-27a,b}$$

At time t':

$$\begin{cases} \bar{x}' = (x' - x_0)C + (y' - y_0)S \\ \bar{y}' = -(x' - x_0)S + (y' - y_0)C \end{cases} \quad \text{or} \quad \begin{cases} x' = \bar{x}'C - \bar{y}'S + x_0 \\ y' = \bar{x}'S + \bar{y}'C + y_0 \end{cases} \tag{8.1-28a,b}$$

where $C = \cos Wt'$ and $S = \sin Wt'$. The displacement functions referred to the space fixed axes are

then obtained by inserting Eqs. 8.1-28a into Eqs. 8.1-26, which then in turn are inserted into Eqs. 8.1-27b to get

$$\begin{cases} x = (x' - x_0)(C + S\dot{\gamma}t') + (y' - y_0)(S - C\dot{\gamma}t') + x_0 \\ y = -(x' - x_0)S + (y' - y_0)C + y_0 \end{cases} \tag{8.1-29}$$

Then by differentiation we obtain

$$\mathbf{E}(0, t') = \begin{pmatrix} C + S\dot{\gamma}t' & S - C\dot{\gamma}t' & 0 \\ -S & C & 0 \\ 0 & 0 & 1 \end{pmatrix} \tag{8.1-30}$$

Notice that the displacement gradient tensor depends on the angular orientation of the turntable at the past time t'. However when we perform the matrix multiplication to form $\mathbf{B} = \{\mathbf{E} \cdot \mathbf{E}^{\dagger}\}$ this dependence drops out

$$\mathbf{B}(0, t') = \begin{pmatrix} 1 + (\dot{\gamma}t')^2 & -\dot{\gamma}t' & 0 \\ -\dot{\gamma}t' & 1 & 0 \\ 0 & 0 & 1 \end{pmatrix}; \quad \mathbf{B}^{-1}(0, t') = \begin{pmatrix} 1 & \dot{\gamma}t' & 0 \\ \dot{\gamma}t' & 1 + (\dot{\gamma}t')^2 & 0 \\ 0 & 0 & 1 \end{pmatrix} \tag{8.1-31}$$

In addition we have given $\mathbf{B}^{-1}$, which we have obtained simply as the inverse of $\mathbf{B}$; in this derivation we used the fact that $\det \mathbf{B} = 1$. The important point about Eqs. 8.1-31 is that the expressions for $\mathbf{B}$ and $\mathbf{B}^{-1}$ are those given in Eqs. 8.1-18 when $\gamma_{yx}(0, t') = \dot{\gamma}t'$. This means that the influence of the rotation clearly present in the displacement gradient tensors has been "filtered out" in the finite strain tensors.

§8.2 QUASI-LINEAR INTEGRAL MODELS

We are now in a position to modify the general linear viscoelastic model to obtain an admissible constitutive equation. We may do this simply by replacing the infinitesimal strain tensor $\boldsymbol{\gamma}(t, t')$ of Eq. 5.2-19 by either of the relative strain tensors $\boldsymbol{\gamma}_{[0]}(t, t')$ or $\boldsymbol{\gamma}^{[0]}(t, t')$ of the previous section.[1] Constitutive equations obtained by using $\boldsymbol{\gamma}_{[0]}(t, t')$ and $\boldsymbol{\gamma}^{[0]}(t, t')$ give rather different predictions outside the linear regime, but several different molecular theories and comparison with experiments (see Problem 8B.4) suggest very strongly that it is more appropriate to replace $\boldsymbol{\gamma}(t, t')$ by $\boldsymbol{\gamma}_{[0]}(t, t')$. Therefore we use the following quasi-linear integral model:

$$\boxed{\boldsymbol{\tau}(t) = \int_{-\infty}^{t} M(t - t')\boldsymbol{\gamma}_{[0]}(t, t')dt'} \tag{8.2-1}$$

where $M(t - t')$ is the *memory function.* We refer to this model as the *Lodge rubberlike liquid.*[2] Since $\boldsymbol{\gamma}_{[0]}$ reduces to $\boldsymbol{\gamma}$ in the limit of small displacement gradients, the model

[1] In place of $\boldsymbol{\gamma}_{[0]}$ we could also use $-\mathbf{B}$, and in place of $\boldsymbol{\gamma}^{[0]}$ we could also use $\mathbf{B}^{-1}$. These replacements do not alter the properties of the constitutive equations, since the materials are incompressible.

[2] A. S. Lodge, *Elastic Liquids*, Academic Press, New York (1964); many rheological properties of this model are worked out in detail in Chapts. 6 and 7. The equation of the form of Eq. 8.2-1 but with $\boldsymbol{\gamma}^{[0]}$ in place of $\boldsymbol{\gamma}_{[0]}$ is sometimes called the equation of *finite linear viscoelasticity* [see W. R. Schowalter, *Mechanics of Non-Newtonian Fluids*, Pergamon, New York (1978), §11.3; and R. Huilgol, *Continuum Mechanics of Viscoelastic Liquids*, Wiley, New York (1975), p. 164].

becomes identical to the general linear viscoelastic model (Eq. 5.2-19) in that limit. Hence the memory function is the same as that of linear viscoelasticity and is related to the relaxation modulus $G(t - t')$ by $M(t - t') = \partial G(t - t')/\partial t'$. The model retains the feature of the general linear viscoelastic model that the integrand is factorized into a product of two functions, one depending on the nature of the specific fluid and the other on the deformation history. We call the model "quasi-linear" because the stress depends linearly on the history of a strain tensor. Keep in mind, however, that $\gamma_{[0]}(t, t')$ is itself nonlinear in the displacement gradients, and that Eq. 8.2-1 therefore really represents a nonlinear model for the stress in terms of the displacements.

The following specific choices for $M(t - t')$ lead to commonly used constitutive equations:

a.
$$M(t - t') = \frac{\eta_0}{\lambda_1^2} \exp\left[-(t - t')/\lambda_1\right] \tag{8.2-2}$$

This gives the *convected Maxwell model* introduced in Chapter 7. It is recognized as a nonlinear version of the Maxwell model in Eq. 5.2-8.

b.
$$M(t - t') = \frac{\eta_0}{\lambda_1^2}\left[\left(1 - \frac{\lambda_2}{\lambda_1}\right) \exp\left[-(t - t')/\lambda_1\right] + 2\lambda_1\lambda_2 \frac{\partial}{\partial t'} \delta(t - t')\right] \tag{8.2-3}$$

This gives the *convected Jeffreys model* (or Oldroyd fluid B) introduced in Chapter 7. It is recognized as a nonlinear version of the Jeffreys model in Eq. 5.2-12.

c.
$$M(t - t') = \sum_{i=1}^{\infty} \frac{\eta_i}{\lambda_i^2} \exp\left[-(t - t')/\lambda_i\right] \tag{8.2-4}$$

This gives the *convected generalized Maxwell model*, which is recognized as a nonlinear modification of Eq. 5.2-15. This model, also called the *Lodge network model*,[3] has been specifically derived from a molecular theory of polymer melts (see Chapter 20). The Rouse and Zimm theories of dilute polymer solutions (see Chapter 15) also give a constitutive equation of the form of Eq. 8.2-1 with the memory function of Eq. 8.2-4; these theories, in contrast to the network theories, give explicit expressions for the parameters η_i and λ_i in terms of the constants describing the mechanical model. In these dilute solution theories, and in the network model of Green and Tobolsky,[4] it is the finite strain tensor $\gamma_{[0]}(t, t')$ that enters naturally in the theory and not the tensor $\gamma^{[0]}(t, t')$. This is the reason for our choice in Eq. 8.2-1 of $\gamma_{[0]}(t, t')$ as the strain tensor used to replace $\gamma(t, t')$ in the quasi-linear models. In the following example we investigate some of the properties of the Lodge rubberlike liquid. A rather complete and extensive investigation of the rheological properties of this model is given by Lodge.[2]

EXAMPLE 8.2-1 Simple Shear Flow of the Lodge Rubberlike Liquid

Consider a time-dependent simple shear flow of a Lodge rubberlike liquid with the flow field $v_x = \dot{\gamma}_{yx}(t)y$ and $v_y = v_z = 0$. Obtain the general expressions for the stress tensor components, and use

[3] A. S. Lodge, *Elastic Liquids*, Academic Press, New York (1964), Chapts. 6 and 7; A. S. Lodge, *Trans. Faraday Soc.*, **52**, 120–130 (1956); A. S. Lodge, R. C. Armstrong, M. H. Wagner, and H. H. Winter, *Pure Appl. Chem.*, **54**, 1349–1359 (1983); see also §20.4.

[4] M. S. Green and A. V. Tobolsky, *J. Chem. Phys.*, **14**, 80–92 (1946).

these to find the material functions for **(a)** steady-state shear flow, **(b)** start-up of shear flow, and **(c)** stress relaxation upon cessation of steady shear flow.

SOLUTION We use the entry for $\gamma_{[0]}(t, t')$ in homogeneous shear flow in Appendix C. When the expressions for the components of $\gamma_{[0]}$ are inserted into Eq. 8.2-1 we obtain for the stress components of interest

$$\tau_{yx}(t) = \int_{-\infty}^{t} M(t - t')\gamma_{yx}(t, t')dt' \tag{8.2-5}$$

$$\tau_{xx}(t) - \tau_{yy}(t) = -\int_{-\infty}^{t} M(t - t')\gamma_{yx}^2(t, t')dt' \tag{8.2-6}$$

$$\tau_{yy}(t) - \tau_{zz}(t) = 0 \tag{8.2-7}$$

where

$$\gamma_{yx}(t, t') = \int_{t}^{t'} \dot{\gamma}_{yx}(t'')dt'' \tag{8.2-8}$$

is the shear strain from t to t'. Note that the shear stress is precisely the same as that predicted from the general linear viscoelastic model in Eq. 5.2-19.

(a) For *steady-state shear flow* $\gamma_{yx}(t, t') = -\dot{\gamma}(t - t')$, where $\dot{\gamma}$ is the shear rate. We then obtain

$$\tau_{yx} = -M_1\dot{\gamma}; \qquad \eta = M_1 \overset{\text{(LNM)}}{=} \sum_i \eta_i \tag{8.2-9}$$

$$\tau_{xx} - \tau_{yy} = -M_2\dot{\gamma}^2; \quad \Psi_1 = M_2 \overset{\text{(LNM)}}{=} 2\sum_i \eta_i\lambda_i \tag{8.2-10}$$

$$\tau_{yy} - \tau_{zz} = 0; \qquad \Psi_2 = 0 \tag{8.2-11}$$

where

$$M_n = \int_0^\infty M(s)s^n\,ds = n\int_0^\infty G(s)s^{n-1}\,ds \tag{8.2-12}$$

and $\overset{\text{(LNM)}}{=}$ means that the particular memory function for the *L*odge *N*etwork *M*odel has been assumed (see Eq. 8.2-4).

Note that η and Ψ_1 are constants for any choice of the memory function. This prediction is not in agreement with most experimental data over a wide range of shear rates. The model also predicts incorrectly that $\Psi_1/2\eta = \int_0^\infty G(s)s\,ds/\int_0^\infty G(s)ds$ is independent of the shear rate. Moreover since the shear stress predicted is identical to that of the linear viscoelastic model, none of the nonlinear effects observed for the shear stresses in these experiments (see Chapter 3) can be described by this model. Also the equalities between the measurable shear quantities in Table 5.3-1 are predicted to hold for stress relaxation, stress growth, constrained recoil, creep and steady-state flow without the limiting process on shear rate (or shear stress).

(b) For *start-up of shear flow* with shear rate $\dot{\gamma}_0$ after time $t = 0$ we have from Eq. 8.2-8

$$\gamma_{yx}(t, t') = -\dot{\gamma}_0 t, \qquad t > 0, t' < 0 \tag{8.2-13}$$

$$\gamma_{yx}(t, t') = -\dot{\gamma}_0(t - t'), \qquad t > 0, t' > 0 \tag{8.2-14}$$

The resulting stresses are

$$\tau_{yx} = -\eta^+\dot{\gamma}_0 = -[M_1 - J_1(t)]\dot{\gamma}_0 \overset{\text{(LNM)}}{=} -\left[\sum_i \eta_i(1 - e^{-t/\lambda_i})\right]\dot{\gamma}_0 \tag{8.2-15}$$

$$\tau_{xx} - \tau_{yy} = -\Psi_1^+\dot{\gamma}_0^2 = -[M_2 - 2tJ_1(t) - J_2(t)]\dot{\gamma}_0^2 \overset{\text{(LNM)}}{=} -\left[2\sum_i \eta_i\lambda_i(1 - (1 + t/\lambda_i)e^{-t/\lambda_i})\right]\dot{\gamma}_0^2 \tag{8.2-16}$$

where

$$J_n(t) = \int_t^\infty M(s)(s - t)^n\, ds \overset{\text{(LNM)}}{=} n!\sum_i \eta_i\lambda_i^{n-1}e^{-t/\lambda_i} \tag{8.2-17}$$

and $\tau_{yy} - \tau_{zz} = 0$. Note that for the Lodge network model $(\eta^+)_{t=0} = (\Psi_1^+)_{t=0} = 0$ and that $(\partial\Psi_1^+/\partial t)_{t=0} = 0$, but $(\partial\eta^+/\partial t)_{t=0} > 0$. The network model does predict correctly that the normal stresses rise more slowly than the shear stresses if there are at least two distinct time constants in the memory function.

(c) For *stress relaxation* upon cessation of a steady shear flow with shear rate $\dot{\gamma}_0$ at time $t = 0$ we have

$$\gamma_{yx}(t, t') = \dot{\gamma}_0 t' \qquad t > 0, t' < 0 \tag{8.2-18}$$

$$\gamma_{yx}(t, t') = 0 \qquad t > 0, t' > 0 \tag{8.2-19}$$

The resulting stresses are

$$\tau_{yx} = -\eta^-\dot{\gamma}_0 = -J_1(t)\dot{\gamma}_0 \overset{\text{(LNM)}}{=} -\left[\sum_i \eta_i e^{-t/\lambda_i}\right]\dot{\gamma}_0 \tag{8.2-20}$$

$$\tau_{xx} - \tau_{yy} = -\Psi_1^-\dot{\gamma}_0^2 = -J_2(t)\dot{\gamma}_0^2 \overset{\text{(LNM)}}{=} -\left[2\sum_i \eta_i\lambda_i e^{-t/\lambda_i}\right]\dot{\gamma}_0^2 \tag{8.2-21}$$

and $\tau_{yy} - \tau_{zz} = 0$. For the Lodge network model it may be shown that the normal stresses relax more slowly than the shear stresses provided there are at least two distinct exponentials in the memory function; this is in qualitative agreement with experimental observations.

§8.3 NONLINEAR INTEGRAL CONSTITUTIVE EQUATIONS

It was demonstrated in Example 8.2-1 that the Lodge rubberlike liquid has a constant viscosity equal to the first moment M_1 of the memory function $M(s)$ (see Eq. 8.2-9). The fact that the viscosity function calculated from that model does not depend on shear rate may not be altered by the choice of different memory functions, but is a direct result of the use of an expression for the stress tensor that is linear in $\boldsymbol{\gamma}_{[0]}(t, t')$ or $\mathbf{B}(t, t')$. In this section we show how the quasi-linear constitutive equation may be modified to give a nonlinear equation capable of describing a shear-rate-dependent viscosity and the shapes of other nonlinear material functions as well. There are several ways to introduce additional nonlinearities into Eq. 8.2-1:

- **a.** Include invariants of $\mathbf{B}$ in the memory function.
- **b.** Allow $\boldsymbol{\gamma}_{[0]}$ to appear nonlinearly in the integrand, for example, by including $\{\boldsymbol{\gamma}_{[0]} \cdot \boldsymbol{\gamma}_{[0]}\}$.

c. Add additional terms with second-, third-, and higher-order integrals containing double, triple, and higher products of $\boldsymbol{\gamma}_{[0]}$ evaluated at different past times t', t'', t'''...

In this section we discuss several constitutive equations that incorporate the notions listed under **(a)** and **(b)**. The matter of multiple integrals is postponed until Chapter 9, inasmuch as such "memory-integral expansions" have not been used for fluid dynamics calculations.

Recall that in §4.1 we modified the Newtonian fluid constitutive equation (linear in $\dot{\boldsymbol{\gamma}}$) to obtain a nonlinear equation capable of describing shear-rate dependent viscosity. The process here is in a way similar to that in §4.1. Just as in §4.1 where we started with a discussion of the scalar invariant $\dot{\gamma} = \sqrt{\frac{1}{2}(\boldsymbol{\gamma}_{(1)} : \boldsymbol{\gamma}_{(1)})}$ of the rate-of-strain tensor, we start this section with a discussion of the scalar invariants of the strain tensors.

We begin by defining the scalar invariants I_1 and I_2 (Eqs. A.3-23 and 24) of the Finger strain tensor $\mathbf{B}(t, t')$ by

$$I_1 = \text{tr } \mathbf{B} \tag{8.3-1}$$

$$I_2 = \tfrac{1}{2}[(\text{tr } \mathbf{B})^2 - \text{tr } (\mathbf{B}^2)] \tag{8.3-2}$$

The third scalar invariant, the determinant of $\mathbf{B}$, need not be considered since for incompressible fluids $\det \mathbf{B} = 1$. Indeed the incompressibility condition allows us to write the Cayley–Hamilton theorem for $\mathbf{B}$ (Eq. A.3-28) in the simple form

$$\mathbf{B}^2 - I_1\mathbf{B} + I_2\boldsymbol{\delta} = \mathbf{B}^{-1} \tag{8.3-3}$$

If we take the trace of Eq. 8.3-3 and use the definitions in Eqs. 8.3-1 and 8.3-2 we may write the invariants as follows

$$I_1 = \text{tr } \mathbf{B} = \text{tr}(\boldsymbol{\delta} - \boldsymbol{\gamma}_{[0]}); \quad I_2 = \text{tr } \mathbf{B}^{-1} = \text{tr}(\boldsymbol{\delta} + \boldsymbol{\gamma}^{[0]}) \tag{8.3-4}$$

These invariants will appear in constitutive equations in this section.

The invariant $\dot{\gamma} = \sqrt{\frac{1}{2}(\boldsymbol{\gamma}_{(1)} : \boldsymbol{\gamma}_{(1)})}$ defined in §4.1 is never negative, that is, for all possible $\boldsymbol{\gamma}_{(1)}$ tensors $\dot{\gamma} \geq 0$. We used this fact for example in the definition of the power-law viscosity function, in which $\dot{\gamma}$ is raised to some power n, which could be a fractional number. In the same way it is useful to know the ranges of the values taken by I_1 and I_2 for real deformations. To understand this range we recall from §8.1 that $\mathbf{B}$ is symmetric and positive definite. This means that the eigenvalues of $\mathbf{B}$ are real and positive and may consequently be written as λ_x^2, λ_y^2, λ_z^2 where the λ's are positive. Then we have

$$I_1 = \lambda_x^2 + \lambda_y^2 + \lambda_z^2; \quad I_2 = \lambda_x^{-2} + \lambda_y^{-2} + \lambda_z^{-2} \tag{8.3-5}$$

The possible combinations of I_1 and I_2 are those that can be generated by the above equations for all combinations of positive λ_x, λ_y, λ_z compatible with the incompressibility condition $\det \mathbf{B} = 1$ which is

$$\lambda_x\lambda_y\lambda_z = 1 \tag{8.3-6}$$

The values of the λ's corresponding to deformations generated by shearfree motions were given in Eqs. 8.1-21 to 23 and may also be found in Appendix C. Without proof we now state that the region of possible I_1 and I_2 values is that bounded on one side by deformations generated in uniaxial elongation ($b = 0$, $\varepsilon < 0$) and on the other side by

deformations generated in biaxial stretching ($b = 0, \varepsilon > 0$); here ε is the Hencky strain. The resulting range is shown in Fig. 8.3-1.

We are now in a position to introduce the two nonlinear single-integral models that are the primary objects of study in this chapter. These are

The K-BKZ Equation[1]

$$\tau(t) = \int_{-\infty}^{t} \left[\frac{\partial V(t-t', I_1, I_2)}{\partial I_1} \gamma_{[0]} + \frac{\partial V(t-t', I_1, I_2)}{\partial I_2} \gamma^{[0]} \right] dt' \tag{8.3-7}$$

and

The Rivlin-Sawyers Equation[2]

$$\tau(t) = \int_{-\infty}^{t} [\psi_1(t-t', I_1, I_2)\gamma_{[0]} + \psi_2(t-t', I_1, I_2)\gamma^{[0]}] dt' \tag{8.3-8}$$

In these equations V and the ψ_i are scalar functions of the arguments indicated for $-\infty < t' \leq t$ and for I_1 and I_2 in the shaded areas shown in Fig. 8.3-1. Certainly the Rivlin-Sawyers model includes the K-BKZ equation but we find it convenient to be able to refer to the equations separately. Note that these constitutive equations include both $\gamma_{[0]}$ and $\gamma^{[0]}$. According to Eq. 8B.3-3 this is tantamount to including $\gamma_{[0]}$ and $\{\gamma_{[0]} \cdot \gamma_{[0]}\}$, that is, to allowing the strain tensor to enter the integrand nonlinearly. Hence Eqs. 8.3-7 and 8 could be formulated entirely in terms of the relative strain tensor $\gamma_{[0]}$. However, in most published works it has been common practice to use $\mathbf{B}$ and $\mathbf{B}^{-1}$, or alternatively $\gamma_{[0]}$ and $\gamma^{[0]}$, and we therefore follow the customary usage. Another point to note is that if the $\gamma^{[0]}$ term is omitted, the second normal-stress coefficient is always zero.

The arguments leading to the K-BKZ equation go back to the ideas proposed in Chapter 5 that polymer melts behave for sudden changes in shape as an elastic solid and for very slow changes in shape as a Newtonian fluid. The K-BKZ equation arises from an ad hoc transformation of a general nonlinear expression for the stress tensor of an ideal elastic solid in large deformations to a constitutive equation for a fluid that combines elastic and viscous ideas.

As an alternative to the K-BKZ equation, the Rivlin-Sawyers constitutive equation is based on the physical assumption that the effects on the stress at time t of the deformations at different past times t' are independent of each other. With this assumption it may be shown from some rather formal arguments[2] that Eq. 8.3-8 represents the most general constitutive equation for isotropic fluids.

Very little work on describing material functions or solving flow problems has been done with the K-BKZ and the Rivlin-Sawyers equations in their general forms shown above. Instead it has been customary to introduce the additional assumptions that the scalar functions V and ψ_i may be written as a product of time-dependent and

[1] Proposed independently by A. Kaye, College of Aeronautics, Cranfield, *Note No. 134* (1962), and B. Bernstein, E. Kearsley, and L. Zapas, *Trans. Soc. Rheol.*, **7**, 391-410 (1963); B. Bernstein, E. A. Kearsley, and L. J. Zapas, *J. Res. Natl. Bur. Stand.*, **68B**, 103-113 (1964). See also L. J. Zapas and T. Craft, *J. Res. Natl. Bur. Stand.*, **69A**, 541-546 (1965), and L. J. Zapas, *J. Res. Natl. Bur. Stand.*, **70A**, 525-532 (1966); E. A. Kearsley and L. J. Zapas, *Trans. Soc. Rheol.*, **20**, 623-637 (1976); L. J. Zapas and J. C. Phillips, *J. Rheol.*, **25**, 405-420 (1981) for data comparisons and B. Bernstein, *Acta Mech.*, **2**, 329-354 (1966), and *Int. J. Nonlinear Mech.*, **4**, 183-200 (1969), for a rather complete compilation of material function expressions.

[2] Proposed by R. S. Rivlin and K. N. Sawyers, *Ann. Rev. Fluid Mech.*, **3**, 117-146 (1971). See also R. V. Chacon and N. Friedman, *Arch. Rat. Mech. Anal.*, **18**, 230-240 (1965); A. D. Martin and V. J. Mizel, *Arch. Rat. Mech. Anal.*, **15**, 353-367 (1964); and R. Huilgol, *Continuum Mechanics of Viscoelastic Liquids*, Wiley, New York (1975).

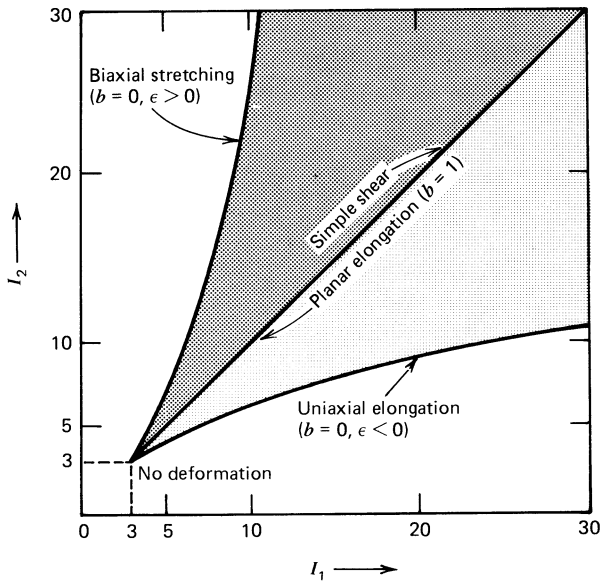

FIGURE 8.3-1. Range of allowable combinations of I_1, I_2 for incompressible materials according to Eqs. 8.3-5 and 6 (shown here for $I_1 < 30$ and $I_2 < 30$). All combinations within the shaded zones are accessible in shearfree flows (see Eqs. 8.1-21 to 23) with combinations in the light gray sector corresponding to $\varepsilon < 0$, and combinations in the dark gray sector corresponding to $\varepsilon > 0$. The line $I_1 = I_2$ that separates the two regions corresponds to both planar elongation and simple shear. The asymptotes of the boundaries are (for large I_1, I_2): $I_1 \sim I_2^2/4$ (for uniaxial elongation) and $I_2 \sim I_1^2/4$ (for biaxial stretching). The point $I_1 = 3$, $I_2 = 3$ corresponds to no deformation gradients. [This kind of sketch was first set forth by K. N. Sawyers, *J. Elast.*, **7**, 99–102 (1977); see also P. K. Currie, *J. Non-Newtonian Fluid Mech.*, **11**, 53–68 (1982); V. K. Stokes, *Trans. ASME*, **48**, 664–666 (1981); L. R. G. Treloar, *The Physics of Rubber Elasticity*, 3rd ed., Oxford University Press, London, (1975), Chap. 10.]

strain-dependent factors as follows:[3]

$$V(t - t', I_1, I_2) = M(t - t')W(I_1, I_2) \tag{8.3-9}$$

$$\psi_i(t - t', I_1, I_2) = M(t - t')\phi_i(I_1, I_2) \tag{8.3-10}$$

In these equations $M(t - t')$ is the linear viscoelastic memory function that appears in Eq. 5.2-19, and W and the ϕ_i are functions defined within the shaded regions shown in Fig. 8.3-1. With these assumptions one arrives at the following constitutive equations, which are still quite flexible since they contain unspecified functions of time and the strain invariants:

The Factorized K–BKZ Equation:

$$\boldsymbol{\tau}(t) = \int_{-\infty}^{t} M(t - t')\left[\frac{\partial W(I_1, I_2)}{\partial I_1}\boldsymbol{\gamma}_{[0]} + \frac{\partial W(I_1, I_2)}{\partial I_2}\boldsymbol{\gamma}^{[0]}\right]dt' \tag{8.3-11}$$

The Factorized Rivlin–Sawyers Equation:

$$\boldsymbol{\tau}(t) = \int_{-\infty}^{t} M(t - t')[\phi_1(I_1, I_2)\boldsymbol{\gamma}_{[0]} + \phi_2(I_1, I_2)\boldsymbol{\gamma}^{[0]}]dt' \tag{8.3-12}$$

[3] Such a factorization was first suggested by J. L. White and N. Tokita, *J. Phys. Soc. Jpn.*, **22**, 719–724 (1967).

The function W in Eq. 8.3-11 is called the *potential function.* In the limit of small displacement gradients, I_1 and I_2 both approach three, and both nonlinear strain tensors simplify to the infinitesimal strain tensor γ introduced in Chapter 5. Consequently, since we require that $M(t - t')$ be the linear viscoelastic memory function, we must require that W and the ϕ_i satisfy the following relations:

$$\left(\frac{\partial W}{\partial I_1}\right)_{3,3} + \left(\frac{\partial W}{\partial I_2}\right)_{3,3} = 1 \tag{8.3-13}$$

$$\phi_1(3, 3) + \phi_2(3, 3) = 1 \tag{8.3-14}$$

Equations 8.3-11 and 12 will be featured in the remainder of this section. These constitutive equations are sufficiently flexible that they can describe many rheological phenomena, and it is anticipated that equations of this form will be increasingly used for numerical flow calculations. Expressions for several material functions derivable from Eqs. 8.3-11 and 12 are displayed in Table 8.3-1.

Several molecular theories for polymeric systems result in constitutive equations in the form of the factorized K-BKZ equation: the Rouse-Zimm theory for dilute polymer solutions (Chapter 15), the Curtiss-Bird ($\varepsilon = 0$) theory for polymer melts (Chapter 19), and the Lodge network theory (Chapter 20). The memory functions and W functions for these models are shown in Table 8.3-2; the Curtiss-Bird ($\varepsilon = 0$) model is further considered in Examples 8.3-3 and 4. In addition several single-integral equations have been proposed that may be considered as empirical modifications of molecularly derived equations or as completely empirical equations. A number of these are shown in Tables 8.3-2 and 3. Some of the proposed empirical equations are of the Rivlin-Sawyers form and may not be written in the K-BKZ form.

In connection with Eqs. 8.3-11 and 12 we note also that:

i. If Eqs. 8.3-11 and 12 are to have retarded-motion expansions, then $W(I_1, I_2)$ and $\phi_j(I_1, I_2)$ must have Taylor expansions[4] about $I_1 = 3$, $I_2 = 3$

$$\begin{aligned} W = {} & W^{(00)} + W^{(10)}(I_1 - 3) + W^{(01)}(I_2 - 3) \\ & + \tfrac{1}{2}W^{(20)}(I_1 - 3)^2 + W^{(11)}(I_1 - 3)(I_2 - 3) \\ & + \tfrac{1}{2}W^{(02)}(I_2 - 3)^2 + \cdots \end{aligned} \tag{8.3-15}$$

$$\phi_j = \phi_j^{(00)} + \phi_j^{(10)}(I_1 - 3) + \phi_j^{(01)}(I_2 - 3) + \cdots \tag{8.3-16}$$

where

$$W^{(mn)} = \left.\frac{\partial^{m+n} W}{\partial I_1^m \partial I_2^n}\right|_{3,3} \tag{8.3-17a}$$

$$\phi_j^{(mn)} = \left.\frac{\partial^{m+n} \phi_j}{\partial I_1^m \partial I_2^n}\right|_{3,3} \tag{8.3-17b}$$

When these Taylor expansions are combined with Eqs. 8.3-11 and 12, the retarded-motion expansion coefficients listed in Table 6.2-2 are obtained (see

[4] O. Hassager, unpublished.

TABLE 8.3-1

Material Functions from the Factorized K-BKZ Equation (Eq. 8.3-11)[a] and the Factorized Rivlin-Sawyers Equation (Eq. 8.3-12)

$$\eta(\dot\gamma) = \int_0^\infty M(s)s(\phi_1 + \phi_2)ds \tag{A}$$

$$\Psi_1(\dot\gamma) = \int_0^\infty M(s)s^2(\phi_1 + \phi_2)ds \tag{B}$$

$$\Psi_2(\dot\gamma) = -\int_0^\infty M(s)s^2\phi_2\, ds \tag{C}$$

$$\eta'(\omega) = \frac{1}{\omega}\int_0^\infty M(s)\sin\omega s\, ds \tag{D}[b]$$

$$\eta''(\omega) = \frac{1}{\omega}\int_0^\infty M(s)(1 - \cos\omega s)ds \tag{E}[b]$$

$$\bar\eta_1(\dot\varepsilon, b) = \frac{1}{\dot\varepsilon}\int_0^\infty M(s)[\phi_1(e^{2\dot\varepsilon s} - e^{-(1+b)\dot\varepsilon s}) + \phi_2(e^{(1+b)\dot\varepsilon s} - e^{-2\dot\varepsilon s})]ds \tag{F}[c]$$

$$\bar\eta_2(\dot\varepsilon, b) = \frac{1}{\dot\varepsilon}\int_0^\infty M(s)[(\phi_1 e^{-\dot\varepsilon s} + \phi_2 e^{\dot\varepsilon s})(e^{b\dot\varepsilon s} - e^{-b\dot\varepsilon s})]ds \tag{G}[c]$$

[a] To obtain the entry for the factorized K-BKZ model replace ϕ_j by $\partial W/\partial I_j$; note that $\phi_j = \phi_j(I_1, I_2)$ and $W = W(I_1, I_2)$, where $I_j = I_j(t, t - s)$.

[b] See Problem 5B.7.

[c] For $0 \le b \le 1$ and $-\infty < \dot\varepsilon < \infty$. When $b = 0$, the function $\bar\eta_1$ becomes $\bar\eta$, and $\bar\eta_2 = 0$.

Problem 9B.8). It is interesting to note that for the K-BKZ fluid the four coefficients $W^{(01)}$, $W^{(20)}$, $W^{(11)}$, and $W^{(02)}$ appear in the retarded-motion coefficients up through third order; the corresponding quantities for the Rivlin-Sawyers fluid are $\phi_2^{(00)}$, $\phi_1^{(10)}$, $(\phi_1^{(01)} + \phi_2^{(10)})$, and $\phi_2^{(01)}$. Because the coefficients $\phi_1^{(01)}$ and $\phi_2^{(10)}$ appear only as a sum, there is at third order no additional flexibility provided by the Rivlin-Sawyers model—that is, the models give equivalent results at the third-order fluid level.

An example of a model not possessing a retarded-motion expansion is the Wagner model of Table 8.3-3. Consequently for this model one cannot use the procedure outlined in Fig. 6.2-2 to obtain perturbation solutions in the limit of slow flow. However, for the purpose of making fluid mechanical calculations outside the slow flow limit, the lack of a retarded-motion expansion is probably not important.

ii. The factorized K-BKZ equation may be written in an alternative form by the use of the chain rule for partial differentiation[5]

$$\frac{1}{2}\sum_k \mathrm{E}_{ik}\frac{\partial W}{\partial \mathrm{E}_{jk}} = -\frac{\partial W}{\partial I_1}\gamma_{[0]ij} - \frac{\partial W}{\partial I_2}\gamma_{ij}^{[0]} + \left(I_2 + \frac{\partial W}{\partial I_1} - \frac{\partial W}{\partial I_2}\right)\delta_{ij} \tag{8.3-18}$$

[5] One use of this expression is illustrated in Example 8.3-3. See also O. Hassager, *J. Non-Newtonian Fluid Mech.*, **9**, 321-328 (1981), in which a variational principle for factorized K-BKZ fluids is given for unsteady-state flows.

TABLE 8.3-2

Examples of Molecular Models Included in the Factorized K-BKZ Model (Eq. 8.3-11)

Model	$M(s)$	$W(I_1, I_2)$	Adjustable Parameters
Rouse-Zimm[a] (Chapter 15)	$-2\eta_s\delta'(s) + \sum_{j=1}^{N} \frac{\eta_j}{\lambda_j^2} e^{-s/\lambda_j}$	I_1	$\eta_s, \eta_0, \lambda_1, \sigma$ in $\lambda_j \doteq \lambda_1/j^\sigma$; $\eta_j = (\eta_0 - \eta_s)\lambda_j/\sum_j \lambda_j$ ($\sigma = 2$ in the Rouse model)
Lodge network[b] (Chapter 20)	$\sum_{j=1}^{N} \frac{\eta_j}{\lambda_j^2} e^{-s/\lambda_j}$	I_1	$n_j, \lambda_j,$ for $j = 1, 2 \ldots$
Tanner-Simmons network rupture[c] (Problem 8B.7)	$\sum_{j=1}^{N} \frac{\eta_j}{\lambda_j^2} e^{-s/\lambda_j}$	I_1, for $I_1 \leq I_0$ I_0, for $I_1 > I_0$	$\eta_j, \lambda_j,$ for $j = 1, 2 \ldots$ I_0
Curtiss-Bird ($\varepsilon = 0$) or Doi-Edwards[d] (Chapter 19)	$\frac{96\eta_0}{\lambda^2} \sum_{\alpha \text{ odd}} e^{-\pi^2\alpha^2 s/\lambda}$	$\frac{5}{4\pi} \int \ln (\mathbf{B}:\boldsymbol{uu}) d\boldsymbol{u}$	η_0 and λ

[a] P. E. Rouse, Jr., *J. Chem. Phys.*, **21**, 1272-1280 (1953); B. H. Zimm, *J. Chem. Phys.*, **24**, 269-278 (1956); the solvent contribution to the stress tensor has been included in Eq. 8.3-11 by the use of the derivative of the Dirac delta function $\delta'(s)$ (see Eq. 5.2-10c).

[b] A. S. Lodge, *Trans. Faraday Soc.*, **52**, 120-130 (1956).

[c] R. I. Tanner and J. M. Simmons, *Chem. Eng. Sci.*, **22**, 1803-1815 (1967).

[d] C. F. Curtiss and R. B. Bird, *J. Chem. Phys.*, **74**, 2016-2025 (1981); **74**, 2026-2033 (1981). In this model $\boldsymbol{u}$ is a unit vector, and $\int \ldots d\boldsymbol{u}$ is an integral over the surface of a unit sphere. See also P. K. Currie, *J. Non-Newtonian Fluid Mech.*, **11**, 53-68 (1982); O. Hassager, *J. Non-Newtonian Fluid Mech.*, **9**, 321-328 (1981). Note that $(\mathbf{B}:\boldsymbol{uu})$ is a scalar and therefore must be expressible as a function of the scalar invariants I_1 and I_2.

where $W = W(I_1, I_2)$. For incompressible fluids the isotropic terms may be omitted in constitutive equations.

iii. Initial value problems with the factorized K-BKZ model will be well posed for finite positive memory functions $M(s)$ when W is monotone in each argument, strictly monotone in I_1 or I_2, and a convex function of $\sqrt{I_1}$ and $\sqrt{I_2}$. We refer to this as the "Renardy condition."[6] An application of this condition is illustrated in the following example.

iv. Standard techniques exist for the determination of M from linear viscoelastic measurements.[7] There is currently no standard technique for the determination of $W(I_1, I_2)$, but beginnings have been made for tackling this difficult problem.[8]

[6] M. Renardy, *Arch. Rat. Mech. Anal.*, **88**, 83-94 (1985). A function $f(x)$ is convex at a point a if in a neighborhood around a we have $f(x) \geq f(a) + (x - a)f'(a)$. If $f''(a) > 0$, then $f(x)$ is strictly convex at a.

[7] J. D. Ferry, *Viscoelastic Properties of Polymers*, 3rd ed., Wiley, New York (1980). See also Example 5.3-7.

[8] J. Meissner, S. E. Stephenson, A. Demarmels, and P. Portmann, *J. Non-Newtonian Fluid Mech.*, **11**, 221-237 (1981); P. Bach and O. Hassager, *Mathematics Research Center Technical Summary Report No. 2755*, University of Wisconsin, Madison (Sept. 1984).

TABLE 8.3-3

Examples of Models Included in the Factorized Rivlin-Sawyers Model (Eq. 8.3-12)[a]

Model	Flow	ϕ_1	ϕ_2	Adjustable Parameters	Comments
Phillips[b]	Simple shear[c]	$(1-q)\exp(-\beta\lvert\gamma_{yx}\rvert)$	$q\exp(-\beta\lvert\gamma_{yx}\rvert)$	α, β	$q = -\Psi_{2,0}/\Psi_{1,0}$ This model has no retarded-motion expansion
	General	Not specified	Not specified		
Wagner[d]	Simple shear[c]	$\exp(-\beta\lvert\gamma_{yx}\rvert)$	0	α, β	$\Psi_{2,0} = 0$ This model has no retarded-motion expansion
	General	$\exp(-\beta\sqrt{\alpha I_1 + (1-\alpha)I_2 - 3}$	0		
Papanastasiou, Scriven, and Macosko[e]	Simple shear[c]	$\dfrac{\alpha}{\alpha + \gamma_{yx}^2}$	0	α, β	$\Psi_{2,0} = 0$
	General	$\dfrac{\alpha}{(\alpha-3) + \beta I_1 + (1-\beta)I_2}$	0		

[a] For a criticism of the Rivlin-Sawyers model see R. G. Larson and K. Monroe, *Rheol. Acta*, **23**, 10-13 (1984).

[b] M. C. Phillips, *J. Non-Newtonian Fluid Mech.*, **2**, 109-121, 123-137, 139-149 (1977).

[c] $v_x = \dot{\gamma}_{yx}(t)y$, $v_y = v_z = 0$; $\gamma_{yx}(t, t') = \int_t^{t'} \dot{\gamma}_{yx}(t'')dt''$.

[d] M. H. Wagner, *Rheol. Acta*, **18**, 33-50 (1979). See also M. H. Wagner and J. Meissner, *Macromol. Chem.*, **181**, 1533-1550 (1980). For further discussion of the Wagner model and its molecular basis see §20.5. In §20.5 the function ϕ_1 is designated by h.

[e] A. C. Papanastasiou, L. E. Scriven, and C. W. Macosko, *J. Rheol.*, **27**, 387-410 (1983).

EXAMPLE 8.3-1 A Nonlinear Single-Integral Constitutive Equation

As an example of a potential function for a factorized K-BKZ constitutive equation consider the following function:[9]

$$W = \begin{cases} K[(1-q)I_1^p + qI_2^p], & \text{for } p > 0 \\ 3[(1-q)\ln I_1 + q \ln I_2], & \text{for } p = 0 \end{cases} \tag{8.3-19}$$

where $K = (1/p)3^{1-p}$ is a factor determined by Eq. 8.3-13, and $p \geq 0$ so that W is a monotone increasing function of I_1 and I_2. For the constitutive equation in Eq. 8.3-11 with the above W function find: **(a)** limits on the two parameters q and p suggested by the Renardy condition, **(b)** expressions for the second-order fluid constants, **(c)** expressions for the viscometric functions. Find also the asymptotic forms for the viscometric functions in the limit of high shear rates for the following memory functions: **(d)** the Maxwell model, **(e)** the Jeffreys model, and **(f)** the Segalman model.

SOLUTION **(a)** If we denote $I_1^{1/2} = x_1$ and $I_2^{1/2} = x_2$ then (for $p > 0$)

$$\frac{\partial W}{\partial x_1} = 2K(1-q)px_1^{2p-1}; \quad \frac{\partial W}{\partial x_2} = 2Kqpx_2^{2p-1} \tag{8.3-20}$$

and

$$\frac{\partial^2 W}{\partial x_1^2} = 2K(1-q)p(2p-1)x_1^{2p-2}; \quad \frac{\partial^2 W}{\partial x_2^2} = 2Kqp(2p-1)x_2^{2p-2} \tag{8.3-21}$$

and $\partial^2 W/\partial x_1 \partial x_2 = 0$. We see that the Renardy conditions are satisfied when

$$0 \leq q \leq 1 \quad \text{and} \quad p \geq 1/2 \tag{8.3-22}$$

which ensures that both second partial derivatives are positive.

(b) To find the second-order fluid constants we expand the potential in I_1 and I_2 around $I_1 = I_2 = 3$

$$\begin{aligned} W &= W(3,3) + \left(\frac{\partial W}{\partial I_1}\right)_{3,3}(I_1 - 3) + \left(\frac{\partial W}{\partial I_2}\right)_{3,3}(I_2 - 3) + \cdots \\ &= (3/p) + (1-q)(I_1 - 3) + q(I_2 - 3) + \cdots \end{aligned} \tag{8.3-23}$$

where we have used $K = (1/p)3^{1-p}$. Then from Table 6.2-2 we see that

$$b_1 = M_1; \quad b_2 = -\tfrac{1}{2}M_2; \quad b_{11} = -qM_2 \tag{8.3-24}$$

and consequently

$$\eta_0 = M_1; \quad \Psi_{1,0} = M_2; \quad \Psi_{2,0} = -qM_2 \tag{8.3-25}$$

where M_n is the nth moment of the memory function as defined in Eq. 8.2-12. We see that $q = -\Psi_{2,0}/\Psi_{1,0}$. This enables us to narrow the useful range of q-values further than given in Eq. 8.3-22. For example if we wish to describe a bulge in Tanners tilted trough (§2.3b) as well as

[9] O. Hassager, unpublished. The separate expression given for $W(p = 0)$ is chosen so that:

$$\frac{\partial W(p=0)}{\partial I_j} = \left.\frac{\partial W(p>0)}{\partial I_j}\right|_{p=0} \quad \text{for } j = 1, 2.$$

rod-climbing (§2.3a) at second order we must have $0 < q < \frac{1}{4}$. This process of using experimental facts to narrow the useful range of parameters has been encountered earlier in §§6.2 and 7.3.

(c) To find the rheological properties in steady simple shear flow we first write the constitutive equation of Eq. 8.3-11:

$$\boldsymbol{\tau} = 3^{1-p}\int_{-\infty}^{t} M(t-t')[(1-q)I_1^{p-1}\boldsymbol{\gamma}_{[0]} + qI_2^{p-1}\boldsymbol{\gamma}^{[0]}]dt' \tag{8.3-26}$$

in which we have used the potential of Eq. 8.3-19 for $p \geq 0$. For steady shear flow with shear rate $\dot{\gamma}$ we obtain the finite strain tensors from Appendix C with $\gamma_{yx} = -\dot{\gamma}s$, where $s = t - t'$; we also find $I_1 = I_2 = 3 + (\dot{\gamma}s)^2$. Thus the relevant stress components become

$$\tau_{yx} = -\left[3^{1-p}\int_0^{\infty} M(s)[3 + (\dot{\gamma}s)^2]^{p-1}s\,ds\right]\dot{\gamma} = -\eta(\dot{\gamma})\dot{\gamma} \tag{8.3-27}$$

$$\tau_{xx} - \tau_{yy} = -\left[3^{1-p}\int_0^{\infty} M(s)[3 + (\dot{\gamma}s)^2]^{p-1}s^2\,ds\right]\dot{\gamma}^2 = -\Psi_1(\dot{\gamma})\dot{\gamma}^2 \tag{8.3-28}$$

and $\Psi_2(\dot{\gamma}) = -q\Psi_1(\dot{\gamma})$. These expressions may be used to compute $\eta(\dot{\gamma})$ or $\Psi_1(\dot{\gamma})$ for any memory function. The limiting slopes of $\eta(\dot{\gamma})$ and $\Psi_1(\dot{\gamma})$ as $\dot{\gamma} \to \infty$ depend on the memory function, as illustrated in the following.

(d) For the single-relaxation-time memory function, corresponding to the Maxwell model in Eq. 8.2-2, we obtain

$$\begin{aligned}\eta &= \left[3^{1-p}\frac{\eta_0}{\lambda_1^2}\int_0^{\infty} e^{-s/\lambda_1}[3(\lambda_1\dot{\gamma})^{-2} + (s/\lambda_1)^2]^{p-1}\,s\,ds\right](\lambda_1\dot{\gamma})^{2p-2} \\ &\sim \left[3^{1-p}\eta_0\int_0^{\infty} e^{-x}x^{2p-1}\,dx\right](\lambda_1\dot{\gamma})^{2p-2} = 3^{1-p}\eta_0\Gamma(2p)(\lambda_1\dot{\gamma})^{2p-2}\end{aligned} \tag{8.3-29}$$

for $\lambda_1\dot{\gamma} \to \infty$. Similarly for Ψ_1 we find the asymptote

$$\Psi_1 \sim \left[3^{1-p}\eta_0\lambda_1\int_0^{\infty} e^{-x}x^{2p}\,dx\right](\lambda_1\dot{\gamma})^{2p-2} = 3^{1-p}\eta_0\lambda_1\Gamma(2p+1)(\lambda_1\dot{\gamma})^{2p-2} \tag{8.3-30}$$

for $\lambda_1\dot{\gamma} \to \infty$ and in this limit we still have $\Psi_2(\dot{\gamma}) = -q\Psi_1(\dot{\gamma})$. We see that we have achieved partial success in that the viscosity function has a power-law shape for large $\dot{\gamma}$. We see that we must require $p > \frac{1}{2}$ to ensure that the shear stress vs. shear rate curve does not show a maximum. This condition is the same as that derived in **(a)**. We also note that the stress ratio

$$\frac{\tau_{xx} - \tau_{yy}}{\tau_{yx}} \sim \frac{\Gamma(2p+1)}{\Gamma(2p)}\lambda_1\dot{\gamma}, \qquad \text{for } \lambda_1\dot{\gamma} \to \infty \tag{8.3-31}$$

Inasmuch as this result is in conflict with the data in Chapter 3 (see particularly Fig. 3.3-8), we try using several other memory functions.

(e) For the memory function in Eq. 8.2-3 corresponding to the Jeffreys model we obtain the asymptotes[10]

$$\eta \sim \eta_0\frac{\lambda_2}{\lambda_1}, \qquad \text{for } \lambda_1\dot{\gamma} \to \infty \tag{8.3-32}$$

[10] The next term in the asymptotic expression for $\eta(\dot{\gamma})$ is proportional to $(\lambda_1\dot{\gamma})^{2p-2}$. This term must be retained to get Eq. 8.3-29 from Eq. 8.3-32 by setting λ_2 equal to zero.

and

$$\Psi_1 \sim 3^{1-p}\eta_0(\lambda_1 - \lambda_2)\Gamma(2p+1)(\lambda_1\dot{\gamma})^{2p-2}, \qquad \text{for } \lambda_1\dot{\gamma} \to \infty \tag{8.3-33}$$

This model may be used with any parameter $p > 0$, but when $p < \frac{1}{2}$ we must choose λ_2/λ_1 so that the shear stress vs. shear rate curve is monotone increasing. The constraint that $p \geq \frac{1}{2}$ obtained in **(a)** is not applicable here, inasmuch as the Renardy condition requires that $M(s)$ be bounded. We also find that

$$\frac{\tau_{xx} - \tau_{yy}}{\tau_{yx}} \sim \left(\frac{\lambda_1}{\lambda_2} - 1\right)3^{1-p}\Gamma(2p+1)(\lambda_1\dot{\gamma})^{2p-1}, \qquad \text{for } \lambda_1\dot{\gamma} \to \infty \tag{8.3-34}$$

We see that it is possible to adjust this ratio to increase with $\lambda_1\dot{\gamma}$, become constant, or eventually decrease with $\lambda_1\dot{\gamma}$ depending on the value of p.

(f) Next we could consider the memory function of Eq. 8.2-4. If we use a finite number of relaxation times, then when the shear rate or frequency exceeds the reciprocal of the smallest relaxation time, the model will fail to give a physically reasonable response. If one uses an infinite number of relaxation times, then one has the problem that these are not experimentally determinable. Therefore we use the Segalman memory function[11] corresponding to the $G(s)$ given in Eq. 5B.2-1 (which is a three-constant empiricism that accounts for a complete spectrum of relaxation times)

$$M(s) = \frac{\eta_0}{\lambda^2\Gamma(1-\nu)}\left(\frac{\lambda}{s}\right)^{\nu+1} e^{-s/\lambda}\left(\nu + \frac{s}{\lambda}\right) \tag{8.3-35}$$

containing three constants: η_0 (zero-shear-rate viscosity); λ (time constant); and ν (a dimensionless parameter between 0 and 1). Substitution of this memory function into Eqs. 8.3-27 and 28 gives $\eta = \eta_0$ and $\Psi_1 = 2(1-\nu)\eta_0\lambda$ in the limit as $\lambda\dot{\gamma} \to 0$.

Now we return to the problem of getting the asymptotic expressions for $\lambda\dot{\gamma} \to \infty$. These turn out to depend on combinations of the p and ν values. For the viscosity we find from Eqs. 8.3-27 and 25

$$\begin{aligned}
\eta &= \left[3^{1-p}\int_0^\infty M(s)[3\dot{\gamma}^{-2} + s^2]^{p-1}\, s\, ds\right]\dot{\gamma}^{2p-2} \\
&\sim \left[3^{1-p}\int_0^\infty M(s)s^{2p-1}\, ds\right]\dot{\gamma}^{2p-2} \\
&= \left[\frac{3^{1-p}\eta_0}{\Gamma(1-\nu)}\int_0^\infty e^{-x}(\nu+x)x^{2p-2-\nu}\, dx\right](\lambda\dot{\gamma})^{2p-2} \\
&= \frac{3^{1-p}\eta_0(2p-1)\Gamma(2p-\nu-1)}{\Gamma(1-\nu)}(\lambda\dot{\gamma})^{2p-2} \qquad \begin{pmatrix}\lambda\dot{\gamma} \to \infty \\ p > (\nu+1)/2\end{pmatrix}
\end{aligned} \tag{8.3-36}$$

The restriction $p > (\nu+1)/2$ must be placed on this result, since it is needed to ensure that the integral does not diverge at $x = s/\lambda = 0$. In the limit as $\nu \to 0$, the Maxwell model result in Eq. 8.3-29 is obtained. Alternatively if we make the change of variable $x = \dot{\gamma}s$ we are led to

$$\begin{aligned}
\eta &= \left[\frac{3^{1-p}\eta_0}{\Gamma(1-\nu)}\int_0^\infty e^{-x/\lambda\dot{\gamma}}x^{-\nu}\left(\nu + \frac{x}{\lambda\dot{\gamma}}\right)(3+x^2)^{p-1}\, dx\right](\lambda\dot{\gamma})^{\nu-1} \\
&\sim \left[\frac{3^{1-p}\eta_0\nu}{\Gamma(1-\nu)}\int_0^\infty \frac{(3+x^2)^{p-1}}{x^\nu}\, dx\right](\lambda\dot{\gamma})^{\nu-1} \qquad \begin{pmatrix}\lambda\dot{\gamma} \to \infty \\ p < (\nu+1)/2\end{pmatrix}
\end{aligned} \tag{8.3-37}$$

which carries with it the restriction that $p < (\nu+1)/2$.

[11] This part of the example was worked out by S. R. Burdette.

The normal stress coefficient Ψ_1 also depends on the p and ν values:

$$\Psi_1 \sim \left[3^{1-p}\int_0^\infty M(s)s^{2p}\,ds\right]\dot{\gamma}^{2p-2}$$
$$= \frac{3^{1-p}2\eta_0\lambda p\Gamma(2p-2)}{\Gamma(1-\nu)}(\lambda\dot{\gamma})^{2p-2} \qquad \begin{pmatrix}\lambda\dot{\gamma}\to\infty\\ p>\nu/2\end{pmatrix} \tag{8.3-38}$$

which simplifies to the Maxwell result in Eq. 8.3-30 when $\nu \to 0$; Eq. 8.3-38 is valid only when $p > \nu/2$. An alternative expression is obtained by using the change of variable $x = \dot{\gamma}s$:

$$\Psi_1 \sim \left[\frac{3^{1-p}\eta_0\lambda\nu}{\Gamma(1-\nu)}\int_0^\infty \frac{(3+x^2)^{p-1}}{x^{\nu-1}}\,dx\right](\lambda\dot{\gamma})^{\nu-2} \qquad \begin{pmatrix}\lambda\dot{\gamma}\to\infty\\ p<\nu/2\end{pmatrix} \tag{8.3-39}$$

and this is valid for $p < \nu/2$.

The asymptotic behavior of the stress ratio as $\lambda\dot{\gamma} \to \infty$ is as follows:

$$\frac{\tau_{xx}-\tau_{yy}}{\tau_{yx}} \propto \begin{cases}(\lambda\dot{\gamma})^0 & p < \dfrac{\nu}{2}\\ (\lambda\dot{\gamma})^{2p-\nu} & \dfrac{\nu}{2} < p < \dfrac{\nu+1}{2}\\ (\lambda\dot{\gamma}) & p > \dfrac{\nu+1}{2}\end{cases} \tag{8.3-40}$$

Therefore the stress ratio will be constant or increase with some power of $\lambda\dot{\gamma}$ between 0 and 1, the behavior depending on the choice of the constants p and ν. The various regions of parameter space are depicted in Fig. 8.3-2. An examination of the various values of the power-law parameters shown in Table 8.3-4 suggests that the model considered here has sufficient capability to describe the limiting behavior of the viscometric functions. From the values of m, n, m', and n', the model parameters η_0, λ, ν, and p can be determined; the parameter q can be obtained from Ψ_2 or $\bar{\eta}$ data.

The curves of the various material functions are shown in Fig. 8.3-3. It can be seen that the shapes of the curves are reasonably satisfactory. With a total of five constants (η_0, λ, ν, p, and q) it is thus possible to describe a wide variety of rheological phenomena, at least qualitatively.

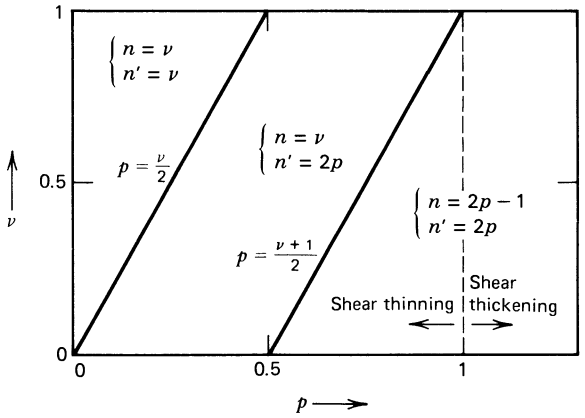

FIGURE 8.3-2. Sketch showing the values of n and n', the "power-law indices" for the high-shear-rate asymptotes of the viscosity and first normal stress coefficient: $\eta \sim m\dot{\gamma}^{n-1}$ and $\Psi_1 \sim m'\dot{\gamma}^{n'-2}$. There are three regions corresponding to different combinations of ν and p.

TABLE 8.3-4

Power-Law Function Parameters for Describing the High Shear Rate Asymptotes of the Viscosity and First Normal Stress Coefficient

	$\eta = m\dot{\gamma}^{n-1}$		$\Psi_1 = m'\dot{\gamma}^{n'-2}$	
Fluid	m Pa·s^n	n	m' Pa·s$^{n'}$	n'
Solutions:[a]				
Hydroxyethylcellulose	21	0.400	30	0.567
Separan	25	0.333	410	0.830
Polyisobutylene	140	0.350	1700	0.677
Melts:[b]				
High-density polyethylene	1.89×10^4	0.40	4.28×10^4	0.41
Low-density polyethylene	0.48×10^4	0.45	1.61×10^4	0.51
Polystyrene	1.56×10^4	0.32	3.31×10^4	0.31
Polypropylene	0.44×10^4	0.50	1.02×10^4	0.51

[a] P. J. Leider, *Ind. Eng. Chem. Fundam.*, **13**, 342–346 (1974).
[b] C. D. Han, K. U. Kim, N. Siskovic, and C. R. Huang, *Rheol. Acta*, **14**, 533–549 (1975), as cited by M. H. Wagner, *Rheol. Acta*, **18**, 33–50 (1979).

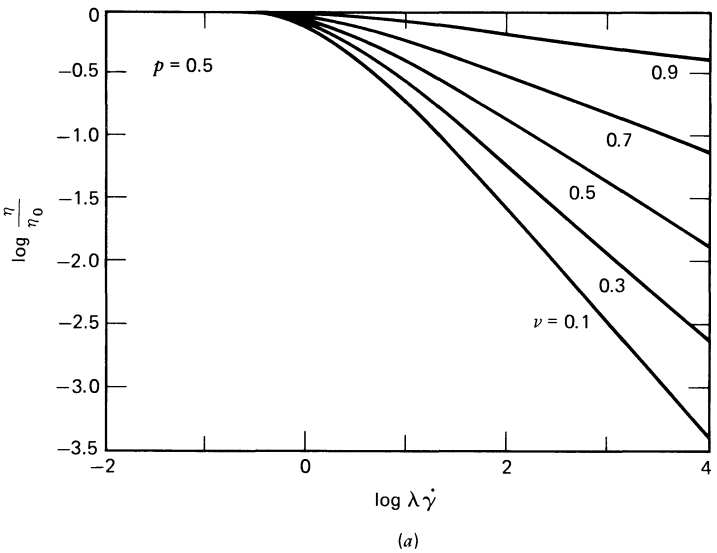

(a)

FIGURE 8.3-3. Material functions computed for a factorized K-BKZ fluid with potential function $W(I_1, I_2)$ given by Eq. 8.3-19 and the memory function $M(s)$ by Eq. 8.3-35: (*a*) viscosity.

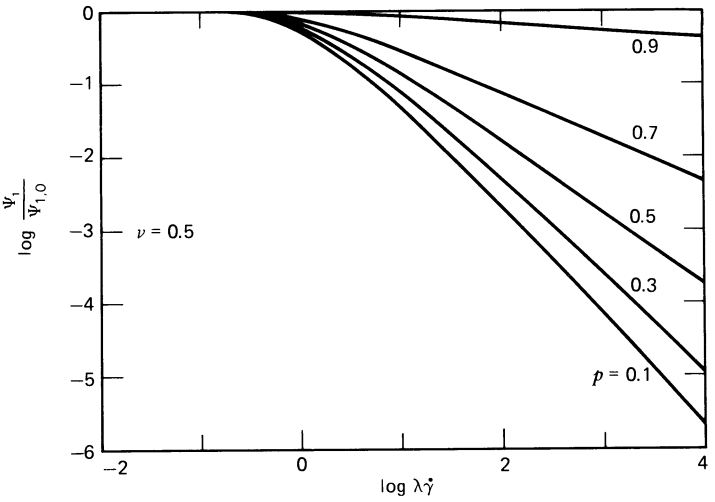

(*b*)

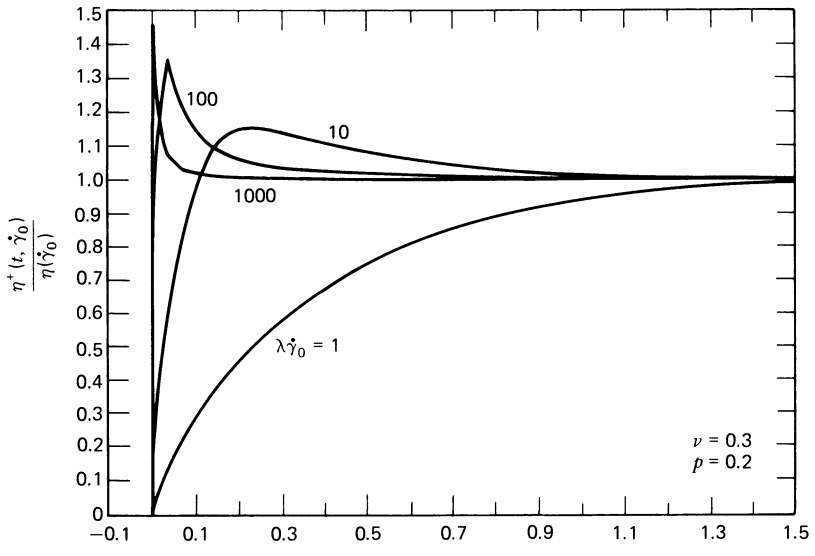

(*c*)

FIGURE 8.3-3. (*b*) first normal stress coefficient; (*c*), stress growth functions.

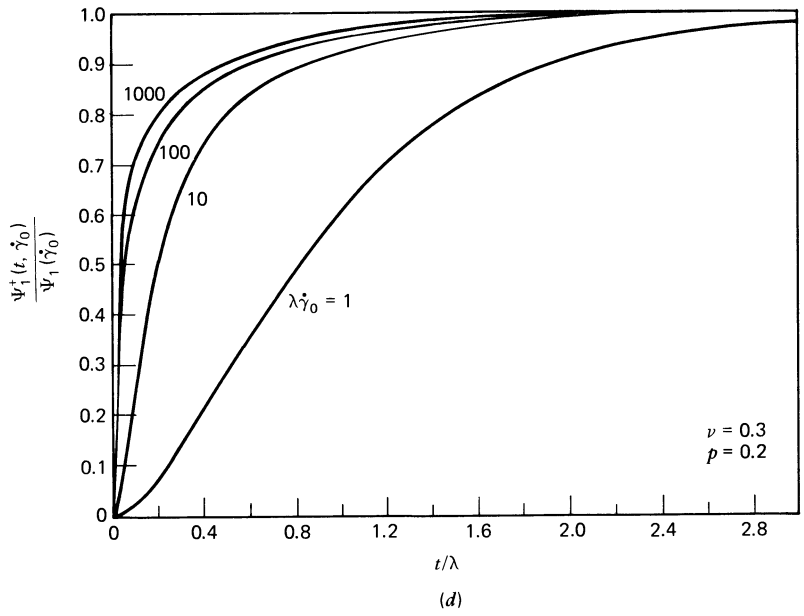

(*d*)

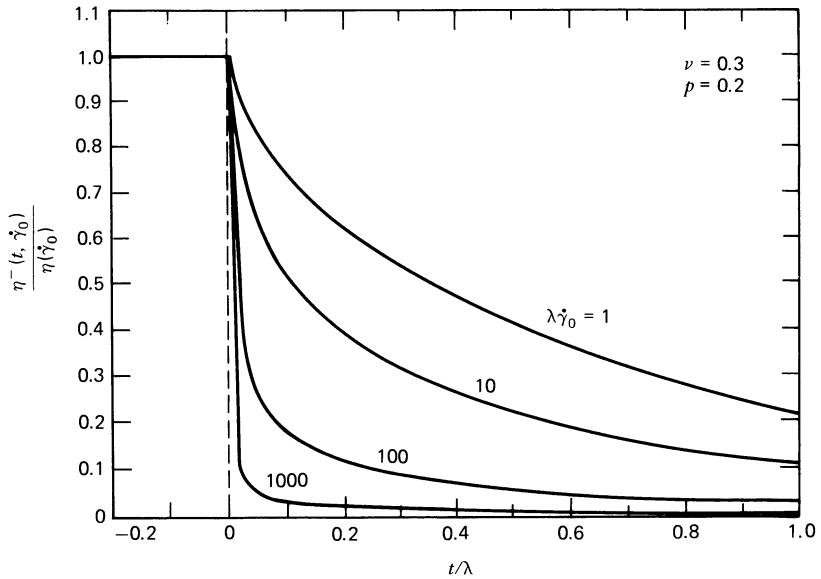

(*e*)

FIGURE 8.3-3. (*d*) stress growth functions; (*e*) stress relaxation functions.

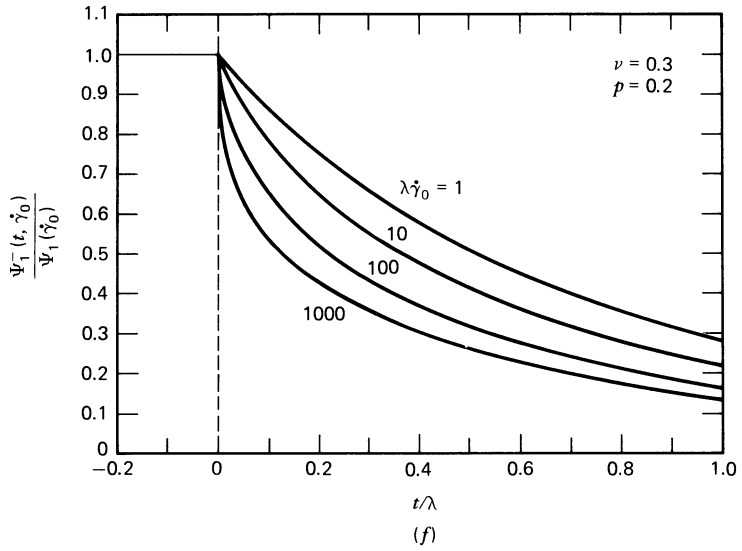

(*f*)

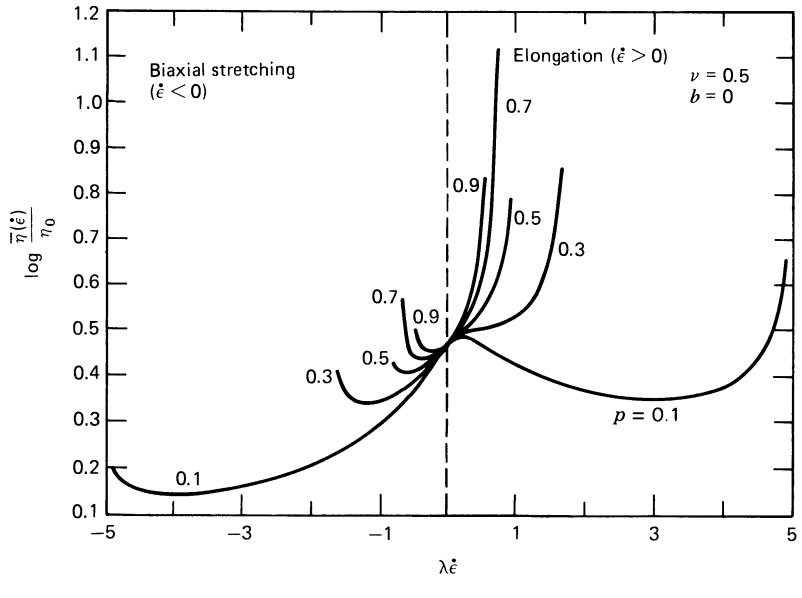

(*g*)

FIGURE 8.3-3. (*f*) stress relaxation functions; (*g*) elongational viscosity ($b = 0$).

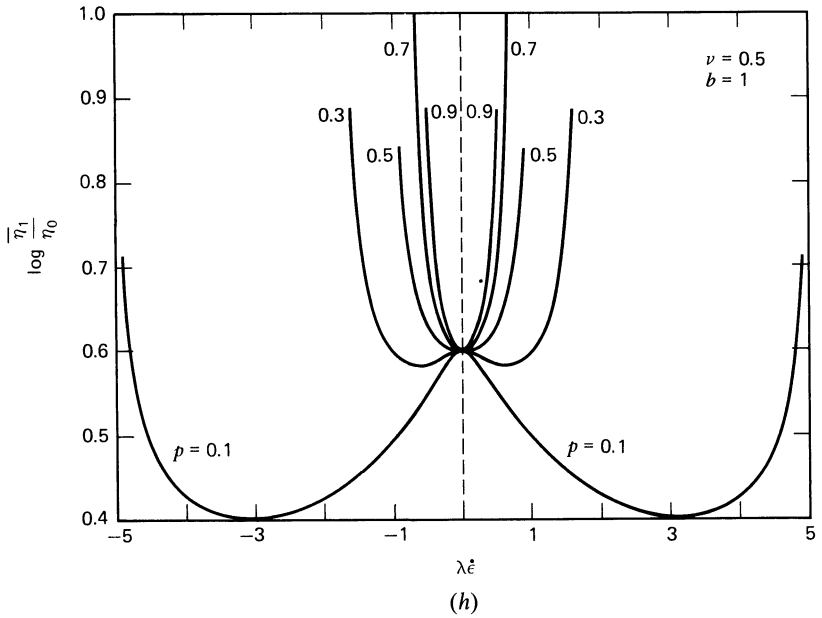

(*h*)

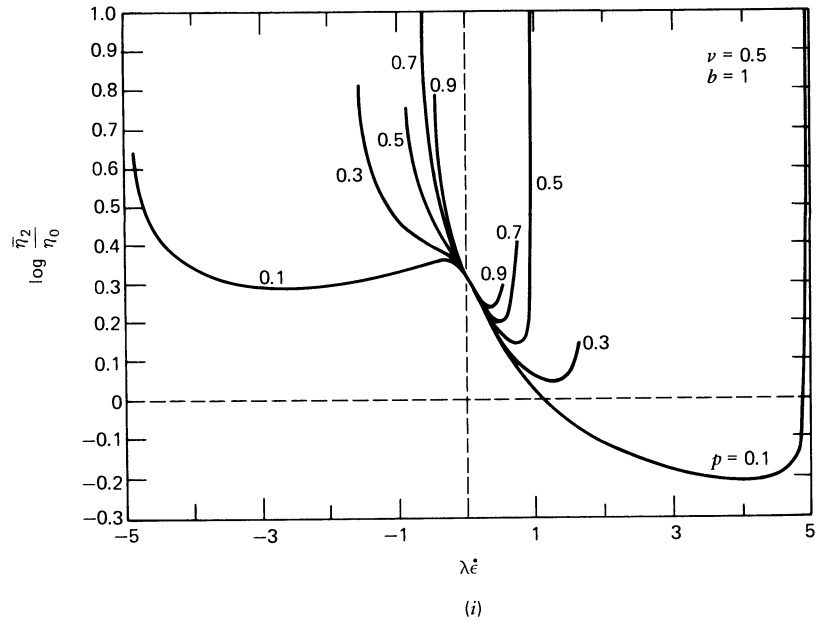

(*i*)

FIGURE 8.3-3. (*h*), (*i*) planar elongational viscosities ($b = 1$). Note in (*h*) that $\bar{\eta}_1(-\dot{\varepsilon}) = \bar{\eta}_1(\dot{\varepsilon})$, and in (*i*) that $\bar{\eta}_2(-\dot{\varepsilon}) = -\bar{\eta}_2(\dot{\varepsilon}) + \bar{\eta}_1(\dot{\varepsilon})$. [Curves calculated by S. R. Burdette.]

EXAMPLE 8.3-2 The Wagner Model

The most carefully tested constitutive equation of the Rivlin-Sawyers type is the Wagner model given in Table 8.3-3. Wagner called $\phi_1(I_1, I_2)$ the "damping function," since it describes the diminishing of the fluid memory by the various kinematic events of the past. Obtain the shear flow and steady elongational flow material functions for this model if $M(t - t')$ is given as a sum of exponentials as in Eq. 8.2-4. Show how the model parameters can be obtained from shear flow experiments.

SOLUTION **(a)** Shear Flow ($v_x = \dot{\gamma}_{yx}(t)y$, $v_y = 0$, $v_z = 0$)
For the particular choice of ϕ_1 in Table 8.3-3 we find for shearing flows

$$\phi_1(I_1, I_2) = e^{-\beta|\gamma_{yx}|} \tag{8.3-41}$$

since $I_1 = I_2 = 3 + \gamma^2_{yx}$ for these flows. A convenient method for determining ϕ_1 is from stress relaxation following a step shear strain of magnitude γ_0 (cf. Table 3.4-1e and §3.4, Experiment e). For the step strain experiment $\gamma_{yx}(t, t') = -\gamma_0[1 - H(t')]$ if the step strain is applied at time $t = 0$; here $H(t)$ is the Heaviside unit step function. By inserting this expression for γ_{yx} into the Wagner model we find

$$\begin{aligned}\tau_{yx} &= \int_{-\infty}^{t} M(t - t')\phi_1(|\gamma_{yx}|)\gamma_{yx}(t, t')dt' \\ &= -\gamma_0 \int_{-\infty}^{0} M(t - t')dt'\phi_1(\gamma_0) \\ &= -\gamma_0 G(t)\phi_1(\gamma_0)\end{aligned} \tag{8.3-42}$$

where $\gamma_{[0]}$ is obtained from Appendix C. Here we have used the facts that $M(t - t') = \partial G(t - t')/\partial t'$ and that $G(t) \to 0$ as $t \to \infty$. Equation 8.3-42 shows that the nonlinear relaxation modulus (Table 3.4-1e) can be factored into a function of time alone and a function of strain alone

$$G(t, \gamma_0) = G(t)\phi_1(\gamma_0) \tag{8.3-43}$$

Experimental data (cf. Figs. 3.4-15 and 16) show that this factorization[12] is indeed observed, except perhaps at very short times, and this provides a justification for the factorization of the K-BKZ and Rivlin-Sawyers models introduced in Eqs. 8.3-11 and 12. The function $G(t)$, which is the linear viscoelastic relaxation modulus, can be determined from the top curve ($\gamma_0 \to 0$) in Fig. 3.4-15 (or from other linear viscoelastic experiments). The strain-dependent part describes the vertical displacement of the relaxation curves in Figs. 3.4-15 and 16. By shifting the large γ_0 curves in Fig. 3.4-15 so as to make them overlap with the top, linear viscoelastic curve, we obtain $\phi_1(\gamma_0)$ as shown in Fig. 8.3-4.

When ϕ_1 is given by the single exponential in Eq. 8.3-41, the data in Fig. 8.3-4 are well described[13] for $\gamma_0 \leq 10$ by $\beta = 0.18$ (dashed curve). In order to improve the description of ϕ_1 for shear flows, Wagner has also used a two-exponential function

$$\phi_1 = ce^{-\beta_1|\gamma_{yx}|} + (1 - c)e^{-\beta_2|\gamma_{yx}|} \tag{8.3-44}$$

where c, β_1, and β_2 are constants. This functional form does not apply to flows other than shearing flow. Fitting Eq. 8.3-44 to the data in Fig. 8.3-4 results in $c = 0.57$, $\beta_1 = 0.31$, and $\beta_2 = 0.106$, which is seen to give a good description of the data for shear strains up to 30. To finish determining the model,

[12] "Strain-time" factorization is also observed for step strain biaxial stretching flows. See P. R. Soskey and H. H. Winter, *J. Rheol.*, **29**, 493-517 (1985), and A. C. Papanastasiou, L. E. Scriven, and C. W. Macosko, *J. Rheol.*, **27**, 387-410 (1983).

[13] M. H. Wagner, *Rheol. Acta*, **15**, 136-142 (1976); **16**, 43-50 (1977); H. M. Laun, *Rheol. Acta*, **17**, 1-15 (1978).

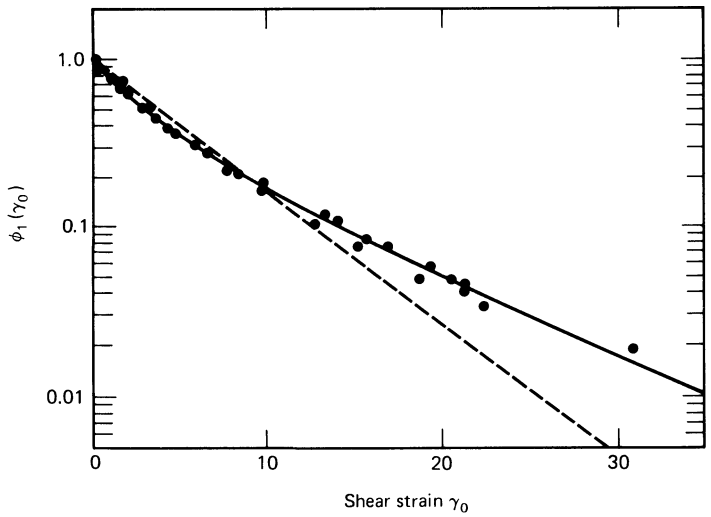

FIGURE 8.3-4. The damping function ϕ_1 as a function of shear strain γ_0 obtained by vertical shifting of the relaxation curves in Fig. 3.4-15. The dashed line corresponds to Eq. 8.3-41 and the solid line to Eq. 8.3-44. [H. M. Laun, *Rheol. Acta*, **17**, 1-15 (1978).]

we must fit $M(t - t')$. This can be done from linear viscoelastic experiments as shown in Example 5.3-7.

It is now of interest to compare the Wagner model predictions with other nonlinear shear flow material functions. We use Eq. 8.3-41 for ϕ_1 to illustrate the calculation of material functions. For steady shear flow with shear rate $\dot{\gamma}$, we have $|\gamma_{yx}| = \dot{\gamma}(t - t')$ so that (with $s = t - t'$)

$$\eta(\dot{\gamma}) = \int_0^\infty M(s)e^{-\beta\dot{\gamma}s}\, s\, ds \tag{8.3-45}$$

$$\Psi_1(\dot{\gamma}) = \int_0^\infty M(s)e^{-\beta\dot{\gamma}s}s^2\, ds \tag{8.3-46}$$

$$\Psi_2(\dot{\gamma}) = 0 \tag{8.3-47}$$

Note that these equations suggest that $\Psi_1(\dot{\gamma}) = -(1/\beta)(d\eta/d\dot{\gamma})$. When $M(s)$ is given as a sum of exponentials the integrals can be performed to give

$$\eta(\dot{\gamma}) = \sum_{p=1}^{\infty} \frac{\eta_p}{(1 + \beta\lambda_p\dot{\gamma})^2} \tag{8.3-48}$$

$$\Psi_1(\dot{\gamma}) = 2\sum_{p=1}^{\infty} \frac{\eta_p\lambda_p}{(1 + \beta\lambda_p\dot{\gamma})^3} \tag{8.3-49}$$

for the shear rate dependence of η and Ψ_1. These predictions with η_p and λ_p given by Table 5.3-2, and $\beta = 0.18$ are compared with experimental data in Fig. 3.3-2 (dashed curves). For comparison, the corresponding predictions for the two-exponential ϕ_1 are shown in Fig. 3.3-2 as the solid curve. Only a minor improvement at large shear rates in the description of Ψ_1 is obtained from the two-exponential form. Similarly, other nonlinear shear flow material functions can be calculated with Eqs. 8.3-41 and 44, and comparisons[13] of some of these with experimental data are given in Figs. 3.4-17 and 19 to 21.

(b) Steady Elongational Flow ($v_x = -\frac{1}{2}\dot{\varepsilon}x$, $v_y = -\frac{1}{2}\dot{\varepsilon}y$, $v_z = \dot{\varepsilon}z$)
For this flow (with $I_1 = 2e^{-\dot{\varepsilon}s} + e^{2\dot{\varepsilon}s}$ and $I_2 = 2e^{\dot{\varepsilon}s} + e^{-2\dot{\varepsilon}s}$) the damping function is

$$\phi_1 = \exp\left[-\beta\sqrt{\alpha(2e^{-\dot{\varepsilon}s} + e^{2\dot{\varepsilon}s}) + (1-\alpha)(2e^{\dot{\varepsilon}s} + e^{-2\dot{\varepsilon}s}) - 3}\right] \tag{8.3-50}$$

The steady elongational viscosity $\bar{\eta}(\dot{\varepsilon})$ is then obtained as

$$\bar{\eta}(\dot{\varepsilon}) = \frac{1}{\dot{\varepsilon}}\int_0^\infty \left\{\sum_{p=1}^{\infty}\frac{\eta_0}{\lambda_p^2}e^{-s/\lambda_p}\right\}\phi_1(e^{2\dot{\varepsilon}s} - e^{\dot{\varepsilon}s})ds \tag{8.3-51}$$

This integral must be done numerically.

Wagner has shown how a combination of shear flow data and transient elongational flow data can be used to obtain the parameter α in the damping function.[14] The ability of the Wagner model to fit a wide variety of shear and elongational flow material functions with only two parameters, α and β, to describe the nonlinear part of the memory function, is impressive.

EXAMPLE 8.3-3 The Doi-Edwards Constitutive Equation

In Volume 2 we consider constitutive equations derived from molecular theory. In Chapter 19 the Curtiss-Bird theory of polymer melts is given. The single-integral constitutive equation obtained in this theory does not fall within the categories listed in Tables 8.3-2 and 3. However a special case of the equation, namely with $\varepsilon = 0$ in Eq. 19.6-9, known as the Doi-Edwards equation, is of the factorized K-BKZ form; see Table 8.3-2 for the potential function for this model. Insert the potential for the Doi-Edwards model from Table 8.3-2 into the K-BKZ model and rewrite the resulting model in terms of $\mathbf{B}^{-1}$.

SOLUTION We use the form of the potential with the E_{ij} shown explicitly. This form is then differentiated with respect to E_{jk} and we form the combination

$$\frac{1}{2}\sum_k E_{ik}\frac{\partial W}{\partial E_{jk}} = \frac{5}{4\pi}\int\frac{\sum_k\sum_m E_{ik}u_k E_{jm}u_m}{\sum_k\sum_m\sum_n E_{nk}u_k E_{nm}u_m}\,d\boldsymbol{u} \tag{8.3-52}$$

Keep in mind that $\boldsymbol{u}$ is a unit vector and $\int\ldots d\boldsymbol{u}$ is shorthand for an integration over the surface of a unit sphere. Note that the expression on the right is symmetric in "i" and "j" as it should be. We then insert this expression into Eq. 8.3-18, which is in turn inserted into the K-BKZ equation to obtain the constitutive equation:[15]

$$\boldsymbol{\tau}(t) = -\frac{5}{4\pi}\int_{-\infty}^{t} M(t-t')\int\hat{\boldsymbol{u}}\hat{\boldsymbol{u}}\,d\boldsymbol{u}\,dt' \tag{8.3-53}$$

where

$$\hat{\boldsymbol{u}} = [\mathbf{E}\cdot\boldsymbol{u}]/|\mathbf{E}\cdot\boldsymbol{u}| \tag{8.3-54}$$

is a unit vector. The two vertical bars in the denominator of Eq. 8.3-54 indicate the magnitude of the vector (see Eq. A.2-17). Note that the strain dependence enters through the displacement gradient tensor $\mathbf{E}(t, t')$. In order to rewrite the constitutive equation in a form containing the strain tensors, we must perform a transformation of variables in the integration over the unit sphere. Specifically we

[14] M. H. Wagner, *Rheol. Acta*, **18**, 33-50, 427-428 (1979); *J. Non-Newtonian Fluid Mech.*, **4**, 39-55 (1978).
[15] R. B. Bird, H. H. Saab, and C. F. Curtiss, *J. Chem. Phys.*, **77**, 4747-4757 (1982); see also Eq. 19.6-9.

wish to transform from the spherical coordinates θ, ϕ of the unit vector $\boldsymbol{u} = \boldsymbol{u}(\theta, \phi)$ to the spherical coordinates $\hat{\theta}$, $\hat{\phi}$ of the unit vector $\hat{\boldsymbol{u}} = \hat{\boldsymbol{u}}(\hat{\theta}, \hat{\phi})$, related to $\boldsymbol{u}$ through Eq. 8.3-54. To do this we need the Jacobian of the transformation (see Problem 8D.1), and we then obtain

$$d\boldsymbol{u} = \frac{\det \boldsymbol{\Delta}}{|\boldsymbol{\Delta} \cdot \hat{\boldsymbol{u}}|^3} d\hat{\boldsymbol{u}} \tag{8.3-55}$$

where $d\boldsymbol{u} = \sin\theta \, d\theta \, d\phi$ and $d\hat{\boldsymbol{u}} = \sin\hat{\theta} \, d\hat{\theta} \, d\hat{\phi}$, and $\boldsymbol{\Delta}$ is the tensor inverse to $\mathbf{E}$. We recall from §8.1 that the determinants of $\mathbf{E}$ and $\boldsymbol{\Delta}$ are equal to unity for incompressible fluids. When this is taken into account and Eq. 8.3-55 is inserted into Eq. 8.3-53 we obtain

$$\boldsymbol{\tau} = -\frac{5}{4\pi} \int_{-\infty}^{t} M(t - t') \int \frac{\hat{\boldsymbol{u}}\hat{\boldsymbol{u}}}{|\boldsymbol{\Delta} \cdot \hat{\boldsymbol{u}}|^3} d\hat{\boldsymbol{u}} \, dt' \tag{8.3-56}$$

If we introduce the expression for the magnitude of the vector in the denominator as the square root of the scalar product of the vector with itself we find that the equation may finally be rewritten as[15]

$$\boldsymbol{\tau} = -\frac{5}{4\pi} \int_{-\infty}^{t} M(t - t') \int \frac{\boldsymbol{u}\boldsymbol{u}}{(\mathbf{B}^{-1} : \boldsymbol{u}\boldsymbol{u})^{3/2}} d\boldsymbol{u} \, dt' \tag{8.3-57}$$

in which we have dropped the circumflex on the integration variable. In this form the deformation history enters through the finite strain tensor $\mathbf{B}^{-1}(t, t')$. In this example we have shown how the constitutive equation for the Doi-Edwards model may be written in three different ways. The form in Eq. 8.3-53 has been used in calculations of shear flow properties,[16] and the form in Eq. 8.3-57 has been used in calculations of elongational flow properties.[17]

EXAMPLE 8.3-4 The Approximate Currie Potential for the Doi-Edwards Model

The following approximate potential function[18] for the Curtiss-Bird ($\varepsilon = 0$) or Doi-Edwards constitutive equation has been used in numerical simulations[19] of viscoelastic flows:

$$W(J) = 5 \ln (J - 1) \tag{8.3-58}$$

where

$$J = I_1 + 2(I_2 + \tfrac{13}{4})^{1/2} \tag{8.3-59}$$

Derive the corresponding approximate constitutive equation and investigate its properties in steady simple shear flow.

SOLUTION The approximate constitutive equation is obtained by substituting Eqs. 8.3-58 and 8.3-59 into Eq. 8.3-11,

$$\boldsymbol{\tau} = 5 \int_{-\infty}^{t} \frac{M(t - t')}{(J - 1)} \left[\boldsymbol{\gamma}_{[0]} + (I_2 + \tfrac{13}{4})^{-1/2} \boldsymbol{\gamma}^{[0]} \right] dt' \tag{8.3-60}$$

[16] H. H. Saab, R. B. Bird, and C. F. Curtiss, *op. cit.*, pp. 4758-4766.

[17] R. B. Bird, H. H. Saab, and C. F. Curtiss, *J. Phys. Chem.*, **86**, 1102-1106 (1982); see also Eq. 19.6-9.

[18] This example is based on P. K. Currie, *J. Non-Newtonian Fluid Mech.*, **11**, 53-68 (1982).

[19] B. Bernstein, D. S. Malkus, and E. T. Olsen, *Int. J. Num. Meth. Fluids*, **5**, 43-70 (1985); D. S. Malkus and B. Bernstein, *J. Non-Newtonian Fluid Mech.*, **16**, 77-116 (1984); S. Dupont, J. M. Marchal, and M. J. Crochet, *J. Non-Newtonian Fluid Mech.*, **17**, 157-183 (1985).

Now for steady shear flow with shear rate $\dot{\gamma}$ we find

$$J = 3 + (\dot{\gamma}s)^2 + (25 + 4(\dot{\gamma}s)^2)^{1/2} \tag{8.3-61}$$

The expressions for the shear stress and normal stress differences then become

$$\tau_{yx} = -\left[5\int_0^\infty \frac{M(s)s}{(J-1)}[1 + (I_2 + \tfrac{13}{4})^{-1/2}]ds\right]\dot{\gamma} = -\eta(\dot{\gamma})\dot{\gamma} \tag{8.3-62}$$

$$\tau_{xx} - \tau_{yy} = -\left[5\int_0^\infty \frac{M(s)s^2}{(J-1)}[1 + (I_2 + \tfrac{13}{4})^{-1/2}]ds\right]\dot{\gamma}^2 = -\Psi_1(\dot{\gamma})\dot{\gamma}^2 \tag{8.3-63}$$

$$\tau_{yy} - \tau_{zz} = \left[5\int_0^\infty \frac{M(s)s^2}{(J-1)}(I_2 + \tfrac{13}{4})^{-1/2}\,ds\right]\dot{\gamma}^2 = -\Psi_2(\dot{\gamma})\dot{\gamma}^2 \tag{8.3-64}$$

These expressions plus the memory function $M(s)$ from Table 8.3-2 determine the viscometric functions over the entire range of shear rates. It is rather simple to obtain the viscometric functions in the limit of small shear rates. To do so we let $\dot{\gamma} = 0$ in the integrals in Eqs. 8.3-62, 63, and 64 so that $I_1 = I_2 = 3$ and $J = 8$. We then find

$$\eta_0 = \int_0^\infty M(s)s\,ds = \eta_0 \tag{8.3-65}$$

$$\Psi_{1,0} = \int_0^\infty M(s)s^2\,ds = \tfrac{1}{5}\eta_0\lambda \tag{8.3-66}$$

$$\Psi_{2,0} = -\tfrac{2}{7}\int_0^\infty M(s)s^2\,ds = -\tfrac{2}{35}\eta_0\lambda \tag{8.3-67}$$

In the limit of high shear rates it may be shown that the viscometric functions exhibit power-law behavior corresponding to $\eta \propto \dot{\gamma}^{-3/2}$, $\Psi_1 \propto \dot{\gamma}^{-2}$, and $\Psi_2 \propto \dot{\gamma}^{-5/2}$.

Even though we have used an approximate expression for the potential, the zero-shear-rate values in Eqs. 8.3-65, 66, and 67 are exact. The ratio of $\Psi_{2,0}/\Psi_{1,0} = -\frac{2}{7}$ means that the Curtiss–Bird ($\varepsilon = 0$) or Doi–Edwards equation incorrectly predicts a depression in the free surface of a fluid near a rotating rod (see Table 6.5-1).[20] Also since the viscosity drops faster than $(\lambda\dot{\gamma})^{-1}$ with shear rate, the equation cannot describe shear flow above a certain critical shear rate.

§8.4 FLOW PROBLEMS IN ONE SPATIAL VARIABLE

In this section we illustrate the solution of flow problems with two examples. In Example 8.4-1 we consider the steady flow of a viscoelastic fluid into a line sink, and in Example 8.4-2 we consider the transient inflation of a spherical viscoelastic film. The particular situations have been chosen for their simplicity and for illustrating two main techniques for the solution of flow problems with integral constitutive equations. We shall refer to these as the Eulerian technique and the Lagrangian technique, respectively.

In the *Eulerian technique*, illustrated in the first example, the dependent variables are the velocity, pressure, and stress. Since the velocity does not enter explicitly into the integral constitutive equation, we must guess a form for the velocity field and then use this guess to

[20] O. Hassager, *J. Rheol.*, **29**, 361–364 (1985).

evaluate the displacement functions and subsequently the stress components. Finally we combine the stress tensor obtained in this way with the equation of motion and attempt to satisfy the resulting equation by suitable choice of adjustable constants or functions in the assumed velocity field.

By contrast in the *Lagrangian technique*, illustrated in the second example, the dependent variables are the particle positions (displacement functions), pressure, and stress. Since an integral constitutive equation can be written explicitly in terms of the displacement functions, these can be combined with the equations of motion to give one or more integro-differential equations for the particle positions as functions of time. The result is an initial value problem in which the particle motion can be determined by forward integration from some time at which the entire past flow history is known.

In certain simple situations analytical solutions may be obtained from the steady Eulerian technique. By contrast the integro-differential equations obtained in the Lagrangian technique must almost always be solved numerically. Note also that whereas applying the Eulerian technique to steady and unsteady problems results in time-independent and time-dependent differential equations, respectively, the Lagrangian technique always results in an unsteady problem. More will be said about these techniques in §8.5; we turn now to the examples. These examples are chosen so that inversion of the displacement functions to calculate $\gamma_{[0]}$ is trivial; a problem in which this inversion is nontrivial is given in Example 10.1-2.

EXAMPLE 8.4-1 Flow of a Viscoelastic Fluid into a Line Sink

Consider the steady two-dimensional plane flow of a Lodge rubberlike liquid (Eq. 8.2-1) moving radially towards the z-axis in a cylindrical coordinate system. Find the velocity field and find the distribution of stresses and pressure in the fluid. Neglect gravitational effects.

SOLUTION We begin by postulating a form for the velocity field: $v_r = v_r(r)$, $v_\theta = 0$, $v_z = 0$. In the cylindrical coordinate system the equation of continuity reduces to

$$\frac{d}{dr}(rv_r) = 0 \tag{8.4-1}$$

This equation may immediately be integrated once to give

$$v_r = -\frac{K}{r} \tag{8.4-2}$$

where K is a constant of integration, and $K \geq 0$ since we assume that the velocity is towards the axis. From an integration over a cylindrical volume of length L and radius r (Fig. 8.4-1) it may be seen that $K = Q/2\pi L$ where Q is the volume rate of flow into the sink. The r-component of Eq. 8.1-14 for the displacement function now reads

$$\frac{dr}{dt} = -\frac{K}{r} \tag{8.4-3}$$

which is to be solved subject to the condition that $r = r'$ at $t = t'$. The final results for the displacement functions then become

$$r = \sqrt{r'^2 - 2K(t - t')}; \quad \theta = \theta'; \quad z = z' \tag{8.4-4}$$

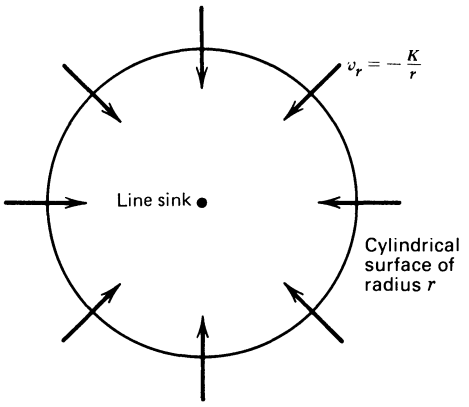

FIGURE 8.4-1. Axisymmetrical flow into a line sink. The volume rate of flow through a cylindrical surface of radius r and length L is $Q = 2\pi KL$.

With these displacement functions we see from Eqs. B.6-7 through 12 that the only nonzero components of $\gamma_{[0]}$ are

$$\gamma_{[0]rr} = 1 - \left(\frac{\partial r}{\partial r'}\right)^2 = -\frac{2K(t-t')}{r^2} \tag{8.4-5a}$$

$$\gamma_{[0]\theta\theta} = 1 - \left(\frac{r}{r'}\frac{\partial \theta}{\partial \theta'}\right)^2 = \frac{2K(t-t')}{r^2 + 2K(t-t')} \tag{8.4-5b}$$

Notice that after the differentiations have been performed, the strain tensor components must be rewritten so that only r, t, and t' appear in the expressions. In order to do this it is necessary to invert the displacement functions in Eq. 8.4-4. When these quantities are substituted into the constitutive equation (Eq. 8.2-1) and when the variable $s = t - t'$ is used, the only nonzero stress tensor components are

$$\tau_{rr}(r) = -\frac{2K}{r^2}\int_0^\infty M(s)\, s\, ds \tag{8.4-6}$$

$$\tau_{\theta\theta}(r) = 2K\int_0^\infty M(s)\frac{s}{r^2 + 2Ks}\, ds \tag{8.4-7}$$

where $s = t - t'$. In the expression for $\tau_{\theta\theta}$ we see why we need to have $K \geq 0$, and that radial flow out from a line source (with $K < 0$) may not be described.

With the above components of the stress tensor, the θ- and z-components of the equation of motion may be satisfied identically by $p = p(r)$, and the radial component of the equation of motion then gives

$$\frac{dp}{dr} = -\rho v_r \frac{dv_r}{dr} - \left(\frac{1}{r}\frac{d}{dr}(r\tau_{rr})\right) + \frac{\tau_{\theta\theta}}{r}$$

$$= +\frac{\rho K^2}{r^3} + 2K\int_0^\infty M(s)s\left[-\frac{1}{r^3} + \frac{1}{r(r^2 + 2Ks)}\right]ds \tag{8.4-8}$$

This is a first-order, separable differential equation for $p(r)$, which may be integrated with the boundary condition that $p = p_\infty$ at $r = \infty$, to give

$$p(r) = p_\infty - \frac{\rho K^2}{2r^2} + \int_0^\infty M(s)\left[\frac{Ks}{r^2} - \tfrac{1}{2}\ln\left(1 + \frac{2Ks}{r^2}\right)\right]ds \tag{8.4-9}$$

and then combination of Eqs. 8.4-6 and 9 gives for π_{rr}

$$\pi_{rr}(r) = p_\infty - \frac{\rho K^2}{2r^2} - \int_0^\infty M(s)\left[\frac{Ks}{r^2} + \tfrac{1}{2}\ln\left(1 + \frac{2Ks}{r^2}\right)\right]ds \tag{8.4-10}$$

This is the general solution to the line-sink flow problem with arbitrary memory function $M(s)$. It is interesting to specialize the above solution to the expression given in Eq. 8.2-3 corresponding to the convected Jeffreys model. We then find

$$\pi_{rr} \sim p_\infty - [\mathrm{Re} + 2 - (1 - (\lambda_2/\lambda_1))](\eta_0 K/r^2) \qquad (r \to 0) \tag{8.4-11}$$

$$\pi_{rr} \sim p_\infty - (\mathrm{Re} + 2)(\eta_0 K/r^2) \qquad (r \to \infty) \tag{8.4-12}$$

where $\mathrm{Re} = \rho K/2\eta_0$ is the Reynolds number. Recall that when $\lambda_2/\lambda_1 = 1$ the convected Jeffreys model becomes a Newtonian fluid, and when $\lambda_2/\lambda_1 = 0$ it becomes a convected Maxwell fluid. We see that $d\pi_{rr}/dr$ near the sink is predicted to be somewhat smaller for an elastic fluid than for a viscous fluid. Moreover we see in Eq. 8.4-11 that inertial (Re), viscous (2), and elastic $(1 - (\lambda_2/\lambda_1))$ terms all have the same r-dependence close to the sink. This latter conclusion is in remarkable contrast with that obtained from the solution of the same flow problem with the third-order fluid (Problem 6B.5) where terms associated with elasticity always dominate inertial and viscous terms close to the sink, and the solution becomes physically unacceptable.

See Problem 8C.1 for the flow from the infinite half space into a line sink located in a plane.

EXAMPLE 8.4-2 Transient Inflation of a Spherical Viscoelastic Film[1]

Consider a thin spherical viscoelastic film forming a bubble initially of radius r_0 and thickness Δr_0 such that $\Delta r_0/r_0 \ll 1$ (Fig. 8.4-2). The bubble has been at rest for a long time with its interior filled with a gas of pressure $p_{g,0}$ equal to the surrounding pressure. At time $t = 0$ the external pressure is suddenly removed, and the bubble begins to expand. It is desired to formulate an integro-differential equation from which the radius of the film may be calculated as function of time. For illustrative purposes use a Lodge rubberlike liquid with the memory function corresponding to the convected Jeffreys model in Eq. 8.2-3. Neglect inertial effects.

SOLUTION We first write the convected Jeffreys model in the form

$$\tau(t) = -\eta_0 \frac{\lambda_2}{\lambda_1}\gamma_{(1)} + \frac{\eta_0}{\lambda_1^2}\left(1 - \frac{\lambda_2}{\lambda_1}\right)\int_{-\infty}^{t} e^{-(t-t')/\lambda_1}\gamma_{[0]}(t, t')dt' \tag{8.4-13}$$

We then introduce a spherical coordinate system and label the coordinates of a typical fluid particle P by r, θ, ϕ at the present time t and by r', θ', ϕ' at a past time t' (see Fig. 8.4-2). From symmetry

[1] For discussions of the related problems of bubble growth and collapse in an infinite sea of liquid see H. Lamb, *Hydrodynamics*, 6th ed., Cambridge University Press (1932), p. 122, and G. K. Batchelor, *An Introduction to Fluid Dynamics*, Cambridge University Press (1967), pp. 486–490. A treatment of the mass-transfer process coupled with the rheological problem has been given in a paper on the dissolution of a gas bubble in a viscoelastic fluid by E. Zana and L. G. Leal, *Ind. Eng. Chem. Fundam.*, **14**, 175–182 (1975). See also J. R. Street, *Trans. Soc. Rheol.*, **12**, 103–131 (1968), and A. C. Papanastasiou, L. E. Scriven, and C. W. Macosko, *J. Non-Newtonian Fluid Mech.*, **16**, 53–75 (1984).

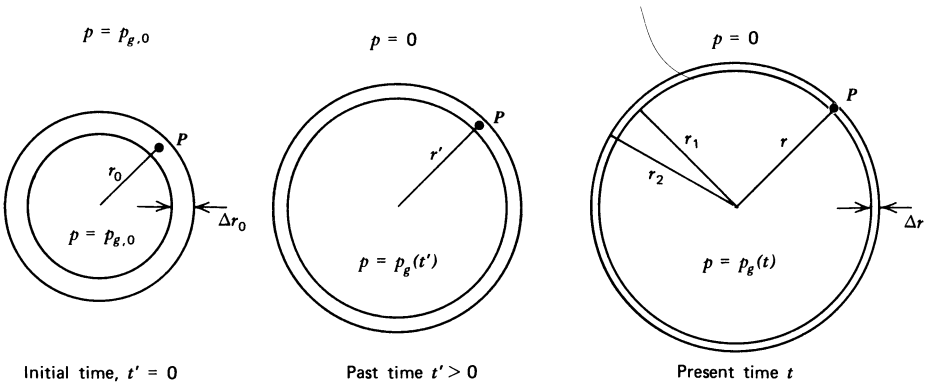

FIGURE 8.4-2. Cross section of a thin viscoelastic film forming a bubble filled with a gas. The bubble is initially at equilibrium with the inside gas pressure equal to the surrounding pressure. At time $t' = 0$ the external pressure is set equal to zero and the bubble expands.

considerations we see that the r-component of the equation of motion in spherical coordinates simplifies for creeping flow to

$$0 = -\frac{\partial p}{\partial r} - \left(\frac{1}{r^2}\frac{\partial}{\partial r}(r^2\tau_{rr}) - \frac{\tau_{\theta\theta} + \tau_{\phi\phi}}{r} \right) \tag{8.4-14}$$

Hence the pressure drop across the film is

$$p_g = -\int_{r_1}^{r_2} \frac{\partial}{\partial r}(p + \tau_{rr})dr = \int_{r_1}^{r_2} \frac{2\tau_{rr} - \tau_{\theta\theta} - \tau_{\phi\phi}}{r}\,dr \doteq (2\tau_{rr} - \tau_{\theta\theta} - \tau_{\phi\phi})\frac{\Delta r}{r} \tag{8.4-15}$$

In the last expression we have introduced the approximation that the stress tensor is constant across the thin film. Let us now calculate the components of the kinematic tensors $\gamma_{(1)}$ and $\gamma_{[0]}$. From Table B.3 we find

$$\gamma_{(1)} = 2\begin{pmatrix} \frac{\partial v_r}{\partial r} & 0 & 0 \\ 0 & \frac{v_r}{r} & 0 \\ 0 & 0 & \frac{v_r}{r} \end{pmatrix} = 2\begin{pmatrix} -2 & 0 & 0 \\ 0 & 1 & 0 \\ 0 & 0 & 1 \end{pmatrix}\frac{1}{r}\frac{dr}{dt} \tag{8.4-16}$$

In the last step of Eq. 8.4-16 we have used the incompressibility condition for the viscoelastic liquid in the film in the form $\text{tr}\,\gamma_{(1)} = 0$. Note also that we have expressed the velocity component as the time derivative of the displacement function. Similarly from Table B.6 we find

$$\begin{aligned} \gamma_{[0]} &= \begin{pmatrix} 1 - \left(\frac{\partial r}{\partial r'}\right)^2 & 0 & 0 \\ 0 & 1 - \left(\frac{r}{r'}\right)^2 & 0 \\ 0 & 0 & 1 - \left(\frac{r}{r'}\right)^2 \end{pmatrix} \\ &= \begin{pmatrix} 1 - \left(\frac{r'}{r}\right)^4 & 0 & 0 \\ 0 & 1 - \left(\frac{r}{r'}\right)^2 & 0 \\ 0 & 0 & 1 - \left(\frac{r}{r'}\right)^2 \end{pmatrix} \end{aligned} \tag{8.4-17}$$

In the last step we have again made use of the incompressibility condition for the viscoelastic liquid, this time in the form $\det(\boldsymbol{\delta} - \boldsymbol{\gamma}_{[0]}) = \det \mathbf{B} = 1$.

Before we combine Eqs. 8.4-16 and 17 with Eq. 8.4-15 we need expressions for Δr and $p_g(t)$ as functions of r. First Δr is obtained from the conservation of liquid in the film

$$r^2 \Delta r = r_0^2 \Delta r_0 \tag{8.4-18}$$

We now approximate the thermodynamic equation of state for the gas inside the bubble by an ideal gas law and assume adiabatic expansion so that

$$p_g(t)V^\gamma = p_{g,0}V_0^\gamma \quad \text{or} \quad p_g(t)r^{3\gamma} = p_{g,0}r_0^{3\gamma} \tag{8.4-19}$$

in which $\gamma = \hat{C}_p/\hat{C}_v$. When Eqs. 8.4-13, 16, 17, 18, and 19 are combined with Eq. 8.4-15 we obtain the desired integro-differential equation for $r(t)$. In dimensionless form this equation may be written

$$\frac{dx}{d\tau} = \frac{1}{(\lambda_2/\lambda_1)\beta}\frac{1}{x^\alpha} - \frac{(1-(\lambda_2/\lambda_1))x}{6(\lambda_2/\lambda_1)\mathrm{De}^2}\int_{-\infty}^{\tau}\left[\left(\frac{x(\tau)}{x(\tau')}\right)^2 - \left(\frac{x(\tau)}{x(\tau')}\right)^{-4}\right]e^{-(\tau-\tau')/\mathrm{De}}d\tau' \tag{8.4-20}$$

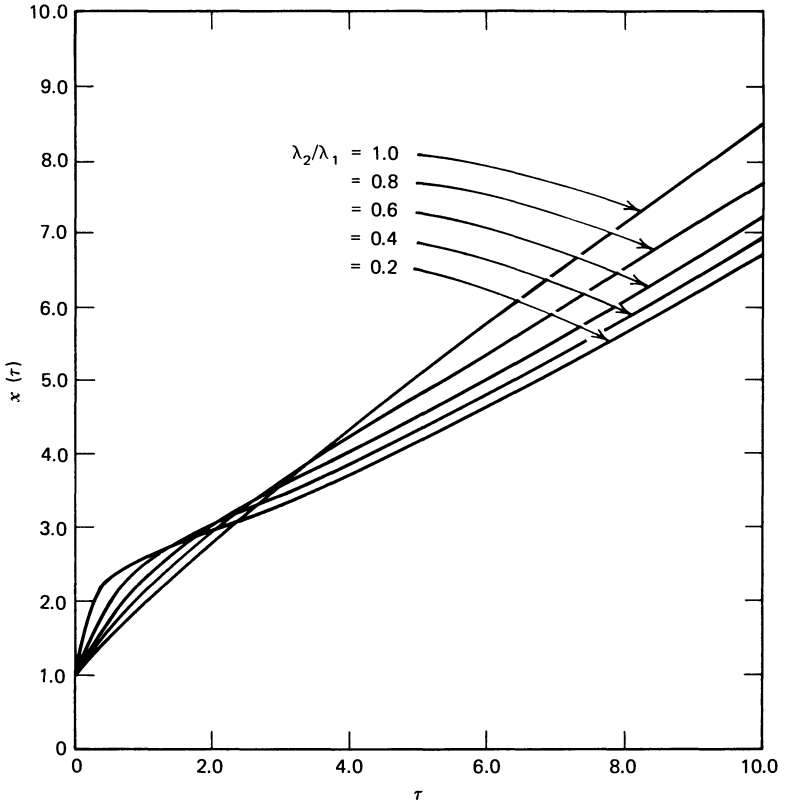

FIGURE 8.4-3. The reduced radius $x(\tau) = r(\tau)/r_0$ versus reduced time $\tau = tp_{g,0}/\eta_0$ as given by the solution of Eq. 8.4-20 for the inflation of a spherical film of a convected Jeffreys model. The parameters are $\alpha = 0.2$, $\beta = 1.0$, and $\mathrm{De} = 2.0$.

where we have introduced the dimensionless quantities

$$x(\tau') = r(t')/r_0 \tag{8.4-21}$$

$$\mathrm{De} = \lambda_1 p_{g,0} \eta_0^{-1}; \quad \tau' = t' p_{g,0} \eta_0^{-1} \tag{8.4-22}$$

$$\alpha = 3\gamma - 4; \quad \beta = 12\Delta r_0/r_0 \tag{8.4-23}$$

Here the Deborah number De is the ratio of the time constant for the fluid (λ_1) to a characteristic time for the process ($\eta_0/p_{g,0}$). Equation 8.4-20 with the condition that $x(\tau') = 1$ for $\tau' \leq 0$ is an initial value problem. For given values of α, β, De, and λ_2/λ_1 we may therefore solve numerically for $x(\tau)$ by a forward integration technique. Figure 8.4-3 shows the reduced radius $x(\tau)$ as a function of the reduced time τ. We have used the values $\alpha = 0.2$ (corresponding to an ideal diatomic gas), $\beta = 1$, De $= 2$, and $\lambda_2/\lambda_1 = 0.2, 0.4, 0.6, 0.8$, and 1.0. We see that a viscoelastic film is predicted to expand somewhat faster than a purely viscous film for small times τ, but that for larger times the viscoelastic film is predicted to expand considerably more slowly than a Newtonian film of the same zero-shear-rate viscosity.

§8.5 FLOW PROBLEMS IN TWO OR THREE SPATIAL VARIABLES

The solution of flow problems in two or three spatial variables for integral models is an area of very active research. The two main techniques, the Eulerian technique and the Lagrangian technique, described in §8.4 are both used in these more complex flow situations. Most research has focused on finite element discretizations to represent velocity, pressure, and displacement fields.

In the *Eulerian technique* a fixed region of space is discretized by a mesh of finite elements. Approximations to the velocity and pressure fields are then constructed from low-order polynomial trial functions on the mesh. The velocity and pressure fields contain the values of velocity and pressure at specified points or "nodes" in the mesh as parameters. Based on the velocity field, the displacement functions and resulting stresses are found, and residuals of the equation of continuity and the equations of motion are computed. Methods are then developed to adjust the velocity and pressure field to minimize a weighted sum of the residuals (cf. §4.3). Some methods[1] have the built-in feature that the equation of continuity is satisfied almost exactly in the final converged solution.

In the *Lagrangian technique*[2] a given amount of fluid is discretized by a mesh of finite elements. Each element node corresponds to a fluid particle, and all fluid particles inside the elements are denoted by unique sets of element coordinates. The motion of the fluid is described by the motion of the element nodes in space. Particles inside the element move with constant element coordinates in a manner determined by the motion of the element nodes. The dependent variables in this Lagrangian discretization then become the coordinates of the element nodes as functions of time and values of the pressure at pressure nodes associated with each element. The object here again is to construct a set of integro-differential equations from which the motion of the nodes may be found by forward integration in time.

[1] B. Bernstein, D. S. Malkus, and E. T. Olsen, *Int. J. Num. Mech. Fluids*, **5**, 43–70 (1985); D. S. Malkus and B. Bernstein, *J. Non-Newtonian Fluid Mech.*, **16**, 77–116 (1984). For other methods see S. Dupont, J. M. Marchal, and M. J. Crochet, *J. Non-Newtonian Fluid Mech.*, **17**, 157–183 (1985); B. Caswell and M. Viryayuthakorn, *J. Non-Newtonian Fluid Mech.*, **12**, 13–29 (1983); H. Court, A. R. Davies, and K. Walters, *J. Non-Newtonian Fluid Mech.*, **8**, 95–117 (1981); M. J. Crochet, A. R. Davies, and K. Walters, *Numerical Simulation of Non-Newtonian Flow*, Elsevier, Amsterdam (1984).

[2] O. Hassager and C. Bisgaard, *J. Non-Newtonian Fluid Mech.*, **12**, 153–164 (1983).

The Eulerian technique seems to have attracted most interest in research developments, possibly because it is somewhat more directly implemented; it has the disadvantage that tracking particles is difficult, since the velocity components rather than the particle positions are used as the dependent variables. The Lagrangian technique, on the other hand, has the advantage that particle tracking is easily and naturally handled.

A detailed discussion of any of the numerical techniques is outside the scope of this textbook. Instead we just give two examples of predictions obtained by the methods. The examples are not problems to be worked step by step, but are intended to illustrate the results obtained.

EXAMPLE 8.5-1 The Hole-Pressure Effect for Flow Across a Transverse Slot

It is desired to illustrate the calculations of the hole-pressure effect for flow across a transverse slot by Malkus and Bernstein,[3] who used the Curtiss-Bird constitutive equation, Eq. 19.6-9, with parameters $\eta_0 = 410$ Pa·s, $\lambda = 9.54$ s, $\varepsilon = 0.375$, and density $\rho = 1363$ kg/m^3. These fluid parameters have been selected to fit measurements of the viscosity function and first normal stress coefficient of a nearly monodisperse solution of polystyrene in a chlorinated biphenyl.[4]

SOLUTION The geometry is shown in Fig. 8.5-1. A fluid is driven by a pressure gradient in the channel, from left to right, and the desired quantity is the "hole pressure"

$$p^* = (\mathscr{P} + \tau_{yy})_1 - (\mathscr{P} + \tau_{yy})_2 \tag{8.5-1}$$

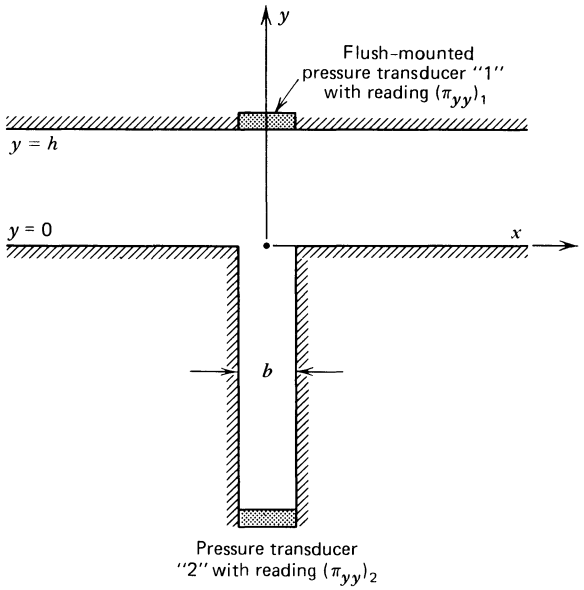

FIGURE 8.5-1. Geometry for plane flow across a transverse slot. Fluid is driven by a pressure gradient from left to right and the velocity field is of the form $v_x = v_x(x, y)$, $v_y = v_y(x, y)$, $v_z = 0$.

[3] D. S. Malkus and B. Bernstein, *J. Non-Newtonian Fluid Mech.*, **13**, 77-116 (1984); corrected calculations have been made by D. S. Malkus, personal communication (1986).

[4] H. H. Saab, R. B. Bird, and C. F. Curtiss, *J. Chem. Phys.*, **77**, 4758-4766 (1982).

Here $(\mathscr{P} + \tau_{yy})_1$ and $(\mathscr{P} + \tau_{yy})_2$ are the values of the total normal stress π_{yy} corrected for gravitational head that are measured by flush-mounted pressure transducers "1" and "2" respectively, located as shown in Fig. 8.5-1. In Fig. 8.5-2 we show the Malkus–Bernstein prediction for p^* as a function of the first normal stress difference $(\tau_{xx} - \tau_{yy})_1$ at the position of pressure transducer "1" based on their numerical solution of the complete flow problem.

In order to facilitate the comparison of the Malkus–Bernstein prediction for p^* with approximate analytical formulas we assume in the following that the slot is sufficiently narrow compared to the channel height ($h \gg b$ in Fig. 8.5-1) that the flow in the neighborhood of pressure transducer "1" is undisturbed by the presence of the slot. Then in the limit of very slow flow, p^* is given by the Tanner and Pipkin analytical relation for second order fluids ($p^* = -(\tau_{xx} - \tau_{yy})/4$; see Eq. 6B.15-1), as shown also in Fig. 8.5-2. The calculations by Malkus and Bernstein[3] cover stress ratios $[(\tau_{xx} - \tau_{yy})/\tau_{yx}]_1$ at pressure transducer "1" up to a maximum of two, and clearly show significant deviations from second-order behavior as evidenced by the discrepancy between the numerical calculations and the Tanner–Pipkin relation in Fig. 8.5-2. Also shown in Fig. 8.5-2 is the prediction for p^* from the Higashitani–Pritchard relation[5] computed by Malkus and Bernstein using the viscometric functions for the Curtiss–Bird model. For this particular constitutive equation, the Higashitani–Pritchard relation apparently differs only slightly from the Tanner–Pipkin relation in the region where both differ significantly from the p^* result obtained from the full numerical solution to the flow problem using the Curtiss-Bird constitutive equation. Experimental measurements,[6] on the other hand, support the validity of the Higashitani–Pritchard relation. Thus here is a situation where numerical simulations and experiments disagree. The reason for this discrepancy is not known.

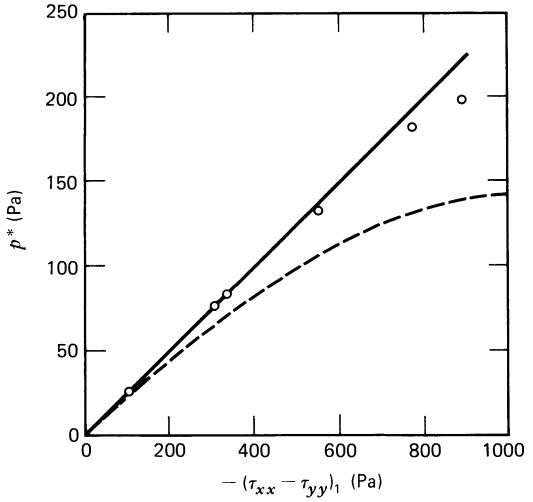

FIGURE 8.5-2. Hole pressure p^* defined by Eq. 8.5-1 as function of the first normal stress difference at pressure transducer "1" in Fig. 8.5-1 for the Curtiss–Bird model, Eq. 19.6-9, with parameters $\eta_0 = 410$ Pa·s, $\lambda = 9.54$ s, $\varepsilon = 0.375$, and density $\rho = 1363$ kg/m^3:

--- Values computed by Malkus and Bernstein by solving the complete flow problem using the Curtiss–Bird model.[3]

○ Values based on the Higashitani–Pritchard relation (Eq. 2.3-15) with $(\tau_{xx} - \tau_{yy})$ and τ_{yx} obtained from the Curtiss–Bird model as computed by Bernstein and Malkus.[3]

— Values from the second-order fluid as given by the Tanner and Pipkin relation ($p^* = -(\tau_{xx} - \tau_{yy})/4$) (Eq. 6B.15-1).

[5] K. Higashitani and W. G. Pritchard, *Trans. Soc. Rheol.*, **16**, 687–696 (1972).

[6] D. Pike and D. G. Baird, *J. Rheol.*, **28**, 439–447 (1984); A. S. Lodge and L. de Vargas, *Rheol. Acta*, **22**, 151–170 (1983); A. S. Lodge, *Polym. News*, **9**, 242–246 (1984).

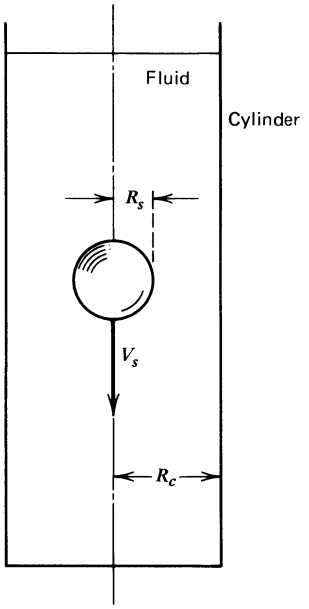

FIGURE 8.5-3. Sphere of radius R_s moving axially with velocity V_s on the centerline of a cylinder of radius R_c.

EXAMPLE 8.5-2 Flow Around a Rigid Sphere Moving Along the Axis of a Cylindrical Tube[2]

A sphere of radius R_s is moving with velocity V_s on the axis of a cylinder of radius R_c as shown in Fig. 8.5-3. The motion of the sphere is caused by a net force F_s acting on the sphere in the direction of V_s. The cylinder is filled with a viscoelastic liquid modeled by a convected Maxwell model with zero-shear-rate viscosity η_0 and time constant λ_1. The dimensionless groups for this problem are the geometric ratio R_s/R_c, the Deborah number De, and a dimensionless force K where

$$\text{De} = \frac{V_s \lambda_1}{R_s} \tag{8.5-2}$$

$$K = \frac{F_s}{6\pi\eta_0 R_s V_s} \tag{8.5-3}$$

It is desired to illustrate the calculations of Hassager and Bisgaard of the relation $K = K(R_s/R_c, \text{De})$.

SOLUTION Hassager and Bisgaard formulate the flow problem as an initial value problem, in which the sphere is at rest in a quiescent fluid for time $t < 0$. Then the force of magnitude F_s is exerted on the sphere for $t \geq 0$, and the resulting transient motion of the sphere and fluid is calculated. Hassager and Bisgaard use a Lagrangian technique, and for moderately small Deborah numbers observe an approach to a steady velocity V_s. The resulting values of De and K as calculated by Hassager and Bisgaard[7] are shown in Fig. 8.5-4.

[7] These results agree closely with results by F. Sugeng and R. I. Tanner, *J. Non-Newtoniaan Fluid Mech.*, **20** 281–292 (1986), who used an Eulerian technique to solve the steady flow problem for the convected Maxwell model in differential form with both a finite element method and a boundary element method; see also M. J. Crochet in *Finite Elements in Fluids*, Vol. 4, ed. R. H. Gallagher, Wiley, New York (1982), pp. 573–579.

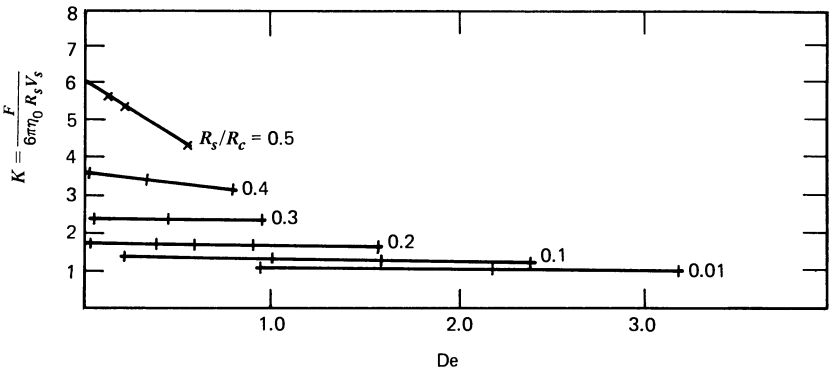

FIGURE 8.5-4. Calculated results[2] for K as a function of De and R_s/R_c for the motion of a sphere in a cylinder as shown in Fig. 8.5-3. + Calculated points. — Interpolation of the calculated points. [O. Hassager and C. Bisgaard, *J. Non-Newtonian Fluid Mech.*, **12**, 153–164 (1983).]

The simulated K-values were compared with experiments for $(R_s/R_c) = 0.3$, 0.4, and 0.5 and a 1% solution of polyacrylamide in glycerine at 293 K, as shown in Fig. 8.5-5. The measurements have been reduced to dimensionless form with the parameters $\eta_0 = 21.0$ Pa·s and $\lambda_1 = 12.0$ s. We see that with this choice of parameters there is good agreement between the measurements and the simulations.

The significance of these values of the parameters $\eta_0 = 21.0$ Pa·s and $\lambda_1 = 12.0$ s might be questioned, since they are determined in an inhomogeneous flow experiment. Certainly from a conceptual point of view it would be simpler to determine η_0 and λ_1 in steady shear flow, for which the Maxwell model has a constant viscosity $\eta(\dot{\gamma}) = \eta_0$ and a first normal stress difference $-(\tau_{xx} - \tau_{yy}) = 2\eta_0\lambda_1\dot{\gamma}^2$. We compare therefore in Fig. 8.5-6 the convected Maxwell model values for the viscosity and first normal stress difference (based on the parameters $\eta_0 = 21.0$ Pa·s and $\lambda_1 = 12.0$ s determined in the sphere experiment) with independent measurements by Prud'homme.[8] The comparison indicates that at least for this particular fluid and model the parameters may be determined equally well in either the sphere experiment or in a steady shear flow experiment. Thus here is a situation where numerical simulations and experiments do agree.

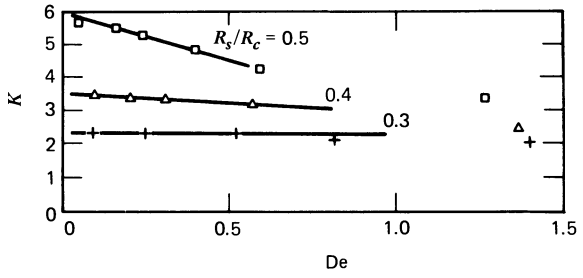

FIGURE 8.5-5. Comparison[2] of calculated results and experiments for K as a function of De and R_s/R_c: □, △, + Experimental data for a 1% solution of polyacrylamide in glycerine at 293 K plotted in dimensionless form with $\eta_0 = 21.0$ Pa·s and $\lambda_1 = 12.0$ s. — Calculated for convected Maxwell model based on Fig. 8.5-4. [O. Hassager and C. Bisgaard, *J. Non-Newtonian Fluid Mech.*, **12**, 153–164 (1983).]

[8] R. K. Prud'homme, private communication.

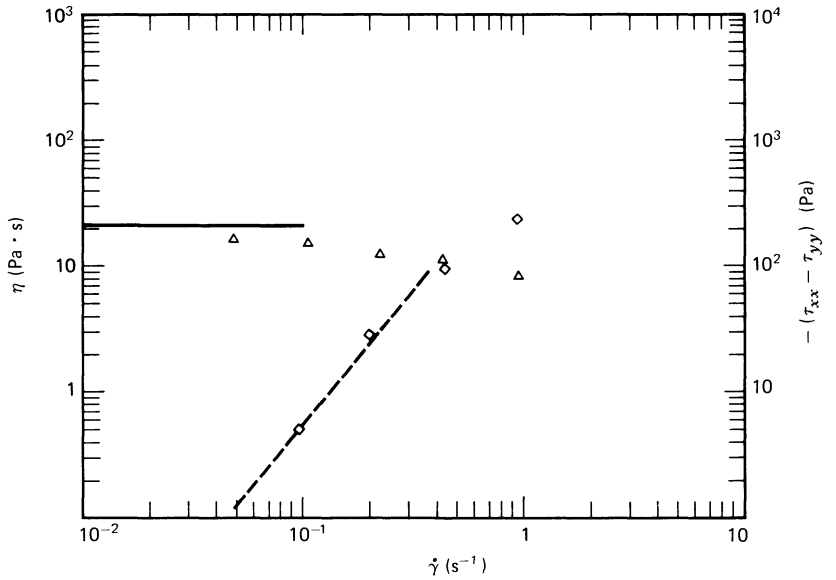

FIGURE 8.5-6. Viscosity η and first normal stress difference $-(\tau_{xx} - \tau_{yy})$ in steady shear flow. Predictions for the convected Maxwell model with parameters $\eta_0 = 21.0$ Pa·s and $\lambda_1 = 12.0$ s are — (for $\eta = \eta_0$) and - - - - - (for $-(\tau_{xx} - \tau_{yy}) = 2\eta_0\lambda_1\dot{\gamma}^2$). Experimental measurements in cone-and-plate geometry (by R. K. Prud'homme[8]) △ for η, and ◇ for $-(\tau_{xx} - \tau_{yy})$.

§8.6 LIMITATIONS OF SINGLE-INTEGRAL MODELS AND RECOMMENDATIONS FOR THEIR USE

The most general constitutive equations considered in this chapter are the K-BKZ and the Rivlin-Sawyers models in Eqs. 8.3-7 and 8.3-8, respectively. These models are too general to be useful for numerical flow calculations, and we have concentrated our discussion on the factorized versions of the two models in Eqs. 8.3-11 and 8.3-12. The factorized K-BKZ equation and the factorized Rivlin-Sawyers model have the following positive features:

i. They include the general linear viscoelastic fluid completely. This means that all of the material presented in Chapter 5 is included in the Rivlin-Sawyers and the K-BKZ equations.

ii. They provide a framework that includes a rather large number of nonlinear constitutive equations both of molecular and empirical origin. It is possible to choose simple empirical functions for $M(s)$ and $W(I_1, I_2)$ (or $\phi_j(I_1, I_2)$) to obtain reasonably satisfactory constitutive equations containing only four or five constants; these constants usually have simple physical meaning and are easy to determine from rheometric data.

iii. They provide a basis for the characterization of polymers, a subject important in connection with many problems relating to quality control. It is possible to use these constitutive equations to interrelate material functions (see, for example, Problem 8C.2).

No constitutive equation will ever be perfect, and the factorized Rivlin-Sawyers and K-BKZ equations also have their limitations:

i. The models generally predict too much recoil in elastic recoil experiments[1] (see, however, comment under **(c)** below).

ii. In certain fast strain experiments, the Rivlin–Sawyers model may form the basis[2] for a work-producing perpetual motion machine which is physically unreasonable.

Since the second limitation does not apply to the K–BKZ equation, we favor it somewhat.

Several considerations must be taken into account in the choice of a specific factorized K–BKZ equation. For example the potential function should be analytic at $(I_1, I_2) = (3, 3)$ in order that the model simplify properly to the retarded-motion expansion. Also the potential function and the memory function should be chosen so that shear stress vs. shear rate curve is monotone increasing. Considerations of this kind were illustrated in connection with Example 8.3-1.

There are some integral models that we have omitted because they cannot be formulated as either Rivlin–Sawyers or K–BKZ equations. In particular we have omitted:

a. *Integral models in which the memory function depends not only on the elapsed time $t - t'$ but also on the strain rate at time t'.*

Examples of such models are the Bird–Carreau[3] and Bogue–Chen[4] models. Models of this type have in the past attracted considerable attention but are no longer used extensively. One serious defect of models that include the strain rate in the memory function is that they do not simplify correctly to a linear viscoelastic model in the limit of small displacement gradients.[5]

b. *Integral models in which the memory function depends on the stress at time t'.*

Examples of such models are the Kaye and Phan-Thien–Tanner network models.[6] This type of model, however, may not be convenient from a computational point of view. Indeed one of the advantages of the integral models of this chapter over differential models is that they are explicit in the stress. In flow simulations this means that the stress components can be eliminated, and the total number of dependent variables may be reduced. However if the stress is included in the memory function this elimination is no longer possible.

c. *Models in which the effect on the stress at time t of the deformations at different past times, t' and t'' say, couple with one another.*

One example of this type of model is the Wagner damping functional model.[1] In this model the function ϕ_1 in Eq. 8.3-12 is replaced by a functional that selects the minimum value of ϕ_1 between times t' and t. This functional is introduced to model "irreversible loss

[1] M. H. Wagner, *Rheol. Acta*, **18**, 681–692 (1979).
[2] R. G. Larson and K. Monroe, *Rheol. Acta*, **23**, 10–13 (1984).
[3] R. B. Bird and P. J. Carreau, *Chem. Eng. Sci.*, **23**, 427–434 (1968); P. J. Carreau, I. F. Macdonald, and R. B. Bird, *ibid.*, 901–911 (1968).
[4] I. Chen and D. C. Bogue, *Trans. Soc. Rheol.*, **16**, 59–78 (1972).
[5] For still other objections, see H. E. van Es and R. M. Christensen, *Trans. Soc. Rheol.*, **17**, 325–330 (1973).
[6] A. Kaye, *Br. J. Appl. Phys.*, **17**, 803–806 (1966); A. S. Lodge, *Rheol. Acta*, **7**, 379–392 (1968); N. Phan-Thien and R. I. Tanner, *J. Non-Newtonian Fluid Mech.*, **2**, 353–365 (1977); N. Phan-Thien, *J. Rheol.*, **22**, 259–283 (1978); R. I. Tanner, *J. Non-Newtonian Fluid Mech.*, **5**, 103–112 (1979). See also §20.5.

of network junctions" (see Chapter 20), and Wagner has shown that this modification significantly improves the description of elastic recovery. Another example of this type of model is the Curtiss–Bird model[7] with $\varepsilon \neq 0$ (Eq. 19.6-9). In this model the contribution to the stress at time t of the strain rate at time t depends upon past states of deformation. We shall see in §9.6 that from a continuum mechanical point of view it is also natural to include the possibility of coupling between deformations at different times in the past and that such coupling contributes to the stress at the present time.

This chapter is the last in a sequence of five chapters, each devoted to a specific type of constitutive equation. It is not possible to recommend any one of these types of constitutive equations to be used for the modeling of the flow properties of polymeric liquids in all possible situations. Rather the choice of constitutive equation depends not only on the material but also on the particular application and the accuracy required by the user; the amount of time available and the computing techniques available may also play important roles in determining the choice of constitutive relation. At this point we wish to formulate some recommendations for a number of different constitutive-equation users:

1. Some rheologists are interested primarily in the experimental characterization of polymeric liquids. This can be done by the determination of the parameters in a model so that the model agrees with the rheometric experiments to the extent possible. For this purpose we recommend the Wagner model or the factorized K–BKZ model. As previously mentioned these automatically include the general linear viscoelastic model of Chapter 5, which has customarily been used by polymer chemists as a basis for the characterization of polymeric liquids in the linear regime.

2. Some fluid mechanicians are interested primarily in the low Reynolds number hydrodynamics of dilute suspensions or emulsions near equilibrium. Questions of interest here may be particle rotation, sedimentation, or deformation and breakup of particle clusters. For this purpose we recommend the retarded-motion expansion of Chapter 6.

3. Some engineers may deal with flow in complex geometric configurations, but may be interested only in rough exploratory calculations. In this situation it must first be determined whether the flow is primarily a shearing flow or an extensional flow. This determination will be based on a physical understanding of the flow situation, and the process will usually also involve some idealization of the geometry. Then for flows that are primarily shearing flows (including those involving heat and mass transfer) we recommend the use of the generalized Newtonian fluid, if necessary in connection with the lubrication approximation or the quasi-steady-state approximation as described in Chapter 4. For flows that involve a mixture of shear and shearfree kinematics or for shearing flows in which normal stress effects are of interest, we recommend the use of single-mode differential models, such as an Oldroyd model or the Giesekus model of Chapter 7.

4. Finally some engineers and fluid dynamicists are interested in precise numerical simulations of flow in complex geometries. For this purpose we recommend the nonlinear models of Chapters 7 and 8. The development of reliable routines for numerical simulations has been the object of much research effort, but is still a largely unresolved problem.[8] It is not possible, therefore, to make more specific recommendations for this last group of users, since any such recommendations will inevitably be altered by future research.

[7] C. F. Curtiss and R. B. Bird, *J. Chem. Phys.*, **74**, 2016–2025, 2026–2033 (1981); *Phys. Today*, **37**(1), 36–43 (1984). R. B. Bird, H. H. Saab, and C. F. Curtiss, *J. Phys. Chem.*, **86**, 1102–1105 (1982); R. B. Bird, H. H. Saab, and C. F. Curtiss, *J. Chem. Phys.*, **77**, 4747–4757 (1982); H. H. Saab, R. B. Bird, and C. F. Curtiss, *ibid.*, 4758–4766 (1982).

[8] See M. J. Crochet and K. Walters, *Ann. Rev. Fluid Mech.*, **15**, 241–260 (1983). For two status reports on numerical methods, see *J. Non-Newtonian Fluid Mech.*, **16**, 1–209 (1984) and **20**, 1–339 (1986).

Gradually there has been a shift in emphasis away from the models in Chapters 4, 5, and 6 and toward those of Chapters 7 and 8, and we expect this trend to continue. Also we expect that molecular-theory-based constitutive equations will replace empirical equations because they have the added advantage of providing extra insight into molecular orientation and stretching. A crucial need is the accumulation of experimental data on material functions, particularly for shearfree flows, and flow-field mappings (by laser Doppler velocimetry, for example), for well characterized fluids over wide ranges of system parameters.

PROBLEMS

8B.1 Potential Functions for Special Models

a. It is desired to demonstrate that two simple integral models in Table 8.3-3 may be formulated as factorized K-BKZ equations for special choices of the parameters. To do this find the potential functions (constructed to be zero at $I_1, I_2 = 3,3$) for the models of Wagner[1] for $\alpha = 1$ and of Papanastasiou et al.[2] for $\beta = 1$.

b. Do the above models obey the Renardy conditions?

Answer: **a.** Wagner: $W = \frac{2}{\beta^2}[1 - (\beta\sqrt{I_1 - 3} + 1)\exp(-\beta\sqrt{I_1 - 3})]$

Papanastasiou-Scriven-Macosko: $W = \alpha \ln[(\alpha + I_1 - 3)/\alpha]$

8B.2 Transient Stretching of a Thin Liquid Filament[3]

Consider a thin liquid filament with one end fixed and one end free. For time $t < t_0$ the filament is at rest with uniform radius R_0, and for $t > t_0$ the filament is being stretched by means of a gravitational acceleration g in the direction of the filament axis and also because of an imposed force on the free end. The initial locations of the fluid particles are described by the coordinates r_0, z_0 for time $t \leq t_0$ (see Fig. 8B.2); the particle locations are given by r, z for time $t > t_0$. The radius of the filament is $R(z_0, t_0, t)$, and for $t > t_0$ it is assumed that $z = z(z_0, t_0, t)$ and $r = r_0 R(z_0, t_0, t)/R_0$.

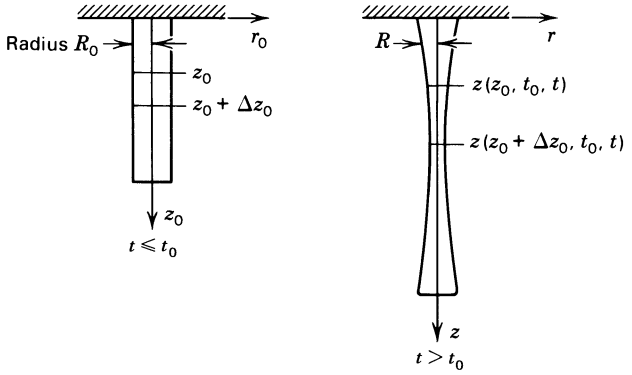

FIGURE 8B.2. Thin liquid filament with one end fixed, shown for times $t \leq t_0$ and $t > t_0$ with cylindrical coordinate r_0, z_0 and r, z. The filament is axisymmetrical with no θ-dependence.

[1] M. H. Wagner, *Rheol. Acta*, **18**, 33-50 (1979).
[2] A. C. Papanastasiou, L. E. Scriven, and C. W. Macosko, *J. Rheol.*, **27**, 387-410 (1983).
[3] P. Markovich and M. Renardy, *J. Non-Newtonian Fluid Mech.*, **17**, 13-22 (1985).

a. Make a mass balance on the material located between z_0 and $z_0 + \Delta z_0$ for $t \leq t_0$ to obtain

$$R(z_0, t_0, t) = \frac{R_0}{\sqrt{\partial z/\partial z_0}} \tag{8B.2-1}$$

where $z = z(z_0, t_0, t)$.

b. Make a momentum balance on the same material to obtain

$$\rho \frac{\partial^2 z}{\partial t^2} = \frac{\partial}{\partial z_0}\left(-\frac{1}{\partial z/\partial z_0}(\tau_{zz} - \tau_{rr}) + \frac{\sigma}{R_0\sqrt{\partial z/\partial z_0}}\right) + \rho g \tag{8B.2-2}$$

where σ is the surface tension. All the constitutive assumptions enter in the expression for the normal stress difference $\tau_{zz} - \tau_{rr}$.

c. Show that for the Newtonian fluid of Eq. 1.2-2

$$\tau_{zz} - \tau_{rr} = -\frac{3}{\partial z/\partial z_0}\frac{\partial^2 z}{\partial t\, \partial z_0} \tag{8B.2-3}$$

d. Show that for the Lodge rubberlike liquid of Eq. 8.2-1

$$\tau_{zz} - \tau_{rr} = -\int_{-\infty}^{t} M(t - t')\left[\left(\frac{\partial z/\partial z_0}{\partial z'/\partial z_0}\right)^2 - \left(\frac{\partial z'/\partial z_0}{\partial z/\partial z_0}\right)\right] dt' \tag{8B.2-4}$$

where $z' = z'(z_0, t_0, t')$.

e. Look up the article by Markovich and Renardy[3] and discuss their numerical solutions of the above evolution equation for $z(z_0, t_0, t)$ for a number of initial and boundary conditions.

8B.3 Properties of Finite Strain Tensors

Consider a particle with coordinates x_i and a neighboring particle with coordinates $x_i + dx_i$ both at time t.

a. Show that the separation, $(ds')^2$, of the two particles at some other time t' is given by

$$(ds')^2 = \sum_i \sum_j B_{ij}^{-1}(t, t')\, dx_i\, dx_j \tag{8B.3-1}$$

and conclude from this that $\mathbf{B}$ and $\mathbf{B}^{-1}$ are positive definite.

b. By using the Cayley–Hamilton theorem, verify that $\boldsymbol{\gamma}^{[0]}$ and $\boldsymbol{\gamma}_{[0]}$ are related by

$$\boldsymbol{\gamma}^{[0]} = (I_2 - I_1)\boldsymbol{\delta} + (I_1 - 2)\boldsymbol{\gamma}_{[0]} + \{\boldsymbol{\gamma}_{[0]} \cdot \boldsymbol{\gamma}_{[0]}\} \tag{8B.3-2}$$

for incompressible fluids.

c. How are the invariants of $\mathbf{B}$ and those of $\boldsymbol{\gamma}_{[0]}$ related?

8B.4 An Alternative to the Lodge Rubberlike Liquid

a. Show that if $\boldsymbol{\gamma}_{[0]}(t, t')$ is replaced by $\boldsymbol{\gamma}^{[0]}(t, t')$ in Eq. 8.2-1, one obtains for steady-state shear flow

$$\tau_{yx} = -M_1\dot{\gamma}; \quad \tau_{xx} - \tau_{yy} = -M_2\dot{\gamma}^2; \quad \tau_{yy} - \tau_{zz} = +M_2\dot{\gamma}^2 \tag{8B.4-1}$$

instead of the results shown in Eqs. 8.2-9 to 11. What experimental data in Chapter 3 show that $\boldsymbol{\gamma}_{[0]}$ is to be preferred?

b. What happens if $\boldsymbol{\gamma}_{[0]}$ in Eq. 8.2-1 is replaced by $(1 - q)\boldsymbol{\gamma}_{[0]} + q\boldsymbol{\gamma}^{[0]}$, where $0 \leq q \leq 1$?

8B.5 Eccentric-Disk Rheometer

The eccentric-disk rheometer of Fig. 3B.1 has been examined in Problem 6B.2 (retarded-motion expansion) and in Problem 7B.9 (convected Maxwell model). Here we analyze the eccentric-disk rheometer by using the factorized Rivlin–Sawyers model.

a. Show that the displacement functions corresponding to the velocity distribution in Eq. 6B.2-1 are

$$x(x', y', z', t', t) = x' \cos W(t - t') - (y' - Az') \sin W(t - t') \tag{8B.5-1}$$

$$y(x', y', z', t', t) = x' \sin W(t - t') + (y' - Az') \cos W(t - t') + Az' \tag{8B.5-2}$$

$$z(x', y', z', t', t) = z' \tag{8B.5-3}$$

Invert the displacement functions by solving for x', y', z'.

b. Find the displacement gradient tensors $\boldsymbol{\Delta}$ and $\mathbf{E}$ for this flow. Check your results by verifying that $\{\boldsymbol{\Delta} \cdot \mathbf{E}\} = \boldsymbol{\delta}$.

c. Then find the Finger and Cauchy strain tensors

$$\mathbf{B} = \begin{pmatrix} 1 + A^2S^2 & A^2S(1 - C) & AS \\ A^2S(1 - C) & 1 + A^2(1 - C)^2 & A(1 - C) \\ AS & A(1 - C) & 1 \end{pmatrix} \tag{8B.5-4}$$

$$\mathbf{B}^{-1} = \begin{pmatrix} 1 & 0 & -AS \\ 0 & 1 & -A(1 - C) \\ -AS & -A(1 - C) & 2A^2(1 - C) + 1 \end{pmatrix} \tag{8B.5-5}$$

in which $S = \sin W(t - t')$ and $C = \cos W(t - t')$

d. Obtain the expressions for τ_{xz} and τ_{yz} using the factorized Rivlin–Sawyers model.

e. Next obtain expressions for $I_1 - 3$ and $I_2 - 3$. Note that, according to Eqs. 8.3-16 and 17b, ϕ_1 and ϕ_2 are given as power series in A^2.

f. Finally obtain the result

$$\lim_{A \to 0} \left(-\frac{\tau_{xz}}{AW} \right) = \eta'(W) \tag{8B.5-6}$$

$$\lim_{A \to 0} \left(-\frac{\tau_{yz}}{AW} \right) = \eta''(W) \tag{8B.5-7}$$

by using Eqs. 5B.7-1 and 2.

8B.6 Planar Elongational Flow

Consider the flow of Eq. 3.1-3 with $b = 1$. Such a flow can be realized approximately for slow flow in the central portion of the crossed-slit apparatus in Fig. 8B.6:

- **a.** Find the displacement functions.
- **b.** Obtain the Finger and Cauchy tensors.
- **c.** Verify the statement in Fig. 8.3-1 that $I_1 = I_2$ for planar elongational flow.
- **d.** For the Lodge elastic liquid, with $M(s) = (\eta_0/\lambda_1^2) \exp(-t/\lambda_1)$, obtain $\bar{\eta}_1(\dot{\varepsilon})$ defined in Eq. 3.5-1. What restrictions must be placed on the result?
- **e.** Show that $\bar{\eta}_1(0) = 4\eta_0$ (cf. Fig. 7.3-8c). Verify that this result is true for the Lodge elastic liquid with any memory function $M(s)$.

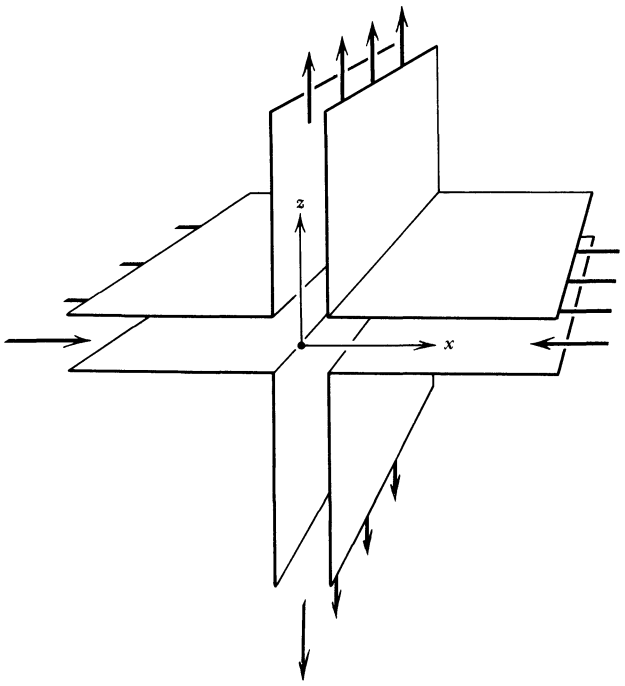

FIGURE 8B.6. Crossed-slit apparatus.

8B.7 The "Network-Rupture Model"

The Lodge rubberlike liquid model (Eq. 8.2-1) includes the idea that the stress in a fluid element at the present time t depends on the strain undergone by the fluid element during all past times t' going from $t' = -\infty$ to $t' = t$. Tanner and Simmons[4] suggest that, as a concentrated polymer solution or polymer melt flows, the "network" of polymer chains is gradually destroyed so that the fluid loses its "memory" of everything that happened t_R time units before t; t_R is called the "rupture time." This is an appealing and simple idea worth investigating. Tanner and Simmons give a general formula for calculating t_R, but for shearing flows t_R is given by the relation $t_R = B/\dot{\gamma}$, where B is a positive constant (characteristic of each fluid) and $\dot{\gamma} = \sqrt{\frac{1}{2}(\boldsymbol{\gamma}_{(1)} : \boldsymbol{\gamma}_{(1)})}$ is the shear rate. Hence in the Lodge rubberlike liquid they suggest replacing $\int_{-\infty}^{t}$ by $\int_{t-t_R}^{t}$.

They also suggest that, instead of using $\boldsymbol{\gamma}_{[0]}(t, t')$ in the integral, one should use a linear combination of $\boldsymbol{\gamma}_{[0]}$ and $\boldsymbol{\gamma}^{[0]}$. Then the Tanner–Simmons model is

$$\boldsymbol{\tau} = \int_{t-t_R}^{t} M(t-t')[(1-q)\boldsymbol{\gamma}_{[0]}(t, t') + q\boldsymbol{\gamma}^{[0]}(t, t')]dt' \tag{8B.7-1}$$

where q is a small, positive constant characteristic of each polymer.

a. Show that for steady-state shear flow

$$\eta = \int_0^{t_R} M(s)s\, ds \tag{8B.7-2}$$

$$\Psi_1 = \int_0^{t_R} M(s)s^2\, ds \tag{8B.7-3}$$

$$\Psi_2 = -q\int_0^{t_R} M(s)s^2\, ds \tag{8B.7-4}$$

[4] R. I. Tanner and J. M. Simmons, *Chem. Eng. Sci.*, **22**, 1803–1815 (1967); R. I. Tanner, *AIChE J.*, **15**, 177–183 (1969).

b. Note that $\Psi_2/\Psi_1 = -q$. What figure in Chapter 3 can you use to evaluate this result, and what is the approximate value of q suggested by the data?

c. Next make a specific choice of the memory function $M(s)$:

$$M(s) = \frac{\eta_0}{\lambda^2} e^{-s/\lambda} \tag{8B.7-5}$$

where η_0 is the zero-shear-rate viscosity and λ is a time constant; this means that the model now contains *four* adjustable parameters: η_0, λ, B, and q. Obtain an expression for the viscosity η as a function of the shear rate $\dot{\gamma}$.

d. In the viscosity found above what are the limiting values of η/η_0 as $\dot{\gamma} \to 0$ and $\dot{\gamma} \to \infty$?

Note: Tanner and Simmons were able to fit experimental data quite well when $M(s)$ was taken to be a sum of exponentials. They found that $\bar{\eta}(\dot{\varepsilon})$ remained finite, and their $\bar{\eta}(\dot{\varepsilon})$ had qualitatively the same shape as that of polymer melt data.

8B.8 Material Functions for the Wagner Model (Segalman Relaxation Modulus)

Use Segalman's memory function $M(s)$ of Eq. 8.3-35. Insert this into Eq. 8.3-12 along with Wagner's ϕ_1 and ϕ_2 functions in Table 8.3-3.

a. Obtain the expressions for $\eta(\dot{\gamma})$ and $\Psi_1(\dot{\gamma})$ for this model.

b. Show that in the limit of zero shear rate

$$\eta = \eta_0; \quad \Psi_1 = 2\eta_0\lambda(1 - v) \tag{8B.8-1}$$

c. Show that in the limit of high shear rates

$$\eta = \eta_0 v(\beta\lambda\dot{\gamma})^{v-1}; \quad \Psi_1 = \eta_0\lambda v(1 - v)(\beta\lambda\dot{\gamma})^{v-2} \tag{8B.8-2}$$

Are these results satisfactory?

8C.1 Flow of a Viscoelastic Fluid into a Line Sink[5]

It is desired to investigate possible generalizations of the plane radial flow problem in Example 8.4-1 to situations with angular dependence of the velocity. That is when Eq. 8.4-2 is replaced by

$$v_r = -\frac{f(\theta)}{r} \tag{8C.1-1}$$

Use the Lodge rubberlike liquid model.

a. Show that the only nonzero components of the $\boldsymbol{\gamma}_{[0]}$ tensor are

$$\gamma_{[0]rr} = -\frac{2fs}{r^2} - \frac{f'^2s^2}{r^2(r^2 + 2fs)} \tag{8C.1-2}$$

$$\gamma_{[0]\theta\theta} = \frac{2fs}{r^2 + 2fs} \tag{8C.1-3}$$

$$\gamma_{[0]r\theta} = \gamma_{[0]\theta r} = \frac{f's}{r^2 + 2fs} \tag{8C.1-4}$$

[5] A. M. Hull, *J. Non-Newtonian Fluid Mech.*, **8**, 327-336 (1981).

b. Show then that the equation of motion is satisfied if it is possible to choose a pressure field p such that

$$\frac{\partial p}{\partial r} = -\int_0^\infty M(s)\frac{4f^2s^2 + f'^2s^2 + r^2f''s}{r^3(r^2 + 2fs)}\,ds \tag{8C.1-5a}$$

$$\frac{\partial p}{\partial \theta} = -\int_0^\infty M(s)\frac{2f's}{r^2 + 2fs}\,ds \tag{8C.1-5b}$$

c. Eliminate p by cross differentiation between Eqs. 8C.1-5a and 5b and show that the resulting equation requires that $f(\theta)$ satisfy

$$f''' + 4f' = 0 \tag{8C.1-6}$$

$$f'(4f^2 + 2ff'' - f'^2) = 0 \tag{8C.1-7}$$

d. Show that the only solutions for $f(\theta)$ that satisfy both equations are

$$f = K \tag{8C.1-8}$$

and

$$f = K\cos^2(\theta - \theta_0) \tag{8C.1-9}$$

Equation 8C.1-8 is the solution in Example 8.4-1, whereas Eq. 8C.1-9 is the Hull solution for flow into a line sink located in an infinite plane, that is, $v_r = 0$ at $\theta = \theta_0 \pm \pi/2$. Verify that θ_0 may be taken to be zero without loss of generality.

e. Show that for the Hull solution (with $\theta_0 = 0$)

$$p = \int_0^\infty M(s)\left[\frac{Ks}{r^2} - \ln\left(1 + \frac{2Ks\cos^2\theta}{r^2}\right)\right]ds + p_\infty \tag{8C.1-10}$$

and

$$\tau_{rr} = -\left[\int_0^\infty F\left(1 + \frac{2Ks}{r^2}\right)ds\right]\cos^2\theta \tag{8C.1-11}$$

$$\tau_{r\theta} = \tau_{\theta r} = -\left[\int_0^\infty F\,ds\right]\sin\theta\cos\theta \tag{8C.1-12}$$

$$\tau_{\theta\theta} = \left[\int_0^\infty F\,ds\right]\cos^2\theta \tag{8C.1-13}$$

where

$$F(r, \theta, s) = \frac{2KM(s)s}{r^2 + 2Ks\cos^2\theta} \tag{8C.1-14}$$

8C.2 Interrelation between Material Functions for the Factorized K-BKZ Model

Consider the stress relaxation after cessation, at time $t = 0$, of the steady shear flow with shear rate $\dot{\gamma}_0$. Show that for $t \geq 0$ the K-BKZ model gives

$$\tau_{yx}|_{t\geq 0} = \dot{\gamma}_0 \int_t^\infty M(s)(t-s)\left(\frac{\partial W}{\partial I_1} + \frac{\partial W}{\partial I_2}\right)_{t-t'=s} ds \tag{8C.2-1}$$

From Eq. B of Table 8.3-1 we see that for $t \leq 0$,

$$(\tau_{xx} - \tau_{yy})|_{t\leq 0} = -\dot{\gamma}_0^2 \int_0^\infty M(s)s^2\left(\frac{\partial W}{\partial I_1} + \frac{\partial W}{\partial I_2}\right)_{t-t'=s} ds \tag{8C.2-2}$$

From these two equations verify that the K-BKZ model predicts that

$$(\tau_{xx} - \tau_{yy})|_{t\leq 0} = 2\dot{\gamma}_0 \int_0^\infty \tau_{yx}\, dt \tag{8C.2-3}$$

This suggests that measuring the area under the stress relaxation curve gives information equivalent to that obtained in a steady-state normal stress measurement.[6]

8D.1 Unit Vector Transformation in Deforming Continua[7]

It is desired to develop the determinant J of the Jacobian matrix of the transformation from spherical coordinates θ, ϕ of the radial unit vector $\boldsymbol{u}(\theta, \phi)$ to spherical coordinates $\hat{\theta}$, $\hat{\phi}$ of the radial unit vector $\hat{\boldsymbol{u}}(\hat{\theta}, \hat{\phi})$, where $\boldsymbol{u}$ and $\hat{\boldsymbol{u}}$ are related by Eq. 8.3-54. Use the following steps:

a. First show that Eq. 8.3-54 can be inverted to yield

$$\boldsymbol{u} = \frac{[\boldsymbol{\Delta}\cdot\hat{\boldsymbol{u}}]}{|\boldsymbol{\Delta}\cdot\hat{\boldsymbol{u}}|} \tag{8D.1-1}$$

b. Instead of the desired transformation consider the transformation from the spherical coordinates $(\hat{r}, \hat{\theta}, \hat{\phi})$ of the position vector $\hat{\boldsymbol{r}}(\hat{r}, \hat{\theta}, \hat{\phi})$ to the spherical coordinates (r, θ, ϕ) of the position vector $\boldsymbol{r}(r, \theta, \phi)$, where $\hat{\boldsymbol{r}}$ and $\boldsymbol{r}$ are related by

$$\boldsymbol{r} = [\boldsymbol{\Delta}\cdot\hat{\boldsymbol{r}}] \tag{8D.1-2}$$

Denote the elements of the Jacobian matrix of the transformation $\hat{r}, \hat{\theta}, \hat{\phi} \rightarrow r, \theta, \phi$ by A_{ij} and show

$$\begin{aligned} J &= (A_{22}A_{33} - A_{23}A_{32})|_{r=|\boldsymbol{\Delta}\cdot\hat{\boldsymbol{r}}|} \\ &= (AA^{11})|_{r=|\boldsymbol{\Delta}\cdot\hat{\boldsymbol{r}}|} \end{aligned} \tag{8D.1-3}$$

where A is the determinant of (A_{ij}), and A^{ij} is an element of the matrix inverse to (A_{ij}).

[6] Equation 8C.2-3 has also been obtained from the kinetic theory of bead-spring chains (see Eq. 15.4-35). Several experiments tend to substantiate this relation: P. Attane, P. LeRoy, J. M. Pierrard, and G. Turrel, *J. Non-Newtonian Fluid Mech.*, **3**, 1-12 (1977), for polystyrene melts and concentrated solutions of polyisobutylene in mineral oil; H. W. Gao, S. Ramachandran, and E. B. Christiansen, *J. Rheol.*, **25**, 213-235 (1981), for concentrated solutions of polystyrene in *n*-butylbenzene.

[7] The development in this problem was supplied to us by A. S. Lodge. A similar derivation is given by S. M. Dinh, Sc.D. Thesis, Massachussetts Institute of Technology, Cambridge (1983).

c. Introduce the notation that the spherical coordinates of $\boldsymbol{r}$ are denoted by ρ_i, with $\rho_1, \rho_2, \rho_3 = r, \theta, \phi$, and the rectangular coordinates of $\boldsymbol{r}$ are x_i. Similarly denote the spherical coordinates of $\hat{\boldsymbol{r}}$ by $\hat{\rho}_i$ and its rectangular coordinates by $\hat{x}_i$. Then show that

$$A_{ij} = \frac{\partial \rho_i}{\partial \hat{\rho}_j} = \sum_m \sum_n \frac{\partial \rho_i}{\partial x_m} \frac{\partial x_m}{\partial \hat{x}_n} \frac{\partial \hat{x}_n}{\partial \hat{\rho}_j} = \sum_m \sum_n \frac{\partial \rho_i}{\partial x_m} \Delta_{mn} \frac{\partial \hat{x}_n}{\partial \hat{\rho}_j} \tag{8D.1-4}$$

$$A^{ij} = \frac{\partial \hat{\rho}_i}{\partial \rho_j} = \sum_m \sum_n \frac{\partial \hat{\rho}_i}{\partial \hat{x}_m} \mathrm{E}_{mn} \frac{\partial x_n}{\partial \rho_j} \tag{8D.1-5}$$

d. Then show that

$$A = (\det \boldsymbol{\Delta}) \frac{\hat{r}^2 \sin \hat{\theta}}{r^2 \sin \theta} \tag{8D.1-6}$$

$$A^{11} = (\hat{\boldsymbol{u}} \cdot [\mathbf{E} \cdot \boldsymbol{u}]) \tag{8D.1-7}$$

e. Combine the above to show that

$$J = \frac{\sin \hat{\theta}}{\sin \theta} \frac{(\det \boldsymbol{\Delta})}{|\boldsymbol{\Delta} \cdot \hat{\boldsymbol{u}}|^3} \tag{8D.1-8}$$

8D.2 Incompressibility Conditions

Consider an arbitrary deformation that is described by the displacement functions Eqs. 8.1-2. It is desired to establish incompressibility conditions by comparing the mass of material contained in a volume $V(t)$, the boundaries of which are fluid particles, at the present time t and at an arbitrary past time t'. By a change of variable in the expression for the mass at t', show that

$$\frac{\rho}{\rho'} = \det \boldsymbol{\Delta} \tag{8D.2-1}$$

where ρ and ρ' denote the fluid density at t and t'. From this deduce

$$\det \boldsymbol{\Delta} = \det \mathbf{E} = 1 \tag{8D.2-2}$$

$$\det \mathbf{B} = \det \mathbf{B}^{-1} = 1 \tag{8D.2-3}$$

for incompressible fluids.